Alexander Bobenko
Christian Klein *Editors*

Computational Approach to Riemann Surfaces

Springer

Lecture Notes in Mathematics 2013

Alexander I. Bobenko · Christian Klein
Editors

Computational Approach to Riemann Surfaces

Springer

Editors
Alexander I. Bobenko
Institut für Mathematik
Technische Universität Berlin
Strasse des 17. Juni 136
10623 Berlin
Germany
bobenko@math.tu-berlin.de

Christian Klein
Institut de
Mathématiques de Bourgogne
Université de Bourgogne
9 avenue Alain Savary
21078 Dijon Cedex
France
christian.klein@u-bourgogne.fr

Cover design: deblik Berlin

Printed on acid-free paper

Preface

Riemann surfaces appear in many branches of mathematics and physics, e.g. in differential and algebraic geometry and the theory of moduli spaces, in topological field theories, quantum chaos and integrable systems. The practical use of Riemann surface theory has been limited for a long time by the absence of efficient computational approaches. In recent years considerable progress has been achieved in the numerical treatment of Riemann surfaces which stimulated further research in the subject and led to new applications. The existing computational approaches follow from the various definitions of Riemann surfaces: via non-singular algebraic curves, as quotients under the action of Fuchsian or Schottky groups, or via polyhedral surfaces.

It is the purpose of the present volume to give a coherent presentation of the existing or currently being developed computational approaches to Riemann surfaces. The authors of the contributions are representants from the groups providing publically available numerical codes in this field. Thus this volume illustrates which software tools are available and how they can be used in practice. In addition examples for solutions to partial differential equations and in surface theory are presented.

In the introduction, A.I. Bobenko presents a comprehensive summary of the theory of compact Riemann surfaces, Abelian differentials, periods on Riemann surfaces, theta functions and uniformization theory. Riemann originally introduced Riemann surfaces as plane algebraic curves. B. Deconinck and M. Patterson have followed this approach together with M. v. Hoeij for a number of years. They have devised several algorithms facilitating different aspects of the effective computation with Riemann surfaces represented by plane algebraic curves. Their algorithms have led to the *algcurves* Maple package: a collection of Maple programs for computations with algebraic curves. B. Deconinck and M. Patterson describe their algorithms, the Maple implementation and give instructive examples. The numerical approach via algebraic curves involves the computation of contour integrals on Riemann surfaces. To study the moduli spaces associated to Riemann surfaces numerically, an efficient computation of these integrals is necessary. J. Frauendiener

and C. Klein present a fully numerical approach based on Gauss integration which provides high accuracy. Explicit solutions of integrable partial differential equations are discussed as applications.

A complementary approach to compact Riemann surfaces is based on the uniformization theory. M. Schmies discusses numerics of the Schottky uniformization of Riemann surfaces and in particular the convergence of Poincaré theta series and their use in the numerical treatment of Riemann surfaces. It is incorporated in the Java project *jtem*. The use of this package is demonstrated for concrete examples from surface theory. R. Hidalgo and M. Seppälä discuss the uniformization of hyperelliptic algebraic curves. Using a method originally due to Myrberg, they construct an algorithm that approximates the generators of a Schottky group uniformizing a given hyperelliptic algebraic curve. D. Crowdy and J. Marshall study conformal mappings for multiply connected domains both analytically and numerically. They discuss a formulae for these mappings in terms of the Schottky–Klein prime function. The latter function is numerically evaluated by using Schottky uniformization.

The relation of Riemann surfaces to polyhedral surfaces offers yet another computational approach. A.I. Bobenko, C. Mercat and M. Schmies discuss the computation of period matrices of Euclidean surfaces by methods of discrete differential geometry. The latter are based on the notions of discrete holomorphicity and discrete Riemann surfaces. As an application period matrices of Lawson surfaces are computed. An interesting object associated to the modular space of Riemann surfaces are determinants of Laplacians. These determinants appear in particular in topological field theories. A. Kokotov presents a review of determinants of Laplacians for surfaces with polyhedral metrics. These determinants are given in terms of explicit functions, and provide a way to study global aspects of the geometry of the associated modular space numerically, an investigation which is currently being performed.

The intended audience of this book is twofold. It can be used as a textbook for a graduate course in numerics of Riemann surfaces. The standard undergraduate background, i.e., calculus and linear algebra, is required. In particular, no knowledge of the theory of Riemann surfaces is expected, the necessary background in this theory is contained in the Introduction chapter.

On the other hand, this book is also written for specialists in geometry and mathematical physics applying the theory of Riemann surfaces in their research. It is the first book on numerics of Riemann surfaces which reflects the progress in this field during the last decade, and it contains original results. There is a growing number of applications where one is interested in the evaluation of concrete characteristics of models analytically described in terms of Riemann surfaces. Many problem settings and computations in this volume are motivated by such concrete applications in geometry and mathematical physics.

Berlin, Dijon   *Alexander I. Bobenko*
June, 2010   *Christian Klein*

Contents

Part IV Discrete Surfaces

List of Contributors

A.I. Bobenko
Institut für Mathematik
Technische Universität Berlin
Strasse des 17. Juni 136
10623 Berlin, Germany
`bobenko@math.tu-berlin.de`

D. Crowdy
Department of Mathematics
Imperial College London
180 Queen's Gate, London, SW7
2AZ, United Kingdom
`d.crowdy@imperial.ac.uk`

B. Deconinck
Department of Applied Mathematics
University of Washington
Seattle WA 98195-2420, USA
`bernard@amath.washington.edu`

J. Frauendiener
Department of Mathematics and
Statistics, University of Otago
P.O. Box 56, Dunedin 9010
New Zealand
and Centre of Mathematics for
Applications, University of Oslo
University of Oslo, P.O. Box 1053
Blindern, NO-0316 Oslo, Norway
`joergf@maths.otago.ac.nz`

R.A. Hidalgo
Departamento de Matemáticas
Universidad Técnica Federico
Santa María, Valparaíso, Chile
`ruben.hidalgo@usm.cl`

C. Klein
Institut de
Mathématiques de Bourgogne
Université de Bourgogne
9 avenue Alain Savary
21078 Dijon Cedex
France
`christian.klein@u-bourgogne.fr`

A. Kokotov
Department of Mathematics and
Statistics, Concordia University
1455 de Maisonneuve Blvd. West
Montreal, Quebec, H3G 1M8 Canada
`alexey@mathstat.concordia.ca`

J.S. Marshall
Department of Mathematics
Imperial College London
180 Queen's Gate, London, SW7
2AZ, United Kingdom
`jonathan.marshall@imperial.ac.uk`

C. Mercat
I3M c.c. 51, Université Montpellier 2
F-34095 Montpellier cedex 5, France
`mercat@math.univ-montp2.fr`

M.S. Patterson
Boeing Research and Technology
2760 160th Ave SE
Bellevue, WA 98008, USA

M. Seppälä
Department of Mathematics, Florida
State University, USA and

Department of Mathematics and
Statistics, University of Helsinki
Finland
`mika.seppala@fsu.edu`

M. Schmies
Institut für Mathematik
Technische Universität Berlin
Strasse des 17. Juni 136
10623 Berlin, Germany
`schmies@math.tu-berlin.de`

Part I Introduction

1

Introduction to Compact Riemann Surfaces

Alexander I. Bobenko

Institut für Mathematik,
Technische Universität Berlin,
Strasse des 17. Juni 136, 10623 Berlin, Germany,
bobenko@math.tu-berlin.de

The theory of Riemann surfaces is a classical field of mathematics where geometry and analysis play equally important roles. The purpose of these notes is to present some basic facts of this theory to make this book more self contained. In particular we will deal with classical descriptions of Riemann surfaces, Abelian differentials, periods on Riemann surfaces, meromorphic functions, theta functions, and uniformization techniques.

Motivated by the concrete point of view on Riemann surfaces of this book we choose essentially an analytic presentation. Concrete analytic tools and constructions available on Riemann surfaces and their applications to the theory are explained in detail. Most of them are proven or accompanied with sketches of proofs. For the same reason, difficult non-constructive proofs of some classical existence results in the theory of Riemann surfaces (such as the existence of conformal coordinates, of holomorphic and Abelian differentials, of meromorphic sections of holomorphic line bundles) are omitted. The language of the geometric approach is explained in the section on holomorphic line bundles.

This chapter is based on the notes of a graduate course given at the Technische Universität Berlin. There exists a huge literature on Riemann surfaces including many excellent classical monographs. Our list [FK92, Jos06, Bos, Bea78, AS60, Gu66, Lew64, Spr81] for further reading is by no means complete.

1.1 Definition of a Riemann Surface and Basic Examples

Let $\mathcal{R}$ be a two-dimensional real manifold, and let $\{U_\alpha\}_{\alpha \in A}$ be an open cover of $\mathcal{R}$, i.e., $\cup_{\alpha \in A} U_\alpha = \mathcal{R}$. A *local parameter (local coordinate, coordinate chart)* is a pair (U_α, z_α) of U_α with a homeomorphism $z_\alpha : U_\alpha \to V_\alpha$ to an open subset $V_\alpha \subset \mathbb{C}$. Two coordinate charts (U_α, z_α) and (U_β, z_β) are called *compatible* if the mapping

$$f_{\beta,\alpha} = z_\beta \circ z_\alpha^{-1} : z_\alpha(U_\alpha \cap U_\beta) \to z_\beta(U_\alpha \cap U_\beta) , \qquad (1.1)$$

which is called a *transition function* is holomorphic. The local parameter (U_α, z_α) will be often identified with the mapping z_a if its domain is clear or irrelevant.

If all the local parameters $\{U_\alpha, z_\alpha\}_{\alpha \in A}$ are compatible, they form a *complex atlas* $\mathcal{A}$ of $\mathcal{R}$. Two complex atlases $\mathcal{A} = \{U_\alpha, z_\alpha\}$ and $\tilde{\mathcal{A}} = \{\tilde{U}_\beta, \tilde{z}_\beta\}$ are compatible if $\mathcal{A} \cup \tilde{\mathcal{A}}$ is a complex atlas. An equivalence class Σ of complex atlases is called a *complex structure*. It can be identified with a maximal atlas $\mathcal{A}^*$, which consists of all coordinate charts, compatible with an atlas $\mathcal{A} \subset \Sigma$.

Definition 1. *A Riemann surface is a connected one-dimensional complex analytic manifold, that is, a connected two-dimensional real manifold $\mathcal{R}$ with a complex structure Σ on it.*

When it is clear which complex structure is considered, we use the notation $\mathcal{R}$ for the Riemann surface.

If $\{U, z\}$ is a coordinate on $\mathcal{R}$ then for every open set $V \subset U$ and every function $f : \mathbb{C} \to \mathbb{C}$, which is holomorphic and bijective on $z(V)$, $\{V, f \circ z\}$ is also a local parameter on $\mathcal{R}$.

The coordinate charts establish homeomorphisms of domains in $\mathcal{R}$ with domains in $\mathbb{C}$. This means that locally the Riemann surface is just a domain in $\mathbb{C}$. But for any point $P \in \mathcal{R}$ there are many possible choices of these homeomorphisms. Therefore one can associate to $\mathcal{R}$ only the notions from the theory of analytic functions in $\mathbb{C}$ that are invariant with respect to biholomorphic maps, i.e. those that one can define without choosing a specific local parameter. For example, one can talk about the angle between two smooth curves γ and $\tilde{\gamma}$ on $\mathcal{R}$ intersecting at some point $P \in \mathcal{R}$. This angle is equal to the one between the curves $z(\gamma)$ and $z(\tilde{\gamma})$ that lie in $\mathbb{C}$ and intersect at the point $z(P)$, where z is some local parameter at P. This definition is invariant with respect to the choice of z.

If $(\mathcal{R}, \Sigma)$ is a Riemann surface, then the manifold $\mathcal{R}$ is oriented.

The simplest examples of Riemann surfaces are any domain (connected open subset) $U \subset \mathbb{C}$ in the complex plane, the whole complex plane $\mathbb{C}$, and the extended complex plane (or *Riemann sphere*) $\hat{\mathbb{C}} = \mathbb{CP}^1 = \mathbb{C} \cup \{\infty\}$. The complex structures on U and $\mathbb{C}$ are defined by single coordinate charts (U, id) and $(\mathbb{C}, id)$. The extended complex plane is the simplest compact Riemann surface. To define the complex structure on it we use two charts $(U_1, z_2), (U_2, z_2)$ with

$$U_1 = \mathbb{C} , \qquad z_1 = z ,$$
$$U_2 = (\mathbb{C}\backslash\{0\}) \cup \{\infty\} , \qquad z_2 = 1/z .$$

The transition functions

$$f_{1,2} = z_1 \circ z_2^{-1} , \quad f_{2,1} = z_2 \circ z_1^{-1} \; : \mathbb{C}\backslash\{0\} \to \mathbb{C}\backslash\{0\}$$

are holomorphic

$$f_{1,2}(z) = f_{2,1}(z) = 1/z .$$

To a large extent the beauty of the theory of Riemann surfaces is due to the fact that Riemann surfaces can be described in many completely different ways. Interrelations between these descriptions make up an essential part of the theory. The basic examples of Riemann surfaces we are going to discuss now are exactly these foundations the whole theory is based on.

1.1.1 Non-Singular Algebraic Curves

Definition 2. *An algebraic curve C is a subset in $\mathbb{C}^2$*

$$C = \{(\mu, \lambda) \in \mathbb{C}^2 \mid \mathcal{P}(\mu, \lambda) = 0\}\,, \tag{1.2}$$

where $\mathcal{P}$ is an irreducible polynomial in λ and μ

$$\mathcal{P}(\mu, \lambda) = \sum_{i=0}^{N} \sum_{j=0}^{M} p_{ij} \mu^i \lambda^j\,.$$

The curve C is called non-singular if

$$\mathrm{grad}_{\mathbb{C}} \mathcal{P}_{|\mathcal{P}=0} = \left(\frac{\partial \mathcal{P}}{\partial \mu}, \frac{\partial \mathcal{P}}{\partial \lambda}\right)_{|\mathcal{P}(\mu,\lambda)=0} \tag{1.3}$$

is nowhere zero on $\mathbb{C}$.

The complex structure on C is defined as follows: the variable λ is taken as local parameter in the neighborhoods of the points where $\partial \mathcal{P}/\partial \mu \neq 0$, and the variable μ is taken as local parameter near the points where $\partial \mathcal{P}/\partial \lambda \neq 0$. The holomorphic compatibility of the introduced local parameters results from the complex version of the implicit function theorem.

The Riemann surface C can be made a compact Riemann surface

$$\hat{C} = C \cup \{\infty^{(1)}\} \cup \ldots \cup \{\infty^N\}$$

by adjoining points $\infty^{(1)}, \ldots, \infty^{(N)}$ at infinity ($\lambda \to \infty, \mu \to \infty$), and introducing admissible local parameters at these points, see Fig. 1.1.

Definition 3. *Let $\mathcal{R}$ be a Riemann surface such that there exists an open subset*

$$U_\infty = U_\infty^{(1)} \cup \ldots \cup U_\infty^{(N)} \subset \mathcal{R}$$

such that $\mathcal{R}\backslash U_\infty$ is compact and $U_\infty^{(n)}$ are homeomorphic to punctured discs

$$z_n : U_\infty^{(n)} \to D\backslash\{0\} = \{z \in \mathbb{C} \mid 0 < |z| < 1\}\,,$$

where the homeomorphisms z_n are holomorphically compatible with the complex structure of $\mathcal{R}$. Then $\mathcal{R}$ is called a compact Riemann surface with punctures.
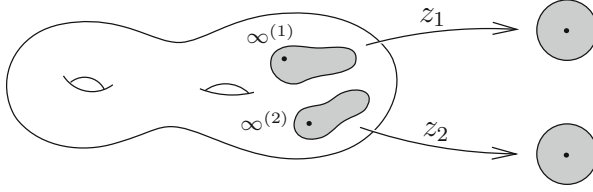
Fig. 1.1. A compact Riemann surface with punctures

Let us extend the homeomorphisms z_n

$$z_n : \hat{U}^{(n)}_\infty = U^{(n)}_\infty \cup \{\infty^{(n)}\} \to D = \{z \mid |z| < 1\} , \tag{1.4}$$

by setting $z_n(\infty^{(n)}) = 0, \quad n = 1, \ldots, N$. A complex atlas for a new Riemann surface

$$\hat{\mathcal{R}} = \mathcal{R} \cup \{\infty^{(1)}\} \cup \ldots \cup \{\infty^{(N)}\}$$

is defined as a union of a complex atlas $\mathcal{A}$ of $\mathcal{R}$ with the coordinate charts (1.4) compatible with $\mathcal{A}$ due to Definition 3. The Riemann surface $\hat{\mathcal{R}}$ is called the *compactification* of the punctured Riemann surface $\mathcal{R}$.

Hyperelliptic Curves

Let us consider the important special case of hyperelliptic curves

$$\mu^2 = \prod_{j=1}^{N} (\lambda - \lambda_j) , \quad N \geq 3 , \quad \lambda_j \in \mathbb{C} . \tag{1.5}$$

When $N = 3$ or 4 the curve (1.5) is called elliptic. The curve is non-singular if all the points λ_j are different

$$\lambda_j \neq \lambda_i , \quad i, j = 1, \ldots, N .$$

In this case the choice of local parameters can be additionally specified. Namely, in the neighborhood of the points (μ_0, λ_0) with $\lambda_0 \neq \lambda_j \quad \forall j$, the local parameter is the homeomorphism

$$(\mu, \lambda) \to \lambda . \tag{1.6}$$

In the neighborhood of each point $(0, \lambda_j)$ it is defined by the homeomorphism

$$(\mu, \lambda) \to \sqrt{\lambda - \lambda_j} . \tag{1.7}$$

For odd $N = 2g + 1$, the curve (1.5) has one puncture ∞

$$P \to \infty \Longleftrightarrow \lambda \to \infty \,,$$

and a local parameter in its neighborhood is given by the homeomorphism

$$z_\infty : (\mu, \lambda) \to \frac{1}{\sqrt{\lambda}} \,. \tag{1.8}$$

For even $N = 2g + 2$ there are two punctures $\infty^\pm$ distinguished by the condition

$$P \to \infty^\pm \Longleftrightarrow \frac{\mu}{\lambda^{g+1}} \to \pm 1 \,, \qquad \lambda \to \infty \,,$$

and the local parameters in the neighborhood of both points are given by the homeomorphism

$$z_{\infty^\pm} : (\mu, \lambda) \to \lambda^{-1} \,. \tag{1.9}$$

Theorem 1. *The local parameters (1.6, 1.7, 1.8, 1.9) describe a compact Riemann surface*

$$\hat{C} = C \cup \{\infty\} \qquad if \ N \ is \ odd \,,$$
$$\hat{C} = C \cup \{\infty^\pm\} \qquad if \ N \ is \ even \,,$$

of the hyperelliptic curve (1.5).

One prefers to consider compact Riemann surfaces and thus the compactification $\hat{C}$ is called *the Riemann surface of the curve C.*

It turns out that all compact Riemann surfaces can be described as compactifications of algebraic curves (see for example [Jos06]).

1.1.2 Quotients Under Group Actions

Definition 4. *Let Δ be a domain in $\mathbb{C}$. A group $G : \Delta \to \Delta$ of holomorphic transformations acts discontinuously on Δ if for any $P \in \Delta$ there exists a neighborhood $V \ni P$ such that*

$$gV \cap V = \emptyset \,, \qquad \forall g \in G \,, \qquad g \neq I \,. \tag{1.10}$$

The quotient space Δ/G is defined by the equivalence relation

$$P \sim P' \Leftrightarrow \exists g \in G : P' = gP \,.$$

By the natural projection $\pi : \Delta \to \Delta/G$ every point is mapped to its equivalence class. Every point $P \in \Delta$ has a neighborhood V satisfying (1.10). Then $U = \pi(V)$ is open and $\pi_{|_V} : V \to U$ is a homeomorphism. Its inversion $z : U \to V \subset \Delta \subset \mathbb{C}$ is a local parameter. One can cover Δ/G by domains of this type. The transition functions are the corresponding group elements g; therefore they are holomorphic.

Theorem 2. *Δ/G is a Riemann surface.*

Tori

Let us consider the case $\Delta = \mathbb{C}$ and the group G generated by two translations

$$z \to z + w , \qquad z \to z + w' ,$$

where $w, w' \in \mathbb{C}$ are two non-parallel vectors, Im $w'/w \neq 0$, see Fig. 1.2. The group G is commutative and consists of the elements

$$g_{n,m}(z) = z + nw + mw' , \qquad n, m \in \mathbb{Z} . \tag{1.11}$$

The factor $\mathbb{C}/G$ has a nice geometrical realization as the parallelogram

$$T = \{z \in \mathbb{C} \mid z = aw + bw', \ a, b \in [0, 1)\} .$$

There are no G-equivalent points in T and on the other hand every point in $\mathbb{C}$ is equivalent to some point in T. Since the edges of the parallelogram T are G-equivalent $z \sim z + w, \ z \sim z + w'$, $\mathcal{R}$ is a compact Riemann surface, which is topologically a torus. We discuss this case in more detail in Sect. 1.5.5.
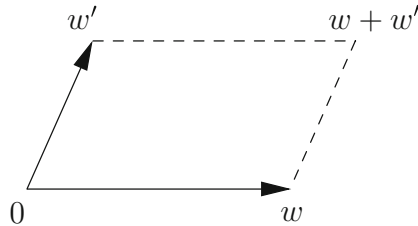
Fig. 1.2. A complex torus

The uniformization theorem (see for example [Jos06]) claims that all compact Riemann surfaces can be obtained as quotients Δ/G.

1.1.3 Polyhedral Surfaces as Riemann Surfaces

One can build a Riemann surface gluing together pieces of the complex plane $\mathbb{C}$.

Consider a finite set of disjoint polygons F_i and identify isometrically pairs of edges in such a way that the result is a compact oriented polyhedral surface $\mathcal{P}$. A polyhedron in 3-dimensional Euclidean space is an example of such a surface.

Theorem 3. *The polyhedral surface $\mathcal{P}$ is a Riemann surface.*
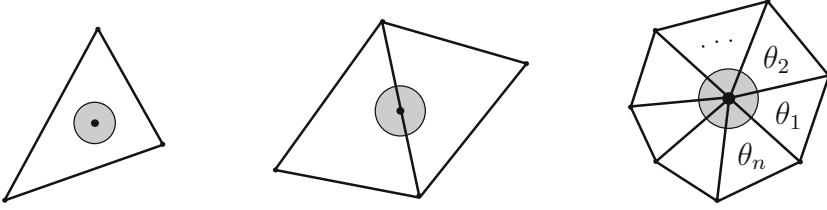
Fig. 1.3. Three kinds of points on a polyhedral surface

In order to define a complex structure on a polyhedral surface let us distinguish three kinds of points (see Fig. 1.3):

1. Inner points of triangles
2. Inner points of edges
3. Vertices

One can map isometrically the corresponding polygon F_i (or pairs of neighboring polygons) into $\mathbb{C}$. This provides local parameters at the points of the first and the second kind. Let P be a vertex and $F_i, \ldots, F_n$ the sequence of successive polygons with this vertex (see the point (iii) above). Denote by θ_i the angle of F_i at P. Then define

$$\gamma = \frac{2\pi}{\sum_{i=1}^n \theta_i} \; .$$

Consider a suitably small ball neighborhood of P, which is the union $U^r = \cup_i F_i^r$, where $F_i^r = \{Q \in F_i \mid \mid Q - P \mid < r\}$. Each F_i^r is a sector with angle θ_i at P. We map it as above into $\mathbb{C}$ with P mapped to the origin and then apply $z \mapsto z^\gamma$, which produces a sector with the angle $\gamma \theta_i$. The mappings corresponding to different polygons F_i can be adjusted to provide a homeomorphism of U^r onto a disc in $\mathbb{C}$. All transition functions of the constructed charts are holomorphic since they are compositions of maps of the form $z \mapsto az + b$ and $z \mapsto z^\gamma$ (away from the origin).

It turns out that any compact Riemann surface can be recovered from some polyhedral surface [Bos].

1.1.4 Complex Structure Generated by the Metric

There is a smooth version of the previous construction. Let $(\mathcal{R}, g)$ be a two-real dimensional orientable differential manifold with Riemannian metric g.

Definition 5. *Two metrics g and $\tilde{g}$ are called conformally equivalent if they differ by a function on $\mathcal{R}$*

$$g \sim \tilde{g} \Leftrightarrow g = f\tilde{g} \,, \qquad f : \mathcal{R} \to \mathbb{R}_+ \,. \tag{1.12}$$

The transformation (1.12) preserves angles. This relation defines classes of conformally equivalent metrics.

Let $(x, y) : U \subset \mathcal{R} \to \mathbb{R}^2$ be a local coordinate. In terms of the complex variable $z = x + iy$ the metric can be written as

$$g = A\mathrm{d}z^2 + 2B\mathrm{d}z\mathrm{d}\bar{z} + \bar{A}\mathrm{d}\bar{z}^2, \qquad A \in \mathbb{C}, B \in \mathbb{R}, B > |A| . \qquad (1.13)$$

Note that the complex coordinate z is *not* compatible with the complex structure we will define on $\mathcal{R}$ with the help of g.

Definition 6. *A coordinate $w : U \to \mathbb{C}$ is called conformal if the metric in this coordinate is of the form*

$$g = \mathrm{e}^{\phi}\mathrm{d}w, \mathrm{d}\bar{w} , \qquad (1.14)$$

i.e., it is conformally equivalent to the standard metric $\mathrm{d}w\mathrm{d}\bar{w}$ of $\mathbb{R}^2 = \mathbb{C}$.

If $F : U \subset \mathbb{R}^2 \to \mathbb{R}^3$ is an immersed surface in $\mathbb{R}^3$ then the first fundamental form $< dF, dF >$ induces a metric on U. When the standard coordinate (x, y) of $\mathbb{R}^2 \supset U$ is conformal, the parameter lines

$$F(x, \Delta m) , \qquad F(\Delta n, y) , \qquad x, y \in \mathbb{R} , \qquad n, m \in \mathbb{Z} , \qquad \Delta \to 0$$

comprise an infinitesimal square net on the surface.

It is easy to show that every compact Riemann surface admits a conformal Riemannian metric. Indeed, each point $P \in \mathcal{R}$ possesses a local parameter $z_P : U_P \to D_P \subset \mathbb{C}$, where D_P is a small open disc. Since $\mathcal{R}$ is compact there exists a finite covering $\cup_{i=1}^{n} U_{P_i} = \mathcal{R}$. For each i choose a smooth function $m_i : D_{P_i} \to \mathbb{R}$ with

$$m_i > 0 \quad \text{on } D_i , \qquad m_i = 0 \quad \text{on } \mathbb{C} \setminus D_i .$$

$m_i(z_{P_i})\mathrm{d}z_{P_i}\mathrm{d}\bar{z}_{P_i}$ is a conformal metric on U_{P_i}. The sum of these metrics over $i = 1, \ldots, n$ yields a conformal metric on $\mathcal{R}$.

Moreover, any metric can be brought to conformal form (1.14) due to the following fundamental theorem.

Theorem 4. *Conformal equivalence classes of metrics on an orientable two-manifold $\mathcal{R}$ are in one to one correspondence with the complex structures on $\mathcal{R}$.*

Let us show how one finds conformal coordinates. The metric (1.13) can be written as follows (we suppose $A \neq 0$)

$$g = s(\mathrm{d}z + \mu\mathrm{d}\bar{z})(\mathrm{d}\bar{z} + \bar{\mu}\mathrm{d}z) , \qquad s > 0 , \qquad (1.15)$$

where

$$\mu = \frac{\bar{A}}{2B}(1 + |\mu|^2) , \qquad s = \frac{2B}{1 + |\mu|^2} .$$

Here $|\mu|$ is a solution of the quadratic equation

$$|\mu| + \frac{1}{|\mu|} = \frac{2B}{|A|} \, ,$$

which can be chosen $|\mu| < 1$. Comparing (1.15) and (1.14) we get

$$\mathrm{d}w = \lambda(\mathrm{d}z + \mu\mathrm{d}\bar{z})$$

or

$$\mathrm{d}w = \lambda(\mathrm{d}\bar{z} + \bar{\mu}\mathrm{d}z).$$

In the first case the map $w(z, \bar{z})$ satisfies the equation

$$w_{\bar{z}} = \mu w_z \tag{1.16}$$

and preserves the orientation $w : \mathbb{C} \supset U \to V \subset \mathbb{C}$ since $|\mu| < 1$. In the second case $w : U \to V$ inverses the orientation.

Equation (1.16) is called the *Beltrami equation* and $\mu(z, \bar{z})$ is called the *Beltrami coefficient*.

By analytic methods (see for example [Spi79]) one can prove that for any Beltrami coefficient μ there exists a local solution to the Beltrami equation in the corresponding functional class. This allows us to introduce local conformal coordinates.

Proposition 1. *Let $\mathcal{R}$ be a two-dimensional orientable manifold with a metric g and a positively oriented atlas $((x_\alpha, y_\alpha) : U_\alpha \to \mathbb{R}^2)_{\alpha \in A}$ on $\mathcal{R}$. Let $(x, y) : U \subset \mathcal{R} \to \mathbb{R}^2$ be one of these coordinate charts around a point $P \in U$, let $z = x + \mathrm{i}y$ and $\mu(z, \bar{z})$ be the Beltrami coefficient and let $w_\beta(z, \bar{z})$ be a solution to the Beltrami equation (1.16) in a neighborhood $V_\beta \subset V = z(U)$ with $P \in U_\beta = z^{-1}(V_\beta)$. Then the coordinate w_β is conformal and the atlas $(w_\beta : U_\beta \to \mathbb{C})_{\beta \in B}$ defines a complex structure on $\mathcal{R}$.*

Only the holomorphicity of the transition function may require a comment. Let $w : U \to \mathbb{C}, \tilde{w} : \tilde{U} \to \mathbb{C}$ be two local parameters with a non-empty intersection $U \cap \tilde{U} \neq \emptyset$. Both coordinates are conformal

$$g = \mathrm{e}^\phi \mathrm{d}w \, \mathrm{d}\bar{w} = \mathrm{e}^{\tilde{\phi}} \mathrm{d}\tilde{w} \, \mathrm{d}\bar{\tilde{w}},$$

which happens in one of the two cases

$$\frac{\partial \tilde{w}}{\partial \bar{w}} = 0 \;\; \text{or} \;\; \frac{\partial \tilde{w}}{\partial w} = 0 \tag{1.17}$$

only. The transition function $\tilde{w}(w)$ is holomorphic and not antiholomorphic since the map $w \to \tilde{w}$ preserves orientation.

Repeating these arguments one observes that conformally equivalent metrics generate the same complex structure, and Theorem 4 follows.

1.2 Holomorphic Mappings

Definition 7. *A mapping*
$$f : M \to N$$

between Riemann surfaces is called holomorphic if for every local parameter (U, z) *on* M *and every local parameter* (V, w) *on* N *with* $U \cap f^{-1}(V) \neq \emptyset$, *the mapping*
$$w \circ f \circ z^{-1} : z(U \cap f^{-1}(V)) \to w(V)$$

is holomorphic.

A holomorphic mapping to $\mathbb{C}$ is called a *holomorphic function*, a holomorphic mapping to $\hat{\mathbb{C}}$ is called a *meromorphic function*.

The following lemma characterizes the local behavior of holomorphic mappings.

Lemma 1. *Let* $f : M \to N$ *be a holomorphic mapping. Then for any* $a \in M$ *there exist* $k \in \mathbb{N}$ *and local parameters* $(U, z), (V, w)$ *such that* $a \in U, f(a) \in V$ *and* $F = w \circ f \circ z^{-1} : z(U) \to w(V)$ *equals*

$$F(z) = z^k. \tag{1.18}$$

Corollary 1. *Let* $f : M \to N$ *be a non-constant holomorphic mapping, then* f *is open, i.e., the image of an open set is open.*

If M is compact then $f(M)$ is compact as a continuous image of a compact set and open due to the previous claim. This implies that in this case the corresponding non-constant holomorphic mapping is surjective and its image $N = f(M)$ compact.

We see that there exist no non-constant holomorphic mappings $f : M \to \mathbb{C}$, which is the issue of the classical Liouville theorem.

Theorem 5. *On a compact Riemann surface there exists no non-constant holomorphic function.*

Non-constant holomorphic mappings of Riemann surfaces $f : M \to N$ are *discrete*: for any point $P \in N$ the set $S_P = f^{-1}(P)$ is discrete, i.e. for any point $a \in M$ there is a neighborhood $V \subset M$ intersecting with S_P in at most one point, $|V \cap S_P| \leq 1$. Non-discreteness of S for a holomorphic mapping would imply the existence of a limiting point in S_P and finally $f = $ const, $f : M \to P \in N$. Non-constant holomorphic mappings of Riemann surfaces are also called *holomorphic coverings*.

Definition 8. *Let* $f : M \to N$ *be a holomorphic covering. A point* $P \in M$ *is called a* branch point *of* f *if it has no neighborhood* $V \ni P$ *such that* $f|_V$ *is injective. A covering without branch points is called* unramified *(ramified or branched covering in the opposite case).*

Note that various definitions of a covering are used in the literature (see for example [Jos06, Bea78]). In particular, often the term "covering" is used for unramified coverings of our definition. Ramified coverings are important in the theory of Riemann surfaces.

The number $k \in \mathbb{N}$ in Lemma 1 can be described in topological terms. There exist neighborhoods $U \ni a, V \ni f(a)$ such that for any $Q \in V \setminus \{f(a)\}$ the set $f^{-1}(Q) \cap U$ consists of k points. One says that f has the *multiplicity* k at a. Lemma 1 allows us to characterize the branch points of a holomorphic covering $f : M \to N$ as the points with the multiplicity $k > 1$. Equivalently, P is a branch point of the covering $f : M \to N$ if

$$\left. \frac{\partial(w \circ f \circ z^{-1})}{\partial z} \right|_{z(P)} = 0 \; , \tag{1.19}$$

where z and w are local parameters at P and $f(P)$ respectively. Due to the chain rule this condition is independent of the choice of the local parameters. The number $b_f(P) = k - 1$ is called the *branch number* of f at $P \in M$. The next lemma follows immediately from Lemma 1.

Lemma 2. *Let $f : M \to N$ be a holomorphic covering. Then the set of branch points*

$$B = \{P \in M \mid b_f(P) > 0\}$$

is discrete. If M is compact, then B is finite.

The projection $A = f(B)$ of the set of branch points is also finite. The number m of preimages for any point in $N \setminus A$ is the same since any two points $Q_1, Q_2 \in N \setminus A$ can be connected by a curve $l \subset N \setminus A$. Combined with the topological characterization of the branch numbers this fact implies the following theorem.

Theorem 6. *Let $f : M \to N$ be a non-constant holomorphic mapping between two compact Riemann surfaces. Then there is a number $m \in \mathbb{N}$ such that f takes every value $Q \in N$ precisely m times, counting multiplicities. That is, for all $Q \in N$*
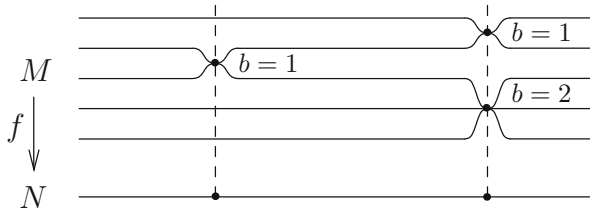
$$\sum_{P \in f^{-1}(Q)} (b_f(P) + 1) = m \; . \tag{1.20}$$

Fig. 1.4. Covering

Definition 9. *The number m above is called the* degree *of f, and the covering f : M → N is called m-sheeted.*

Applying Theorem 6 to holomorphic mappings $f : \mathcal{R} \to \hat{\mathbb{C}}$ we get

Corollary 2. *A non-constant meromorphic function on a compact Riemann surface assumes every value m times, where m is the number of its poles (counting multiplicities).*

1.2.1 Algebraic Curves as Coverings

Let C be a non-singular algebraic curve (1.2) and $\hat{C}$ its compactification. The map

$$(\mu, \lambda) \to \lambda \tag{1.21}$$

is a holomorphic covering $\hat{C} \to \hat{\mathbb{C}}$. If N is the degree of the polynomial $\mathcal{P}(\mu, \lambda)$ in μ

$$\mathcal{P}(\mu, \lambda) = \mu^N p_N(\lambda) + \mu^{N-1} p_{N-1}(\lambda) + \ldots + p_0(\lambda) \,,$$

where all $p_i(\lambda)$ are polynomials, then $\lambda : \hat{C} \to \hat{\mathbb{C}}$ is an N-sheeted covering, see Fig. 1.4.

The points with $\partial \mathcal{P}/\partial \mu = 0$ are the branch points of the covering $\lambda : C \to \mathbb{C}$. At these points $\partial \mathcal{P}/\partial \lambda \neq 0$, and μ is a local parameter. The derivative of λ with respect to the local parameter vanishes

$$\frac{\partial \lambda}{\partial \mu} = -\frac{\partial \mathcal{P}/\partial \mu}{\partial \mathcal{P}/\partial \lambda} = 0 \,,$$

which characterizes (1.19) the branch points of the covering (1.21). In the same way the map $(\mu, \lambda) \mapsto \mu$ is a holomorphic covering of the μ-plane. The branch points of this covering are the points with $\partial \mathcal{P}/\partial \lambda = 0$.

Hyperelliptic Curves

Before we consider the hyperelliptic case let us recall a conventional description of the Riemann surface of the function $\mu = \sqrt{\lambda}$. One takes two copies of the complex plane $\mathbb{C}$ with cuts $[0, \infty]$ and glues them together crosswise along this cut (see Fig. 1.5). The image in Fig. 1.5 visualizes the points of the curve

$$C = \{(\mu, \lambda) \in \mathbb{C}^2 \mid \mu^2 = \lambda\} \,,$$

and the point $\lambda = 0$ gives an idea of a branch point.

The compactification $\hat{C}$ of the hyperelliptic curve

$$C = \{(\mu, \lambda) \in \mathbb{C}^2 \mid \mu^2 = \prod_{i=1}^{N}(\lambda - \lambda_i)\} \tag{1.22}$$
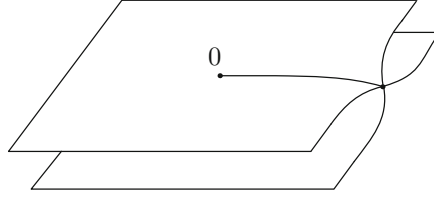
Fig. 1.5. Riemann surface of $\sqrt{\lambda}$

is a two sheeted covering of the extended complex plane $\lambda : \hat{C} \to \hat{\mathbb{C}}$. The branch points of this covering are

$$(0, \lambda_i), \ i = 1, \ldots, N \text{ and } \infty \text{ for } N = 2g + 1 \, ,$$
$$(0, \lambda_i), \ i = 1, \ldots, N \qquad \text{for } N = 2g + 2 \, ,$$

with the branch numbers $b_\lambda = 1$ at these points. Only the branching at $\lambda = \infty$ possibly needs some clarification. The local parameter at $\infty \in \hat{\mathbb{C}}$ is $1/\lambda$, whereas the local parameter at the point $\infty \in \hat{C}$ of the curve $\hat{C}$ with $N = 2g + 1$ is $1/\sqrt{\lambda}$ due to (1.8). In these coordinates the covering mapping reads as (compare with (1.18))

$$\frac{1}{\lambda} = \left(\frac{1}{\sqrt{\lambda}} \right)^2 ,$$

which shows that $b_\lambda(\infty) = 1$.

One can imagine the Riemann surface $\hat{C}$ with $N = 2g + 2$ as two Riemann spheres with the cuts

$$[\lambda_1, \lambda_2], [\lambda_3, \lambda_4], \ldots, [\lambda_{2g+1}, \lambda_{2g+2}]$$

glued together crosswise along the cuts. Figure 1.6 presents a topological image of this Riemann surface. The image in Fig. 1.7 shows the Riemann surface "from above" or "the first" sheet on the covering $\lambda : C \to \mathbb{C}$.

Hyperelliptic curves possess a holomorphic involution

$$h : (\mu, \lambda) \to (-\mu, \lambda) \, , \tag{1.23}$$
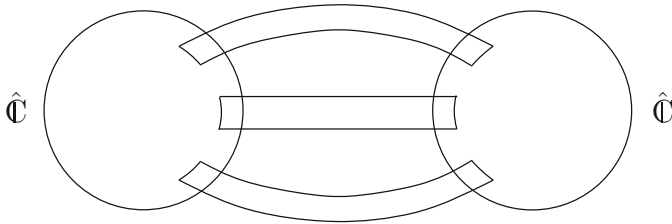
Fig. 1.6. Topological image of a hyperelliptic surface
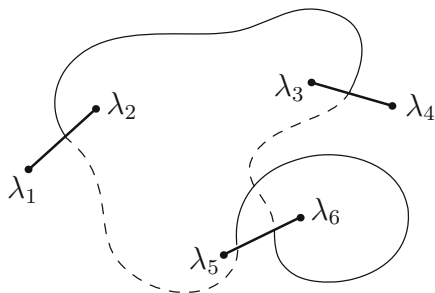
Fig. 1.7. Hyperelliptic surface C as a two-sheeted cover. The parts of the curves on C that lie on the second sheet are indicated by *dotted lines*

which interchanges the sheets of the covering $\lambda : \hat{C} \to \hat{\mathbb{C}}$. It is called the *hyperelliptic involution*. The branch points of the covering are the fixed points of h.

The cuts in Fig. 1.7 are conventional and belong to the image shown in Fig. 1.7 and not to the hyperelliptic Riemann surface itself, which is determined by its branch points alone. In particular, the two images shown in Fig. 1.8 correspond to the same Riemann surface and to the same covering $(\mu, \lambda) \to \lambda$.
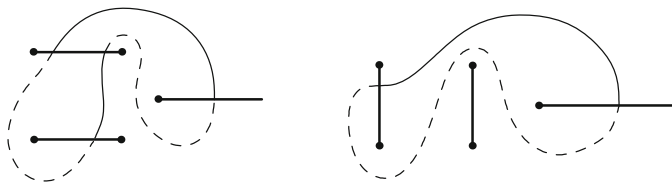
Fig. 1.8. Two equivalent images of the same hyperelliptic Riemann surface

1.2.2 Symmetric Riemann Surfaces as Coverings

The construction of Sect. 1.1.2 can be also applied to Riemann surfaces.

Theorem 7. *Let $\mathcal{R}$ be a (compact) Riemann surface and let G be a finite group of holomorphic automorphisms[1] of order $|G|$. Then $\mathcal{R}/G$ is a Riemann surface with the complex structure determined by the condition that the canonical projection*

$$\pi : \mathcal{R} \to \mathcal{R}/G$$

is holomorphic. This is an $|G|$-sheeted covering, ramified at the fixed points of G.

---

[1] This group is always finite if the genus ≥ 2.

The canonical projection π defines an $|G|$-sheeted covering. Denote by

$$G_{P_0} = \{g \in G \mid gP_0 = P_0\}$$

the *stabilizer* of P_0. It is always possible to choose a neighborhood U of P_0, which is invariant with respect to all elements of G_{P_0} and such that $U \cap gU = \emptyset$ for all $g \in G \setminus G_{P_0}$. Let us normalize the local parameter z on U by $z(P_0) = 0$. The local parameter w in $\pi(U)$, which is $|G_{P_0}|$-sheetedly covered by U is defined as the product of the values of the local parameter z at all equivalent points lying in U. In terms of the local parameter z all the elements of the stabilizer are represented by the functions $\tilde{g} = z \circ g \circ z^{-1}$: $z(U) \to z(U)$, which vanish at $z = 0$. Since $\tilde{g}(z)$ are also invertible they can be represented as $\tilde{g}(z) = zh_g(z)$ with $h_g(0) \neq 0$. Finally the $w - z$ coordinate charts representation of π

$$w \circ \pi \circ z^{-1} : z \to z^{|G_{P_0}|} \prod_{g \in G_{P_0}} h_g(z)$$

shows that the branch number of P_0 is $|G_{P_0}|$.

The compact Riemann surface $\hat{C}$ of the hyperelliptic curve

$$\mu^2 = \prod_{n=1}^{2N} (\lambda^2 - \lambda_n^2) , \qquad \lambda_i^2 \neq \lambda_j^2, \ \lambda_k \neq 0 \tag{1.24}$$

has the following group of holomorphic automorphisms

$$h : (\mu, \lambda) \to (-\mu, \lambda)$$
$$i_1 : (\mu, \lambda) \to (\mu, -\lambda)$$
$$i_2 = hi_1 : (\mu, \lambda) \to (-\mu, -\lambda) .$$

The hyperelliptic involution h interchanges the sheets of the covering $\lambda :$ $\hat{C} \to \hat{\mathbb{C}}$, therefore the factor $\hat{C}/h$ is the Riemann sphere. The covering

$$\hat{C} \to \hat{C}/h = \hat{\mathbb{C}}$$

is ramified at all the points $\lambda = \pm\lambda_n$.

The involution i_1 has four fixed points on $\hat{C}$: two points with $\lambda = 0$ and two points with $\lambda = \infty$. The covering

$$\hat{C} \to \hat{C}_1 = \hat{C}/i_1 \tag{1.25}$$

is ramified at these points. The mapping (1.25) is given by

$$(\mu, \lambda) \to (\mu, \Lambda) , \qquad \Lambda = \lambda^2 ,$$

and $\hat{C}_1$ is the Riemann surface of the curve

$$\mu^2 = \prod_{n=1}^{2N} (\Lambda - \lambda_n^2) .$$

The involution i_2 has no fixed points. The covering

$$\hat{C} \to \hat{C}_2 = \hat{C}/i_2 \qquad\qquad (1.26)$$

is unramified. The mapping (1.26) is given by

$$(\mu, \lambda) \to (M, \Lambda) , \qquad M = \mu\lambda, \ \Lambda = \lambda^2 ,$$

and $\hat{C}_2$ is the Riemann surface of the curve

$$M^2 = \Lambda \prod_{n=1}^{2N} (\Lambda - \lambda_n^2) .$$

1.3 Topology of Riemann Surfaces

1.3.1 Spheres with Handles

We have seen in Sect. 1.1 that any Riemann surface is a two-dimensional orientable real manifold. In this section we present basic facts about the topology of these manifolds focusing on the compact case. We start with an intuitive fundamental classification theorem.

Theorem 8. (and Definition) *Every compact Riemann surface is homeomorphic to a sphere with handles (i.e., a topological manifold homeomorphic to a sphere with handles in Euclidean 3-space). The number $g \in \mathbb{N}$ of handles is called the* genus *of $\mathcal{R}$. Two manifolds with different genera are not homeomorphic.*
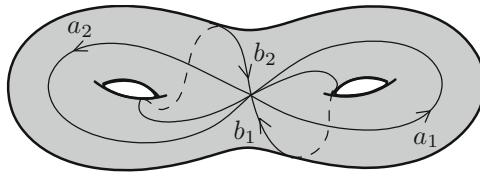
Fig. 1.9. A sphere with 2 handles

The genus of the compactification $\hat{C}$ of the hyperelliptic curve (1.22) with $N = 2g + 1$ or $N = 2g + 2$ is equal to g.

For many purposes it is convenient to use planar images of spheres with handles.

Proposition 2. *Let Π_g be a sphere $S^2 \cong \mathbb{R}^2 \cup \{\infty\}$ with 2g holes bounded by the non-intersecting curves*

$$\gamma_1, \gamma_1', \ldots, \gamma_g, \gamma_g' \, . \tag{1.27}$$

and identify the curves $\gamma_i \approx \gamma_i'$, $i = 1, \ldots, g$ in such a way that the orientations of these curves with respect to Π_g are opposite (see Fig. 1.10). Then Π_g is homeomorphic to a sphere with g handles.
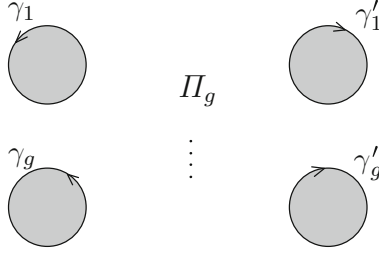
Fig. 1.10. A planar image of a sphere with g handles

To check this claim one should cut up all the handles of a sphere with g handles.

A normalized simply-connected image of a sphere with g handles is described in the following proposition.

Proposition 3. *Let F_g be a 4g-gon with the edges*

$$a_1, b_1, a_1', b_1', \ldots, a_g, b_g, a_g', b_g' \, , \tag{1.28}$$

listed in the order of traversing the boundary of F_g and the boundary curves

$$a_i \approx a_i', b_i \approx b_i', \ i = 1, \ldots, g$$

are identified in such a way that the orientations of the edges a_i and a_i' as well as b_i and b_i' with respect to F_g are opposite (see Fig. 1.11). Then F_g is homeomorphic to a sphere with g handles. The sphere without handles ($g = 0$) is homeomorphic to a 2-gon with the edges identified.

This claim is visualized in Figs. 1.12 and 1.13. One choice of closed curves $a_1, b_1, \ldots, a_g, b_g$ on a sphere with handles is shown in Fig. 1.9.

Let us consider *a triangulation* $\mathcal{T}$ of $\mathcal{R}$, i.e., a set $\{T_i\}$ of topological triangles, which are glued along their edges (the identification of vertices or edges of individual triangles is not excluded), and which comprise $\mathcal{R}$. More generally, one can consider cell decompositions of $\mathcal{R}$ into topological polygons $\{T_i\}$. Obviously, compact Riemann surfaces possess finite triangulations.
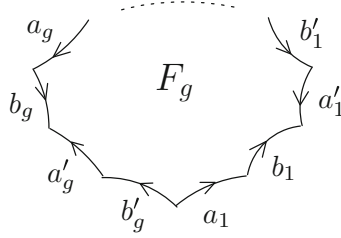
Fig. 1.11. Simply-connected image of a sphere with g handles
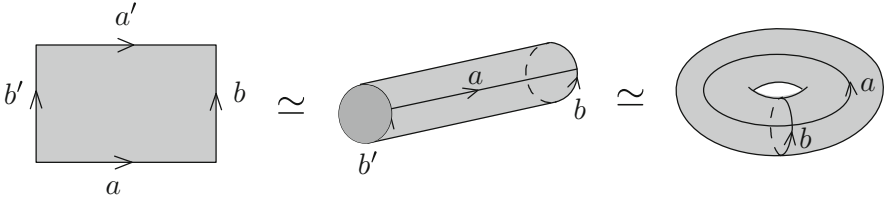
Fig. 1.12. Gluing a torus
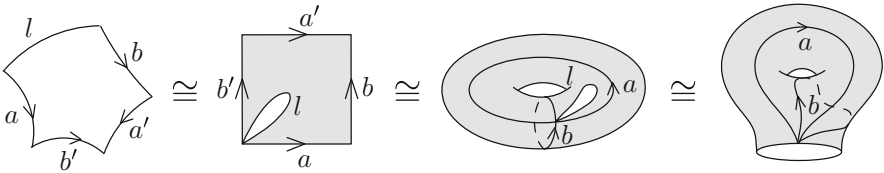
Fig. 1.13. Gluing a handle

Definition 10. *Let $\mathcal{T}$ be a triangulation of a compact two-real dimensional manifold $\mathcal{R}$ and F be the number of triangles, E the number of edges, V the number of vertices of $\mathcal{T}$. The number*

$$\chi = F - E + V \tag{1.29}$$

is called the Euler characteristic *of $\mathcal{R}$.*

Proposition 4. *The Euler characteristic $\chi(\mathcal{R})$ of a compact Riemann surface $\mathcal{R}$ is independent of the triangulation of $\mathcal{R}$.*

A differential geometric proof of this fact is based on the Gauss–Bonnet theorem (see for example [Spi79]). Introduce a conformal metric $\mathrm{e}^u\, \mathrm{d}z\, \mathrm{d}\bar{z}$ on a Riemann surface (see Sect. 1.1.4). The Gauss–Bonnet theorem provides us with the following formula for the Euler characteristic

$$\chi(\mathcal{R}) = \frac{1}{2\pi} \int_{\mathcal{R}} K \,, \tag{1.30}$$

where

$$K = -2u_{z\bar{z}}\mathrm{e}^{-u}$$

is the curvature of the metric. The right hand side in (1.30) is independent of the triangulation, the left hand side is independent of the metric we introduced on $\mathcal{R}$. This proves that the Euler characteristic is a topological invariant of $\mathcal{R}$.

A triangulation of the simply-connected model F_g of Proposition 3 gives a formula for χ in terms of the genus.

Corollary 3. *The Euler characteristic $\chi(\mathcal{R})$ of a compact Riemann surface $\mathcal{R}$ of genus g is equal to*

$$\chi(\mathcal{R}) = 2 - 2g \ . \tag{1.31}$$

Theorem 9 (Riemann–Hurwitz). *Let $f : \hat{\mathcal{R}} \to \mathcal{R}$ be an N-sheeted covering of the compact Riemann surface $\mathcal{R}$ of genus g. Then the genus $\hat{g}$ of $\hat{\mathcal{R}}$ is equal to*

$$\hat{g} = N(g - 1) + 1 + \frac{b}{2} \ , \tag{1.32}$$

where

$$b = \sum_{P \in \hat{\mathcal{R}}} b_f(P) \tag{1.33}$$

is the total branching number.

This formula is equivalent to the corresponding identity for the Euler characteristic

$$\chi(\hat{\mathcal{R}}) = N\chi(\mathcal{R}) - b \ .$$

The latter follows easily if one chooses a triangulation of $\mathcal{R}$ so that the set of its vertices contains the projection to $\mathcal{R}$ of all branch points of the covering.

1.3.2 Fundamental Group

Let γ be a closed curve with initial and terminal point P, i.e., a continuous map $\gamma : [0, 1] \to \mathcal{R}$ with $\gamma(0) = \gamma(1) = P$.

Definition 11. *Two closed curves γ^1, γ^2 on $\mathcal{R}$ with the initial and terminal point P are called homotopic if one can be continuously deformed to the another, i.e., if there exists a continuous map $\gamma : [0, 1] \times [0, 1] \to \mathcal{R}$ such that $\gamma(t, 0) = \gamma^1(t)$, $\gamma(t, 1) = \gamma^2(t)$, $\gamma(0, \lambda) = \gamma(1, \lambda) = P$. The set of homotopic curves forms a homotopy class, which we denote by $\Gamma = [\gamma]$.*

There is a natural composition of such curves:

$$\gamma_1 \cdot \gamma_2(t) = \begin{cases} \gamma_1(2t) & 0 \le t \le \frac{1}{2} \\ \gamma_2(2t - 1) & \frac{1}{2} \le t \le 1 \ , \end{cases}$$

which is well-defined also for the corresponding homotopic classes

$$\Gamma_1 \cdot \Gamma_2 = [\gamma_1 \cdot \gamma_2] \ .$$

The set of homotopy classes of curves forms a group $\pi_1(\mathcal{R}, P)$ with the multiplication defined above. The curves that can be contracted to a point correspond to the identity element of the group. It is easy to see that the groups $\pi_1(\mathcal{R}, P)$ and $\pi_1(\mathcal{R}, Q)$ based at different points are isomorphic as groups, and one can omit the second argument in the notation. The elements of this group are freely homotopic closed curves (i.e. cycles without reference to the base point P).

Definition 12. *The group* $\pi_1(\mathcal{R})$ *is called the* fundamental group *of* $\mathcal{R}$*.*

Examples
1. Sphere with N holes
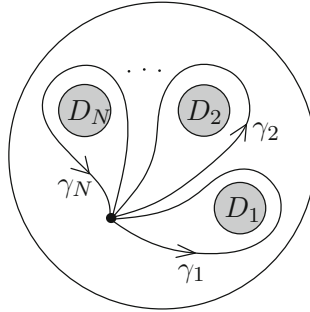
Fig. 1.14. Fundamental group of a sphere with N holes

The fundamental group is generated by the homotopy classes of the closed curves $\gamma_1, \ldots, \gamma_N$ each going around one of the holes (Fig. 1.14). The curve $\gamma_1 \gamma_2 \ldots \gamma_N$ can be contracted to a point, which implies the relation

$$\Gamma_1 \Gamma_2 \ldots \Gamma_N = 1 \tag{1.34}$$

in $\pi_1(S^2 \setminus \{\bigcup_{n=1}^{N} D_n\})$.

2. Compact Riemann surface of genus g
It is convenient to consider the $4g$-gon model F_g (Fig. 1.15). The curves $a_1, b_1, \ldots, a_g, b_g$ are closed on $\mathcal{R}$. Their homotopy classes, which we denote by $A_1, B_1, \ldots, A_g, B_g$ generate $\pi_1(\mathcal{R})$. The contractible boundary of F_g implies the only relation in the fundamental group:

$$A_1 B_1 A_1^{-1} B_1^{-1} \ldots A_g B_g A_g^{-1} B_g^{-1} = 1 \ . \tag{1.35}$$
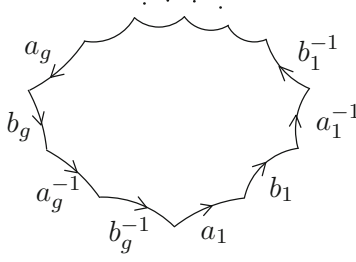
Fig. 1.15. Fundamental group of a compact surface of genus g

1.3.3 First Homology Group

Formal sums of points $\sum n_i P_i$, oriented curves γ_i,

$$\gamma = \sum n_i \gamma_i \in C_1$$

and oriented domains D_i,

$$D = \sum n_i D_i \in C_2$$

with integer coefficients $n_i \in \mathbb{Z}$ form abelian groups C_0, C_1 and C_2 respectively. The elements of these groups are called *0-chains*, *1-chains* and *2-chains*, respectively.

The boundary operator ∂ maps the corresponding elements to their oriented boundaries, defining the group homomorphisms $\partial : C_1 \to C_0, \partial : C_2 \to C_1$.

C_1 contains two important subgroups, of cycles and of boundaries. A closed oriented curve γ is called a *cycle* (i.e. $\partial \gamma = 0$), and $\gamma = \partial D$ is called a *boundary*. We denote these subgroups by

$$Z = \{\gamma \in C_1 \mid \; \partial \gamma = 0\} \,, \qquad B = \partial C_2 \,.$$

Because $\partial^2 = 0$, every boundary is a cycle and we have $B \subset Z \subset C_1$. Two elements of C_1 are called *homologous* if their difference is a boundary:

$$\gamma_1 \sim \gamma_2, \; \gamma_1, \gamma_2 \in C_1 \Leftrightarrow \gamma_1 - \gamma_2 \in B, \text{ i.e. } \exists D \in C_2 : \delta D = \gamma_1 - \gamma_2 \,.$$

Definition 13. *The factor group*

$$H_1(\mathcal{R}, \mathbb{Z}) = Z/B$$

is called the first homology *group of $\mathcal{R}$.*

Freely homotopic closed curves are homologous. However, the converse is false in general, as one can see from the example in Fig. 1.16.
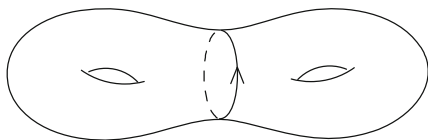
Fig. 1.16. A cycle homologous to zero but not homotopic to a point

The first homology group is the fundamental group "made commutative". More precisely

$$H_1(\mathcal{R}, \mathbb{Z}) = \frac{\pi(\mathcal{R})}{[\pi(\mathcal{R}), \pi(\mathcal{R})]} \ ,$$

where the denominator is the commutator subgroup, i.e., the subgroup of $\pi(\mathcal{R})$ generated by all elements of the form $ABA^{-1}B^{-1}$, $A, B \in \pi(\mathcal{R})$.

To introduce intersection numbers of elements of the first homology group it is convenient to represent them by smooth cycles. Every element of $H_1(\mathcal{R}, \mathbb{Z})$ can be represented by a C^∞-cycle without self-intersections. Moreover, given two elements of $H_1(\mathcal{R}, \mathbb{Z})$ one can represent them by smooth cycles intersecting transversally in a finite number of points.

Let γ_1 and γ_2 be two curves intersecting transversally at the point P. One associates to this point a number $(\gamma_1 \circ \gamma_2)_P = \pm 1$, where the sign is determined by the orientation of the basis $\gamma_1'(P), \gamma_2'(P)$ as it is shown in Fig. 1.17.
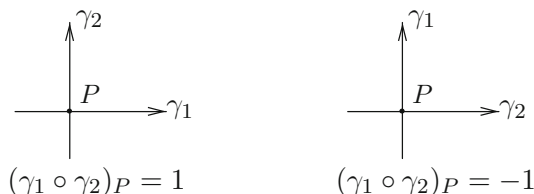
Fig. 1.17. Intersection number at a point

Definition 14. *Let γ_1, γ_2 be two smooth cycles intersecting transversally in finitely many points. The* intersection number *of γ_1 and γ_2 is defined by*

$$\gamma_1 \circ \gamma_2 = \sum_{P \in \gamma_1 \cap \gamma_2} (\gamma_1 \circ \gamma_2)_P \ . \tag{1.36}$$

Lemma 3. *The intersection number of any boundary with any cycle vanishes.*

Since (1.36) is bilinear it is enough to check the statement for a boundary of a domain $\beta = \delta D$ and a simple cycle γ. This follows from the fact that the cycle γ enters D as many times as it leaves D (see Fig. 1.18).
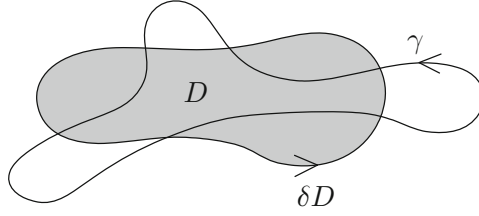
Fig. 1.18. $\gamma \circ \delta D = 0$

To define the intersection number for homology classes represent $\gamma, \gamma' \in H_1(\mathcal{R}, \mathbb{Z})$ by C^∞-cycles

$$\gamma = \sum_i n_i \gamma_i, \qquad \gamma' = \sum_j m_j \gamma'_j,$$

where γ_i, γ'_j are smooth curves intersecting transversally. Define $\gamma \circ \gamma' = \sum_{ij} n_i m_j \gamma_i \circ \gamma'_j$. Due to Lemma 3 the intersection number is well defined for homology classes.

Theorem 10. *The intersection number is a bilinear skew-symmetric map*

$$\circ : H_1(\mathcal{R}, \mathbb{Z}) \times H_1(\mathcal{R}, \mathbb{Z}) \to \mathbb{Z} .$$

Examples

1. The homology group of a sphere with N holes
The homology group is generated by the loops $\gamma_1, \ldots, \gamma_{N-1}$ (see Fig. 1.14). For the homology class of the loop γ_N one has

$$\gamma_N = -\sum_{i=1}^{N-1} \gamma_i ,$$

since $\sum_{i=1}^{N} \gamma_i$ is a boundary.

2. Homology group of a compact Riemann surface of genus g
Since the homotopy group is generated by the cycles $a_1, b_1, \ldots, a_g, b_g$ shown in Fig. 1.15 this is also true for the homology group. The intersection numbers of these cycles are as follows:

$$a_i \circ b_j = \delta_{ij} , \qquad a_i \circ a_j = b_i \circ b_j = 0 . \tag{1.37}$$

The cycles $a_1, b_1, \ldots, a_g, b_g$ constitute a basis of the homology group. Their intersection numbers imply the linear independence.

Definition 15. *A homology basis $a_1, b_1, \ldots, a_g, b_g$ of a compact Riemann surface of genus g with the intersection numbers (1.37) is called* canonical basis *of cycles.*

A canonical basis of cycles is by no means unique. Let (a, b) be a canonical basis of cycles. We represent it by a $2g$-dimensional vector

$$\begin{pmatrix} a \\ b \end{pmatrix} , \quad a = \begin{pmatrix} a_1 \\ \vdots \\ a_g \end{pmatrix} , \quad b = \begin{pmatrix} b_1 \\ \vdots \\ b_g \end{pmatrix} .$$

Any other basis $(\tilde{a}, \tilde{b})$ of $H_1(\mathcal{R}, \mathbb{Z})$ is then given by the transformation

$$\begin{pmatrix} \tilde{a} \\ \tilde{b} \end{pmatrix} = A \begin{pmatrix} a \\ b \end{pmatrix} , \qquad A \in GL(2g, \mathbb{Z}) . \tag{1.38}$$

Substituting the right hand side of (1.38) in

$$J = \begin{pmatrix} \tilde{a} \\ \tilde{b} \end{pmatrix} \circ (\tilde{a}, \tilde{b}) , \qquad J = \begin{pmatrix} 0 & I \\ -I & 0 \end{pmatrix}$$

we obtain that the basis $(\tilde{a}, \tilde{b})$ is canonical if and only if A is symplectic, $A \in Sp(g, \mathbb{Z})$, i.e.,

$$J = AJA^T . \tag{1.39}$$

Two examples of canonical cycle bases are presented in Figs. 1.19 and 1.20. The curves b_i in Fig. 1.19 connect identified points of the boundary curves and are therefore closed. In Fig. 1.20 the parts of the cycles lying on the "lower" sheet of the covering are marked by dotted lines.
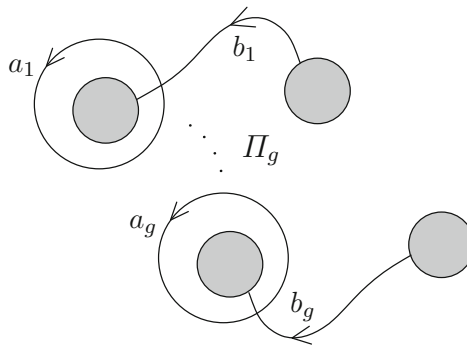
Fig. 1.19. A canonical cycle basis for the planar model Π_g of a compact Riemann surface

1.4 Abelian Differentials

Differentials on a Riemann surface are much easier to handle than functions, and they are the basic tool to investigate and construct functions.
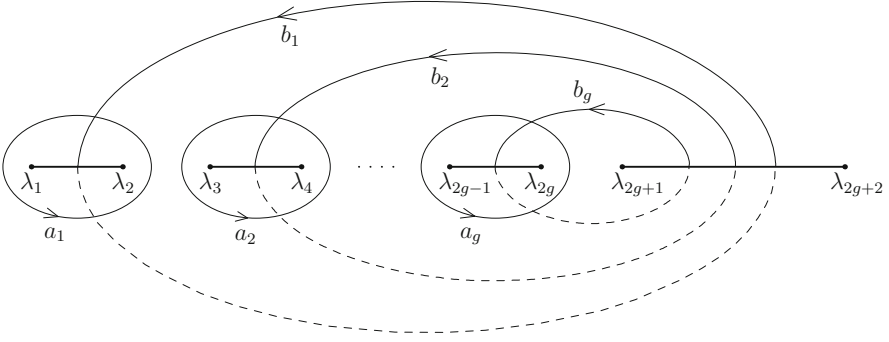
Fig. 1.20. A canonical cycle basis of a hyperelliptic Riemann surface

1.4.1 Differential Forms and Integration Formulas

If smooth complex valued functions $f(z, \bar{z})$, $p(z, \bar{z})$, $q(z, \bar{z})$, $s(z, \bar{z})$ are assigned to each local coordinate on $\mathcal{R}$ such that

$$
\begin{aligned}
f &= f(z, \bar{z}) \,, \\
\omega &= p(z, \bar{z})\mathrm{d}z + q(z, \bar{z})\mathrm{d}\bar{z} \,, \\
S &= s(z, \bar{z})\mathrm{d}z \wedge \mathrm{d}\bar{z}
\end{aligned}
\tag{1.40}
$$

are invariant under coordinate changes (1.1), one says that the function (0-form) f, the differential (1-form) ω and the 2-form S are defined on $\mathcal{R}$.

The 1-form ω is called a form of type (1,0) (resp. a form of type (0,1)) if it may locally be written $\omega = p\,\mathrm{d}z$ (resp. $\omega = q\,\mathrm{d}\bar{z}$). The space of differentials is obviously a direct sum of the subspaces of (1,0) and (0,1) forms.

The exterior product of two 1-forms ω_1 and ω_2 is the 2-form

$$
\omega_1 \wedge \omega_2 = (p_1 q_2 - p_2 q_1)\mathrm{d}z \wedge \mathrm{d}\bar{z} \,.
$$

The differential operator d, which transforms k-forms into $(k+1)$-forms is defined by

$$
\begin{aligned}
\mathrm{d}f &= f_z \mathrm{d}z + f_{\bar{z}}\mathrm{d}\bar{z} \,, \\
\mathrm{d}\omega &= (q_z - p_{\bar{z}})\mathrm{d}z \wedge \mathrm{d}\bar{z} \,, \\
\mathrm{d}S &= 0 \,.
\end{aligned}
\tag{1.41}
$$

Definition 16. *A differential* $\mathrm{d}f$ *is called* exact. *A differential* ω *with* $\mathrm{d}\omega = 0$ *is called* closed.

Using (1.41), one can also easily check that

$$
\mathrm{d}^2 = 0
$$

whenever d^2 is defined and

$$\mathrm{d}(f\omega) = \mathrm{d}f \wedge \omega + f\mathrm{d}\omega \tag{1.42}$$

for any function f and 1-form ω. This implies in particular that any exact form is closed.

One can integrate differentials over 1-chains (i.e., smooth oriented curves and their formal sums), $\int_\gamma \omega$, and 2-forms over 2-chains (formal sums of oriented domains): $\int_D S$.

The most important integration formula is

Theorem 11 (Stokes's theorem). *Let D be a 2-chain with a piecewise smooth boundary ∂D. Then Stokes's formula*

$$\int_D \mathrm{d}\omega = \int_{\partial D} \omega \tag{1.43}$$

holds for any differential ω.

The difference of two homologic curves $\gamma - \tilde{\gamma}$ is a boundary for some D, which implies

Corollary 4. *A differential ω is closed, $\mathrm{d}\omega = 0$, if and only if for any two homological paths γ and $\tilde{\gamma}$*

$$\int_\gamma \omega = \int_{\tilde{\gamma}} \omega$$

holds.

Corollary 5. *Let ω be a closed differential, F_g be a simply connected model of Riemann surface of genus g (see Sect. 1.3) and P_0 be some point in F_g. Then the function*

$$f(P) = \int_{P_0}^{P} \omega \,, \qquad P \in F_g \,,$$

where the integration path lies in F_g is well-defined on F_g.

Let $\gamma_1, \ldots, \gamma_n$ be a homology basis of $\mathcal{R}$ and ω a closed differential. Periods of ω are defined by

$$\Lambda_i = \int_{\gamma_i} \omega \,.$$

Any closed curve γ on $\mathcal{R}$ is homological to $\sum n_i \gamma_i$ with some $n_i \in \mathbb{Z}$, which implies

$$\int_\gamma \omega = \sum n_i \Lambda_i \,,$$

i.e., Λ_i generate the lattice of periods of ω. In particular, if $\mathcal{R}$ is a Riemann surface of genus g with canonical homology basis $a_1, b_1, \ldots, a_g, b_g$, we denote the corresponding periods by

$$A_i = \int_{a_i} \omega \,, \qquad B_i = \int_{b_i} \omega \,.$$

Theorem 12 (Riemann's bilinear relations). *Let $\mathcal{R}$ be a Riemann surface of genus g with a canonical basis a_i, b_i, $i = 1, \ldots, g$ and let ω and ω' be two closed differentials on $\mathcal{R}$ with periods A_i, B_i, A_i', B_i', $i = 1, \ldots, g$. Then*

$$\int_{\mathcal{R}} \omega \wedge \omega' = \sum_{j=1}^{g} (A_j B_j' - A_j' B_j) \,. \tag{1.44}$$

The Riemann surface $\mathcal{R}$ cut along all the cycles a_i, b_i, $i = 1, \ldots, g$ of the fundamental group is the simply connected domain F_g with the boundary (see Figs. 1.11 and 1.15)

$$\partial F_g = \sum_{i=1}^{g} a_i + a_i^{-1} + b_i + b_i^{-1} \,. \tag{1.45}$$

Stokes's theorem with $D = F_g$ implies

$$\int_{\mathcal{R}} \omega \wedge \omega' = \int_{\partial F_g} \omega'(P) \int_{P_0}^{P} \omega \,,$$

where P_0 is some point in F_g and the integration path $[P_0, P]$ lies in F_g.

The curves a_j and a_j^{-1} of the boundary of F_g are identical on $\mathcal{R}$ but have opposite orientation. For the points P_j and P_j' lying on a_j and a_j^{-1} respectively and coinciding on $\mathcal{R}$ we have (see Fig. 1.21)

$$\omega'(P_j) = \omega'(P_j') \,, \qquad \int_{P_0}^{P_j} \omega - \int_{P_0}^{P_j'} \omega = \int_{P_j'}^{P_j} \omega = -B_j \,. \tag{1.46}$$

In the same way for the points $Q_j \in b_j$ and $Q_j' \in b_j^{-1}$ coinciding on $\mathcal{R}$ one gets

$$\omega'(Q_j) = \omega'(Q_j') \,, \qquad \int_{P_0}^{Q_j} \omega - \int_{P_0}^{Q_j'} \omega = \int_{Q_j'}^{Q_j} \omega = A_j \,. \tag{1.47}$$

Substituting, we obtain

$$\int\limits_{\partial F_g} \omega'(P) \int\limits_{P_0}^{P} \omega = \sum_{j=1}^{g} \left(- B_j \int\limits_{a_j} \omega' + A_j \int\limits_{b_j} \omega' \right) = \sum_{j=1}^{g} (A_j B_j' - A_j' B_j) \,.$$

Finally, to complete the proof of Riemann's bilinear identity, one checks directly that the right hand side of (1.44) is invariant under the transformation (1.38, 1.39). Therefore the claim holds for an arbitrary canonical basis of $H_1(\mathcal{R}, \mathbb{C})$.
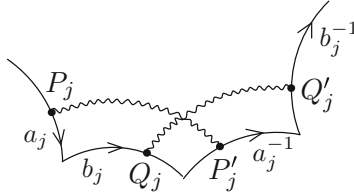
Fig. 1.21. Illustrating the proof of the Riemann bilinear relation

1.4.2 Abelian Differentials of the First, Second and Third Kind

Definition 17. *A differential ω on a Riemann surface $\mathcal{R}$ is called holomorphic (or an Abelian differential of the first kind) if in any local chart it is represented as*

$$\omega = h(z)\mathrm{d}z$$

where $h(z)$ is holomorphic. The differential $\bar\omega$ is called anti-holomorphic.

Holomorphic and anti-holomorphic differentials are closed.

Holomorphic differentials form a complex vector space $H^1(\mathcal{R}, \mathbb{C})$. It is not difficult to show that the dimension of this space is at most g. Indeed, Riemann's bilinear identity with $\omega' = \bar\omega$ implies that the periods A_j, B_j of a holomorphic differential ω satisfy

$$\mathrm{Im} \sum_{j=1}^{g} A_j \bar B_j < 0 \,. \tag{1.48}$$

Thus, if all a-periods of the holomorphic differential ω are zero then $\omega \equiv 0$. If $\omega_1, \dots, \omega_{g+1}$ are holomorphic, then there exists a linear combination of them with all zero a-periods, i.e., the differentials are linearly dependent.

Theorem 13. *The dimension of the space of holomorphic differentials of a compact Riemann surface is equal to its genus*

$$\dim H^1(\mathcal{R}, \mathbb{C}) = g(\mathcal{R}) \,.$$

The existence part of this theorem is more difficult and can be proved by analytic methods [FK92]. However, when the Riemann surface $\mathcal{R}$ is concretely described, one can usually present a basis $\omega_1, \ldots, \omega_g$ of holomorphic differentials explicitly.

On a hyperelliptic curve one can check the holomorphicity using the corresponding local coordinates described in Sect. 1.1.1.

Theorem 14. *The differentials*

$$\omega_j = \frac{\lambda^{j-1}\mathrm{d}\lambda}{\mu}, \qquad j = 1, \ldots, g \tag{1.49}$$

form a basis of holomorphic differentials of the hyperelliptic Riemann surface

$$\mu^2 = \prod_{i=1}^{N}(\lambda - \lambda_i) \qquad \lambda_i \neq \lambda_j , \tag{1.50}$$

where $N = 2g + 2$ or $N = 2g + 1$.

Another example is the holomorphic differential

$$\omega = \mathrm{d}z$$

on the torus $\mathbb{C}/G$ of Sect. 1.3. Here z is the coordinate of $\mathbb{C}$.

Since a differential with all zero a-periods vanishes identically, the matrix of a-periods $A_{ij} = \int_{a_i} \omega_j$ of any basis ω_j, $j = 1, \ldots, g$ of $H^1(\mathcal{R}, \mathbb{C})$ is invertible. The basis can be normalized.

Definition 18. *Let a_j, b_j, $j = 1, \ldots, g$ be a canonical basis of $H_1(\mathcal{R}, \mathbb{Z})$. The dual basis of holomorphic differentials ω_k, $k = 1, \ldots, g$, normalized by*

$$\int_{a_j} \omega_k = 2\pi\mathrm{i}\delta_{jk}$$

is called canonical basis of differentials.

We consider also differentials with singularities.

Definition 19. *A differential Ω is called meromorphic or Abelian differential if in any local chart $z : U \to \mathbb{C}$ it is of the form*

$$\Omega = g(z)\mathrm{d}z ,$$

where $g(z)$ is meromorphic. The integral $\int_{P_0}^{P} \Omega$ of a meromorphic differential is called the Abelian integral.

Let z be a local parameter at the point P, $z(P) = 0$ and

$$\Omega = \sum_{k=N(P)}^{\infty} g_k z^k \mathrm{d}z , \qquad N \in \mathbb{Z} \tag{1.51}$$

be the representation of the differential Ω at P. The numbers $N(P)$ and g_{-1} do not depend on the choice of the local parameter and are characteristics of Ω alone. $N(P)$ is called the *order of the point P*. If $N(P)$ is negative $-N(P)$ is called the *order of the pole* of Ω at P. The number g_{-1} is called the *residue* of Ω at P. It can also be defined by

$$\mathrm{res}_P \Omega \equiv g_{-1} = \frac{1}{2\pi \mathrm{i}} \int_\gamma \Omega , \tag{1.52}$$

where γ is a small closed simple loop going around P in the positive direction.

Let S be the set of singularities of Ω

$$S = \{P \in \mathcal{R} \mid N(P) < 0\} .$$

S is discrete, and if $\mathcal{R}$ is compact then S is also finite.

Computing the integral of an Abelian differential Ω along the boundary of the simply connected model F_g by residues, one obtains

$$\sum_{P_j \in S} \mathrm{res}_{P_j} \Omega = 0 . \tag{1.53}$$

Definition 20. *A meromorphic differential with singularities is called an Abelian differential of the second kind if the residues are equal to zero at all singular points. A meromorphic differential with non-zero residues is called an Abelian differential of the third kind.*

The residue identity (1.53) motivates the following choice of basic meromorphic differentials. The differential of the second kind $\Omega_R^{(N)}$ has only one singularity. It is at the point $R \in \mathcal{R}$ and is of the form

$$\Omega_R^{(N)} = \left(\frac{1}{z^{N+1}} + O(1) \right) \mathrm{d}z , \tag{1.54}$$

where z is a local parameter at R with $z(R) = 0$. The Abelian differential $\Omega_R^{(N)}$ depends on the choice of the local parameter z. The Abelian differential of the third kind Ω_{RQ} has two singularities at the points R and Q with

$$\mathrm{res}_R \Omega_{RQ} = -\mathrm{res}_Q \Omega_{RQ} = 1 ,$$

$$\Omega_{RQ} = \left(\frac{1}{z_R} + O(1) \right) \mathrm{d}z_R \qquad \text{near } R ,$$

$$\Omega_{RQ} = \left(-\frac{1}{z_Q} + O(1) \right) \mathrm{d}z_Q \qquad \text{near } Q , \tag{1.55}$$

where z_R and z_Q are local parameters at R and Q with $z_R(R) = z_Q(Q) = 0$. For the corresponding Abelian integrals this implies

$$\int^P \Omega_R^{(N)} = -\frac{1}{Nz^N} + O(1) \qquad P \to R ,\qquad (1.56)$$

$$\int^P \Omega_{RQ} = \log z_R + O(1) \qquad P \to R ,$$

$$\int^P \Omega_{RQ} = -\log z_Q + O(1) \qquad P \to Q . \qquad (1.57)$$

The Abelian integrals of the first and second kind are single-valued on F_g. The Abelian integral of the third kind Ω_{RQ} is single-valued on $F_g \setminus [R, Q]$, where $[R, Q]$ is a cut from R to Q lying inside F_g.

One can add Abelian differentials of the first kind to $\Omega_R^{(N)}$ and Ω_{RQ} preserving the form of the singularities. By addition of a proper linear combination $\sum_{i=1}^g \alpha_i \omega_i$ the differential can be normalized as follows:

$$\int_{a_j} \Omega_R^{(N)} = 0 , \qquad \int_{a_j} \Omega_{RQ} = 0 \qquad (1.58)$$

for all a-cycles $j = 1, \ldots, g$.

Definition 21. *The differentials $\Omega_R^{(N)}$, Ω_{RQ} with the singularities (1.54), (1.55) and all zero a-periods (1.58) are called the normalized Abelian differentials of the second and third kind.*

Theorem 15. *Given a compact Riemann surface $\mathcal{R}$ with a canonical basis of cycles $a_1, b_1, \ldots, a_g, b_g$, points $R, Q \in \mathcal{R}$, a local parameter z at R, and $N \in \mathbb{N}$, there exist unique normalized Abelian differentials $\Omega_R^{(N)}$ and Ω_{RQ} of the second and third kind, respectively.*

The proof of the uniqueness is simple. The holomorphic difference of two normalized differentials with the same singularities has all zero a-periods and therefore vanishes identically. Like in the case of holomorphic differentials, the existence can be shown by analytic methods [FK92].

Abelian differentials of the second and third kind can be normalized by a more symmetric condition than (1.58). Namely, all the periods can be normalized to be purely imaginary

$$\mathrm{Re} \int_\gamma \Omega = 0 , \qquad \forall \gamma \in H_1(\mathcal{R}, \mathbb{Z}) .$$

Corollary 6. *The normalized Abelian differentials form a basis in the space of Abelian differentials on $\mathcal{R}$.*

Again, as in the case of holomorphic differentials, we present the basis of Abelian differentials of the second and third kind in the hyperelliptic case

$$\mu^2 = \prod_{k=1}^{M} (\lambda - \lambda_k) \, .$$

Denote the coordinates of the points R and Q by

$$R = (\mu_R, \lambda_R) \, , \qquad Q = (\mu_Q, \lambda_Q) \, .$$

We consider the case when both points R and Q are finite $\lambda_R \neq \infty$, $\lambda_Q \neq \infty$. The case $\lambda_R = \infty$ or $\lambda_Q = \infty$ is reduced to the case we consider by a fractional linear transformation. If R is not a branch point, then to get a proper singularity we multiply $d\lambda/\mu$ by $1/(\lambda - \lambda_R)^n$ and cancel the singularity at the point $\pi R = (-\mu_R, \lambda_R)$.

The following differentials are of the third kind with the singularities (1.55)

$$\hat{\Omega}_{RQ} = \left(\frac{\mu + \mu_R}{\lambda - \lambda_R} - \frac{\mu + \mu_Q}{\lambda - \lambda_Q} \right) \frac{d\lambda}{2\mu} \quad \text{if} \quad \mu_R \neq 0 \, , \quad \mu_Q \neq 0 \, ,$$

$$\hat{\Omega}_{RQ} = \left(\frac{\mu + \mu_R}{\mu(\lambda - \lambda_R)} - \frac{1}{\lambda - \lambda_Q} \right) \frac{d\lambda}{2} \quad \text{if} \quad \mu_R \neq 0 \, , \quad \mu_Q = 0 \, ,$$

$$\hat{\Omega}_{RQ} = \left(\frac{1}{\lambda - \lambda_R} - \frac{1}{\lambda - \lambda_Q} \right) \frac{d\lambda}{2} \quad \text{if} \quad \mu_R = \mu_Q = 0 \, .$$

If R is not a branch point, $\mu_R \neq 0$, then the differentials

$$\hat{\Omega}_R^{(N)} = \frac{\mu + \mu_R^{[N]}}{(\lambda - \lambda_R)^{N+1}} \frac{d\lambda}{2\mu} \, ,$$

where $\mu_R^{[N]}$ is the Taylor series at R up to the term of order N,

$$\mu_R^{[N]} = \mu_R + \left. \frac{\partial \mu}{\partial \lambda} \right|_R (\lambda - \lambda_R) + \ldots + \frac{1}{N!} \left. \frac{\partial^N \mu}{\partial \lambda^N} \right|_R (\lambda - \lambda_R)^N \, ,$$

have singularities at R of the form

$$\left(z^{-N-1} + o(z^{-N-1}) \right) dz \tag{1.59}$$

where $z = \lambda - \lambda_R$. If R is a branch point, $\mu_R = 0$, the following differentials have the singularities (1.59) with $z = \sqrt{\lambda - \lambda_R}$

$$\hat{\Omega}_R^{(N)} = \frac{d\lambda}{2(\lambda - \lambda_R)^n \mu} \sqrt{\prod_{\substack{i=1 \\ i \neq R}}^{N} (\lambda_R - \lambda_i)} \quad \text{for} \quad N = 2n - 1 \, ,$$

$$\hat{\Omega}_R^{(N)} = \frac{d\lambda}{2(\lambda - \lambda_R)^n} \quad \text{for} \quad N = 2n - 2 \, .$$

Taking proper linear combinations of these differentials with different values of N we obtain the singularity (1.54). The normalization (1.58) is obtained by addition of holomorphic differentials (1.46)

1.4.3 Periods of Abelian Differentials: Jacobi Variety

Definition 22. *Let a_j, b_j, $j = 1, \ldots, g$, be a canonical homology basis of $\mathcal{R}$ and let ω_k, $k = 1, \ldots, g$, be the dual basis of $H^1(\mathcal{R}, \mathbb{C})$. The matrix*

$$B_{ij} = \int_{b_i} \omega_j \tag{1.60}$$

is called the period matrix *of $\mathcal{R}$.*

Theorem 16. *The period matrix is symmetric and its real part is negative definite,*

$$B_{ij} = B_{ji} \,, \tag{1.61}$$
$$\mathrm{Re}(B\alpha, \alpha) \ < 0 \,, \qquad \forall \alpha \in \mathbb{R}^g \setminus \{0\} \,. \tag{1.62}$$

The symmetry of the period matrix follows from the Riemann bilinear identity (1.44) with $\omega = \omega_i$ and $\omega' = \omega_j$. The definiteness (1.62) is another form of (1.48).

The period matrix depends on the homology basis. Let us use the column notations

$$\begin{pmatrix} \tilde{a} \\ \tilde{b} \end{pmatrix} = \begin{pmatrix} \mathsf{A} & \mathsf{B} \\ \mathsf{C} & \mathsf{D} \end{pmatrix} \begin{pmatrix} a \\ b \end{pmatrix}, \qquad \begin{pmatrix} \mathsf{A} & \mathsf{B} \\ \mathsf{C} & \mathsf{D} \end{pmatrix} \in Sp(g, \mathbb{Z}) \,. \tag{1.63}$$

Let $\omega = (\omega_1, \ldots, \omega_g)$ be the canonical basis of holomorphic differentials dual to (a, b). Labeling columns of the matrices by differentials and rows by cycles we get

$$\int_{\tilde{a}} \omega = 2\pi\mathsf{i}\mathsf{A} + \mathsf{B}B, \qquad \int_{\tilde{b}} \omega = 2\pi\mathsf{i}\mathsf{C} + \mathsf{D}B.$$

The canonical basis of $H^1(\mathcal{R}, \mathbb{C})$ dual to the basis $(\tilde{a}, \tilde{b})$ is given by the right multiplication

$$\tilde{\omega} = 2\pi\mathsf{i}\omega(2\pi\mathsf{i}\mathsf{A} + \mathsf{B}B)^{-1}.$$

This implies the following transformation formula for the period matrix.

Lemma 4. *The period matrices B and $\tilde{B}$ of the Riemann surface $\mathcal{R}$ corresponding to the homology basis (a, b) and $(\tilde{a}, \tilde{b})$ respectively are related by*

$$\tilde{B} = 2\pi\mathsf{i}(\mathsf{D}B + 2\pi\mathsf{i}\mathsf{C})(\mathsf{B}B + 2\pi\mathsf{i}\mathsf{A})^{-1}, \tag{1.64}$$

where $\mathsf{A}, \mathsf{B}, \mathsf{C}, \mathsf{D}$ are the coefficients of the symplectic matrix (1.63).

Using the Riemann bilinear identity one can express the periods of the normalized Abelian differentials of the second and third kind in terms of the normalized holomorphic differentials. Choosing $\omega = \omega_j$ and $\omega' = \Omega_R^{(N)}$ or $\omega' = \Omega_{RQ}$ in the Riemann bilinear identity we obtain the following representations.

Lemma 5. *Let* $\omega_j, \Omega_R^{(N)}, \Omega_{RQ}$ *be the normalized Abelian differentials from Definition 21. Let* z *be a local parameter at* R *with* $z(R) = 0$ *and*

$$\omega_j = \sum_{k=0}^{\infty} \alpha_{k,j} z^k \mathrm{d}z \tag{1.65}$$

the representation of the normalized holomorphic differentials at R. *The periods of* $\Omega_R^{(N)}$, Ω_{RQ} *are equal to:*

$$\int_{b_j} \Omega_R^{(N)} = \frac{1}{N} \alpha_{N-1,j} \tag{1.66}$$

$$\int_{b_j} \Omega_{RQ} = \int_Q^R \omega_j , \tag{1.67}$$

where the integration path $[R, Q]$ *in (1.67) does not cross the cycles* a, b.

Let Λ be the lattice

$$\Lambda = \{2\pi\mathrm{i}N + BM, \ N, M \in \mathbb{Z}^g\}$$

generated by the periods of $\mathcal{R}$. It defines an equivalence relation in $\mathbb{C}^g$: two points of $\mathbb{C}^g$ are equivalent if they differ by an element of Λ.

Definition 23. *The complex torus*

$$\mathrm{Jac}(\mathcal{R}) = \mathbb{C}^g/\Lambda$$

is called the Jacobi variety *of* $\mathcal{R}$. *The map*

$$\mathcal{A} : \mathcal{R} \to \mathrm{Jac}(\mathcal{R}) , \qquad \mathcal{A}(P) = \int_{P_0}^{P} \omega , \tag{1.68}$$

where $\omega = (\omega_1, \ldots, \omega_g)$ *is the canonical basis of holomorphic differentials and* $P_0 \in \mathcal{R}$, *is called the* Abel map.

1.5 Meromorphic Functions on Compact Riemann Surfaces

1.5.1 Divisors and the Abel Theorem

In order to analyze functions and differentials on Riemann surfaces, one characterizes them in terms of their zeros and poles. It is convenient to consider formal sums of points on $\mathcal{R}$. (Later these points will become zeros and poles of functions and differentials).

Definition 24. *A formal linear combination*

$$D = \sum_{j=1}^{N} n_j P_j , \qquad n_j \in \mathbb{Z} , \; P_j \in \mathcal{R} \tag{1.69}$$

is called a divisor *on the Riemann surface $\mathcal{R}$. The sum*

$$\deg D = \sum_{j=1}^{N} n_j$$

is called the degree *of D.*

The set of all divisors with the obviously defined group operations

$$n_1 P + n_2 P = (n_1 + n_2)P , \qquad -D = \sum_{j=1}^{N} (-n_j)P_j$$

forms an Abelian group $\mathrm{Div}(\mathcal{R})$. A divisor (1.69) with all $n_j \geq 0$ is called *positive* (or integral, or effective). This notion allows us to define a partial ordering in $\mathrm{Div}(\mathcal{R})$

$$D \leq D' \iff D' - D \geq 0 .$$

Definition 25. *Let f be a meromorphic function on $\mathcal{R}$ and let $P_1, \ldots, P_M$ be its zeros with multiplicities $p_1, \ldots, p_M > 0$ and $Q_1, \ldots, Q_N$ its poles with multiplicities $q_1, \ldots, q_N > 0$. The divisor*

$$D = p_1 P_1 + \ldots + p_M P_M - q_1 Q_1 - \ldots - q_N Q_N = (f)$$

is called the divisor of f *and is denoted by (f). A divisor D is called* principal *if there exists a function f with $(f) = D$.*

Obviously we have

$$(fg) = (f) + (g) ,$$

where f and g are two meromorphic functions on $\mathcal{R}$.

Definition 26. *Two divisors D and D' are called* linearly equivalent *if the divisor $D - D'$ is principal. The corresponding equivalence class is called the* divisor class.

We denote linearly equivalent divisors by $D \equiv D'$. Divisors of Abelian differentials are also well-defined. We have already seen that the order of the point $N(P)$ defined by (1.51) is independent of the choice of a local parameter and is a characteristic of the Abelian differential. The set of points $P \in \mathcal{R}$ with $N(P) \neq 0$ is finite.

Definition 27. *The divisor of an Abelian differential Ω is*

$$(\Omega) = \sum_{P \in \mathcal{R}} N(P) P \ ,$$

where $N(P)$ is the order of the point P of Ω.

Since the quotient of two Abelian differentials

$$\Omega_1 / \Omega_2$$

is a meromorphic function any two divisors of Abelian differentials are linearly equivalent. The corresponding class is called *canonical*. We will denote it by $\mathcal{C}$.

Any principal divisor can be represented as the difference of two positive linearly equivalent divisors

$$(f) = D_0 - D_\infty \ , \qquad D_0 \equiv D_\infty \ ,$$

where D_0 is the zero divisor and D_∞ is the pole divisor of f. Corollary 2 implies that

$$\deg(f) = 0 \ ,$$

i.e., all principal divisors have zero degree. All canonical divisors have the same degree.

The Abel map is defined for divisors in a natural way

$$\mathcal{A}(D) = \sum_{j=1}^{N} n_j \int_{P_0}^{P_j} \omega \ . \tag{1.70}$$

If the divisor D is of degree zero, then $\mathcal{A}(D)$ is independent of P_0

$$D = P_1 + \ldots + P_N - Q_1 - \ldots - Q_N \ ,$$

$$\mathcal{A}(D) = \sum_{i=1}^{N} \int_{Q_i}^{P_i} \omega \ . \tag{1.71}$$

Theorem 17 (Abel's theorem).   *The divisor $D \in \mathrm{Div}\,(\mathcal{R})$ is principal if and only if:*

(1) $\deg D = 0$
(2) $\mathcal{A}(D) \equiv 0$

The necessity of the first condition is already shown in Corollary 2. Let f be a meromorphic function with the divisor

$$(f) = P_1 + \ldots + P_N - Q_1 - \ldots - Q_N$$

(these points need not be different). Then

$$\Omega = \frac{\mathrm{d}f}{f} = \mathrm{d}(\log f)$$

is an Abelian differential of the third kind. Since periods of Ω are integer multiples of $2\pi\mathrm{i}$, it can be represented as

$$\Omega = \sum_{i=1}^{N} \Omega_{P_i Q_i} + \sum_{k=1}^{g} n_k \omega_k$$

with $n_k \in \mathbb{Z}$. The representation (1.67) for the b-periods of the normalized differentials of the third kind implies $\mathcal{A}(D) \equiv 0$.

Corollary 7. *All linearly equivalent divisors are mapped by the Abel map to the same point of the Jacobian*

$$\mathcal{A}((f) + D) = \mathcal{A}(D) .$$

The Abel theorem can be formulated in terms of any basis $\tilde{\omega} = (\tilde{\omega}_1, \ldots, \tilde{\omega}_g)$ of holomorphic differentials. In this case the second condition of the theorem reads

$$\sum_{i=1}^{N} \int_{Q_i}^{P_i} \tilde{\omega} \equiv 0 \quad (\text{mod periods of } \tilde{\omega}).$$

1.5.2 The Riemann–Roch Theorem

Let D_∞ be a positive divisor on $\mathcal{R}$. A natural problem is to describe the vector space of meromorphic functions with poles at D_∞ only. More generally, let D be a divisor on $\mathcal{R}$. Let us consider the vector space

$$L(D) = \{f \text{ meromorphic functions on } \mathcal{R} \mid (f) \geq -D \text{ or } f \equiv 0\}.$$

Let us split

$$-D = D_0 - D_\infty$$

into negative and positive parts

$$D_0 = \sum n_i P_i , \qquad D_\infty = \sum m_k Q_k ,$$

where both D_0 and D_∞ are positive. The space $L(D)$ of dimension

$$l(D) = \dim L(D)$$

consists of the meromorphic functions with zeros of order at least n_i at P_i and with poles of order at most m_k at Q_k.

Similarly, let us denote by

$$H(D) = \{\Omega \text{ Abelian differential on } \mathcal{R} \mid (\Omega) \geq D \text{ or } \Omega \equiv 0\}$$

the corresponding vector space of differentials, and by

$$i(D) = \dim H(D)$$

its dimension, which is called the *index of speciality* of D.

It is easy to see that $l(D)$ and $i(D)$ depend only on the divisor class of D, and

$$i(D) = l(C - D) \, , \tag{1.72}$$

where C is the canonical divisor class. Indeed, let Ω_0 be a non-zero Abelian differential and $C = (\Omega_0)$ be its divisor. The map $H(D) \to L(C - D)$ defined by

$$H(D) \ni \Omega \longrightarrow \frac{\Omega}{\Omega_0} \in L(C - D)$$

is an isomorphism of linear spaces, which implies $i(D) = l(C - D)$.

Theorem 18 (Riemann–Roch theorem). *Let $\mathcal{R}$ be a compact Riemann surface of genus g and D a divisor on $\mathcal{R}$. Then*

$$l(D) = \deg D - g + 1 + i(D) \, . \tag{1.73}$$

This identity can be proved by an analysis of the singularities and the periods of the differential df for a function $f \in L(D)$. However the proof is rather involved [FK92].[2] Many important results can be easily obtained from this fundamental theorem.

Since the index $i(D)$ is non-negative one has

Theorem 19 (Riemann's inequality). *For any divisor D*

$$l(D) \geq \deg D + 1 - g \, .$$

This has the following immediate consequence.

Corollary 8. *For any positive divisor D with $\deg D = g + 1$ there exists a non-constant meromorphic function in $L(D)$.*

Let us consider a divisor on a Riemann surface of genus zero which consists of one point $D = P$. Riemann's inequality implies $l(P) \geq 2$. There exists a non-trivial function f with 1 pole on $\mathcal{R}$. It is a holomorphic covering $f : \mathcal{R} \to \hat{\mathbb{C}}$. Since f has only one pole, every value is assumed once (Corollary 2), therefore $\mathcal{R}$ and $\hat{\mathbb{C}}$ are conformally equivalent.

Corollary 9. *Any Riemann surface of genus 0 is conformally equivalent to the complex sphere $\hat{\mathbb{C}}$.*

---

[2] Note the difference in notations by the sign of D. Our space $L(D)$ is identified with the space of holomorphic sections of the holomorphic line bundle $L[D]$ (see Sect. 1.7).

Corollary 10. *The degree of the canonical class is*

$$\deg C = 2g - 2 \ . \tag{1.74}$$

The Riemann–Roch theorem implies for the canonical divisor

$$\deg C = l(C) + g - 1 - i(C) \ .$$

Since the spaces of holomorphic differentials and functions are g- and 1-dimensional respectively, using (1.72), $l(C) = i(0) = g, i(C) = l(0) = 1$, one arrives at (1.74).

Corollary 11. *On a compact Riemann surface there is no point where all holomorphic differentials vanish simultaneously.*

Indeed, suppose there exists such a point $P \in \mathcal{R}$, i.e., $i(P) = g$. The Riemann–Roch theorem for the divisor $D = P$ implies $l(P) = 2$, i.e., there exists a non-constant meromorphic function f with only one simple pole. This implies that $f : \mathcal{R} \to \hat{\mathbb{C}}$ is bi-holomorphic, in particular $g = 0$.

1.5.3 Jacobi Inversion Problem

Now we come to more complicated properties of the Abel map. Let us fix a point $P_0 \in \mathcal{R}$. From corollary 11 of the Riemann–Roch theorem we know that all holomorphic differentials do not vanish simultaneously. Therefore $d\mathcal{A}(P) = \omega(P) \neq 0$, which shows that the Abel map is an immersion (the differential of the map vanishes nowhere on $\mathcal{R}$).

Proposition 5. *The Abel map*

$$\mathcal{A} : \mathcal{R} \to Jac(\mathcal{R})$$

$$P \mapsto \int_{P_0}^{P} \omega \tag{1.75}$$

is an embedding, i.e., the map (1.75) is an injective immersion.

The injectivity follows from Abel's theorem. Suppose there exist $P_1, P_2 \in \mathcal{R}$ with $\mathcal{A}(P_1) = \mathcal{A}(P_2)$, i.e., the divisor $P_1 - P_2$ is principal. Functions with one pole do not exist for Riemann surfaces of genus $g > 0$, thus the points must coincide $P_1 = P_2$.

The Jacobi variety of a Riemann surface of genus one is a one-dimensional complex torus, which is itself a Riemann surface of genus one (see Sect. 1.1.2).

Corollary 12. *A Riemann surface of genus one is conformally equivalent to its Jacobi variety.*

Although the next theorem looks technical (see for example [FK92] for the proof), it is an important result often used.

Theorem 20 (Jacobi inversion problem). *Let $\mathcal{D}_g$ be the set of positive divisors of degree g. The Abel map on this set*

$$\mathcal{A} : \mathcal{D}_g \rightarrow Jac(\mathcal{R})$$

is surjective, i.e., for any $\xi \in Jac(\mathcal{R})$ there exists a degree g positive divisor $P_1 + \ldots + P_g \in \mathcal{D}_g$ (the P_i need not be different) satisfying

$$\sum_{i=1}^{g} \int_{P_0}^{P_i} \omega = \xi. \tag{1.76}$$

1.5.4 Special Divisors and Weierstrass Points

Definition 28. *A positive divisor D of degree $\deg D = g$ is called* special *if $i(D) > 0$, i.e., there exists a holomorphic differential ω with*

$$(\omega) \geq D . \tag{1.77}$$

The Riemann–Roch theorem implies that (1.77) is equivalent to the existence of a non-constant function f with $(f) \geq -D$. Since the space of holomorphic differentials is g-dimensional, (1.77) is a homogeneous linear system of g equations in g variables. This shows that most of the positive divisors of degree g are non-special.

Definition 29. *A point $P \in \mathcal{R}$ is called the* Weierstrass point *if the divisor $D = gP$ is special.*

The Weierstrass points are special points of $\mathcal{R}$. Weierstrass points exists on Riemann surfaces of genus $g > 1$. They coincide with the zeros of the holomorphic q-differential $H dz^q$ with $q = g(g+1)/2$ and

$$H := \det \begin{pmatrix} h_1 & \cdots & h_g \\ h_1' & \cdots & h_g' \\ \vdots & & \vdots \\ h_1^{(g-1)} & \cdots & h_g^{(g-1)} \end{pmatrix}, \tag{1.78}$$

where $\omega_k = h_k(z)dz$ are the local representations of a basis of holomorphic differentials. Indeed, H vanishes at P_0 if and only if the matrix in (1.78) has a non-zero vector $(\alpha_1, \ldots, \alpha_g)^T$ in the kernel. In this case the differential $\sum_{k=1}^{g} \alpha_k h_k$ has a zero of order g at P_0, which implies $i(gP_0) > 0$.

The number of the Weierstrass points is bounded by the number of zeros of H, which is $g^3 - g$.

1.5.5 Hyperelliptic Riemann Surfaces

Let $\mathcal{R}$ be a compact Riemann surface of a hyperelliptic curve as in Theorem 1. On this Riemann surface there exist meromorphic functions with precisely two poles counting multiplicities. Examples of such functions are λ and $\frac{1}{\lambda - \lambda_0}$ with arbitrary λ_0. This observation leads to an equivalent definition of hyperelliptic Riemann surfaces.

Definition 30. *A compact Riemann surface $\mathcal{R}$ of genus $g \geq 2$ is called hyperelliptic if there exists a positive divisor D on $\mathcal{R}$ with*

$$\deg D = 2 \,, \qquad l(D) \geq 2 \,.$$

A non-constant meromorphic function Λ in $L(D)$ defines a two-sheeted covering of the complex sphere

$$\Lambda : \mathcal{R} \to \hat{\mathbb{C}} \,. \tag{1.79}$$

All the ramification points of this covering have branch numbers 1.

It is not difficult to show that two hyperelliptic Riemann surfaces are conformally equivalent if and only if their branch points differ by a fractional linear transformation. The branch points can be used as parameters in the moduli space of hyperelliptic curves. The complex dimension of this space is $2g - 1$. Indeed, there are $2g + 2$ branch points and three of them can be normalized to $0, 1, \infty$ by a fractional linear transformation. We see that for $g = 2$ this dimension coincides with the complex dimension $3g - 3$ of the space of Riemann surfaces of genus g (see Sect. 1.8.1). This simple observation shows that there exist non-hyperelliptic Riemann surfaces of genus $g \geq 3$.

Theorem 21. *Any Riemann surface of genus $g = 2$ is hyperelliptic.*

This is not difficult to prove. The zero divisor (ω) of a holomorphic differential on a Riemann surface $\mathcal{R}$ of genus 2 is of degree $2 = 2g - 2$. Since $i((\omega)) > 0$, the Riemann–Roch theorem implies $l((\omega)) \geq 2$.

Special divisors on hyperelliptic Riemann surfaces are characterized by the following simple property.

Proposition 6. *Let $\mathcal{R}$ be a hyperelliptic Riemann surface and let $\lambda : \mathcal{R} \to \hat{\mathbb{C}}$ be the corresponding two-sheeted covering (1.5) with branch points $\lambda_k, k = 1 \ldots, N$. A positive divisor D of degree g is singular if and only if it contains a pair of points (μ_0, λ_0), $(-\mu_0, \lambda_0)$ with the same λ-coordinate $\lambda_0 \neq \lambda_k$ or a double branch point $2(0, \lambda_k)$.*

D being a special divisor implies that there exists a differential ω with $(\omega) \geq D$. The differential ω is holomorphic, and due to Theorem 14 it can be represented as

$$\omega = \frac{P_{g-1}(\lambda)}{\mu} \mathrm{d}\lambda \,,$$

where $P_{g-1}(\lambda)$ is a polynomial of degree $g - 1$. The differential ω has $g - 1$ pairs of zeros

$$(\mu_n, \lambda_n), \ (-\mu_n, \lambda_n) \ , \ n = 1, \ldots, g - 1, \ P_{g-1}(\lambda_n) = 0 \ .$$

Since D is of degree g it must contain at least one of these pairs.

1.6 Theta Functions

1.6.1 Definition and Simplest Properties

Consider a g-dimensional complex torus $\mathbb{C}^g / \Lambda$ where Λ is a lattice of full rank:

$$\Lambda = AN + BM \ , \qquad A, B \in gl(g, \mathbb{C}) \ , \ N, M \in \mathbb{Z}^g \ , \qquad (1.80)$$

and the $2g$ columns of A, B are $\mathbb{R}$-linearly independent. Non-constant mero-morphic functions on $\mathbb{C}^g / \Lambda$ exist only (see, for example, [Sie71]) if the complex torus is an *Abelian torus*, i.e., if by an appropriate linear choice of coordinates on $\mathbb{C}^g$ the lattice (1.80) can be reduced to a special form: A is a diagonal matrix of the form

$$A = 2\pi\mathrm{i} \ \mathrm{diag}(a_1 = 1, \ldots, a_g) \ , \quad a_k \in \mathbb{N} \ , \ a_k \text{ divides } a_{k+1} \ ,$$

and B is a symmetric matrix with negative real part. An Abelian torus with $a_1 = \ldots = a_g = 1$ is called *principally polarized*. Jacobi varieties of Riemann surfaces are principally polarized Abelian tori. Meromorphic functions on Abelian tori are constructed in terms of theta functions, which are defined by their Fourier series.

Definition 31. *Let B be a symmetric $g \times g$ matrix with negative real part. The* theta function *is defined by the following series*

$$\theta(z) = \sum_{m \in \mathbb{Z}^g} \exp\{\frac{1}{2}(Bm, m) + (z, m)\} \ , \qquad z \in \mathbb{C} \ .$$

Here

$$(Bm, m) = \sum_{ij} B_{ij} m_i m_j \ , \quad (z, m) = \sum_j z_j m_j \ .$$

Since B has negative real part, the series converge absolutely and defines an entire function on $\mathbb{C}^g$.

Proposition 7. *The theta function is even,*

$$\theta(-z) = \theta(z) \ ,$$

and possesses the following periodicity property:

$$\theta(z + 2\pi\mathrm{i}N + BM) = \exp\{-\frac{1}{2}(BM, M) - (z, M)\}\theta(z) \ , \quad N, M \in \mathbb{Z}^g \ . \ (1.81)$$

More generally one introduces *theta functions with characteristics* $[\alpha, \beta]$

$$\theta \begin{bmatrix} \alpha \\ \beta \end{bmatrix} (z) = \sum_{m \in \mathbb{Z}^g} \exp \left\{ \frac{1}{2}(B(m+\alpha), m+\alpha) + (z + 2\pi \mathrm{i}\beta, m+\alpha) \right\}$$

$$= \theta(z + 2\pi \mathrm{i}\beta + B\alpha) \exp \left\{ \frac{1}{2}(B\alpha, \alpha) + (z + 2\pi \mathrm{i}\beta, \alpha) \right\} , \quad (1.82)$$

$$z \in \mathbb{C}^g, \ \alpha, \beta \in \mathbb{R}^g .$$

with the transformation law

$$\theta \begin{bmatrix} \alpha \\ \beta \end{bmatrix} (z + 2\pi \mathrm{i}N + BM) = \quad (1.83)$$

$$\exp \left\{ -\tfrac{1}{2}(BM, M) - (z, M) + 2\pi \mathrm{i}((\alpha, N) - (\beta, M)) \right\} \ \theta \begin{bmatrix} \alpha \\ \beta \end{bmatrix} (z) .$$

1.6.2 Theta Functions of Riemann Surfaces

From now on we consider an Abelian torus which is a Jacobi variety, $\mathbb{C}/\Lambda = Jac(\mathcal{R})$. By combining the theta function with the Abel map, one obtains the following useful map on a Riemann surface:

$$\Theta(P) := \theta(\mathcal{A}_{P_0}(P) - d) , \qquad \mathcal{A}_{P_0}(P) = \int_{P_0}^{P} \omega . \quad (1.84)$$

Here we incorporated the base point $P_0 \in \mathcal{R}$ in the notation of the Abel map, and the parameter $d \in \mathbb{C}^g$ is arbitrary. The periodicity properties of the theta function (1.81) imply the following

Proposition 8. $\Theta(P)$ *is an entire function on the universal covering* $\tilde{\mathcal{R}}$ *of* $\mathcal{R}$. *Under analytical continuation* $\mathcal{M}_{a_k}, \mathcal{M}_{b_k}$ *along a- and b-cycles on the Riemann surface, it is transformed as follows:*

$$\mathcal{M}_{a_k} \Theta(P) = \Theta(P) ,$$

$$\mathcal{M}_{b_k} \Theta(P) = \exp\{ -\tfrac{1}{2}B_{kk} - \int_{P_0}^{P} \omega_k + d_k \} \Theta(P) . \quad (1.85)$$

The zero divisor (Θ) *of* $\Theta(P)$ *on* $\mathcal{R}$ *is well defined.*

Theorem 22. *The theta function* $\Theta(P)$ *either vanishes identically on* $\mathcal{R}$ *or has exactly g zeros (counting multiplicities):*

$$\deg(\Theta) = g .$$

Suppose $\Theta \not\equiv 0$. As in Sect. 1.4 consider the simply connected model F_g of the Riemann surface. The differential $\mathrm{d} \log \Theta$ is well defined on F_g and the number of zeros of Θ is equal to

$$\deg(\Theta) = \frac{1}{2\pi \mathrm{i}} \int_{\partial F_g} \mathrm{d} \log \Theta(P) .$$

using the periodicity properties of Θ we get (see Theorem 12 for notation) for the values of $d \log \Theta$ at the corresponding points

$$d \log \Theta(Q'_j) = d \log \Theta(Q_j), \ d \log \Theta(P'_j) = d \log \Theta(P_j) - \omega_j(P_j) . \quad (1.86)$$

For the number of zeros of the theta function this implies

$$\deg(\Theta) = \frac{1}{2\pi i} \sum_{j=1}^{g} \int_{a_j} \omega_j = \ .$$

A similar but more involved computation [FK92] of the integral

$$I_k = \frac{1}{2\pi i} \int_{\partial F_g} d \log \Theta(P) \int_{P_0}^{P} \omega_k .$$

implies the following Jacobi inversion problem for the zeros of (Θ).

Proposition 9. *Suppose $\Theta \not\equiv 0$. Then its g zeros $P_1, \ldots, P_g$ satisfy*

$$\sum_{i=1}^{g} \int_{P_0}^{P_i} \omega = d - K , \quad (1.87)$$

where K is the vector of Riemann constants

$$K_k = \pi i + \frac{B_{kk}}{2} - \frac{1}{2\pi i} \sum_{j \neq k} \int_{a_j} \omega_j \int_{P_0}^{P} \omega_k . \quad (1.88)$$

One can easily check that $K \in Jac(\mathcal{R})$ is well defined by (1.88), i.e., it is independent of the integration path. On the other hand, K depends on the choice of the base point P_0.

1.6.3 Theta Divisor

Let us denote by J_k the set of equivalence classes (of linearly equivalent divisors, see Sect. 1.5.1) of divisors of degree k. The Abel theorem and the Jacobi inversion imply a canonical identification of J_g and the Jacobi variety

$$J_g \ni D \longleftrightarrow \mathcal{A}(D) \in Jac(\mathcal{R}) .$$

The zero set of the theta function of a Riemann surface, which is called the *theta divisor* can be characterized in terms of divisors on $\mathcal{R}$ as follows. Take a non-special divisor $\tilde{D} = P_1 + \ldots + P_g$ and distinguish one of its points $\tilde{D} = P_1 + D, \ D \in J_{g-1}$. Proposition 9 implies that $\theta(\int^P \omega - \mathcal{A}(\tilde{(D)})) - K)$ vanishes in particular at P_1, and one has $\theta(\mathcal{A}(D) - K) = 0$. Since non-special divisors form a dense set, one has this identify for any $D \in J_{g-1}$. Moreover, this identity gives a characterization of the theta divisor [FK92].

Theorem 23. *The theta divisor is isomorphic to the set J_{g-1} of equivalence classes of positive divisors of degree $g - 1$:*

$$\theta(e) = 0 \Leftrightarrow \exists D \in J_{g-1}, D \geq 0 : \; e = \mathcal{A}(D) + K \; .$$

For any $D \in J_{g-1}$ the expression $\mathcal{A}(D) + K \in Jac(\mathcal{R})$ is independent of the choice of the initial integration point P_0.

Using this characterization of the theta divisor one can complete the description of Proposition 9 of the divisor of the function Θ

Theorem 24. *Let $\Theta(P) = \theta(\mathcal{A}_{P_0}(P) - d)$ be the theta function (1.84) on a Riemann surface and let the divisor $D \in J_g$, $D \geq 0$ be a Jacobi inversion (1.76) of $d - K$,*

$$d = \mathcal{A}(D) + K \; .$$

Then the following alternative holds:
    (i) $\Theta \equiv 0$ iff $i(D) > 0$, i.e., if the divisor D is special.
    (ii) $\Theta \not\equiv 0$ iff $i(D) = 0$, i.e., if the divisor D is non-special. In the last case, D is precisely the zero divisor of Θ.

The evenness of the theta function and Theorem 23 imply that $\theta(d - \mathcal{A}(P)) \equiv 0$ is equivalent to the existence (for any P) of a positive divisor D_P of degree $g - 1$ satisfying $\mathcal{A}(D) + K - \mathcal{A}(P) = \mathcal{A}(D_P) + K$. Due to the Abel theorem the last identity holds if and only if the divisors D and $D_P + P$ are linearly equivalent, i.e., if there exists a function in $L(D)$ vanishing at the (arbitrary) point P. In terms of the dimension of $L(D)$ the last property can be formulated as $l(D) > 1$, which is equivalent to $i(D) > 0$.

Suppose now that D is non-special. Then, as we have shown above, $\Theta \not\equiv 0$, and Proposition 9 implies for the zero divisor of Θ

$$\mathcal{A}((\Theta)) = \mathcal{A}(D) \; .$$

The non-speciality of D implies $D = (\Theta)$.

Although the vector of Riemann constants K appeared in Proposition 9 just as a result of computation, K plays an important role in the theory of theta functions. The geometrical nature of K is partially clarified by the following

Proposition 10.
$$2K = -\mathcal{A}(C) \; ,$$

where C is a canonical divisor.

Indeed, take an arbitrary positive $D_1 \in J_{g-1}$. Due to Theorem 23 the theta function vanishes at $e = \mathcal{A}(D_1) + K$. Theorem 23 applied to $\theta(-e) = 0$ implies the existence of a positive divisor $D_2 \in J_{g-1}$ with $-e = \mathcal{A}(D_2) + K$. For $2K$ this gives

$$2K = \mathcal{A}(D_1 + D_2) \; .$$

It is not difficult to show that this representation (where $D_1 \in J_{g-1}$ is arbitrary) implies $l(D_1 + D_2) \geq g$, or equivalently $i(D_1 + D_2) > 0$, i.e., the divisor $D_1 + D_2$ is canonical.

The vanishing of theta functions at some points follows from their algebraic properties.

Definition 32. *Half-periods of the period lattice*

$$\Delta = 2\pi i \alpha + B\beta \,, \qquad \alpha = (\alpha_1, \ldots, \alpha_g)\,, \beta = (\beta_1, \ldots, \beta_g), \quad \alpha_k, \beta_k \in \left\{0, \frac{1}{2}\right\}.$$

are called half periods or theta characteristics. *A half period is called* even (odd) *if* $4(\alpha, \beta) = 4\sum \alpha_k \beta_k$ *is even (odd).*

We denote the theta characteristic by $\Delta = [\alpha, \beta]$. The theta function $\theta(z)$ vanishes in all odd theta characteristics

$$\theta(\Delta) = \theta(-\Delta + 4\pi i \alpha + 2B\beta) = \theta(-\Delta) \exp(-4\pi i(\alpha, \beta)) \,.$$

To any odd theta characteristic Δ there corresponds a positive divisor D_Δ of degree $g - 1$,

$$\Delta = \mathcal{A}(D_\Delta) + K \,. \tag{1.89}$$

Since 2Δ belongs to the lattice of $Jac(\mathcal{R})$, doubling of (1.89) yields

$$\mathcal{A}(2D_\Delta) = -2K = \mathcal{A}(C) \,.$$

The next corollary follows from the Abel theorem.

Corollary 13. *For any odd theta characteristic Δ there exists a holomorphic differential ω_Δ with*

$$(\omega_\Delta) = 2D_\Delta \,. \tag{1.90}$$

In particular all zeros of ω_Δ are of even multiplicity.

Note, that identity (1.90) is an identity on divisors and not only on equivalence classes of divisors.

The differential ω_Δ can be described explicitly in theta functions.

To any point z of the Abelian torus one can associate a number $s(z)$ determined by the condition that all partial derivatives of θ up to order $s(z)-1$ vanish at z and at least one partial derivative of order $s(z)$ does not vanish at z. For most of the points $s = 0$. The points of the theta divisor are precisely those with $s > 0$. In particular, $s(\Delta) > 0$ for any odd theta characteristic Δ. An odd theta characteristic Δ is called *non-singular* iff $s(\Delta) = 1$.

Let $D = P_1 + \ldots + P_{g-1}$ be a positive divisor of degree $g - 1$. Consider the function $f(P_1, \ldots, P_{g-1}) = \theta(\mathcal{A}(D) + K)$ of $g - 1$ variables. Since f vanishes

identically, differentiating it with respect to P_k one sees that the holomorphic differential

$$h = \sum_i \frac{\partial \theta}{\partial z_i}(e)\omega_i$$

with $e = \mathcal{A}(D) + K$ vanishes at all points P_k. Let Δ be an odd non-singular theta characteristic. Then $D_\Delta \in J_{g-1}$ is uniquely determined by the identity (1.89), i.e., $i(D_\Delta) = 1$. Indeed, if D_Δ is not determined by its Abel image then it is linearly equivalent to a divisor $P + D_{g-2}$, $D_{g-2} \in J_{g-2}$ with an arbitrary point P. Repeating the arguments with the differential h above we see that it vanishes identically on $\mathcal{R}$, i.e., all the derivatives of the theta function $\theta(\Delta)$ vanish. This contradicts the non-singularity of Δ. Finally, we arrive at the following explicit description the one-dimensional ($i(D_\Delta) = 1$) space of holomorphic differentials vanishing at D_Δ.

Proposition 11. *Let Δ be a non-singular odd theta characteristic and D_Δ the corresponding (1.89) positive divisor of degree $g - 1$. Then the holomorphic differential ω_Δ of Corollary 13 is given by the expression*

$$\omega_\Delta = \sum_{i=1}^{g} \frac{\partial \theta}{\partial z_i}(\Delta)\omega_i \; ,$$

where ω_i are normalized holomorphic differentials.

We finish this section with Riemann's complete description of the theta divisor. The proof of this classical theorem can be found for example in [FK92, Lew64]. It is based on considerations similar to the ones in this section, but technically more involved.

Theorem 25. *The following two characterizations of a point $e \in Jac(\mathcal{R})$ are equivalent:*

- *The theta function and all its partial derivatives up to order $s-1$ vanish in e and at least one partial derivative of order s does not vanish at e.*
- *$e = \mathcal{A}(D) + K$ where D is a positive divisor of degree g and $i(D) = s$.*

1.7 Holomorphic Line Bundles

In this section some results of the previous sections are formulated in the language of holomorphic line bundles. This language is useful for generalizations to manifolds of higher dimension, where one does not have concrete tools as in the case of Riemann surfaces, and where one has to rely on more abstract geometric constructions.

1.7.1 Holomorphic Line Bundles and Divisors

Let (U_α, z_α) be coordinate charts of an open cover $\cup_{\alpha \in A} U_\alpha = \mathcal{R}$ of a Riemann surface. The geometric idea behind the concept of a holomorphic line bundle

is the following. One takes the union $U_\alpha \times \mathbb{C}$ over all $\alpha \in A$ and "glues" them together by identifying $(P, \xi_\alpha) \in U_\alpha \times \mathbb{C}$ with $(P, \xi_\beta) \in U_\beta \times \mathbb{C}$ for $P \in U_\alpha \cap U_\beta$ linearly holomorphically, i.e., $\xi_\beta = g(P)\xi_\alpha$ where $g(P) : U_\alpha \cap U_\beta :\to \mathbb{C}$ is holomorphic.

Let us make this "constructive" definition rigorous. Denote by

$$\mathcal{O}^*(U) \subset \mathcal{O}(U) \subset \mathcal{M}(U)$$

the sets of nowhere vanishing holomorphic functions, of holomorphic functions and of meromorphic functions on $U \subset \mathcal{R}$, respectively. A holomorphic line bundle is given by its *transition functions*, which are holomorphic non-vanishing functions $g_{\alpha\beta} \in \mathcal{O}^*(U_\alpha \cap U_\beta)$ satisfying

$$g_{\alpha\beta}(P)g_{\beta\gamma}(P) = g_{\alpha\gamma}(P) \qquad \forall P \in U_\alpha \cap U_\beta \cap U_\gamma . \tag{1.91}$$

This identity implies in particular $g_{\alpha\alpha} = 1$ and $g_{\alpha\beta}g_{\beta\alpha} = 1$.

Introduce on triples $[P, U_\alpha, \xi]$, $P \in U_\alpha, \alpha \in A, \xi \in \mathbb{C}$ the following equivalence relation:

$$[P, U_\alpha, \xi] \sim [Q, U_\beta, \eta] \Leftrightarrow P = Q \in U_\alpha \cap U_\beta, \ \eta = g_{\beta\alpha}\xi . \tag{1.92}$$

Definition 33. *The union of $U_\alpha \times \mathbb{C}$ identified by the equivalence relation (1.92) is called a* holomorphic line bundle $L = L(\mathcal{R})$. *The mapping $\pi : L \to \mathcal{R}$ defined by $[P, U_\alpha, \xi] \mapsto P$ is called the canonical projection. The linear space $L_P := \pi^{-1}(P) \cong \{P\} \times \mathbb{C}$ is called the* fibre *of L over P.*

The line bundle with all $g_{\alpha\beta} = 1$ is called *trivial*.

A set of meromorphic functions $\phi_\alpha \in \mathcal{M}(U_\alpha)$ such that $\phi_\alpha/\phi_\beta \in \mathcal{O}^*(U_\alpha \cap U_\beta)$ for all α, β is called a *meromorphic section* ϕ of a line bundle $L(\mathcal{R})$ defined by the transition functions

$$g_{\alpha\beta} = \phi_\alpha/\phi_\beta .$$

Note that the divisor (ϕ) of the meromorphic section ϕ is well defined by $(\phi)\big|_{U_\alpha} = (\phi_\alpha)\big|_{U_\alpha}$. In the same way one defines a line bundle $L(U)$ and its sections on an open subset $U \subset \mathcal{R}$. Bundles are locally trivializable, i.e., there always exist local sections: a local holomorphic section over U_α can be given simply by

$$U_\alpha \ni P \mapsto [P, U_\alpha, 1]. \tag{1.93}$$

One immediately recognizes that holomorphic (Abelian) differentials (see Definitions 17, 19) are holomorphic (meromorphic) sections of a holomorphic line bundle. This line bundle, given by the transition functions

$$g_{\alpha\beta}(P) = \frac{dz_\beta}{dz_\alpha}(P) ,$$

is called the *canonical bundle* and denoted by K.

Obviously a line bundle is completely determined by a meromorphic section. In Sects. 1.4 and 1.5.5 we dealt with meromorphic sections directly and formulated results in terms of sections without using the bundle language.

Let L be a holomorphic line bundle (1.92) with trivializations (1.93) on U_α. Local sections

$$U_\alpha \ni P \mapsto [P, U_\alpha, h_\alpha(P)] \,,$$

where $h_\alpha \in \mathcal{O}^*(U_\alpha)$ define another holomorphic line bundle L' which is called (holomorphically) *isomorphic* to L. We see that fibres of isomorphic holomorphic line bundles can be holomorphically identified $h_\alpha : L(U_\alpha) \to L'(U_\alpha)$. This is equivalent to the following definition.

Definition 34. *Two holomorphic line bundles L and L' are isomorphic if their transition functions are related by*

$$g'_{\alpha\beta} = g_{\alpha\beta} \frac{h_\alpha}{h_\beta} \tag{1.94}$$

with some $h_\alpha \in \mathcal{O}^*(U_\alpha)$.

We have seen that holomorphic line bundles can be described by their meromorphic sections. Therefore it is not suprising that holomorphic line bundles and divisors are intimately related. To each divisor one can naturally associate a class of isomorphic holomorphic line bundles. Let D be a divisor on $\mathcal{R}$. Consider a covering $\{U_\alpha\}$ such that each point of the divisor belongs to only one U_α. Take $\phi_\alpha \in \mathcal{M}(U_\alpha)$ such that the divisor of ϕ_α is presicely the part of D lying in U_α,

$$(\phi_\alpha) = D_\alpha := D \mid_{U_\alpha} \ .$$

For example take $\phi_\alpha = z_\alpha^{n_i}$, where z_α is a local parameter vanishing at the point $P_i \in U_\alpha$ of the divisor $D = \sum n_i P_i$. The so defined meromorphic section ϕ determines a line bundle L associated with D. If $\phi'_\alpha \in \mathcal{M}(U_\alpha)$ are different local sections with the same divisor $D = (\phi')$, then $h_\alpha = \phi'_\alpha/\phi_\alpha \in \mathcal{O}^*(U_\alpha)$ and ϕ' determines a line bundle L' isomorphic to L. We see that a divisor D determines not a particular line bundle but a class of isomorphic line bundles together with corresponding meromorphic sections ϕ such that $(\phi) = D$. This relation is clearly an isomorphism. Let us denote by $L[D]$ isomorphic line bundles determined by D.

It is natural to get rid of sections in this relation and to describe line bundles in terms of divisors.

Lemma 6. *The holomorphic line bundles $L[D]$ and $L[D']$ are isomorphic if and only the corresponding divisors D and D' are linearly equivalent.*

Indeed, choose a covering $\{U_\alpha\}$ such that each point of D and D' belongs to only one U_α. Take $h \in \mathcal{M}(\mathcal{R})$ with $(h) = D - D'$. This function is holomorphic on each $U_\alpha \cap U_\beta$, $\alpha \neq \beta$. If ϕ is a meromorphic section of $L[D]$ then $h\phi$

is a meromorphic section of $L[D']$, which implies (1.94) for the transition functions. Conversely, let ϕ and ϕ' be meromorphic sections of isomorphic line bundles $L[D]$ and $L[D']$ respectively, $(\phi) = D, (\phi') = D'$. Identity (1.94) implies that $\phi_\alpha h_\alpha / \phi'_\alpha$ is a meromorphic function on $\mathcal{R}$. The divisor of this function is $D - D'$, which yields $D \equiv D'$.

It turns out that Lemma 6 implies a classification of holomorphic line bundles. Namely, every holomorphic line bundle L comes as a bundle associated to the divisor $L = L[(\phi)]$ of a meromorphic section ϕ, and every holomorphic line bundle possesses a meromorphic section. The proofs of the last fact are based on homological methods and are rather involved [GH94, Gu66, Spr81]. We arrive at the following fundamental classification theorem.

Theorem 26. *There is a one to one correspondence between classes of isomorphic holomorphic line bundles and classes of linearly equivalent divisors.*

The degree $\deg D$ is called the *degree* of the line bundle $L[D]$.

Thus, holomorphic line bundles are classified by elements of J_n (see Sect. 1.6.3), where n is the degree of the bundle $n = \deg L$. Due to the Abel theorem and Jacobi inversion, elements of J_n can be identified with the points of the Jacobi variety. Namely, choose some $D_0 \in J_n$ as a reference point. Then due to the Abel theorem the class of divisor $D \in J_n$ is given by the point

$$\mathcal{A}(D - D_0) = \int_{D_0}^{D} \omega \in Jac(\mathcal{R}) \ .$$

Conversely, due to the Jacobi inversion, given some $D_0 \in J_n$, to any point $d \in Jac(\mathcal{R})$ there corresponds $D \in J_n$ satisfying $\mathcal{A}(D - D_0) = d$.

1.7.2 Picard Group: Holomorphic Spin Bundle

We will not distinguish isomorphic line bundles and denote by $L[D]$ the isomorphic line bundle associated with the divisor class D.

The set of line bundles can be equipped with an Abelian group structure. If L and L' are bundles with transition functions $g_{\alpha\beta}$ and $g'_{\alpha\beta}$ respectively, then the line bundle. $L'L^{-1}$ is defined by the transition functions $g'_{\alpha\beta} g_{\alpha\beta}^{-1}$.

Definition 35. *The Abelian group of line bundles on $\mathcal{R}$ is called the* Picard group *of $\mathcal{R}$ and denoted by $Pic(\mathcal{R})$*

Let ϕ and ϕ' be meromorphic sections of L and L' respectively. Then ϕ'/ϕ is a meromorphic section of $L'L^{-1}$. For the divisors of the sections one has $(\phi'/\phi) = (\phi') - (\phi)$. The classification Theorem 26 implies the following

Theorem 27. *The Picard group $Pic(\mathcal{R})$ is isomorphic to the group of divisors $Div(\mathcal{R})$ modulo linear equivalence.*

Holomorphic q-differentials of Sect. 1.5.4 are holomorphic sections of the bundle K^q.

Corollary 14. *Holomorphic line bundles L_1, L_2, L_3 satisfy*

$$L_3 = L_2 L_1^{-1}$$

if and only if

$$\deg L_3 = \deg L_2 - \deg L_1 \quad and \quad \mathcal{A}(D_3 - D_2 + D_1) = 0 \ ,$$

where D_i are the divisors corresponding to $L_i = L[D_i]$.

For the proof one uses the characterization of line bundles via their meromorphic sections ϕ_1, ϕ_2, ϕ_3 and applies the Abel theorem to the meromorphic function $\phi_3\phi_1/\phi_2$.

Since the canonical bundle K is of even degree one can define a "square root" of it.

Definition 36. *A holomorphic line bundle S satisfying*

$$SS = K$$

is called a holomorphic spin bundle. *Holomorphic (meromorphic) sections of S are called holomorphic (meromorphic) spinors.*

Spinors are differentials of order $1/2$. In local coordinates they are given by expressions $s(z)\sqrt{dz}$ where $s(z)$ is holomorphic (meromorphic) for holomorphic (meromorphic) spinors.

Proposition 12. *There exist exactly 4^g non-isomorphic spin bundles on a Riemann surface of genus g.*

This fact can be shown using the description of classes of isomorphic holomorphic line bundles by the elements of the Jacobi variety, see the end of Sect. 1.7.1. The classes of linearly equivalent divisors are isomorphic to points of the Jacobi variety

$$D \in J_n \leftrightarrow d = \mathcal{A}(D - nP_0) \in Jac(\mathcal{R}) \ ,$$

where P_0 is a reference point $P_0 \in \mathcal{R}$. For the divisor class D_S of a holomorphic spin bundle Corollary 14 implies

$$\deg D_S = g - 1 \quad and \quad 2\mathcal{A}(D_S) = \mathcal{A}(C) \ ,$$

where C is the canonical divisor. Proposition 10 provides us with the general solution to this problem,

$$\mathcal{A}(D_S) = -K + \Delta \ ,$$

where K is the vector of Riemann constants and Δ is one of the 4^g half-periods of Definition 32. Due to the Jacobi inversion the last equation is solvable

(the divisor $D_S \in J_{g-1}$ is not necessarily positive) for any Δ. We denote by $D_\Delta \in J_{g-1}$ the divisor class corresponding to the half-period Δ and by S_Δ the corresponding holomorphic spin bundle $S_\Delta := L[D_\Delta]$. The line bundles with different half-periods can not be isomorphic since the images of their divisors in the Jacobi variety are different.

Note that we obtained a geometrical interpretation for the vector of Riemann constants.

Corollary 15. *Up to a sign the vector of Riemann constants is the image under the Abel map of the divisor of the holomorphic spin bundle with the zero theta characteristic*

$$K = -\mathcal{A}(D_{[0,0]} - (g-1)P_0) \, .$$

This corollary clarifies the dependence of K_{P_0} on the base point and on the choice of the canonical homology basis.

Finally, let us give a geometric interpretation of the Riemann–Roch theorem. Denote by $h^0(L)$ the dimension of the space of holomorphic sections of the line bundle L.

Theorem 28 (Riemann–Roch theorem). *For any holomorphic line bundle $\pi : L \to \mathcal{R}$ over a Riemann surface $\mathcal{R}$ of genus g*

$$h^0(L) = \deg L - g + 1 + h^0(KL^{-1}) \, . \tag{1.95}$$

This theorem is just a reformulation of Theorem 18. Indeed, let $D = (\phi)$ be the divisor of a meromorphic section of the line bundle $L = L[D]$ and let h be a holomorphic section of L. The quotient h/ϕ is a meromorphic function with the divisor $(h/\phi) \geq -D$. On the other hand, given $f \in \mathcal{M}(\mathcal{R})$ with $(f) \geq -D$ the product $f\phi$ is a holomorphic section of L. We see that the space of holomorphic sections of L can be identified with the space of meromorphic functions $L(D)$ defined in Sect. 1.5.2. Similarly, holomorphic sections of KL^{-1} can be identified with Abelian differentials with divisors $(\Omega) \geq D$. This is the space $H(D)$ of Sect. 1.5.2 and its dimension is $i(D)$. Now the claim follows from (1.73).

The Riemann–Roch theorem does not allow us to compute the number of holomorphic sections of a spin bundle. The identity (1.95) implies only that $\deg S = g - 1$. A computation of $h^0(S)$ is a rather delicate problem. It turns out that the dimension of the space of holomorphic sections of S_Δ depends on the theta characteristic Δ and is even for even theta characteristics and odd for odd theta characteristics [Ati71]. Spin bundles with non-singular theta characteristics have no holomorphic sections if the characteristic is even and have a unique holomorphic section if the characteristic is odd.

Results of Sect. 1.6.3 allow us to show this easily for odd theta characteristics. Take the differential ω_Δ of Corollary 13. The square root of it $\sqrt{\omega_\Delta}$ is a holomorphic section of S_Δ.

Proposition 13. *Spin bundles S_Δ with odd theta characteristics Δ possess global holomorphic sections.*

If Δ is a non-singular theta characteristic then the corresponding positive divisor D_Δ of degree $g - 1$ is unique (see the proof of Proposition 11). This implies the uniqueness of the differential with $(\omega) = D_\Delta$ and $h^0(S_\Delta) = 1$. This holomorphic section is given by

$$\sqrt{\sum_{i=1}^{g} \frac{\partial \theta}{\partial z_i}(\Delta)\omega_i} \ .$$

1.8 Schottky Uniformization

1.8.1 Schottky Group

Let $C_1, C_1', \ldots, C_N, C_N'$ be a set of $2N$ mutually disjoint Jordan curves on $\hat{\mathbb{C}}$. They comprise the boundary of a domain $\Pi \subset \hat{\mathbb{C}}$ which is a topological sphere with $2N$ holes (see Fig. 1.22). Let us assume that the curves C_n and C_n' are identified by $\sigma C_n = C_n'$ where σ is a loxodromic transformation,

$$\frac{\sigma_n z - B_n}{\sigma_n z - A_n} = \mu_n \frac{z - B_n}{z - A_n} \ , \quad |\mu_n| < 1, \quad n = 1, \ldots, N \ , \tag{1.96}$$

which maps the exterior of C_n to the interior of C_n'. The points A_n, B_n are the fixed points of this transformation.

Fractional-linear transformations can be canonically identified with the elements of the matrix group $\mathrm{PSL}(2,\mathbb{C})$:

$$\begin{pmatrix} a\ b \\ c\ d \end{pmatrix} \ \leftrightarrow \ \sigma z = \frac{az - b}{cz - d} \ , \quad a, b, c, d \in \mathbb{C} \ , \quad ad - bc = 1 \ . \tag{1.97}$$

The canonical matrix representation of the transformation (1.96) is as follows

$$\begin{pmatrix} a\ b \\ c\ d \end{pmatrix} = \frac{1}{A - B} \begin{pmatrix} A\sqrt{\mu} - \frac{B}{\sqrt{\mu}} & AB(\frac{1}{\sqrt{\mu}} - \sqrt{\mu}) \\ \sqrt{\mu} - \frac{1}{\sqrt{\mu}} & \frac{A}{\sqrt{\mu}} - B\sqrt{\mu} \end{pmatrix} \ .$$

The derivative of the transformation (1.97) is $\sigma' z = (cz + d)^{-2}$. It is an isometry for the points satisfying $|cz + d| = 1$. These points comprise the *isometric circle* C_σ of σ with the center at $-\frac{d}{c}$ and the radius $\frac{1}{|c|}$. The isometric circles C_σ and $C_{\sigma^{-1}}$ of the transformations (1.96) have equal radii and are disjoint.

Definition 37. *The group G generated by the transformations $\sigma_1, \ldots, \sigma_N$ is called a* Schottky group. *If all the boundary curves C_n, C_n' are circles the Schottky group is called* classical.
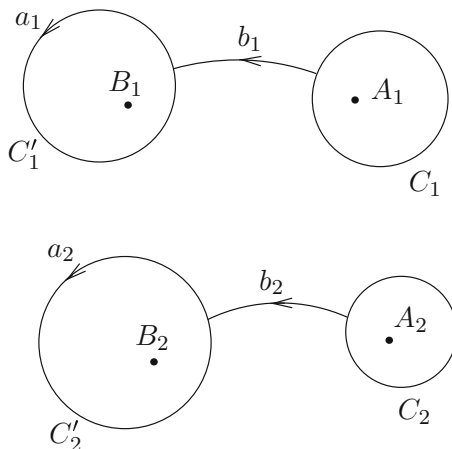
Fig. 1.22. The fundamental domain Π of a Schottky group with a canonical homology basis. The cycles a_n coincide with the positively oriented C_n' ; b_n run on Π between the points $z_n \in C_n$ and $\sigma_n z_n \in C_n'$

These groups were introduced in [Sch87] by Schottky who has established their fundamental properties and investigated their automorphic functions. The domain Π is the fundamental domain of the group G. The existence of nonclassical (for an arbitrary system of generators) Schottky groups is shown in [Mar74]. A special case of classical Schottky groups are the Schottky groups with fundamental domains bounded by isometric circles of their generators. General Schottky groups can be characterized as free, purely loxodromic finitely generated discontinuous groups [Mas67].

The limit set $\Lambda(G)$ of the Schottky group is the closure of the fix points of all its elements. The discontinuity set $\Omega(G) = \mathbb{C} \setminus \Lambda(G)$ factorized with respect to G is a compact Riemann surface $\Omega(G)/G$ of genus N. According to the classical uniformization theorem [Fo29] any compact Riemann surface of genus N can be represented in this form.

Theorem 29 (Schottky uniformization). *Let $\mathcal{R}$ be a Riemann surface of genus N with a set of homologically independent simple disjoint loops $v_1, \ldots, v_N$. Then there exists a Schottky group G such that*

$$\mathcal{R} = \Omega(G)/G ,$$

and the fundamental domain $\Pi(G)$ is conformally equivalent to $\mathcal{R}$ cut along the loops $v_1, \ldots, v_N$.

Under the Schottky uniformization the loops v_n are mapped to the boundary curves C_n, C_n'. The loop system $v_1, \ldots, v_N$ generates a subgroup of the homology group $H_1(\mathcal{R}, \mathbb{Z})$. Two loop systems generating the same subgroup

determine the same Schottky group but with a different choice of generators. The Schottky groups G and G' corresponding to the loop systems generating different subgroups of $H_1(\mathcal{R}, \mathbb{Z})$ are different.

The Schottky group is parametrized by the fix points $A_1, B_1, \ldots, A_N, B_N$ of the generators and their trace parameters $\mu_1, \ldots, \mu_N$. The Schottky groups G and G' with the parameters $A_1, B_1, \ldots, A_N, B_N$ and $A'_1, B'_1, \ldots, A'_N, B'_N$ which differ by a common fractional-linear transformation uniformize the same Riemann surface. This parameter counting gives the correct number $3N-3$ for the complex dimension of the moduli space of Riemann surfaces of genus N.

It is unknown whether every Riemann surface can be uniformized by a classical Schottky group.

The Schottky uniformization of $\mathcal{R}$ is determined by a half basis of $H_1(\Omega(G)/G, \mathbb{Z})$, and it is natural to choose a canonical basis of $H_1(\mathcal{R}, \mathbb{Z})$ respecting this structure. Such a canonical basis of cycles is illustrated in Fig. 1.22: the cycle a_n coincides with the positively oriented curve C'_n, and the cycle b_n connects the points $z_n \in C_n$ and $\sigma_n z_n \in C'_n$, and the b-cycles are mutually disjoint.

1.8.2 Holomorphic Differentials as Poincaré Series

Denote by G_n the subgroup of the Schottky group G generated by σ_n. The cosets G/G_n and $G_m \backslash G/G_n$ are the sets of all elements

$$\sigma = \sigma_{i_1}^{j_1} \ldots \sigma_{i_k}^{j_k} \,, \quad i \in \{1, \ldots, N\} \,, \ j \in \mathbb{Z} \setminus \{0\} \,,$$

such that $i_k \neq n$ and for $G_m \backslash G/G_n$ in addition $i_1 \neq m$.

The following theorem is classical (see [Bur92, Bak97]).

Theorem 30. *If the Poincaré series*

$$\omega_n = \sum_{\sigma \in G/G_n} \left(\frac{1}{z - \sigma B_n} - \frac{1}{z - \sigma A_n} \right) \mathrm{d}z \tag{1.98}$$

are absolutely convergent on $\Pi(G)$, they are holomorphic differentials of the Riemann surface $\Omega(G)/G$ normalized in the canonical basis shown in Fig. 1.22. The period matrix is

$$B_{nm} = \sum_{\sigma \in G_m \backslash G/G_n} \log\{B_m, \sigma B_n, A_m, \sigma A_n\} \,, \quad m \neq n \,,$$

$$B_{nn} = \log \mu_n + \sum_{\sigma \in G_n \backslash G/G_n} \log\{B_n, \sigma B_n, A_n, \sigma A_n\} \,, \tag{1.99}$$

where the curly brackets denote the cross-ratio

$$\{z_1, z_2, z_3, z_4\} = \frac{(z_1 - z_2)(z_3 - z_4)}{(z_2 - z_3)(z_4 - z_1)} \,.$$

The series (1.98) have no poles in $\Pi(G)$. The normalization $\int_{a_m} \omega_n = 2\pi i \delta_{nm}$ follows from a computation of residues. Indeed, if $\sigma = \sigma_{i_1}^{j_1} \ldots \sigma_{i_k}^{j_k}$, $\sigma \neq I$, then both the points σB_n and σA_n are inside of C'_{i_1} when $j_1 > 0$, and inside of C_{i_1} when $j_1 < 0$. Only for $\sigma = I$ the images σB_n and σA_n are separated: B_n is inside of C'_n and A_n is inside of C_n.

The series (1.98) are (-2)-dimensional Poincaré series and can be written in a slightly different form

$$\omega_n = \sum_{\sigma \in G_n \backslash G} \left(\frac{1}{\sigma z - B_n} - \frac{1}{\sigma z - A_n} \right) \sigma' z \mathrm{d}z \ , \quad \sigma' z = \frac{1}{(cz+d)^2} \ .$$

In this form it is easy to see that $\omega_n(\sigma z) = \omega_n(z)$, so ω_n is a holomorphic differential on $\mathcal{R} = \Omega(G)/G$. Using the invariance of the cross-ratio with respect to fractional-linear transformations

$$\{\sigma z_1, \sigma z_2, \sigma z_3, \sigma z_4\} = \{z_1, z_2, z_3, z_4\}$$

one can derive (1.99) from the definition of the period matrix.

The problem of convergence of Poincaré series describing holomorphic differentials is a non-trivial problem of crucial importance since one cannot rely on computations with divergent series. This problem is ignored in some applied papers. For general Schottky groups and even for classical ones the (-2)-dimensional Poincaré theta series can be divergent. However, the convergence of these series is guaranteed if the fundamental domain $\Pi(g)$ is "circle decomposable":

Assume that the Schottky group is classical and that $2N - 3$ circles $L_1, \ldots, L_{2N-3}$ can be fixed on the fundamental domain $\Pi(G)$ so that the following conditions are satisfied:

- (a) The circles $L_1, \ldots, L_{2N-3}, C_1, C'_1, \ldots, C_N, C'_N$ are mutually disjoint.
- (b) The circles $L_1, \ldots, L_{2N-3}$ divide $\Pi(G)$ into $2N - 2$ regions $T_1, \ldots, T_{2N-2}$.
- (c) Each T_i is bounded by exactly three circles.

Such Schottky groups are called *circle decomposable* (see Fig. 1.23 for an example of a circle decomposable Schootky group). In particular, each Schottky group which has an invariant circle is circle decomposable by circles orthogonal to the invariant circle.

The following elegant geometric convergence result is due to Schottky [Sch87] (see also [FK65] for a proof).

Theorem 31 (Schottky condition). *(-2)-dimensional Poincaré theta series corresponding to a circle decomposable Schottky group is absolutely convergent on the whole fundamental domain of G.*
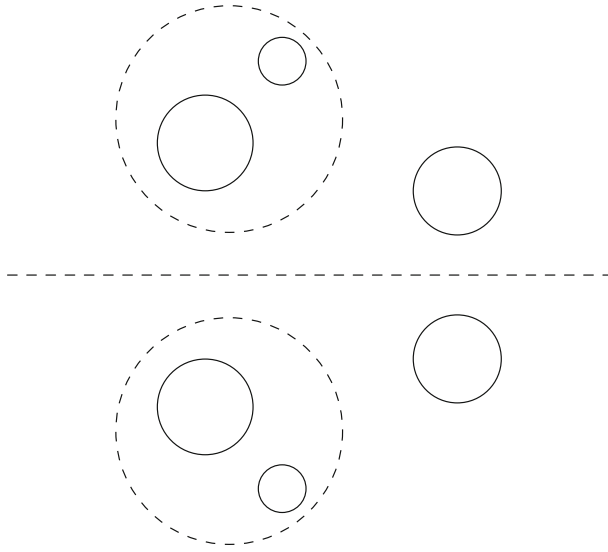
Fig. 1.23. The fundamental domain of a circle decomposable Schottky group

The convergence of (-2)-dimensional Poincaré theta series can be proved also in the case when the circles C_n, C_n', $n = 1, \ldots, N$ are small and far enough apart. The corresponding estimations can be found in [Bur92, Bak97] and in the contribution by Schmies in this volume.

The convergence of the Poincaré theta series can be characterized in terms of the metrical properties of the limiting set $\Lambda(G)$. If ν is the minimal dimension for which the $(-\nu)$-dimensional Poincaré theta series converge absolutely, then the Hausdorff measure of $\Lambda(G)$ is equal to $\frac{\nu}{2}$. In particular, the 1-dimensional Hausdorff measure of $\Lambda(G)$ of a Schottky group with divergent (-2)-dimensional Poincaré theta series is infinite. Examples of such classical Schottky groups with fundamental domains bounded by isometric circles can be found in [Myr16, Aka67]. The class of Schottky groups with convergent (-2)-dimensional Poincaré theta series is geometrically characterized in [Bow79].

1.8.3 Schottky Uniformization of Real Riemann Surfaces

As it was mentioned in the preceding sections the problem of convergence of the Poincaré theta series for the holomorphic differentials is of crucial importance. Another important problem for the practical application of Schottky uniformization is to determine the *Schottky space* $S = (A_1, B_1, \mu_1, \ldots, A_N, B_N, \mu_N) \subset \mathbb{C}^{3N}$ of the uniformizing Schottky groups. Both problems are so difficult that solving them for general Riemann surfaces seems hopeless.

The situation is more fortunate in the case of real Riemann surfaces, which is the most important for applications. In this case one can find a Schottky uniformization with convergent Poincaré series and describe the Schottky space S [Bob88, BBE+94]. Here we present the main ideas of this method.

Definition 38. *A Riemann surface $\mathcal{R}$ with an anti-holomorphic involution $\tau : \mathcal{R} \to \mathcal{R}$ is called a* real Riemann surface*. The connected components $X_1, \ldots, X_m$ of the set of fix points of τ are called real ovals. If $\mathcal{R} \setminus \{X_1, \ldots, X_m\}$ has two connected components the Riemann surface is called* of decomposing type.

There are real Riemann surfaces without fix point of τ. Let $\mathcal{R}$ be of decomposing type and $\mathcal{R}_+$ and $\mathcal{R}_-$ be two components of $\mathcal{R} \setminus \{X_1, \ldots, X_m\}$. Both $\mathcal{R}_\pm$ are Riemann surfaces of type (g, m), i.e., they are homeomorphic to a surface of genus $g = \frac{N+1-m}{2}$ with m boundary components.

Theorem 32. *Every real Riemann surface of decomposing type possesses a Schottky uniformization by a Fuchsian group G of the second kind. The Poincaré theta series of dimension -2 of G are absolutely convergent.*

The main idea behind this theorem is that in this case the Schottky group is of Fuchsian type. Indeed, consider the classical Fuchsian uniformization of the surface $\mathcal{R}_+ = H/G$. Here H is the upper half plane $H = \{z \in \mathbb{Z}, \Im z > 0\}$ and the group G is a purely hyperbolic Fuchsian group of the second kind [Fo29]. The matrix elements (1.97) of all the group elements of G are real and satisfy $|a+d| > 2$. The group G is generated by the hyperbolic transformations $\alpha_1, \beta_1, \ldots, \alpha_g, \beta_g$ and $\gamma_1, \ldots, \gamma_m$, $m > 0$, satisfying the constraint

$$\alpha_1 \beta_1 \alpha_1^{-1} \beta_1^{-1} \ldots \alpha_g \beta_g \alpha_g^{-1} \beta_g^{-1} \gamma_1 \ldots \gamma_m = I \ .$$

Extending the action of G to the lower half-plane $\overline{H} = \{z \in \mathbb{Z}, \Im z < 0\}$ we obtain another component $\mathcal{R}_- = \overline{H}/G$. The elements

$$\sigma_i = \alpha_i, \sigma_{g+i} = \beta_i, \sigma_{2g+j} = \gamma_j, \quad i = 1, \ldots, g; \ j = 1, \ldots, m-1$$

acting on the whole Riemann sphere $\hat{\mathbb{C}}$ generate a free, purely hyperbolic group, which is a Schottky group uniformizing the Riemann surface $\mathcal{R}$. It possesses an invariant circle, which is the real line, and therefore is circle decomposable. The convergence of the Poincaré series follows from Theorem 31. Note that the Schottky group is classical since the fundamental domain of the Fuchsian group can be chosen to be bounded by geodesics in the hyperbolic geometry. These geodesics are arcs of circles orthogonal to the real line.

The Schottky uniformization of real Riemann surfaces of decomposing type described above looks as follows. The circles C_n, C_n', $n = 1, \ldots, N$ are orthogonal to the real axis and their discs are disjoint (see Fig. 1.24 for the special case of M-curves). The order of circles is arbitrary. Every pair C_n, C_n' determines a hyperbolic transformation σ_n. The transformations $\sigma_1, \ldots, N$ generate a Schottky group uniformizing a real Riemann surface of decomposing

type. The number of real ovals is determined by the arrangement of the circles C_n, C_n', $n = 1, \ldots, N$. The Schottky parameters are real,

$$(A_1, B_1, \mu_1, \ldots, A_N, B_N, \mu_N) \in \mathbb{R}^{3N}, \quad 0 < \mu_n < 1, n = 1, \ldots, N .$$

The description of the Schottky space can be obtained from an analysis of the invariant lines of the group elements of G (see [Kee65, Nat04]). We present here the result for the case of M-curves.
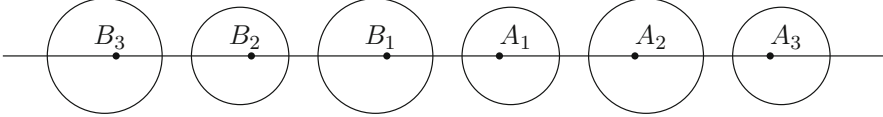
Fig. 1.24. Schottky uniformization of an M-curve

A real Riemann surface $\mathcal{R}$ of genus N with maximal possible number $m = N + 1$ of real ovals is called an *M-curve*. The real ovals decompose it into two components $\mathcal{R}_\pm$ which are topological spheres with $N + 1$ holes. The Schottky space S is described as follows [Bob88, BBE+94]:

$$B_N < B_{N-1} < \ldots < B_1 < A_1 < \ldots < A_N , \quad 0 < \sqrt{\mu_n} < 1, n = 1, \ldots, N ,$$

$$\{B_n, B_{n+1}, A_n, A_{n+1}\} > \left(\frac{\sqrt{\mu_n} + \sqrt{\mu_{n+1}}}{1 + \sqrt{\mu_n \mu_{n+1}}} \right)^2 , \quad n = 1, \ldots, N - 1 .$$

1.8.4 Schottky Uniformization of Hyperelliptic M-Curves

By imposing an additional symmetry to the Schottky data one obtains hyperelliptic Riemann surfaces. The additional constraint

$$B_n = -A_n, \quad n = 1, \ldots, N , \tag{1.100}$$

in the previous description of M-curves gives all hyperelliptic M-curves. All the considerations simplify in this case (see [BBE+94] for details).

In particular the fundamental domain Π of the Schottky group can be chosen symmetric with respect to the involution $\pi z = -z$. The boundary circles C_n, C_n' can be chosen to be the isometric circles of the corresponding hyperbolic generators. The center c_n and the radius r_n of C_n are as follows:

$$c_n = A_n \frac{1 + \mu_n}{1 - \mu_n} , \quad r_n = 2A_n \frac{\sqrt{\mu_n}}{1 - \mu_n} .$$

The involutions $\tau z = \bar{z}$ and $\tilde{\tau} = \tau \pi z = -\bar{z}$ are anti-holomorphic, and τ is the one with $N + 1$ real ovals. The Schottky group G is the subgroup of

index 2 of the group generated by the inversions i_n in the circles C_n and $\tilde{\tau}$, in particular $\sigma_n = \tilde{\tau} i_n$, $\sigma_n^{-1} = i_n \tilde{\tau}$. The intersection points of the circles C_n with the real axis

$$z_n^{\pm} = A_n \frac{1 \pm \sqrt{\mu_n}}{1 \mp \sqrt{\mu_n}}$$

as well as $z = 0$ and $z = \infty$ are the fix points of the hyperelliptic involution π.

The reduction (1.100) simplifies the period matrix,

$$B_{nm} = \sum_{\sigma \in G_m \backslash G / G_n} \log \left(\frac{A_m - \sigma(A_n)}{A_m - \sigma(-A_n)} \right)^2 ,$$

$$B_{nn} = \log \mu_n + \sum_{\sigma \in G_n \backslash G / G_n} \log \left(\frac{A_n - \sigma(A_n)}{A_n - \sigma(-A_n)} \right)^2$$

and the description of the Schottky set,

$$0 < A_1 < \ldots < A_N, \quad 0 < \sqrt{\mu_n} < 1 \, , n = 1, \ldots, N \, ,$$

$$\left(\frac{1 - \sqrt{\mu_n}}{1 - \sqrt{\mu_n}} \right) \left(\frac{1 - \sqrt{\mu_{n+1}}}{1 - \sqrt{\mu_{n+1}}} \right) > \frac{A_n}{A_{n+1}}, \quad n = 1, \ldots, N - 1 \, .$$

A meromorphic function $\lambda : \mathcal{R} \to \hat{\mathbb{C}}$ with double pole (at $z = \infty$) defining a two-sheeted covering (see Sect. 1.5.5) is given by the Poincaré theta series

$$\lambda(z) = \sum_{\sigma \in G} ((\sigma z)^2 - (\sigma 0)^2) \, .$$

The corresponding hyperelliptic curve is

$$\mu^2 = \lambda \prod_{n=1}^{N} (\lambda - \lambda(z_n^-))(\lambda - \lambda(z_n^+)) \, .$$

Acknowledgment

References

[Aka67]   Akaza, T.: Singular sets of some Kleinian groups. II. Nagoya Math. J. **29**, 149–162 (1967)

[AS60]   Ahlfors, L., Sario, L.: Riemann surfaces. Princeton mathematical series, vol. 26, xi+382 pp. Princeton University Press, Princeton, N.J. (1960)

[Ati71]   Atiyah, M.: Riemann surfaces and spin structures. Ann. Sci. École Norm.
           Sup. (4), **4**, 47–62 (1971)
[Bak97]   Baker, H.F.: Abelian functions. Abel's theorem and the allied theory of
           theta functions, Reprint of the 1897 original, xxxvi+684 pp. Cambridge
           University Press, Cambridge (1995)
[Bea78]   Beardon, A.F.: A Primer on Riemann Surfaces. London Math. Society
           Lecture Notes series, vol. 78, x+188 pp. Cambridge University Press,
           Cambridge (1984)
[BBE+94]   Belokolos, E.D., Bobenko, A.I., Enolskii V.Z., Its, A.R., Matveev, V.B.:
           Algebro-geometric approach to nonlinear integrable equations. Springer
           Series in Nonlinear Dynamics, xii+337 pp. Springer, Berlin (1994)
[Bob88]   Bobenko, A.I.: Schottky uniformization and finite-gap integration. Sov.
           Math. Dokl. **36**(1), 38–42 (1988)
[Bos]   Bost, J.-B.: Introduction to Compact Riemann Surfaces, Jacobians,
           and Abelian Varieties. In: Waldschmidt, M., Moussa, P., Luck, J.-M.,
           Itzykson, C. (eds.) From Number Theory to Physics, pp. 64–211.
           Springer, Berlin (1992)
[Bow79]   Bowen, R.: Hausdorff dimension of quasicircles. Inst. Hautes E'tudes Sci.
           Publ. Math. **50**, 11–25 (1979)
[Bur92]   Burnside, W.: On a class of automorphic functions. Proc. Lond. Math.
           Soc. **23**, 49–88, 281–295 (1892)
[FK92]   Farkas, H.M., Kra, I.: Riemann Surfaces. Second edition, Graduate Texts
           in Mathematics, vol. 71, xvi+363 pp. Springer, New York (1992)
[Fo29]   Ford, L.R.: Automorphic Functions, vii+333 pp. McGraw-Hill, New York
           (1929)
[FK65]   Fricke, R., Klein, F.: Vorlesungen über die Theorie der automorphen
           Funktionen. Johnson Reprint Corp., New York; B.G. Teubner Verlags-
           gesellschaft, Stuttgart, xiv+634 pp., xiv+668 pp. (1965)
[GH94]   Griffiths, P., Harris J.: Principles of Algebraic Geometry. Reprint of the
           1978 original, Wiley Classics Library, xiv+813 pp. Wiley, New York
           (1994)
[Gu66]   Gunning, R.: Lectures on Riemann Surfaces. Princeton Math. Notes,
           iv+254 pp. Princeton University Press, Princeton, N.J. (1966)
[Jos06]   Jost, J.: Compact Riemann Surfaces. An introduction to contemporary
           mathematics. 3d edition, Universitext, xviii+277 pp. Springer, Berlin
           (2006)
[Kee65]   Keen, L.: Canonical polygons for finitely generated Fuchsian groups.
           Acta Math. **115**, 1–16 (1965)
[Lew64]   Lewittes, J.: Riemann surfaces and the theta functions. Acta Math. **111**,
           35–61 (1964)
[Mar74]   Marden, A.: Schottky groups and Circles. In: Contribut. to Analysis,
           Collect. of Papers dedicated to Lipman Bers, pp. 273–278. Academic,
           New York (1974)
[Mas67]   Maskit, B.: A characterization of Schottky groups. J. Anal. Math. **19**,
           227–230 (1967)
[Myr16]   Myrberg, P.J.: Zur Theorie der Konvergenz der Poincaréschen Reihen. I,
           II. Ann. Acad. Sci. Fenn. (A) **9**(4), 1–75 (1916)
[Nat04]   Natanzon, S.M.: Moduli of Riemann surfaces, real algebraic curves, and
           their superanalogs. Translations of Mathematical Monographs, vol. 225,
           viii+160 p. AMS, Providence, RI (2004)

[Schm]   Schmies, M.: Computing Poincaré theta Series for Schottky Groups. In:
           Bobenko, A.I., Klein, Ch. (eds.) Lecture Notes in Mathematics 2013,
           pp. 165–181. Springer, Berlin (2011)
[Sch87]   Schottky, F.: Über eine specielle Function, welche bei einer bestimmten
           linearen Transformation ihres Argumentes unverändert bleibt. J. Reine
           Angew. Math. **101**, 227–272 (1887)
[Sie71]   Siegel, C.L.: Topics in complex functions theory. Vol. II: Automorphic
           functions and Abelian integrals. Interscience Tracts in Pure and Applied
           Mathematics, vol. 25, ix+193 pp. Wiley, New York (1971)
[Spi79]   Spivak, M.: A Comprehensive Introduction to Differential Geometry,
           vol. 1–5, 2d edn. Publish or Perish, Boston (1979)
[Spr81]   Springer, G.: Introduction to Riemann Surfaces. 2nd ed., 309 p. Chelsea
           Publishing Co., New York (1981)

Part II Algebraic Curves

2

Computing with Plane Algebraic Curves and Riemann Surfaces: The Algorithms of the Maple Package "Algcurves"

Bernard Deconinck[1] and Matthew S. Patterson[2]

[1] Department of Applied Mathematics, University of Washington
Seattle WA 98195-2420, USA,
`bernard@amath.washington.edu`
[2] Boeing Research and Technology
2760 160th Ave SE
Bellevue, WA 98008, USA

2.1 Introduction

In this chapter, we present an overview of different algorithms for computing with compact connected Riemann surfaces, obtained from desingularized and compactified plane algebraic curves. As mentioned in Chap. 1 [Bob11], all compact connected Riemann surfaces may be represented this way. The Maple package "algcurves", largely developed by the authors and Mark van Hoeij contains implementations of these algorithms. A few recent additions to the "algcurves" package are not due to the authors or Mark van Hoeij. The algorithm behind those commands are not discussed here as they have no bearing on anything associated with Riemann surfaces.

Because some of the algorithms presented here are algebraic in nature, they rely on exact arithmetic, which implies that the coefficients of the algebraic curves are required to have an exact representation. Most importantly, floating point numbers are not allowed as coefficients for these algorithms. The reason for not allowing floating point numbers is that the geometry of the Riemann surface is highly dependent on the accuracy of the coefficients in its algebraic curve representation. If an algebraic curve has singularities, then, almost surely, the nature of these singularities will be affected by inaccuracies in the coefficients of the curve. This may affect the algebraic algorithms discussed below, such as those for the calculation of the genus, homology and holomorphic 1-forms on the Riemann surface. Users of the "algcurves" package can consider floating point coefficients, but these need to be converted to a different form (rational, for instance), before the programs will accept the input. Furthermore, since we are using algebraic curves to represent Riemann surfaces, the algebraic curves are always considered over the

complex numbers. Throughout this chapter, "calculation" is used when exact results are obtained, whereas "computation" is used for numerical results.

Apart from the restriction to an exact representation, all of the algorithms discussed in detail in this chapter are general in the sense that they apply to all compact connected Riemann surfaces. An appendix is presented discussing the use of a few algorithms that apply to a restricted class of algebraic curves and Riemann surfaces, such as elliptic and hyperelliptic surfaces. This appendix contains many examples, but no detailed explanation of the specifics of the algorithms.

All of the descriptions of the algorithms of the main body of this chapter are preceded by the next section which outlines the connection between plane algebraic curves and Riemann surfaces with a level of detail appropriate for what follows. The work reviewed here may be found in [DvH01, DP07a, Pat07, vH95, vH94]. The examples of the implementations use commands available in Maple 11 (Released Spring 2007). A few commands are used that are not available in Maple 11 yet. They are identified as such in the text.

2.2 Relationship Between Plane Algebraic Curves and Riemann Surfaces

In this section, some required background from the theory of Riemann surfaces is introduced. More details can be found in such standard references as [FK92, Spr57]. Excellent places to read up on Riemann surfaces and how they relate to plane algebraic curves that do not require an extensive background are the monographs by Brieskorn and Knörrer [BK86] and Griffiths [Gri89].

Consider a plane algebraic curve, defined over the complex numbers $\mathbb{C}$, i.e., consider the subset of $\mathbb{C}^2$ consisting of all points (x, y) satisfying a polynomial relation in two variables x and y with complex coefficients:

$$f(x,y) = a_n(x)y^n + a_{n-1}(x)y^{n-1} + \ldots + a_1(x)y + a_0(x) = 0 . \qquad (2.1)$$

Here $a_j(x)$, $j = 0, \ldots, n$ are polynomials in x. Write $a_j(x) = \sum_i a_{ij}x^i$, where the coefficients a_{ij} are complex numbers. Assuming $a_n(x)$ does not vanish identically, n is the degree of $f(x, y)$ considered as a polynomial in y. We only consider irreducible algebraic curves, so $f(x, y)$ cannot be written as the product of two non-constant polynomials with complex coefficients.

Let d denote the degree of $f(x, y)$ as a polynomial in x and y, i.e., d is the largest $i + j$ for which the coefficient a_{ij} of $x^i y^j$ in $f(x, y)$ is non-zero. The behavior at infinity for both x and y is examined by homogenizing $f(x, y) = 0$ by letting

$$x = X/Z , \quad y = Y/Z , \qquad (2.2)$$

and investigating

$$F(X, Y, Z) = Z^d f(X/Z, Y/Z) = 0 . \qquad (2.3)$$

Here $F(X, Y, Z)$ is a homogeneous polynomial equation of degree d. Finite points $(x, y) \in \mathbb{C}^2$ on the algebraic curve correspond to triples $(X : Y : Z)$ with $Z \neq 0$. Since for these points $(X : Y : Z) = (X/Z : Y/Z : 1)$, we may equate $Z = 1$, so finite points can be denoted unambiguously by (x, y) instead of $(X/Z, Y/Z)$. Points at infinity correspond to triples $(X : Y : Z)$, with $Z = 0$. Hence, at a point at infinity, at least one of the two coordinate functions x or y is infinite. Because $F(X, Y, 0)$ is a homogeneous polynomial of degree d, there are at most d points at infinity.

The algebraic curve can have singular points. An algorithm to efficiently calculate the singular points of an algebraic curve is discussed in Sect. 2.5. Here we briefly discuss singularities as they need to be dealt with in order to construct the Riemann surface from an algebraic curve. Finite singular points on the algebraic curve specified by $f(x, y) = 0$ satisfy $f(x, y) = 0 = \partial_x f(x, y) = \partial_y f(x, y)$. Points at infinity can also be singular. Singular points at infinity satisfy $\partial_X F(X, Y, Z) = \partial_Y F(X, Y, Z) = \partial_Z F(X, Y, Z) = 0$ (then also $F(X, Y, Z) = 0$, by Euler's theorem for homogeneous functions). Desingularizing the algebraic curve results in a Riemann surface, i.e., a one-dimensional complex-analytic manifold (so it is two-dimensional over the real numbers; it is a surface). There are various ways of desingularizing algebraic curves. Our methods use Puiseux series, as detailed in Sect. 2.3. Each nonsingular point on the algebraic curve corresponds to one place[1] on the Riemann surface, whereas a singular point on the algebraic curve can correspond to multiple places on the Riemann surface.

In what follows, Γ is used to denote the Riemann surface obtained by desingularizing and compactifying (by adding the places at infinity) the algebraic curve represented by $f(x, y) = 0$. All Riemann surfaces obtained this way are connected (because $f(x, y)$ is irreducible) and compact (because the points at infinity are included). Conversely, as stated in Chap. 1 it is known that every compact connected Riemann surface can be obtained as described above [BBE+94, Spr57]. From here on out, all Riemann surfaces considered are understood to be connected and compact. We use $\hat{\Gamma}$ to denote the compactified, not desingularized algebraic curve.

2.3 Puiseux Series

Many of the algorithms presented in the next sections make use of local coordinates on an algebraic curve. For our algorithms, this local behavior is understood using Puiseux expansions. These expansions allow us to distinguish between regular points, branch points and singular points. Further, in addition to determine the nature of singular points, Puiseux expansions characterize

---

[1] We use the term "point" to denote a value in the complex x-plane. On the other hand, "place" is used to denote a location on the Riemann surface Γ, or, unambiguously, a location on the desingularized plane algebraic curve.

the topology of an algebraic curve near branch points. One way to look at this is that Puiseux series are our way to desingularize the algebraic curves we are working with. There are other ways of doing so, all with their advantages and disadvantages. A popular alternative is the use of quadratic transformations to "lift" the singular plane algebraic curve to a higher-dimensional nonsingular curve [Abh90].

Newton's Theorem, which we summarize below, completely describes the local behavior of a plane algebraic curve. Over the neighborhoods of a regular point $x = \alpha$ the coordinate function y is given locally as a series in ascending powers of $x - \alpha$ [Bli66]. Near a branch point however, y is given necessarily by a series with ascending fractional powers in $x - \alpha$. Such series are known as *Puiseux series*. It is common to choose a local parameter, say t, such that x and y are written as Laurent series in that local parameter.[2] That is, if α is a branch point of order r, then $t^r = x - \alpha$, and y is written as a Laurent series in t. A pair $(x(t), y(t))$ is referred to as a Puiseux expansion as it is equivalent to a Puiseux series.

2.3.1 Newton's Theorem

In a lift of the neighborhood of $x = \alpha$, the n y-roots of (2.1) are determined by a number $\leq n$ of pairs of expansions of the form

$$P_j = \left(x = \alpha + t^{r_j}, y = \beta_j t^{s_j} + \beta_j' t^{s_j'} + \cdots \right) \tag{2.4}$$

with $r_j, s_j, s_j', \ldots \in \mathbb{Z}$, $t \in \mathbb{C}$, $\alpha, \beta_j, \beta_j', \ldots \in \mathbb{C}$. Here $|r_j|$ is the number (the *branching number*) of y-roots that merge at place P_j. If $|r_j| > 1$ for one of the P_j, then α is a branch point and P_j is a branch place. For $|t| > 0$, a place P_j represents $|r_j|$ distinct y-values and $\sum_j |r_j| = n$. The coefficients $\beta, \beta', \ldots$ are all non zero; only a finite number of the integer exponents $s_j < s_j' < \ldots$ are negative; and $|r_j|$ is coprime with at least one of the $s_j, s_j', \ldots$. For places over $x = \infty$, one has $\alpha = 0$ and $r_j < 0$, i.e., $x = 1/t^{-r_j}$. A Puiseux expansion evaluated at $t = 0$ is called a *center*.

The algorithm to compute Puiseux expansions implemented in the "algcurves" package is essentially that described by Newton in letters to Oldenburg and Leibniz [BK86]. A treatment of the algorithm with much detail may be found, for instance, in [Wal62]. The paper by van Hoeij [vH94] discusses a modern implementation of the algorithm, most importantly providing a method allowing one to determine how many terms of the expansions are required to guarantee distinct branches are recognized as such.

---

[2] For finite points, only Taylor series in the local parameter are required. Laurent series with a finite number of singular terms are necessary to encompass points at infinity.
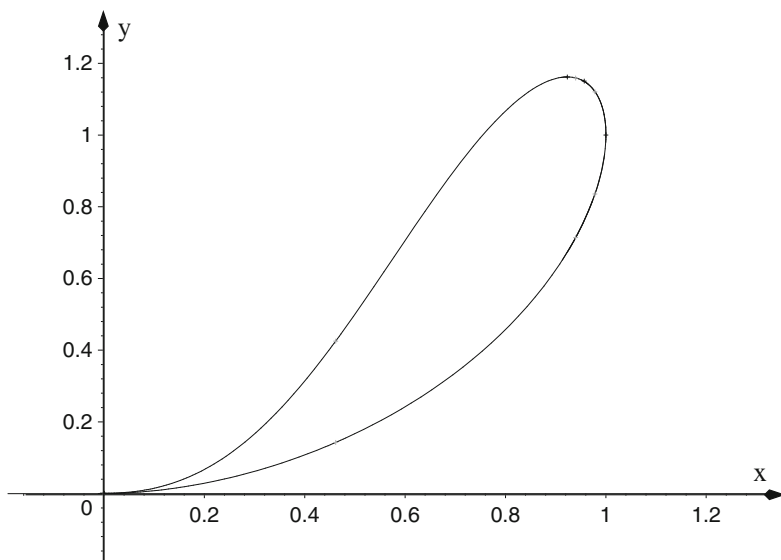
Fig. 2.1. The real graph of the Ramphoid cusp curve

Example. Consider the curve

$$f(x, y) = (x^2 - x + 1)y^2 - 2x^2y + x^4 = 0 . \tag{2.5}$$

Note that for this example $a_n(x) = x^2 - x + 1$ is not constant, a fact complicating the calculation of Puiseux expansions [Bli66]. Nevertheless, such computations are still possible. The curve (2.5) is known as a "ramphoid cusp" because of the structure of the real part of the graph at the origin [Wal62], as shown in Fig. 2.1. The graph was produced using the command plot_real_curve of the "algcurves" package. We compute the local structure of this curve at two different x-values. First we compute the expansions over $x = 0$, which is not a zero of a_n, and second, the expansions over one of the roots of $a_n(x) = 0$.

The command puiseux used below computes the y-expansions of $f(x, y) = 0$ over $x = 0$. To give zero as the fourth argument of this command implies that the procedure calculates as many terms as are necessary to distinguish separate expansions.

```
># read in the package
>with(algcurves):
># define the algebraic curve
>f:=x^4+x^2*y^2-2*x^2*y-y^2*x+y^2:
># compute the Puiseux expansions over x=0
>puiseux(f,x=0,y,0);
```

$$\left\{ x^2 + x^{5/2} \right\}$$

Note that $x = 0$ is a branch point by virtue of the fractional power in the second term. This one expansion represents two distinct places for $|x| > 0$. To recover both roots near $x = 0$ one 'conjugates' the series using the r-th roots of unity, where r is the greatest common denominator of the exponents of the series. Thus, one makes the r substitutions $x \mapsto e^{2\pi i j/r} x$, $j = 1, \ldots, r$. In this case, the $r = 2$ different y-roots are

$$y = \left\{ x^2 + x^{5/2} + \cdots, x^2 - x^{5/2} + \cdots \right\}.$$

If, instead of 0, the fourth argument is specified to be a positive integer value M, then the expansions are computed up to x^M. For example, if $M = 4$, then the $x^{7/2}$ term is included, but terms of order x^4 and higher are not.

```
>puiseux(f,x=0,y,4);
```

$$\left\{ x^2 + x^{5/2} + x^3 + \frac{1}{2} x^{7/2} \right\}$$

```
>puiseux(f,x=0,y,5);
```

$$\left\{ x^2 + x^{5/2} + x^3 + \frac{1}{2} x^{7/2} - \frac{5}{8} x^{9/2} \right\}$$

Including a fifth argument t in the call to `puiseux` changes the output. In this case the output is a pair of expansions in the local parameter t.

```
>f:=x^4+x^2*y^2-2*x^2*y-y^2*x+y^2:
># compute the Puiseux expansions using local coordinate t
>puiseux(f,x=0,y,0,t);
```

$$\{[x = t^2, y = t^4 + t^5]\}$$

2.4 Integral Basis

We start by explaining the concept of an integral basis. Integral bases are used in all aspects of algebra, but they have become particularly important with the rise of computer algebra systems, as their construction often allows convenient calculation of many other derived quantities. An example of this in our chapter is the use of the integral basis for the calculation of the holomorphic 1-forms on a Riemann surface, see Sect. 2.9. Another example is their use in the algorithmic integration in finite terms of algebraic functions.

Consider the coordinate functions x and y on the Riemann surface Γ. These two functions are algebraically dependent, by the defining equation $f(x, y) = 0$. Denote by $A(\Gamma)$ the part of the Riemann surface where both x

and y are finite. Also, let $O_{A(\Gamma)}$ be the set of all meromorphic functions on the Riemann surface that have no poles in $A(\Gamma)$. For example, $O_{A(\Gamma)}$ contains $\mathbb{C}[x, y]$, the set of all polynomials in x and y: since in $A(\Gamma)$ both x and y are finite, any polynomial of x and y results in a finite value as well. If the algebraic curve has no finite singularities, then every meromorphic function on the Riemann surface without poles in $A(\Gamma)$ can be represented as a polynomial in x and y, hence $O_{A(\Gamma)} = \mathbb{C}[x, y]$ if the curve has no finite singularities. In general, $O_{A(\Gamma)}$ is the integral closure of $\mathbb{C}[x, y]$ in the meromorphic functions on A: it is the set of all meromorphic functions g on $A(\Gamma)$ which satisfy a monic polynomial equation

$$g^m + \gamma_{m-1}(x, y)g^{m-1} + \ldots + \gamma_1(x, y)g + \gamma_0(x, y) = 0 , \qquad (2.6)$$

for a certain positive integer m and coefficients $\gamma_i(x, y)$, $i = 0, 1, \ldots, m-1$ from $\mathbb{C}[x, y]$. Note that for $m = 1$ we get $\mathbb{C}[x, y] \subset O_{A(\Gamma)}$, so all polynomials in x and y are in $O_{A(\Gamma)}$. An integral basis $\{\beta_0, \ldots, \beta_{n-1}\}$ of $O_{A(\Gamma)}$ can be computed such that every element of $O_{A(\Gamma)}$ can be written as a linear combination of $\beta_0, \ldots, \beta_{n-1}$ with coefficients that are polynomial in x only.

An efficient method to calculate an integral basis of $O_{A(\Gamma)}$, using Puiseux expansions, is given in [vH94]. The algorithm is as follows. We put $\beta_0 = 1$. To construct β_k, $k = 1, \ldots, n - 1$, we repeat the following steps:

1. Make the guess $\beta_k = y^k$. Actually, the algorithm in [vH94] uses the guess $\beta_k = y\beta_{k-1}$, which is more efficient. The examples below are easier to work out with $\beta_k = y^k$. The results, of course, are equivalent.
2. Define V to be the set of all elements v,

$$v = \sum_{j=0}^{k} w_j(x)y^j , \qquad (2.7)$$

   where the $w_j(x)$ are rational functions of x, such that v is regular on $A(\Gamma)$, modulo the linear combinations of β_j, $j = 1, \ldots, k$, where the coefficients of the linear combinations are polynomial in x.
3. If V is not empty, we choose an element $\hat{v}$ of V of the form

$$\hat{v} = \frac{\sum_{j=0}^{k} \hat{w}_j(x)\beta_j}{k(x)} . \qquad (2.8)$$

   Here $\hat{w}_j(x)$, $j = 1, \ldots, k$ and $k(x)$ are polynomial in x. Also, $\hat{w}_k(x) \equiv 1$.
4. We replace our guess for β_k with $\hat{v}$, and repeat from step 2.

It is shown in [vH94] that the set V becomes smaller at every step, thus the algorithm terminates. We now briefly discuss this method using two examples.

Example. Consider the algebraic curve defined by

$$f(x, y) = y^3 - x^7 + 2x^3y = 0 . \qquad (2.9)$$

This curve has one finite singular point at $(x, y) = (0, 0)$. The Puiseux expansions at this point are

$$P_1 : (x = t, y = t^4/2 + \ldots) , \quad P_2 : (x = -2t^2, y = 4t^3 + \ldots). \qquad (2.10)$$

- We start with $\beta_0 = 1$.
- Our first guess is $\beta_1 = y$. With this guess, the set V consists of all elements $v = w_0(x) + w_1(x)y$ that do not contain any polynomial part that is of first degree in y. Since we are interested in the behavior at the origin $x = y = 0$, we can represent v as

$$v = \frac{w_{0,-1}}{x} + \frac{w_{0,-2}}{x^2} + \ldots + \frac{w_{0,-p}}{x^p} + \left(\frac{w_{1,-1}}{x} + \frac{w_{1,-2}}{x^2} + \ldots + \frac{w_{1,-q}}{x^q} \right) y ,$$
$$(2.11)$$

for some positive integers p and q.

Imposing the regularity of this expression at the singular point requires the vanishing of $w_{0,k}$, $k = -1, -2, \ldots$, and of $w_{1,k}$, $k \neq -1$. Thus v has to be proportional to y/x. This leads us to our second guess for β_1, namely $\beta_1 = y/x$. We now repeat the above. With this new guess we find that v cannot have a polynomial part in x, nor a part that is linear in y and at worst has a first-order pole at $x = 0$. As a result, the set V is empty, and we conclude that $\beta_1 = y/x$.

- Our first guess for β_2 is $\beta_2 = y^2$ and the set V consists of all elements $v = w_0(x) + w_1(x)y + w_2(x)y^2$, modulo polynomials in x, multiplied by 1, y/x or y^2. Again using a Laurent series approach and imposing regularity at the places P_1 and P_2 we find that v is of the form $v = w_{2,-1}y^2/x + w_{2,-2}y^2/x^2 + w_{2,-3}y^2/x^3$. Several choices are possible. If we make the worst choice (i.e., the choice leading to the longest iteration) and make our new guess $\beta_2 = y^2/x$, we repeat this loop, only to conclude that the new set V contains elements of the form $w_{2,-2}y^2/x^2 + w_{2,-3}y^2/x^3$, a few more iterations lead us to our final guess: $\beta_2 = y^2/x^3$. With this guess we determine the set V to be empty.

This concludes the construction of the integral basis for this example. As a last check, we verify explicitly that y/x and y^2/x^3 satisfy monic polynomial equations with coefficients that are polynomials in x and y. Indeed:

$$\left(\frac{y}{x} \right)^3 + 2x \left(\frac{y}{x} \right) - x^4 = 0 , \quad \left(\frac{y^2}{x^3} \right)^2 + 2 \left(\frac{y^2}{x^3} \right) - xy = 0 . \qquad (2.12)$$

The command `integral_basis` calculates this integral basis immediately:

```
># load the algcurves package
>with(algcurves):
># define the algebraic curve
```
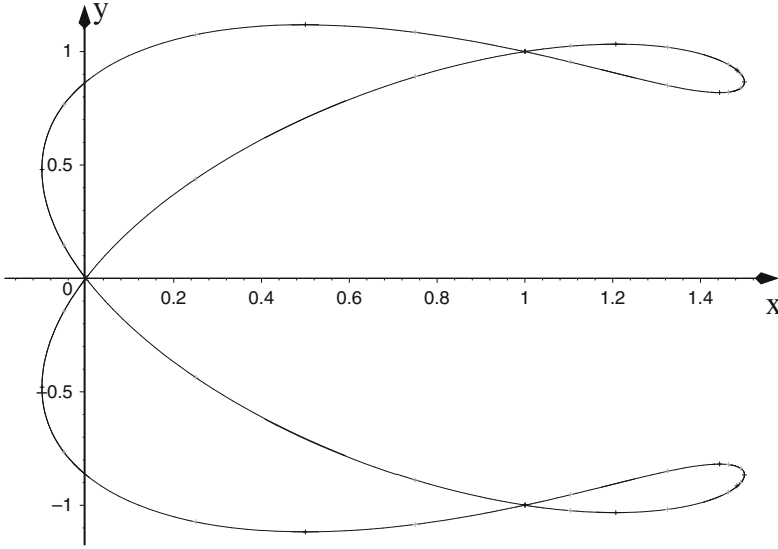
Fig. 2.2. The real graph of the Ampersand curve

```
>f:=y^3-x^7+2*x^3*y:
># calculate an integral basis for f(x,y)=0
>integral_basis(f,x,y);
```

$$\left[1, \frac{y}{x}, \frac{y^2}{x^3}\right]$$

Example. Consider the algebraic curve defined by

$$f(x,y) = (y^2 - x^2)(x - 1)(2x - 3) - 4(x^2 + y^2 - 2x)^2 = 0 \,. \qquad (2.13)$$

This curve is known as the Ampersand curve. Its graph for $(x, y) \in \mathbb{R}^2$ is shown in Fig. 2.2. The figure was produced using the `plot_real_curve` command of the "algcurves" package. The curve has three finite singular points (all double points): at $(x, y) = (0, 0)$, $(1, 1)$ and $(1, -1)$. The Puiseux expansions specifying the places at these points are:

$$(0,0): \begin{cases} P_1: (x = t, y = t\sqrt{19/3} + \ldots) \,, \\ P_2: (x = t, y = -t\sqrt{19/3} + \ldots) \,, \end{cases} \qquad (2.14)$$

$$(1,1): \begin{cases} P_3: (x = 1 + t, y = 1 + t(\sqrt{33} - 1)/16 + \ldots) \,, \\ P_4: (x = 1 + t, y = 1 - t(\sqrt{33} + 1)/16 + \ldots) \,, \end{cases} \qquad (2.15)$$

$$(1,-1): \begin{cases} P_5: (x = 1 + t, y = -1 + t(\sqrt{33} + 1)/16 + \ldots) \,, \\ P_6: (x = 1 + t, y = -1 - t(\sqrt{33} - 1)/16 + \ldots) \,. \end{cases} \qquad (2.16)$$

The other two places over $x = 0$ are regular; they are needed in the following calculation of the integral basis of (2.13).

- We start with $\beta_0 = 1$.
- Our first guess for β_1 is $\beta_1 = y\beta_0 = y$. With this guess, the set V consists of all elements $v = w_0(x) + w_1(x)y$ without any polynomial parts of first degree in y. Since we are interested in the behavior at the origin and at the singular points with $x = 1$, we represent v using a partial fraction decomposition as

$$
v = \frac{v_{0,-1}}{x} + \frac{v_{0,-2}}{x^2} + \ldots + \frac{w_{0,-1}}{x-1} + \frac{w_{0,-2}}{(x-1)^2} + \ldots +
$$
$$
\left(\frac{v_{1,-1}}{x} + \frac{v_{1,-2}}{x^2} + \ldots + \frac{w_{1,-1}}{x-1} + \frac{w_{1,-2}}{(x-1)^2} + \ldots \right) y . \quad (2.17)
$$

Here, and in the rest of this example, the dots denote that more terms may appear, but only a finite number. Imposing the regularity of this expression at the two regular places with $x = 0$ enforces $v_{j,k} = 0$, for all choices of j and k. Next, imposing the regularity of the remaining expression at P_3 to P_6 yields too many conditions, resulting in all coefficients being equated to zero. Thus $\beta_1 = y$.

- Our first guess for β_2 is $\beta_2 = y^2$ and the set V consists of all elements $v = w_0(x) + w_1(x)y + w_2(x)y^2$, modulo polynomials in x, multiplied by 1, y or y^2. Again using a partial fraction approach we write

$$
v = \frac{v_{0,-1}}{x} + \frac{v_{0,-2}}{x^2} + \ldots + \frac{w_{0,-1}}{x-1} + \frac{w_{0,-2}}{(x-1)^2} + \ldots +
$$
$$
\left(\frac{v_{1,-1}}{x} + \frac{v_{1,-2}}{x^2} + \ldots + \frac{w_{1,-1}}{x-1} + \frac{w_{1,-2}}{(x-1)^2} + \ldots \right) y +
$$
$$
\left(\frac{v_{2,-1}}{x} + \frac{v_{2,-2}}{x^2} + \ldots + \frac{w_{2,-1}}{x-1} + \frac{w_{2,-2}}{(x-1)^2} + \ldots \right) y^2 . \quad (2.18)
$$

We first impose the regularity conditions originating from the singular and regular points corresponding to $x = 0$. These only affect the coefficients $v_{j,k}$. From the Puiseux series P_1 and P_2, it follows immediately that $v_{j,k} = 0$ for $k < -2$. The remaining $v_{j,k}$ all vanish to ensure the regularity of v at the regular points over $x = 0$. Thus, at this stage the most general element of V is of the form

$$
v = \frac{w_{0,-1}}{x-1} + \frac{w_{0,-2}}{(x-1)^2} + \ldots + \left(\frac{w_{1,-1}}{x-1} + \frac{w_{1,-2}}{(x-1)^2} + \ldots \right) y +
$$
$$
\left(\frac{w_{2,-1}}{x-1} + \frac{w_{2,-2}}{(x-1)^2} + \ldots \right) y^2 . \quad (2.19)
$$

Regularity of v at the places P_3, ..., P_6 implies that all denominators in (2.19) are powers of t. Using the zeroth order Puiseux expansions at these places, we find that v reduces to

$$v = \frac{y^2 - 1}{x - 1}\left(w_{2,-1} + \frac{w_{2,-2}}{x - 1} + \frac{w_{2,-3}}{(x-1)^2} + \dots\right) . \qquad (2.20)$$

Lastly, all coefficients $w_{2,k}$ vanish for $k \neq -1$ as there are no numerators left to cancel their singularity. Thus,

$$v = w_{2,-1}\frac{y^2 - 1}{x - 1} , \qquad (2.21)$$

and we are led to choose $\beta_2 = (y^2 - 1)/(x - 1)$. With this choice, we determine the new set V to be empty. Thus we have determined the third element of the integral basis.

- To find the final element of the integral basis for (2.13), we initially guess $\beta_3 = y^3$. A similar to the above, but lengthier calculation results in

$$v = v_{3,-1}\frac{y(y^2 - 3/4)}{x} + \frac{y^2 - 1}{x - 1}(w_{3,-1}y + w_{2,-1}) . \qquad (2.22)$$

To choose a new representative for β_3, we impose (2.8), which leads to the choice

$$\beta_3 = \frac{4y^3 - xy - 3}{4x(x - 1)} . \qquad (2.23)$$

With this choice the new set V is found to be empty, thus we have finished the determination of the integral basis of (2.13).

The command `integral_basis` agrees with our calculation of the integral basis:

```
># load the algcurves package
>with(algcurves):
># define the algebraic curve
>f:=(y^2-x^2)*(x-1)*(2*x-3)-4*(x^2+y^2-2*x)^2:
># calculate an integral basis for f(x,y)=0
>integral_basis(f,x,y);
```

$$\left[1, y, \frac{-1 + y^2}{-1 + x}, \frac{y^3}{(-1 + x)x} - \frac{y(x + 3)}{4(-1 + x)x}\right]$$

A few simple algebraic manipulations confirm this integral basis to be identical to the one constructed for this example above.

2.5 Singularities of a Plane Algebraic Curve

The singularities of a plane algebraic curve are those points that prevent us from identifying the compactified algebraic curve with a Riemann surface. In order to obtain a Riemann surface from a plane algebraic curve, these singularities need to be resolved. There are various ways of doing this. A popular way (e.g. [Abh90]) is the use of quadratic transformations, to essentially unravel the behavior at the singular points by adding extra dimensions. Our approach is different. As discussed in Sect. 2.3, we employ Puiseux series. These do not allow us to unravel the behavior at the singular points, but they do allow us to determine how to pass through singular points. They determine a coordinate chart of the singular point, with which a coordinate atlas may be built, leading to the manifold structure required for a Riemann surface.

2.5.1 Computing the Singularities

Let us consider finite singularities first. We will consider singularities at infinity at the end of this section. Let $R(x)$ be the resultant of $f(x,y)$ and $\partial_y f(x,y)$ [Gri89]. In other words,

$$R(x) = \tag{2.24}$$

$$\det \begin{pmatrix}
a_n & a_{n-1} & \cdots & a_1 & a_0 & 0 & \cdots & 0 \\
0 & a_n & a_{n-1} & \cdots & a_1 & a_0 & \cdots & 0 \\
\vdots & \ddots & & & & & \ddots & \vdots \\
0 & \cdots & a_n & a_{n-1} & \cdots & a_1 & a_0 & 0 \\
0 & \cdots & 0 & a_n & a_{n-1} & \cdots & a_1 & a_0 \\
na_n & (n-1)a_{n-1} & \cdots & a_1 & 0 & \cdots & 0 & 0 \\
0 & na_n & (n-1)a_{n-1} & \cdots & a_1 & 0 & \cdots & 0 \\
\vdots & \ddots & & & & & \ddots & \vdots \\
0 & \cdots & 0 & na_n & (n-1)a_{n-1} & \cdots & a_1 & 0 \\
0 & 0 & \cdots & 0 & na_n & (n-1)a_{n-1} & \cdots & a_1
\end{pmatrix}.$$

Here all the coefficients a_k, $k = 0, \ldots, n$, are as in (2.1), thus they are functions of x. The zeros of $R(x)$ are the x-coordinates of the places that satisfy

$$f(x,y) = 0 , \quad \partial_y f(x,y) = 0 . \tag{2.25}$$

Since singularities correspond to more than one place on the Riemann surface, we seek the roots of $R(x) = 0$ that have multiplicity 2 or higher. Let $S = (x_1, \ldots, x_s)$ be the list of these roots. For each $x_k \in S$, we solve

$$f(x_k, y) = 0 . \tag{2.26}$$

Denote the solutions of this equation by $(y_{k1}, \ldots, y_{kn})$ (some entries may be repeated). This results in a number of places (x_k, y_{kj}), $k = 1, \ldots, s$, $j = 1, \ldots, n$. Those places that satisfy

$$\partial_x f(x_k, y_{kj}) = 0 \, , \quad k = 1, \ldots, s, \;\; j = 1, \ldots, n, \tag{2.27}$$

are singular points of the algebraic curve specified by (2.1). Using homogeneous coordinates, these points are denoted $(x_k, y_{kj}, 1)$.

For singular points at infinity, we proceed as follows. The points at infinity are found by solving the homogeneous polynomial equation of degree d (see (2.3))

$$F(X, Y, 0) = 0 = X^d F(1, Y/X, 0) = Y^d F(X/Y, 1, 0) \, . \tag{2.28}$$

This results in d points, possibly repeated, written in homogeneous coordinates as $(X_j, Y_j, 0)$, $j = 1, \ldots, d$. Among these points those that satisfy

$$F_X(X, Y, Z) = F_Y(X, Y, Z) = F_Z(X, Y, Z) = 0 \, , \tag{2.29}$$

are singular points. Incorporating the newly found singular points at infinity, we denote the set of all singular points as

$$\mathcal{S} = \{P_1, \ldots, P_S\} \, , \tag{2.30}$$

where S denotes the number of distinct singularities of the algebraic curve.

Each singularity on an algebraic curve is categorized by three numbers: m, δ, and R: its multiplicity, its delta invariant and its number of local branches, respectively. In rough terms, for a point P on the algebraic curve, m is the number of tangent lines at P (counting a tangent line as many times as its multiplicity), δ is the number of ordinary double points that coalesce to form the singularity at P, and R is the number of local branches that emanate from P. A common approach [BK86, Abh90, Wal62] is to compute these numbers by employing successive quadratic transformations $(x, y) \mapsto (x, yx)$ to "blow up" or resolve singularities into "infinitely near" but distinguishable curve components. Instead, the algorithms of the "algcurves" package use Puiseux expansions to compute m, δ and R.

Note that triples (X, Y, Z) corresponding to places at infinity may be brought to the origin by an appropriate transformation [Abh90], so it suffices to discuss the computation of m, δ and R for affine triples $(\alpha, \beta, 1)$ which are well defined by the pair (α, β). Further, using $x \mapsto x - \alpha$, all affine places corresponding to (α, β) are brought to places $(0, \beta)$ over $x = 0$. In the descriptions below, we assume such transformations have been executed, to simplify the discussion.

2.5.2 Branching Number of a Singularity

The number R of local branches at $(0, \beta)$ is determined by computing all the Puiseux expansions over $x = 0$, and counting how many of them have y-value β at the center. In other words, $R = \sum_j |r_j|$, where the sum runs over all places at the singular point.

2.5.3 Multiplicity of a Singularity

The multiplicity of a place $P = (0, \beta)$ on the plane algebraic curve defined by $f(x, y) = 0$ is the number of (complex) tangent lines that meet there once multiple tangencies are properly counted [Gri89].

Over a regular point $x = \alpha$ there are n distinct y-values, each yielding a distinct pair (α, β_j). Thus the multiplicity of a pair (α, β_j) over a regular point α is necessarily one. Over a singular point, sets of the n branches of the algebraic cover coalesce at least one of the β_j. Suppose that some number, say ℓ, of branches all coalesce at $(\alpha = 0, \beta)$. Then the multiplicity of $(\alpha = 0, \beta)$ (and thus that of the homogeneous triple $(\alpha = 0, \beta, 1)$ is the sum of the multiplicities of each of the ℓ branches. The multiplicity of each branch is calculated from the Puiseux expansions whose centers are $(\alpha = 0, \beta)$: define the lines $L(x, y) = a(x - \alpha) + b(y - \beta) = 0$, with $a, b \in \mathbb{C}$. To properly count the tangencies at place $P = (t^r, \beta + \beta' t^s + \cdots)$ with center $(\alpha = 0, \beta)$, we calculate the valuation of $L(t^r, \beta' t^s + \cdots)$ (*i.e.*, the exponent of the lowest power of t in $L(t^r, \beta' t^s + \cdots)$) and minimize it over all a and b [Wal62].

One may see that the multiplicity of $P = (t^r, \beta + \beta' t^s + \cdots)$ is the minimum of r and s. Indeed, we calculate the minimum intersection multiplicity of expansion P with lines through $(0, \beta)$ given by (a) $x = 0$ and (b) $y = \beta$. (a) First, any line of the form $ax = 0$ (or, L with $a \neq 0$, $b = 0$) evaluated at P_i results in $at^r = 0$. Thus the valuation of $L(x, y) = 0$ is r for any value of $a \neq 0$. (b) Next, any line for which $b \neq 0$, when intersected with P, is given by $L = at^r + b(\beta + \beta' t^s + \cdots - \beta) = at^r + b(\beta' t^s + \cdots) = 0$. If $r \leq s$, then the valuation is r. Otherwise, the valuation is s.

2.5.4 Delta Invariant of a Singularity

A singular point is said to be an *ordinary singular point* if all the branches at this point intersect transversely (i.e., all tangent lines at the point to these branches are distinct). The delta invariant δ of an ordinary m-tuple center (α, β) is the number of transverse intersections that occur there. For instance, 4 lines crossing transversely at (α, β) may be "perturbed" slightly to create a situation with $4(4 - 1)/2$ intersections, each a transverse intersection of two lines. The delta invariant of any ordinary m-tuple singularity (α, β) is the number $\delta = m(m - 1)/2$, where m is the multiplicity of the center (α, β).

Suppose the branches do not cross transversely at (α, β), in other words (α, β) is not an ordinary m-tuple center. Then δ is instead defined to be the number of linear conditions imposed by the Puiseux expansions with center (α, β) on the construction of the integral basis of Sect. 2.4, but without incorporating the singularities not at (α, β). This definition encompasses the one above, which only holds for ordinary m-tuple centers.

The "algcurves" command `singularities` uses a formula which allows for the computation of the delta invariant directly in terms of the quantities associated with the Puiseux series at the singular point (see, for instance, [Kir92]).

To explain the formula used to compute the delta invariant δ of the center $(0, \beta)$, it is necessary to introduce the intersection index Int_P of Puiseux expansion P. Suppose all the places with center $(0, \beta)$ are given by $P_1, \ldots, P_m$, and let r_j be the branching number of P_j. Further, suppose $\hat{y}_j(x)$ is a series in powers of the local coordinate x^{1/r_j}, each with constant term β. Recall that upon 'conjugation' using the r_j-th roots of unity, $\hat{y}_j$ accounts for r_j y-roots of $f(0, y) = 0$. Thus, near $x = 0$, f may be factored as

$$f = \Pi_{j=1}^{m} \Pi_{k=1}^{r_j} \left(y - \hat{y}_j(e^{2i\pi k/r_j} x) \right) * \Pi_{j=m+1}^{n}(y - \hat{y}_j(x)) , \qquad (2.31)$$

where $\hat{y}_j(0) \neq \beta$ for $m+1 < j \leq n$. Rewriting (2.31) more simply as a product of n factors, without regard to the places from which those factors arose, we have

$$f = \Pi_{k=1}^{n}(y - \widetilde{y}_k(x)) . \qquad (2.32)$$

The intersection index Int_{P_j} at place P_j is then given by

$$\mathrm{Int}_{P_j} = \sum_{k=1,\, k \neq j}^{n} \mathrm{ord}_x(\hat{y}_j(x) - \widetilde{y}_k(x)) , \qquad (2.33)$$

where $\mathrm{ord}_x(g(x))$ denotes the lowest, possibly fractional, exponent of x appearing in $g(x)$. The delta invariant of the center $(0, \beta)$ is then given by

$$\delta_{(0,\beta)} = \sum_{j=1}^{m} \frac{r_j \mathrm{Int}_{P_j} - r_j + 1}{2} . \qquad (2.34)$$

Example. Recall from Sect. 2.3 that the ramphoid cusp given by $f = (x^2 - x + 1)y^2 - 2x^2 y + x^4 = 0$ is described near $x = 0$ by the single Puiseux series $y = x^2 + x^{5/2} + \cdots$. To recover both roots of $f(0, y) = 0$, we conjugate over the square roots of unity. Thus, near $x = 0$, f may be factored as

$$f = (y - x^2 - x^{5/2} + \cdots)(y - x^2 + x^{5/2} + \cdots) . \qquad (2.35)$$

Int_P is the lowest exponent in x appearing in the expression obtained by substituting $y = x^2 + x^{5/2} + \cdots$ into the right-hand factor in (2.35):

$$\mathrm{Int}_P = \mathrm{ord}_x(x^2 + x^{5/2} + \cdots - x^2 + x^{5/2} + \cdots) = 5/2 .$$

Noting there is only one place over $x = 0$, and the branching number there is 2, the delta invariant of the center $(0,0)$ is, by (2.34), $((5/2)2 - 2 + 1)/2 = 2$.

Example. Consider the plane algebraic curve defined by $f = y^3 - x^7 + 2x^3 y = 0$. The Puiseux expansions over $x = 0$ are

$$\bar{y}_1 = x^4/2 + \cdots , \quad \bar{y}_2 = -\mathrm{i}\sqrt{2}x^{3/2} - x^4/4 + \cdots ,$$

thus, near $x = 0$, f may be factored as

$$\left(y - x^4/2 + \cdots\right)\left(y + i\sqrt{2}x^{3/2} + 2x^4 + \cdots\right)\left(y - i\sqrt{2}x^{3/2} + 2x^4 + \cdots\right).$$
(2.36)

First we calculate the contribution to (2.34) from $\bar{y}_1$. The branching number in this case is $r_1 = 1$. The quantity Int_{P_1} is the order in x of

$$\left(x^4/2 + \cdots + i\sqrt{2}x^{3/2} + 2x^4 + \cdots\right)\left(x^4/2 + \cdots - i\sqrt{2}x^{3/2} + 2x^4 + \cdots\right),$$

which is $3/2 + 3/2 = 3$. Therefore the contribution to $\delta_{(0,0)}$ from $\bar{y}_1$ is $((1)(3) - 1 + 1)/2 = 3/2$. Next, we calculate the contribution from $\hat{y}_2$. The branching number in this case is 2, and Int_2 is the lowest exponent in x in the result of substituting $y = \bar{y}_2$ into the first and third factors of (2.36):

$$\text{Int}_{P_2} = \text{ord}_x\left(\left(-i\sqrt{2}x^{3/2} - x^4/4 + \cdots - x^4/2 + \cdots\right) * \cdots\right.$$
$$\left.\cdots * \left(-i\sqrt{2}x^{3/2} - x^4/4 + \cdots + -i\sqrt{2}x^{3/2} + 2x^4 - \cdots\right)\right)$$
$$= 3$$

Thus the contribution due to $\bar{y}_2$ is $((2)(3) - 2 + 1)/2 = 5/2$, and $\delta_{(0,0)} = 3/2 + 5/2 = 4$.

Next we present a few examples of the use of the `singularities` command of the "algcurves" package to calculate with singularities of plane algebraic curves. We restrict the coefficients of the polynomials in the examples to be integers to keep the output relatively simple. The Maple implementation is in no way restricted to such curves.

The output of the command `singularities` is a set of lists, one list for each singularity. Each list consists of the homogeneous coordinates representation of the singularity P, followed by, in order, the multiplicity m, the delta invariant δ and the number of local branches R at P. The procedure computes all singularities up to conjugation. Thus if a singularity $[\text{RootOf}(\_Z^2 - 2), 1, 1]$ is present in the output, and if $\text{RootOf}(\_Z^2 - 2)$ does not appear as a coefficient in the curve, then $[-\text{RootOf}(\_Z^2 - 2), 1, 1]$ is a singular point as well but is suppressed in the output. Here we have adopted the Maple notation $\text{RootOf}(\_Z^2 - 2)$ to denote the roots of the equation $Z^2 - 2 = 0$. In other words, $\text{RootOf}(\_Z^2 - 2)$ is a placeholder for both $\sqrt{2}$ and $-\sqrt{2}$.

Example. The curve $f = y^2 + x^3 - x^2 = 0$ has a node, that is an ordinary double point, at the origin and a branch point at $x = 1$. Figure 2.3 shows the real graph of $f(x, y) = 0$. In this example we compute m, δ and R for the singularity at $(0, 0)$ (or in homogeneous coordinates, $(0 : 0 : 1)$). First, we calculate the Puiseux expansions over $x = 0$.
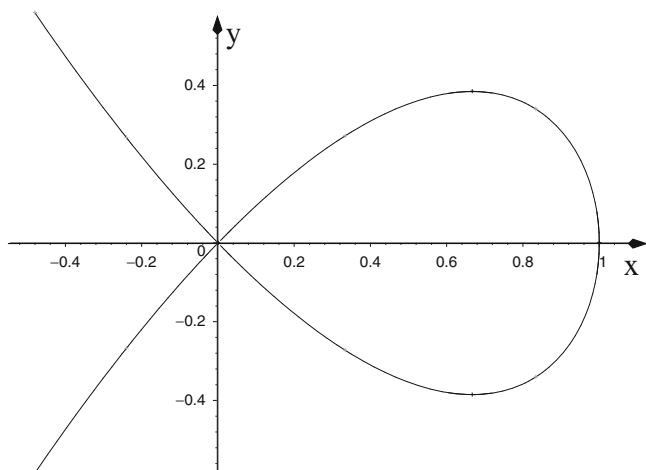
Fig. 2.3. The real part of the graph of $y^2 + x^3 - x^2 = 0$ displays an ordinary double point, also known as a node, at the origin $x = y = 0$. The figure was produced using the `plot_real_curve` command

```
># read in the package
>with(algcurves):
># define the algebraic curve
>f:=y^2+x^3-x^2:
># compute the Puiseux expansions over x=0
>puiseux(f,x=0,y,0,t);
```

$$\{[x = t, y = -t], [x = t, y = t]\}$$

There are two expansions over $x = 0$, both with center $(0,0)$: therefore $R = 2$. Consider the first expansion. The exponent of t for the x-series is one, as is the lowest exponent for the y-series. The minimum of these two exponents is one, thus the multiplicity of the first expansion is one. A similar argument with the second expansion gives that its multiplicity is also one, resulting in a total multiplicity for the singularity of $m = 2$. The two branches cross transversely, thus $(0,0)$ is an ordinary double point with delta invariant given by $\delta = 2(2 - 1)/2 = 1$. We confirm this using the command `singularities`.

```
>singularities(f,x,y);
```

$$\{[[0, 0, 1], 2, 1, 2]\}$$

Thus the origin is a singular point with multiplicity $m = 2$, delta invariant $\delta = 1$ and branching number $R = 2$.
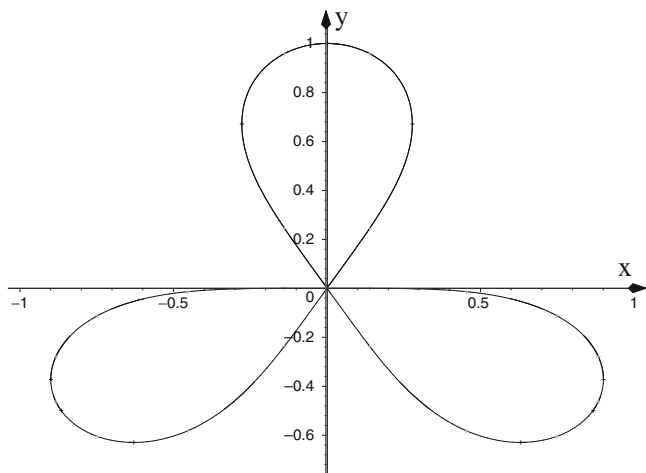
Fig. 2.4. The real part of the graph of $(x^2 + y^2)^3 + 3x^2y - y^3 = 0$ shows the presence of a singularity at the origin which is an ordinary triple point. The figure was produced using the `plot_real_curve` command

Example. The real graph of the algebraic curve defined by

$$f = y^6 + 3x^2y^4 - y^3 + 3x^4y^2 + 3x^2y + x^6$$
$$= (x^2 + y^2)^3 + 3x^2y - y^3 \tag{2.37}$$

is a trefoil whose lobes meet at the origin, as shown in Fig. 2.4. As before, we compute the Puiseux series over $x = 0$ and, using these expansions, explain the output of the command `singularities`.

```
># define the algebraic curve
>f:=(x^2 +y^2)^3 + 3x^2y - y^3:
># compute the Puiseux expansions over x=0
>puiseux(f,x=0,y,0,t);
```

$$\{[x = t, y = \text{RootOf}(\_Z^2 + \_Z + 1)], [x = t, y = t\,\text{RootOf}(\_Z^2 - 3)],$$
$$[x = t, y = 0], [x = t, y = 1]\}$$

Note that the first and last expansions in the set above do not have centers at the origin. Further, as explained above, the expansion $[x = t, y = t\,\text{RootOf}(\_Z^2 - 3)]$ represents two places (that is $(t, \sqrt{3}t + \cdots)$ and $(t, -\sqrt{3}t + \cdots)$), each with the same center (namely $(0, 0)$). Thus there are three local expansions with center $(0, 0)$. As the three branches have distinct slopes, the origin is an ordinary triple point. Thus its delta invariant is $3(2)/2 = 3$.

```
>singularities(f,x,y);
```

$$[[\text{RootOf}(\_Z^2 + 1), 1, 0], 3, 3, 3], [[0, 0, 1], 3, 3, 3]$$

As the singularities are computed up to conjugation, the first triple in the set above represents the two (non-affine) homogeneous triples $(i : 1 : 0)$ and $(-i : 1 : 0)$, each having the same values for m, δ and R. The sum of the delta invariants is 9 and not 6 as might be expected from the above output.

2.6 Genus of a Riemann Surface

In this section, we discuss how one algorithmically computes the genus of a Riemann surface associated with a possibly singular plane algebraic curve. The algorithm relies on the various quantities discussed in the previous sections. The genus is an important ingredient for the algorithms of the following sections on the computation of the Riemann matrix (Sect. 2.10) and the Abel map (Sect. 2.11).

Once the delta invariants of all singularities (finite and infinite) are known, the genus is given by $(d-1)(d-2)/2$ minus the sum of all the delta invariants [Abh90]:

$$g = \frac{(d-1)(d-2)}{2} - \sum_{P \in \mathcal{S}} \delta_P \ . \tag{2.38}$$

Example. In what follows, a few examples of the output of the `genus` command are given. If the polynomial given as input can be factored, the `genus` command returns -1. We consider two algebraic curves defined by $f_j(x, y) = 0$, $j = 1, 2$:

$$f_1 = y^4 - y^2 x + x^2 \ , \tag{2.39}$$
$$f_2 = y^3 - (x^3 + y)^2 + 1 \ . \tag{2.40}$$

The first of these curves, $f_1(x, y) = 0$ is reducible. The second one is a curve of genus 4.

```
>#  load the algcurves package
>with(algcurves):
>#  define the algebraic curve
>f1:=y^4-y^2 x+x^2:
>#  calculate the genus of f1(x,y)=0
>genus(f1,x,y);
>Warning, negative genus so the curve is reducible
```

$$-1$$

```
>#  factor the curve
>evala(AFactor(f1));
```

$$\left(y^2 + \frac{-1 - \mathrm{RootOf}(\_Z\char94 2 + 3)}{2} x \right) \left(y^2 + \frac{-1 + \mathrm{RootOf}(\_Z\char94 2 + 3)}{2} x \right)$$

```
># define the algebraic curve
>f2:=y^3-(x^3+y)^2+1:
># calculate the genus of f2(x,y)=0
>genus(f2,x,y);
```

$$4$$

```
># the same result is obtained if we switch the order of
># the variables
>genus(f2,y,x);
```

$$4$$

2.7 Monodromy of a Plane Algebraic Curve

The monodromy of a plane algebraic curve is the input for Tretkoff–Tretkoff's algorithm [TT84] for the construction of a homology basis of a Riemann surface, as discussed in Sect. 2.8. In this section we study an algorithm to compute the monodromy of a plane algebraic curve.

An algebraic curve gives rise to a covering of the Riemann sphere.[3] The monodromy of a plane algebraic curve encodes how the different sheets of this covering glue together to form one smooth whole.

The calculation of the monodromy group of an algebraic covering $y(x)$ requires several ingredients. First, we select a *base point* $x = a$ in the complex x-plane. This base point is a finite regular point of the algebraic covering $y(x)$, i.e., for $x = a$, n distinct finite y-values exist. These n y-values may be assigned an order, $(y_1, y_2, \ldots, y_n)$. This ordering of the n y-values labels the sheets of the algebraic covering $y(x)$. For each branch point b one chooses a path γ_b in the complex x-plane which starts and ends at $x = a$ and encircles only the branch point $x = b$, counterclockwise. Next, the n-tuple $(y_1, y_2, \ldots, y_n)$ is analytically continued around this path γ_b. When one returns to $x = a$, a new n-tuple is found, which has the same entries as $(y_1, y_2, \ldots, y_n)$, but reshuffled: $(y_{\sigma_b(1)}, y_{\sigma_b(2)}, \ldots, y_{\sigma_b(n)})$. The permutation σ_b is read off from this reshuffled vector. The collection of the permutations at all branch points (including any singular branch points and points at infinity) determines the monodromy group of the algebraic curve (2.1). More background on the monodromy group is found in [DFN85], whereas [TT84] provides more details that are useful for the later use of the monodromy of a plane algebraic curve in computing the homology of the associated Riemann surface. We now discuss the steps of the monodromy computation more systematically.

---

[3] In fact, Riemann introduced the concept of a Riemann surface to examine this multivaluedness [Rie90].

1. *The problem points of the analytic continuation:* The algebraic curve (2.1) defines an n-sheeted covering $y(x)$ of the extended complex x-plane. For all but a finite number of values of x in the extended complex plane $\mathbb{C} \bigcup \{\infty\}$ there are n values for $y(x)$ in $\mathbb{C} \bigcup \{\infty\}$. A value for x corresponds to a singularity or a *branch point* if and only if there are fewer than n values for $y(x)$. A branch point of this n-sheeted covering is defined as an x-value $x = b$ where the vector of roots $\mathbf{y}(x)$ does not return to its original value when one analytically continues $\mathbf{y}(x)$ once along a small circle around $x = b$.

   The notion of problem points $P = \{b_1, b_2, \ldots, b_m\}$ was introduced in [DvH01] for the purpose of singling out the finite x-values corresponding to those places on the algebraic curve that require special treatment for the purposes of numerical analytic continuation. The problem points contain the collected x-values giving rise to singular points, branch points and points for which $y = \infty$. In short, the problem points are all finite x-values for which the equation $f(x, y) = 0$ gives rise to fewer than n finite and distinct roots y.

   The set of problem points is found by calculating (a) the roots of $\Delta(x) = 0$, where $\Delta(x)$ is the discriminant of $f(x, y)$, see (2.24), namely the resultant of $f(x, y)$ and $f_y(x, y)/a_n(x)$ [vdW91], and (b) the roots of $a_n(x) = 0$. If x is a root of the latter equation, then the equation $f(x, y) = 0$ effectively drops in degree, resulting in some roots y being infinite. Note that the addition of the roots of $a_n(x) = 0$ is necessary due to the definition of the discriminant. Since both the discriminant $\Delta(x)$ and $a_n(x)$ are polynomials in x, the number of problem points is finite. The discriminant points are either branch points or singular points. Singular points may have non-trivial monodromy in which case they are also branch points. In the algorithms, the problem points are the union of roots of $a_n(x) = 0$ or $\Delta(x) = 0$.

2. *Encircling the problem points:* In order to compute the monodromies of the covering $y(x)$, the vector $\mathbf{y}(x)$ is analytically continued along paths encircling the problem points. Though the monodromy of the roots of $a_n(x) = 0$ and certain singular points is trivial, the paths for the analytical continuation of the $y(x)$ also stay away from these points to avoid numerical problems. In order to simplify control of the numerical accuracy, the paths stay a (finite) distance $r(b_i)$ away from each problem point b_i. Thus, to every problem point b_i, we associate a radius $r(b_i)$ as follows:

$$r(b_i) = \frac{2}{5} \rho(b_i, \{b_1, b_2, \ldots, b_m\} \setminus \{b_i\}), \qquad (2.41)$$

where ρ denotes distance. In other words, $r(b_i)$ is two fifths of the distance of b_i to the next nearest problem point. The ratio $2/5$ is somewhat arbitrary; other numbers between 0 and $1/2$ might be used. Important is that the circles $C(b_i, r(b_i))$ do not intersect each other.

3. *The choice of the base point:* A base point a is chosen such that $x = a$ is at least a distance $r(b_s)$ away from the nearest problem point b_s, and such that the real part of a is smaller than the real parts of any of the b_i. By the latter choice, the arguments of $b_i - a$ are between $-\pi/2$ and $\pi/2$. For plane algebraic curves defined by (2.1) with real coefficients, the base point is chosen to be real.

4. *Labeling of the sheets:* At the base point $x = a$ there are n distinct finite y-values. These are determined numerically as the solutions of $f(a, y) = 0$. Let these n y-values be assigned an order $(y_1, y_2, \ldots, y_n)$, which is denoted as $\boldsymbol{y}(a)$. Assigning such an order to these y-values labels the sheets of the covering $y(x)$: sheet one is the sheet containing y_1, sheet 2 is the sheet containing y_2, and so on. Note that because $x = a$ is at least a distance $r(b_s)$ away from the nearest problem point b_s, the values $(y_1, y_2, \ldots, y_n)$ are well separated.

5. *Ordering the problem points of the analytic continuation:* A consistent ordering needs to be imposed on the problem points. We choose to order these points according to their argument with respect to the base point: if $\arg(b_i - a) < \arg(b_j - a)$, then b_i precedes b_j in the ordering, where $\arg(\cdot)$ denotes the argument function. If $\arg(b_i - a) = \arg(b_j - a)$, then b_i precedes b_j in the ordering if $|b_i - a| < |b_j - a|$. This ordering results in an ordered m-tuple of problem points: $(b_1, b_2, \ldots, b_m)$. The same notation is used for the ordered problem points as for the elements of the non-ordered set.

6. *Choice of the paths:* Next, we choose paths for the analytic continuation. These paths are composed of line segments and semi-circles. The simplest path $L(b_i)$ around b_i consists of one line segment from a to $b_i - r(b_i)$. This is followed by the circle $C(b_i, r(b_i))$, starting at $b_i - r(b_i)$. Successively, a line segment is followed from $b_i - r(b_i)$, back to a. However, if this path intersects one of the circles $C(b_j, r(b_j))$, $j \neq i$, we modify the path to another one that is homotopic[4] to it. If a path intersects one of the circles $C(b_j, r(b_j))$, $j \neq i$, this indicates that it comes close to the problem point b_j. As a consequence, the sheets of the covering would not be well separated along the path, which complicates the numerical analytical continuation. Therefore we wish to avoid this. The situation may be remedied as indicated in Fig. 2.5: the path takes a detour along a semi-circle around b_j. Whether this semi-circle goes above or below b_j depends on the relative positions of a, b_i and b_j. The semi-circle is chosen such that the new path is deformable to $L(b_i)$, without crossing any problem points of the analytic continuation.

   This process is iterated, until a path is obtained, which stays at least $r(b_j)$ away from b_j, for $j = 1, 2, \ldots, m$. The iteration of this process is not sufficient to ensure that the chosen path is homotopic to the straight-line path from the base point a to $b_i - r(b_i)$. To ensure that a correct path is

---

[4] In this context we call two paths homotopic to each other if they may be continuously deformed to one another without crossing any problem points.
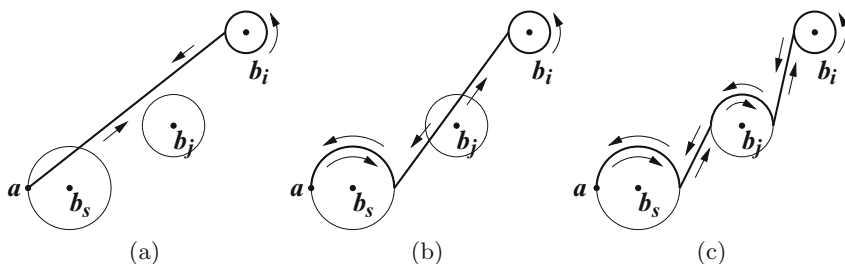
Fig. 2.5. Choosing the path from $x = a$ to $x = b_i$. The path around b_i is indicated in a *thick black line*. (a) The simplest path intersects $C(b_s, r(b_s))$. (b) This is remedied by a new path which is homotopic to the previous one. The new path intersects $C(b_j, r(b_j))$. (c) This is remedied by another path, which is homotopic to both previous paths

chosen, our implementation explicitly checks for the presence of problem points between the chosen path and the straight-line path. If such points are present, the path is modified to go around them, after which the check procedure is re-iterated.

7. *Numerical analytic continuation:* Consider two non-problem points $x = x_1$ and $x = x_2$. Corresponding to x_1 is an ordered n-tuple $\boldsymbol{y}(x_1)$. When a path is followed in the complex x-plane from x_1 to x_2, the entries of $\boldsymbol{y}(x_1)$ follow paths on the cover to the roots of $f(x_2, y) = 0$, which gives rise to an n-tuple $\boldsymbol{y}(x_2)$, whose ordering is induced by the ordering of $\boldsymbol{y}(x_1)$. If x_1 and x_2 are relatively close to each other so that the path between them deviates little from a straight-line segment and provided it does not pass through or near any problem points, then

$$\boldsymbol{y}(x_2) = \boldsymbol{y}(x_1) + \boldsymbol{y}'(x_1)(x_2 - x_1) + \vartheta(|x_2 - x_1|^2) , \qquad (2.42)$$

and the last term is small when x_2 and x_1 are sufficiently close (to make this precise one needs to bound the second derivative of $\boldsymbol{y}(x)$ to find a bound for $\vartheta(|x_2 - x_1|^2)$). Here $\boldsymbol{y}'(x_1)$ is the n-tuple of derivatives to $\boldsymbol{y}(x)$ at x_1. Using implicit differentiation we have

$$\boldsymbol{y}'(x_1) = -\left(\frac{f_x(x_1, y_1(x_1))}{f_y(x_1, y_1(x_1))}, \frac{f_x(x_1, y_2(x_1))}{f_y(x_1, y_2(x_1))}, \ldots, \frac{f_x(x_1, y_n(x_1))}{f_y(x_1, y_n(x_1))} \right) , \quad (2.43)$$

where a subindex x or y denotes partial differentiation and $y_i(x_1)$, $i = 1, \ldots, n$ denotes the i-th component of $\boldsymbol{y}(x_1)$. Under the above conditions, the first two terms of (2.42) give a good approximation to $\boldsymbol{y}(x_2)$. Having the unordered entries of $\boldsymbol{y}(x_2)$ at our disposal and comparing them with the ordered approximation $\boldsymbol{y}(x_1) + \boldsymbol{y}'(x_1)(x_2 - x_1)$ allows us to determine the ordering of these entries, resulting in the ordered n-tuple $\boldsymbol{y}(x_2)$. Clearly, in order to avoid matching up the entries of $\boldsymbol{y}(x_2)$ with the wrong

entries of the ordered approximation, the numerically acceptable size of $|x_2 - x_1|$ depends on the absolute differences between the components of $\boldsymbol{y}(x_2)$.

If $|x_2 - x_1|$ is not small, or if the path connecting them deviates significantly from a straight-line segment, then an analytic continuation from $\boldsymbol{y}(x_1)$ to $\boldsymbol{y}(x_2)$ is obtained by iterating the above process along sufficiently small segments of the path, such that the necessary conditions above are satisfied. Note that $\boldsymbol{y}(x_2)$ is dependent on the path chosen from x_1 to x_2. For brevity of notation, this dependence is not made explicit.

8. *The monodromy group:* For the set $\{b_1, \ldots, b_m\}$ of branch points, consider the paths γ_k generating the fundamental group $\pi_1(\mathbb{C}P^1 \setminus \{b_1, \ldots, b_m\})$ which satisfy the relation $\gamma_1 \ldots \gamma_m = id$ (see Fig. 1.15 in Chap. 1). After analytic continuation of $\boldsymbol{y}(a)$ along the path γ_k around b_k, the entries of $\boldsymbol{y}(a)$ are recovered, but they are shuffled by the permutation σ_{b_k}:

$$\Pi(b_k)\boldsymbol{y}(a) = \Pi(b_k)(y_1(a), y_2(a), \ldots, y_n(a))$$
$$= \left(y_{\sigma_{b_k}(1)}, y_{\sigma_{b_k}(2)}, \ldots, y_{\sigma_{b_k}(n)} \right) , \qquad (2.44)$$

where $\Pi(b_k)$ denotes the action of analytic continuation along γ_k. The collection of all σ_{b_k} generates the monodromy group of the covering, which is represented here as a subgroup of S_n, the group of permutations of $\{1, 2, \ldots, n\}$. Note that this representation depends on the choice of the labeling of the y-values at $x = a$, so it is only unique up to conjugation. More details are found in [DFN85].

Despite the numerical nature of the analytic continuation of $\boldsymbol{y}(x)$, it is possible to identify $\boldsymbol{y}(x)$ uniquely after a full cycle around a point, since there is only a finite number of components of $\boldsymbol{y}(x)$. Thus the monodromy is obtained exactly.

9. *Infinity:* The point $x = \infty$ might also be a branch point. The corresponding permutation σ_∞ is computed by encircling all problem points in a clockwise sense. On the base of the covering, this is equivalent to encircling the point at infinity in a counter-clockwise sense. If this permutation is not the identity, then the point $x = \infty$ is a branch point. Otherwise it is not.

Having found this permutation, the program performs one of many internal checks by verifying that

$$\sigma_\infty \circ \sigma_{b_m} \circ \sigma_{b_{m-1}} \circ \ldots \circ \sigma_{b_2} \circ \sigma_{b_1} = 1 . \qquad (2.45)$$

Since a closed path in the extended complex x-plane that encircles all branch points is homotopic to a point, analytic continuation along such a path will not permute the entries of $\boldsymbol{y}(a)$. Alternatively, we could use (2.45) to compute σ_∞, but this eliminates a possible check. In what follows, it is always assumed that the list $b_1, b_2, \ldots, b_m$ includes $x = \infty$ if it is a branch point. In this case, σ_∞ is also assumed to be included in the permutation list $\sigma_{b_1}, \ldots, \sigma_{b_m}$.

Example. We use the above algorithm to compute a representation of the monodromy group for the algebraic covering $y(x)$ corresponding to $F(x,y) = y^3 - (x^3+y)^2 + 1 = 0$: the command `monodromy(f,x,y)` gives a list with three elements. The first element is the choice of the base point $x = a$. The second element is $\boldsymbol{y}(a)$, which is a list of $n = 3$ elements. The third element is a list of the branch points b_i with corresponding permutations σ_{b_i}, given in disjoint cycle notation.

```
># load the algcurves package
>with(algcurves):
># define the algebraic curve
>f:=y^3-(x^3+y)^2+1:
># calculate the monodromy representation for y(x)
>m:=monodromy(f,x,y,'showpaths'):
># the base point x=a
>m[1];
```

$$-1.27297541004$$

```
># the sheets y(a)
>m[2];
```

$$[.0907534141676 - 1.99219212537i, .0907534141676 + 1.99219212537i,$$
$$.818493171665]$$

```
># the branch points with their permutations
>m[3];
```

$$[[-.573843481646 - .993926065804i, [[2, 3]]],$$
$$[-1.03977417810 - .167751539921i, [[2, 3]]],$$
$$[-.372303356542 - .644848329360i, [[1, 2]]],$$
$$[.374609993952 - .984346622390i, [[1, 3]]],$$
$$[.665164184143 - .816595082469i, [[2, 3]]],$$
$$[.744606713085, [[1, 2]]], [1.14768696329, [[1, 3]]],$$
$$[.665164184143 + .816595082469i, [[1, 3]]],$$
$$[.374609993952 + .984346622390i, [[2, 3]]],$$
$$[-.372303356542 + .644848329360i, [[1, 2]]],$$
$$[-1.03977417810 + .167751539921i, [[1, 3]]],$$
$$[-.573843481646 + .993926065804i, [[1, 3]]]]$$

Thus, starting from the ordered sheets 1, 2 and 3 above the base point $x = -0.724402557170$ (i.e., from the ordered y-values $0.0907534141676 - 1.99219212537i, 0.0907534141676 + 1.99219212537i, 0.818493171665$), and encircling $x = 0.374609993952 - .984346622390i$, one finds that sheet 1 has
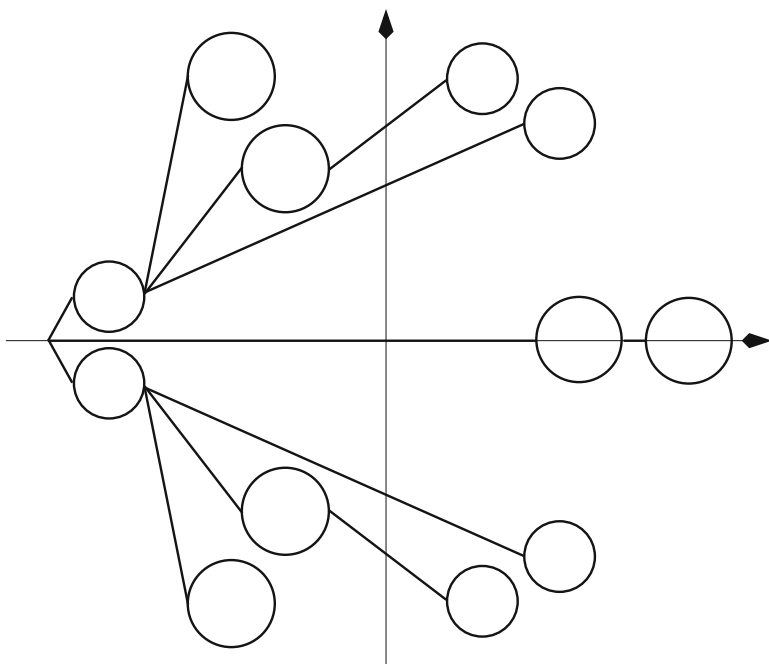
Fig. 2.6. The complex x-plane and the paths followed for the analytic continuation of $\boldsymbol{y}(x)$, with $y^3 - (x^3 + y)^2 + 1 = 0$. The base point $x = a$ is at the left

become sheet 3 and sheet 3 has become sheet 1. Sheet 2 was not affected by encircling this branch point. The optional argument `showpaths` produces Fig. 2.6. This shows the paths followed in the complex x-plane for the analytic continuation of $\boldsymbol{y}(x)$.

Remarks

- The reader should note that throughout the above procedures, no mentioning is ever made of branch cuts. Any book on complex analysis will state that the choice of branch cuts is irrelevant for many purposes. This is clear from the presentation above: branch cuts are never introduced! Branch cuts provide a recipe for performing analytic continuation, by specifying the range of the argument function. They are also often convenient means for understanding the geometry of the Riemann surface under investigation: In practice they are artificial boundaries on the Riemann surface delimiting the several sheets. They loose much of their practical value when one leaves the realm of hyperelliptic surfaces. In the above, branch cuts could have been introduced as segments from the base point to the branch points.
- The construction of the paths for a general plane algebraic curve is a hard problem. Most of the algorithms discussed in this chapter rely on local
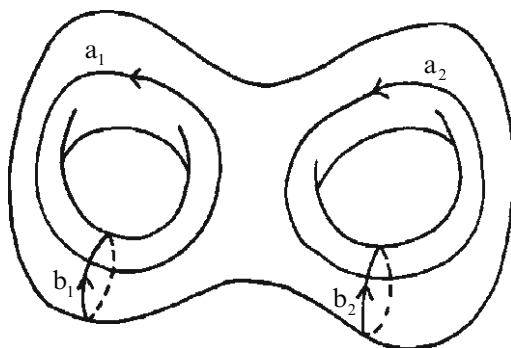
Fig. 2.7. A genus 2 surface with a canonical basis of cycles

analytic structures near specific points. The construction of the paths is the main part of the algorithms, where the global geometry of the curve is encoded. It is relatively easy to construct examples, where the location of the problem points is such that the iterative algorithm described above does not terminate unless the user-specified accuracy is sufficiently high. In such cases the user may get an error message making exactly this statement, asking the user to increase the accuracy and to try again.

- Recent work by Adrien Poteaux [Pot07] has resulted in an algorithm for the computation of the monodromy of a plane algebraic curve that gives correct results, without requiring user interaction. The algorithm appears to be competitive in that it is computationally not significantly more expensive than that described above.

2.8 Homology of a Riemann Surface

With the monodromy of a plane algebraic curve at our disposal, in this section we construct a basis for the homology of the Riemann surface obtained from such an algebraic curve. We define a cycle to be a closed, oriented, smooth or piecewise smooth curve. Since a Riemann surface of genus g is topologically equivalent to a sphere with g handles, on a surface of genus > 1 there are cycles (those encircling the handles or the holes) which cannot be deformed to points. As stated in Chap. 1, on a Riemann surface Γ of genus g, it is possible to choose $2g$ nonhomologous cycles such that their intersection indices are as follows:

$$a_i \circ a_j = 0, \quad b_i \circ b_j = 0, \quad a_i \circ b_j = \delta_{ij}, \quad i, j = 0, \ldots, g, \tag{2.46}$$

where δ_{ij} is the Kronecker delta: it is one if $i = j$ and zero otherwise. A basis for the homology of the Riemann surface Γ with these intersection indices is called a canonical basis of cycles. Figure 2.7 illustrates the canonical homology

basis for a $g = 2$ surface. Notice that a canonical basis for the homology is not uniquely determined by the intersection conditions (2.46).

A combinatorial algorithm for the calculation of a canonical basis for the homology of a Riemann surface specified by its monodromy structure was published by C. L. Tretkoff and M. D. Tretkoff in 1984 [TT84]. The monodromies computed in the previous section allow us to use the methods of [TT84].

Since our implementation follows the Tretkoff–Tretkoff algorithm, we limit our discussion of it. Full details may be found in [TT84]. A short geometrical sketch of the algorithm is as follows:

1. Choose a base point $x = a$ as before. In practice, this is the same base point as for the monodromy algorithm.
2. Indicate all places on the Riemann surface Γ, corresponding to $x = a$ contained in $\boldsymbol{y}(a)$. This gives n places $A_i = (a, y_i(a))$, $i = 1, 2, \ldots, n$ on the Riemann surface, which effectively label the sheets of Γ.
3. Let $x = b$ denote a branch point in the complex x-plane. Denote one of the disjoint cycles of the corresponding permutation σ_b by τ. Then the sheets labeled by A_k, with $k \in \tau$ meet at a branch place B on the Riemann surface, with x-value b. Similarly, each one of the disjoint cycles of any σ_b corresponds one-to-one to a branch place on the Riemann surface, with $x = b$. In particular, the number of branch places on the Riemann surface with $x = b$ is the number of disjoint cycles in σ_b, not including fixed points. The total number of places on the Riemann surface with $x = b$ is the number of disjoint cycles in σ_b, including fixed points. In what follows, we denote the disjoint cycle in σ_b corresponding to B by τ_B.
   Now, on the Riemann surface, indicate all branch places, including branch places at infinity. Let t denote the total number of branch places and B_i, $i = 1, 2, \ldots, t$ the branch places on the Riemann surface.
4. Next join every branch place B_i to each place A_j, for which $j \in \tau_{B_i}$, $i = 1, \ldots, t$, using paths which only meet at the places B_i and A_j. Thus, every branch place B_i is connected to all places A_j which can be reached by paths emanating from B_i with no other branch places B_j, $j \neq i$ on this connection.
   This creates a non-directed graph on the Riemann surface, with $n + t$ vertices.
5. This graph is reduced to a *spanning tree* by removing a number of edges, say r edges. Denote these edges by e_i, $i = 1, \ldots, r$.
6. This spanning tree contains no closed paths, by definition. Adding to it the removed edge e_1 gives rise to a unique closed path on the Riemann surface. Fix an orientation on this closed path, thus defining a cycle c_1.
7. Similarly, every other removed edge e_k gives rise to a closed path on the Riemann surface. If this path has any edges in common with the cycles $c_1, c_2, \ldots, c_{k-1}$, then an orientation is induced from these cycles on the cycle c_k. Otherwise, an orientation is chosen. This way, a collection of r cycles $c_1, \ldots, c_r$ is obtained on the Riemann surface.

Tretkoff and Tretkoff [TT84] show that the cycles constructed above are all nontrivial, i.e., they cannot be contracted to a point. Furthermore,

$$r = 2g + n - 1 \, , \tag{2.47}$$

where g is the genus of the Riemann surface.

Since $n > 1$ (otherwise $y(x)$ is a single-valued function), $r > 2g$. Thus the above construction results in more cycles than are required for a basis of the homology, which has dimension $2g$.

In [TT84], Tretkoff–Tretkoff present an algorithmic way to cut the above-mentioned graph on the Riemann surface across the edges $e_1, \ldots, e_r$. This results in a planar graph which contains cut copies of the cycles $c_1, \ldots, c_r$. They show how this planar graph is used to find the intersection numbers $K_{ij} = c_i \circ c_j$, $i, j = 1, \ldots, r$, resulting in an $r \times r$ intersection matrix $\boldsymbol{K} = (K_{ij})_{i,j=1}^{g} = (c_i \circ c_j)_{i,j=1}^{g}$. Because only $2g$ of the cycles $c_1, \ldots, c_r$ are independent, the rank of this matrix is $2g$. Furthermore, an $r \times r$ matrix $\boldsymbol{\alpha}$ with integer entries and determinant ± 1 exists such that

$$\boldsymbol{\alpha K \alpha}^T = \boldsymbol{J} = \begin{pmatrix} \boldsymbol{0}_g & \boldsymbol{I}_g & \boldsymbol{0}_{g,n-1} \\ -\boldsymbol{I}_g & \boldsymbol{0}_g & \boldsymbol{0}_{g,n-1} \\ \boldsymbol{0}_{n-1,g} & \boldsymbol{0}_{n-1,g} & \boldsymbol{0}_{n-1,n-1} \end{pmatrix} \, , \tag{2.48}$$

with $\boldsymbol{0}_g$ being the $g \times g$ zero matrix, $\boldsymbol{I}_g$ the $g \times g$ identity matrix and $\boldsymbol{0}_{p,q}$ the $p \times q$ zero matrix. We now define the cycles

$$a_i = \sum_{j=1}^{r} \alpha_{ij} c_j, \quad b_i = \sum_{j=1}^{r} \alpha_{i+g,j} c_j, \quad i = 1, \ldots, g \, . \tag{2.49}$$

It is straightforward to check that these cycles satisfy (2.46). Hence the cycles $a_1, \ldots, a_g$, $b_1, \ldots, b_g$ define a canonical basis of cycles for the homology of the Riemann surface. The non-uniqueness of such a basis is a restatement of the non-uniqueness of the matrix $\boldsymbol{\alpha}$. This matrix is the transformation matrix from the basis of cycles $c_1, \ldots, c_r$ to the canonical basis. Its first $2g$ rows prescribe the linear combination of the cycles $c_1, \ldots, c_r$ which results in the canonical basis. Its last $n - 1$ rows confirm the dependence of the cycles $c_1, \ldots, c_r$:

$$\sum_{j=1}^{r} \alpha_{ij} c_j = 0, \quad i = 2g + 1, \ldots, 2g + n - 1 \, . \tag{2.50}$$

Example. In the following example, we compute a canonical basis for the homology of the Riemann surface of genus 3 corresponding to $y^3 - (x^2 + y)^2 + 1 = 0$. Note that the example is a little different from that used to illustrate the use of the monodromy command, so as to demonstrate what happens when $x = \infty$ is a branch point. The command `homology(f,x,y)` results in a table. This table has the following entries:

1. `basepoint:` the base point $x = a$ for the analytic continuation of the algebraic covering $y(x)$.

2. `sheets:` the ordered n-tuple $\boldsymbol{y}(a)$.
3. `cycles:` the cycles $c_1, c_2, \ldots, c_r$. The cycles are given as lists. The first element of the cycle c_k specifies the starting sheet $y_i(a)$, by displaying i. The second element is a branch point $x = b$ in the complex x-plane, together with the disjoint cycle of σ_b, which contains i. The third element is a sheet $y_j(a)$, given by j. This part of the cycle c_k is read as: "From sheet i proceed to sheet j, by encircling the point $x = b$". It is possible that $x = b$ needs to be encircled more than once, in order to get from sheet i to sheet j. Having arrived at sheet j, this process now repeats. The list is cyclical, meaning that after encircling the last branch point, one arrives again at the initial sheet, so as to obtain a cycle on the Riemann surface.
4. `linearcombination:` the first $2g$ rows of the matrix $\boldsymbol{\alpha}$, as discussed above.
5. `canonicalcycles:` the result of combining `linearcombination` and `cycles`. Each of the cycles $a_1, \ldots, a_g, b_1, \ldots, b_g$ is given as a list. Adding these lists gives a basis element of the canonical basis of cycles. Usually, only one list is necessary for each canonical-basis element. Since the canonical-basis elements are obtained from the information in both `cycles` and `linearcombination`, their representation is typically more complicated. Also, instead of specifying the disjoint cycle of the permutation at the branch point, the number of times one needs to encircle the branch point in the complex x-plane counterclockwise is given. If this number is negative, the branch point needs to be encircled clockwise as many times as the absolute value of the number.
6. `genus:` this entry gives the genus of the Riemann surface, by halving the dimension of the canonical basis. This topological calculation is completely independent of the one using Puiseux expansions, used by the `genus` algorithm [vH95] discussed in Sect. 2.6.

```
>#  load the algcurves package
>with(algcurves):
>#  define the algebraic curve
>f:=y^3-(x^2+y)^2+1=0:
>#  calculate the homology of the Riemann surface
>#  corresponding to f.
>h:=homology(f,x,y):
>#  the base point x=a
>h[basepoint];
```

$$-1.46431608476$$

```
>#  the sheet labels y(a)
>h[sheets];
```

$$[-.951818492315 - .577121407841i, -.951818492315 + .577121407841i,$$
$$2.90363698463]$$

```
>#  the cycles c_1,...,c_r
>eval(h[cycles]);
```

$\text{table}([1 = [1,[-.256859579359 - 1.04991843161i, [1,2]],$
$\qquad 2,[-1.22951879712, [1,2]]],$
$\quad 2 = [1,[1.22951879712, [1,3]], 3, [.256859579359 + 1.04991843161i, [1,3]]],$
$\quad 3 = [1,[-.256859579359 - 1.04991843161i, [1,2]],$
$\qquad 2,[-.256859579359 + 1.04991843161i, [1,2]]],$
$\quad 5 = [1,[1.22951879712, [1,3]], 3, [\infty, [1,2,3]]],$
$\quad 4 = [1,[-.256859579359 - 1.04991843161i, [1,2]], 2, [\infty, [1,2,3]]],$
$\quad 7 = [1,[-.256859579359 - 1.04991843161i, [1,2]],$
$\qquad 2,[-.642525578033, [2,3]], 3, [1.22951879712, [1,3]]],$
$\quad 6 = [1,[-.256859579359 - 1.04991843161i, [1,2]],$
$\qquad 2,[.256859579359 - 1.04991843161i, [2,3]], 3, [1.22951879712, [1,3]]],$
$\quad 8 = [1,[-.256859579359 - 1.04991843161i, [1,2]],$
$\qquad 2,[.642525578033, [2,3]], 3, [1.22951879712, [1,3]]])$

```
>#  the first 2g rows of the matrix alpha:
>h[linearcombination];
```

$$\begin{pmatrix} 1 & 0 & 0 & 0 & 0 & 0 & 0 & 0 \\ 0 & 1 & 0 & 0 & 0 & 0 & 0 & 0 \\ 0 & 0 & 1 & -1 & 0 & 0 & 0 & 0 \\ 0 & 0 & 0 & 0 & 1 & 0 & 1 & 0 \\ 1 & 0 & 0 & 0 & 1 & 0 & 0 & 0 \\ 0 & 0 & 0 & 1 & -1 & 0 & -1 & 0 \end{pmatrix}$$

```
>#  the canonical-basis cycles
>eval(h[canonicalcycles]);
```

$\text{table}([b[1] = [[1,[-.256859579359 - 1.04991843161i, 1],$
$\qquad 2,[-.642525578033, 1], 3, [\infty, 1]]],$
$\quad a[3] = [[1,[\infty, 1], 2, [-.256859579359 + 1.04991843161i, -1]]],$
$\quad a[2] = [[1,[1.22951879712, 1], 3, [.256859579359 + 1.04991843161i, -1]]],$
$\quad a[1] = [[1,[-.256859579359 - 1.04991843161i, 1], 2, [-1.22951879712, -1]]],$
$\quad b[2] = [[1,[-.256859579359 - 1.04991843161i, 1],$
$\qquad 2,[-1.22951879712, -1], 1, [1.22951879712, 1], 3, [\infty, 1]]],$
$\quad b[3] = [[2,[\infty, 1], 3, [-.642525578033, -1]]]$
$\qquad])$

Thus, the cycle c_1 is as follows: start on sheet 1 (thus $x = -1.46431608476$, $y = -0.951818492315 - 0.577121407841$i); encircle branch point $x = -0.256859579359 - 1.04991843161$i to arrive at sheet 2 (thus $x = -1.46431608476$, $y = -0.951818492315 + 0.577121407841$i); encircle branch point $x = -1.22951879712$ to arrive back at sheet 1 (thus $x = -1.46431608476$, $y = -0.951818492315 - 0.577121407841$i, once again).

Using the linear combination matrix from the above example, the cycle b_1 is given by $b_1 = c_5 + c_7$, which is rewritten as: start from sheet 1 ($x = -1.46431608476$, $y = -0.951818492315 - 0.577121407841$i); encircle branch point $x = -0.256859579359 - 1.04991843161$i once counterclockwise, ending up at sheet 2 ($x = -1.46431608476$, $y = -0.951818492315 + 0.577121407841$i); encircle branch point $x = -0.642525578033$ one time counterclockwise, and end up at sheet 3 ($x = -1.46431608476$, $y = 2.90363698463$); encircle branch point $x = \infty$ one time counterclockwise, and find yourself back at sheet 1 (back at $x = -1.46431608476$, $y = -0.951818492315 - 0.577121407841$i). Remember that any negative "encircling numbers" imply that the branch point should be encircled clockwise, as is necessary, for instance, for cycle a_3.

Remarks

- Our implementation of the Tretkoff–Tretkoff algorithm [TT84] in "algcurves" is not the first program to implement this algorithm [TT84]. Such a program in Turbo Pascal was already announced in [BT92]. A rewrite in C++ was also communicated to the authors in 1999 (Berry and Tretkoff, Private communication, 1999).These programs start from a representation of the monodromy group of a Riemann surface and construct from it a canonical basis for the homology. To the best of our knowledge, the Maple program `homology`, presented here, is the only program that calculates a canonical basis for the homology of a compact connected Riemann surface defined via the equation of a plane algebraic curve with exact coefficients.
- Since it is entirely combinatorial, the homology algorithm is guaranteed to return the correct result if it received the correct input in the form of the monodromy structure of a plane algebraic curve. The algorithm relies on the monodromy algorithm, which may require the user to increase the default accuracy, as discussed in the Remarks at the end of Sect. 2.7.

2.9 Holomorphic 1-Forms on a Riemann Surface

A basis for the holomorphic 1-forms on a Riemann surface specified by an algebraic curve is given by the span of $\{\omega_1, \ldots, \omega_g\}$, where $\omega_1, \ldots, \omega_g$ are linearly independent holomorphic differentials on the surface. Consider the case of the extended complex x-plane, i.e., the Riemann sphere. Let $R(x)$ be a non-zero meromorphic function on the Riemann sphere. Since meromorphic functions on the Riemann sphere are rational functions, $R(x) = p_n(x)/q_m(x)$,

with $p_n(x)$ and $q_m(x)$ polynomials in x of degrees n and m respectively. Then $\omega = R(x) \, dx$ is by definition a meromorphic differential on the Riemann sphere, i.e., a differential whose only singularities are poles. This differential has poles at the zeros of $q_m(x)$. Hence, in order for ω to be holomorphic, $q_m(x)$ is constant. Without loss of generality, let $q_m(x) = 1$. Furthermore, using $\tau = 1/x$ as a local parameter at $x = \infty$, we can write $\omega = -p_n(1/\tau) \, d\tau/\tau^2$ at infinity. Hence ω has a pole at infinity unless $p_n(1/\tau)$ has at least a double root at $\tau = 0$, but this is impossible. Thus on the Riemann sphere no non-zero holomorphic differentials exist. However, for genus greater than zero, the situation is different; non-zero holomorphic differentials do exist.

The holomorphic differentials are all of the form (see [BK86] or [Noe83])

$$\omega_k = \frac{P_k(x,y)}{\partial_y f(x,y)} dx \ . \tag{2.51}$$

Here $P_k(x,y) = \sum_{i+j \le d-3} c_{kij} x^i y^j$ is a polynomial in x and y of degree at most $d-3$, where as before d is the degree of $f(x,y)$ as a polynomial in x and y. Clearly there are no more than $(d-1)(d-2)/2$ linearly independent polynomials $P_k(x,y)$ of this form. These polynomials, for which the differential $\omega = P(x,y)/\partial_y F(x,y) \, dx$ has no poles in A, are referred to as the *adjoint polynomials*. If the curve $\hat{\Gamma}$ (recall, $\hat{\Gamma}$ is the compactified algebraic curve, whose corresponding Riemann surface is Γ) is nonsingular, then all polynomials $P(x,y)$ of degree $\le d-3$ give rise to a holomorphic differential $\omega = P(x,y)/\partial_y F(x,y) \, dx$. This is of course consistent with the genus of a nonsingular plane algebraic curve of degree d being exactly $(d-1)(d-2)/2$ [BK86], as was already stated in Sect. 2.6.

The denominator $\partial_y F(x,y)$ vanishes at the branch points of $y(x)$ as well as at the singular points, whereas the differential dx vanishes (using local coordinates) only at the branch points of $y(x)$. Therefore, in order for the differential ω_k not to have poles at the singular points, the numerator $P_k(x,y)$ has to vanish at the singular points. Noether [Noe83] showed that on the algebraic curve at a singular point P of multiplicity m_P the adjoint polynomial $P_k(x,y)$ vanishes with multiplicity at least $m_P - 1$. Imposing regularity of the differentials (2.51) at a point P imposes a number of independent linear conditions on the coefficients c_{kij} of the polynomial $P_k(x,y)$. The number of such conditions is equal to the delta invariant δ_P of the singularity P, see Sect. 2.5.

For every singular point, there are $m_P(m_P - 1)/2$ linear conditions which are easily computed. These arise from the fact that $P_k(x,y)$ should vanish at P with multiplicity $m_P - 1$. If $\delta_P = m_p(m_P - 1)/2$ this is a sufficient number of linear equations. Otherwise $\delta_P > m_P(m_P - 1)/2$, and more linear equations are required. Singular points P with $\delta_P > m_P(m_P - 1)/2$ are called special singularities. These extra linear conditions are obtained by using the Puiseux expansions at the singular points at sufficiently high order: direct substitution of the Puiseux expansion in the candidate expression for the

holomorphic differential results in different combinations of the coefficients that necessarily vanish to avoid the presence of singular behavior. Singular points at infinity require a similar treatment, after representing the plane algebraic curve in homogeneous coordinates (X, Y, Z) and equating X or Y to 1.

A different way to obtain the adjoint polynomials is through the use of the Newton polygon [Nov01]. Given the equation $f(x, y) = 0$ for the algebraic curve $\hat{\Gamma}$, its Newton polygon $\mathcal{N}(\hat{\Gamma})$ is the convex hull of all points in the (i, j) plane for which the coefficient of $x^i y^j$ in the equation is nonzero. For each interior point (i, j) (not including boundary points) of $\mathcal{N}(\hat{\Gamma})$, one may construct a meromorphic differential

$$\omega_{ij} = \frac{x^{i-1} y^{j-1}}{\partial_y f(x, y)} dx \ . \tag{2.52}$$

If the algebraic curve is nonsingular, the number of differentials so obtained is exactly g, and all are holomorphic [Nov01]. However, if the curve is singular, linear combinations of these differentials have to be identified that are holomorphic in each set of local coordinates. As above, using the Puiseux expansions at the singular points, this leads to a sufficient number of linear conditions on the coefficients of these linear combinations. As the following example shows, this approach has the advantage that generically fewer candidate differentials are found, simplifying the calculations to incorporate the behavior at the singularities.

Example. We use the familiar example of a hyperelliptic curve to illustrate the above two approaches. Let

$$f(x, y) = y^2 - P_{2g+1}(x) \ , \tag{2.53}$$

where $P_{2g+1}(x)$ is a polynomial of degree $2g + 1$ in x, with only single roots. The corresponding algebraic curve has genus g [Gri89], and there is only one singular point, namely at infinity.

Using the first approach, our candidate holomorphic differentials are

$$\omega_k = \frac{P_k(x, y)}{y} dx \ , \tag{2.54}$$

where $k = 1, \ldots, (d-1)(d-2)/2$, with $d = 2g + 1$. Thus there are $(d-1)$ $(d-2)/2 = g(2g-1)$ possible differentials. For large genera, the discrepancy between the number of independent holomorphic differentials and the number of candidate differentials increases quadratically.

On the other hand, using the Newton polygon approach, we obtain

$$\omega_{ij} = \frac{x^{i-1} y^{j-1}}{\partial_y f(x, y)} dx \ , \tag{2.55}$$
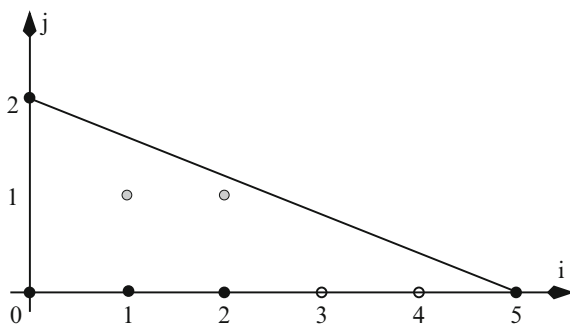
Fig. 2.8. The Newton polygon for a generic hyperelliptic curve of genus $g = 2$, represented in Weierstrass form

where $j = 1$ to avoid the boundary of the polygon, and $i = 1, \ldots, g$. A Newton polygon for the $g = 2$ case is illustrated in Fig. 2.8. We see that, at least for this simple example, the Newton polygon immediately gives a basis of the holomorphic differentials of the correct dimension.

The `differentials` command from the "algcurves" package uses neither of these approaches. A convenient way to determine the adjoint polynomials $P_k(x, y)$ is to use a theorem of Mñuk [Mn97]. This way relies on the computation of an integral basis, see Sect. 2.4. Denote the set of all adjoint polynomials by $\mathrm{Adj}(\hat{\Gamma})$. The elements of $\mathrm{Adj}(\hat{\Gamma})$ are polynomials $P(x, y) \in \mathbb{C}[x, y]$ for which the differential $\omega = P(x, y)/\partial_y F(x, y)\, \mathrm{d}x$ has no poles in A. Then, for any element $f \in O_{A(\Gamma)}$, $f\omega$ also has no poles in A. In fact one can show that in this case $fP(x, y)$ is again a polynomial, and hence is in $\mathrm{Adj}(\hat{\Gamma})$, see [Mn97]. Denoting by $O_{A(\Gamma)} \cdot \mathrm{Adj}(\hat{\Gamma})$ the set of products of elements of $O_{A(\Gamma)}$ with elements of $\mathrm{Adj}(\hat{\Gamma})$, this statement is written as $O_{A(\Gamma)} \cdot \mathrm{Adj}(\hat{\Gamma}) \subset \mathrm{Adj}(\hat{\Gamma}) \subset \mathbb{C}[x, y]$, since all elements of $\mathrm{Adj}(\hat{\Gamma})$ are by definition polynomials in x and y. Theorem 3.3 in [Mn97] shows that this condition determines the adjoint polynomials completely:

$$\mathrm{Adj}(\hat{\Gamma}) = \left\{ P(x, y) \mid O_{A(\Gamma)} \cdot P(x, y) \subset \mathbb{C}[x, y] \right\} . \tag{2.56}$$

Using this result, the linear conditions on the coefficients c_{ij} of $P(x, y) = \sum_{i+j \leq d-3} c_{ij} x^i y^j$ arising from the finite singularities are easily found: having found an integral basis $\{\beta_1, \ldots, \beta_n\}$, the above equation is equivalent to demanding that all products $\beta_j P(x, y)$, $j = 1, \ldots, n$ are polynomials in x and y. Using the equation $f(x, y) = 0$, powers of y^n and higher are eliminated from the quantities $\beta_j P(x, y)$. Then these quantities are all reduced to the form $G_j(x, y)/H_j(x)$, with $G_j(x, y)$ a polynomial in x and y, and $H_j(x)$ a polynomial in x. This is rewritten as $G_j(x, y)/H_j(x) = Q_j(x, y) + R_j(x, y)/H_j(x)$, with the degree of $R_j(x, y)$ as a polynomial in x less than the degree of $H_j(x)$. The condition (2.56) from Mñuk's theorem then states that all coefficients of $R_j(x, y)$ as a polynomial in x and y are zero. These coefficients are linear

combinations of the c_{ij}, and they now are equated to zero. After obtaining similar conditions from the singular points at infinity (see below), the total set of linear equations for the coefficients c_{ij} is solved. The solution set of these equations is g-dimensional, because there are g linearly independent holomorphic differentials and Mñuk proves that (2.56) completely determines the holomorphic differentials. By computing a set of g independent solutions and substituting these in $P(x, y)$, a set of g linearly independent adjoint polynomials $P_k(x, y)$ is found, and hence by (2.51) a basis $\omega_1, \ldots, \omega_g$ for the holomorphic 1-forms is found.

If $\hat{\Gamma}$ has special singular points at infinity, a similar reasoning applies, but only after transforming (2.51) such that it is expressed using the coordinate functions $(X/Y, Z/Y)$ or $(Y/X, Z/X)$. Here $(X : Y : Z)$ are the homogeneous coordinates introduced before. Recall that for finite points on $\hat{\Gamma}$, $Z \neq 0$, so that finite points can be denoted by (X, Y), with $Z = 1$. Similarly, for infinite points $Z = 0$, but at least one of X or Y is non-zero. If at a point at infinity $X \neq 0$, then $(X : Y : Z) = (1 : Y/X : Z/X)$. In this case, we put $X = 1$; then $\hat{y} = Y/X$ and $\hat{z} = Z/X$ are good local coordinate functions near this point at infinity. Otherwise, if $X = 0$ but $Y \neq 0$, then $\tilde{x} = X/Y$ and $\tilde{z} = Z/Y$ are good local coordinates. In the first case, the differential is transformed to the new coordinate functions using $x = X/Z = 1/\hat{z}, y = Y/Z = \hat{y}/\hat{z}$. In the second case, the transformation is $x = X/Z = \tilde{x}/\tilde{z}$, $y = Y/Z = 1/\tilde{z}$. This transformation is now applied to the equation for the plane algebraic curve (2.1) and the equation for the adjoint polynomial $P(x, y) = \sum_{i+j \leq d-3} c_{ij} x^i y^j$. This results in two equations: an equation for the algebraic curve in the new coordinates and a polynomial $\bar{P}$ in the new coordinates, namely the numerator of $P(x, y)$ under the transformation. The coefficients of this new polynomial $\bar{P}$ are linear combinations of the coefficients c_{ij}. Finding an integral basis for the algebraic curve in the new coordinate functions and applying Mñuk's result (2.56) gives linear conditions on the coefficients c_{ij}, in addition to the ones obtained using the coordinate functions x and y for the finite points.

If for some singular points at infinity $X = 0$, while for others $Y = 0$, then this process may have to be repeated a total of three times, using all three sets of coordinate functions (x, y), $(\hat{x}, \hat{z})$ and $(\tilde{y}, \tilde{z})$.

Example. Using $f(x, y) = y^3 + 2x^7 - x^3 y$, we illustrate the above method and construct the holomorphic differentials. From (2.51), all holomorphic differentials are of the form $\omega = P(x, y)/(3y^2 - x^3)\mathrm{d}x$, with $P(x, y) = \sum_{i+j \leq 4} c_{ij} x^i y^j$ a polynomial in x and y of degree at most 4. This gives rise to 15 undetermined coefficients c_{ij}. Expressed in homogeneous coordinates $(X : Y : Z)$, the singular points are $P_1 = (0 : 0 : 1)$ and $P_2 = (0 : 1 : 0)$. The second singular point P_2 is infinite and the conditions it imposes on the coefficients of $P(x, y)$ are derived after we find the conditions imposed from P_1.

The multiplicity of $P_1 = (0 : 0 : 1)$ is $m_{P_1} = 3$, its delta invariant is $\delta_{P_1} = 4$. Since $\delta_{P_1} = 4 > 3 = m_{P_1}(m_{P_1} - 1)/2$, the integral basis method is used. The integral basis is found (see Sect. 2.4) to be $\{1, y/x, y^2/x^3\}$. Hence all

elements of $O_{A(\Gamma)}$ are of the form $f = f_1(x) + f_2(x)y/x + f_3(x)y^2/x^3$, where $f_j(x)$, $j = 1, 2, 3$ are polynomials in x.

The integral basis gives rise to the conditions that $P(x, y), yP(x, y)/x$ and $y^2 P(x, y)/x^3$ are polynomials in x and y. Clearly only the last two of these result in any conditions on the coefficients. Demanding that $yP(x, y)/x$ is a polynomial in x and y, gives $c_{00} = 0 = c_{01}$. Demanding that $y^2 P(x, y)/x^3$ is a polynomial in x and y gives $c_{10} = 0 = c_{20}$. As expected, the singular point P_1 results in $\delta_{P_1} = 4$ conditions on the coefficients c_{ij}.

We now turn to the singular point at infinity $P_2 = (0 : 1 : 0)$. Since $y_{P_2} \neq 0$, $(\tilde{x}, \tilde{z})$ are good coordinate functions near this point. After homogenizing $y^3 + 2x^7 - x^3 y = 0$ and equating $Y = 1$, we find $\tilde{z}^4 + 2\tilde{x}^7 - \tilde{x}^3 \tilde{z}^3 = 0$ and this algebraic curve now has a singular point at $(\tilde{x}, \tilde{z}) = (0, 0)$. The transformed adjoint polynomial is $\bar{P}(\tilde{x}, \tilde{z}) = \sum_{i+j \leq 4} c_{ij} \tilde{x}^i \tilde{z}^{4-(i+j)}$. Again, the integral basis method is used, since $\delta_{P_2} = 9 > 6 = m_{P_2}(m_{P_2} - 1)/2$. An integral basis is $\{1, \tilde{z}/\tilde{x}, \tilde{z}^2/\tilde{x}^3, \tilde{z}^3/\tilde{x}^5\}$. Imposing that $\tilde{z}\bar{P}(\tilde{x}, \tilde{z})/\tilde{x}$, $\tilde{z}^2 \bar{P}(\tilde{x}, \tilde{z})/\tilde{x}^3$ and $\tilde{z}^3 \bar{P}(\tilde{x}, \tilde{z})/\tilde{x}^5$ are polynomials in $\tilde{x}$ and $\tilde{z}$ demands that all $c_{ij} = 0$, except c_{30} and c_{11}, which are undetermined. Hence the most general adjoint polynomial is

$$P(x, y) = c_{11}xy + c_{30}x^3 . \tag{2.57}$$

Thus a basis of holomorphic differentials for the Riemann surface specified by $y^3 + 2x^7 - x^3 y = 0$ is

$$\omega_1 = \frac{xy}{3y^2 - x^3}\mathrm{d}x , \qquad \omega_2 = \frac{x^3}{3y^2 - x^3}\mathrm{d}x , \tag{2.58}$$

which provides an independent confirmation that the genus of the Riemann surface considered in this example is $g = 2$. The calculation of the holomorphic differentials of the Riemann surface specified by $y^3 + 2x^7 - x^3 y = 0$ using Maple is given below.

```
># load the algcurves package
>with(algcurves):
># define the algebraic curve
>f:=y^3+2*x^7-x^3*y:
># calculate the holomorphic differentials
>differentials(f,x,y);
```

$$\left[\frac{x^3 dx}{3y^2 - x^3}, \frac{xydx}{3y^2 - x^3} \right]$$

2.10 Period Matrix of a Riemann Surface

The values of the integrals of the holomorphic 1-forms along the cycles of the homology are closely related to the geometric and analytic structure of the Riemann surface under consideration [Sie88]. In fact, Torelli's theorem [Gri89] states that, up to isomorphisms, a Riemann surface is determined by these

integrals. The values of the integrals are referred to as the periods of the holomorphic differentials. Given bases of both the homology $\{a_i, b_i, i = 1, \ldots, g\}$ and for the holomorphic 1-forms $\{\omega_i, i = 1, \ldots, g\}$, a period matrix $\boldsymbol{\Omega}$ of the Riemann surface Γ is given by

$$\boldsymbol{\Omega} = (\boldsymbol{A}\ \boldsymbol{B}), \tag{2.59}$$

which is a $g \times 2g$ matrix, consisting of two $g \times g$ blocks:

$$\boldsymbol{A} = (A_{ij})_{i,j=1}^{g}, \quad A_{ij} = \oint_{a_j} \omega_i, \tag{2.60}$$

$$\boldsymbol{B} = (B_{ij})_{i,j=1}^{g}, \quad B_{ij} = \oint_{b_j} \omega_i. \tag{2.61}$$

A canonical basis for the holomorphic 1-forms for a canonical basis of the homology is defined by the normalization

$$\oint_{a_j} \hat{\omega}_i = \delta_{ij}. \tag{2.62}$$

With this basis of holomorphic 1-forms , $\hat{\boldsymbol{A}} \equiv \boldsymbol{I}$, the $g \times g$ identity matrix. The resulting $\hat{\boldsymbol{B}}$ is called a Riemann matrix. If $(\boldsymbol{A}\ \boldsymbol{B})$ is the period matrix obtained from a non-normalized basis of the holomorphic 1-forms, then a Riemann matrix $\hat{\boldsymbol{B}}$ for the Riemann surface is determined by

$$\hat{\boldsymbol{B}} = \boldsymbol{A}^{-1}\boldsymbol{B}. \tag{2.63}$$

The Riemann matrix depends on the chosen basis of the homology. This is discussed below. It follows from the Riemann relations [Gri89,Spr57] (a consequence of Stokes' theorem, see Chap. 1) that the Riemann matrix is symmetric and the eigenvalues of its imaginary part are positive definite. Our algorithm never imposes these conditions on the Riemann matrix, as they do not allow us to make the algorithm more efficient or accurate. As a consequence, the symmetry of the Riemann matrix within the accuracy specified provides an excellent check on the the computational results. The positivity of the eigenvalues of the imaginary part may be checked as well, but requires a little more effort on the part of the user.

Having obtained a canonical basis for the homology and the holomorphic differentials of a Riemann surface using the algorithms of the previous sections, a period matrix is found by evaluation of the integrals (2.60) and (2.61). Once a period matrix is found, the Riemann matrix for the Riemann surface follows from (2.63).

Using (2.49),

$$\oint_{a_j} \omega_i = \sum_{k=1}^{r} \alpha_{jk} \oint_{c_k} \omega_i , \quad \oint_{b_j} \omega_i = \sum_{k=1}^{r} \alpha_{g+j,k} \oint_{c_k} \omega_i , \tag{2.64}$$

and the computation of a period matrix reduces to the computation of the integrals $\oint_{c_k} \omega_i$, $k = 1, \ldots, r$ for the holomorphic differential ω_i. By construction, the cycles c_k consists of line segments and semi-circles in the complex x-plane lifted to the Riemann surface. Each one of these line segments or semi-circles is parameterized by $x = \gamma(t)$, with $0 \leq t \leq 1$. The lifting of $x = \gamma(t)$, denoted by $y = \tilde{\gamma}(y_0, t)$, is obtained by specifying a starting value y_0 of y (essentially the sheet number), and by analytically continuing this value y_0 along $x = \gamma(t)$. Hence $\tilde{\gamma}(y_0, 0) = y_0$ and $f(\gamma(t), \tilde{\gamma}(y_0, t)) = 0$. Thus we have to numerically evaluate integrals of the type

$$\int_0^1 \frac{P_i(\gamma(t), \tilde{\gamma}(y_0, t))}{\partial_y F(\gamma(t), \tilde{\gamma}(y_0, t))} \gamma'(t) \mathrm{d}t \ . \tag{2.65}$$

The "algcurves" implementation of our algorithm evaluates these integrals using Maple's numerical integration routine. This has the effect that the user can specify the number of significant digits to be used for the computations. If `Digits` is the number of significant digits the user specified, the command `periodmatrix(f,x,y)` attempts to return the periodmatrix of the Riemann surface specified by the plane algebraic curve $f = F(x, y)$ with at least `Digits`-3 significant digits. If this number of significant digits is not attained, a warning is issued. The numerical evaluation of the integrals is slow, since for every evaluation of the integrand numerical analytic continuation is required. As expected, if the user requires more significant digits more computer time is used.

Example. First we compute a Riemann matrix for the Riemann surface specified by $f(x, y) = y^3 + x^4 + x^2$. The genus of this surface is 2, and thus the surface is hyperelliptic [Gri89]. As the reader may verify, the use of the birational transformation

$$u = \frac{y}{x}, \quad v = \frac{2x^3 + y^3}{x^3} \tag{2.66}$$

reduces the equation $f(x, y) = 0$ to

$$v^2 = u^6 - 4, \tag{2.67}$$

which is of the standard form of a hyperelliptic curve of genus 2. Using this, it is possible to calculate the Riemann matrix associated to $f(x, y) = 0$ analytically:

$$\hat{B} = \begin{pmatrix} 1 + \dfrac{2\mathrm{i}}{\sqrt{3}} & -1 - \dfrac{\mathrm{i}}{\sqrt{3}} \\ -1 - \dfrac{\mathrm{i}}{\sqrt{3}} & 1 + \dfrac{2\mathrm{i}}{\sqrt{3}} \end{pmatrix} \ . \tag{2.68}$$

```
># load the algcurves package
>with(algcurves):
># define the algebraic curve
```

```
>f:=y^3+x^4+x^2:
># calculate a period matrix for the Riemann surface
># corresponding to f
>pm:=periodmatrix(f,x,y):
># use only 5 significant digits, for display purposes
>evalf(pm,5);
```

$$
\begin{pmatrix}
.9999999971 + 1.154700542i & -.9999999950 - .5773502479i \\
-.9999999920 - .5773502773i & 1.000000016 + 1.154700531i
\end{pmatrix}
$$

```
>PM:=Matrix([[1+2*I/s,-1-I/s],[-1-I/s,1-2*I/s]]);
```

$$
\mathrm{PM} := \begin{pmatrix}
1 + \dfrac{2i}{\sqrt{3}} & -1 - \dfrac{i}{\sqrt{3}} \\
-1 - \dfrac{i}{\sqrt{3}} & 1 + \dfrac{2i}{\sqrt{3}}
\end{pmatrix}
$$

```
> evalf(PM);
```

$$
\begin{pmatrix}
1. + 1.154700539i & -1. - .5773502693i \\
-1. - .5773502693i & 1. + 1.154700539i
\end{pmatrix}
$$

We see that the "algcurves" implementation gives the promised accuracy.

Example. This example computes a period matrix and a Riemann matrix for the Riemann surface specified by the algebraic curve given by $f(x,y) = y^3 + 2x^7 - x^3y = 0$. Since for this example, an exact answer is not known, the accuracy of the output is estimated by the absolute values of the anti-symmetric part of the Riemann matrix.

```
># load the algcurves package
>with(algcurves):
># define the algebraic curve
>f:=y^3+2*x^7-x^3*y:
># calculate a period matrix for the Riemann surface
># corresponding to f
>pm:=periodmatrix(f,x,y):
># use only 5 significant digits, for display purposes
>evalf(pm,5);
```

$$
\begin{pmatrix}
-.71618 - .98573i & 1.1588 - 2.3480i & -1.2184i & 1.9715i \\
-1.8496 + .60096i & -1.1431 + 2.7753i & -1.9448i & -1.2019i
\end{pmatrix}
$$

```
># calculate a Riemann matrix for the Riemann matrix
># corresponding to f
>rm:=evalf(periodmatrix(f,x,y,Riemann),10);
```

$$
\begin{pmatrix}
.2360680016 + 1.175570489i & -.1180339855 - .3632712593i \\
-.1180339976 - .3632712768i & -.5000000061 + .36327127i
\end{pmatrix}
$$

```
># load the linalg package
>with(linalg):
># compute the anti-symmetric part of rm
>evalm(rm-transpose(rm));
```

$$
\begin{pmatrix}
0 & 0.121\ 10^{-7} + 0.175\ 10^{-7} \\
-0.121\ 10^{-7} - 0.175\ 10^{-7} & 0
\end{pmatrix}
$$

```
># increase the digits used in computations to 20.
>Digits:=20;
># calculate a Riemann matrix using 20 digits.
>rm:=periodmatrix(f,x,y,Riemann):
># compute the anti-symmetric part of rm
>evalm(rm-transpose(rm));
```

$$
\begin{pmatrix}
0 & 0.41\ 10^{-18} + 0.1\ 10^{-19} \\
-0.41\ 10^{-18} - 0.1\ 10^{-19} & 0
\end{pmatrix}
$$

If the roles of the coordinate functions x and y are switched, x is regarded as an algebraic function of y, $x = x(y)$. This results in an entirely different monodromy. Thus, the coordinate representation of the homology and which cycles are chosen as basis elements may be completely different. The period matrix computation results in a different but symplectically equivalent period matrix, see Chap. 1.

2.11 Abel Map Associated with a Riemann Surface

The Abel map $\boldsymbol{\mathcal{A}}$ from a genus g Riemann surface Γ to its Jacobian $J(\Gamma) = \mathbb{C}^g/\Lambda(\Gamma)$ is defined as

$$
\boldsymbol{\mathcal{A}}(P_0, P) = (\mathcal{A}_i(P_0, P))_{i=1}^g , \quad \mathcal{A}_i(P_0, P) = \int_{P_0}^P \hat{\omega}_i , \tag{2.69}
$$

where P_0, P are places on Γ, and $\hat{\omega}_i$ is the i-th normalized holomorphic 1-form. Also, $\Lambda(\Gamma)$ is the fundamental period lattice associated with the Riemann surface:

$$
\Lambda(\Gamma) = \{\boldsymbol{M} + \hat{\boldsymbol{B}}\boldsymbol{N}, \ \boldsymbol{M}, \boldsymbol{N} \in \mathbb{Z}^g\} . \tag{2.70}
$$

The same path from P_0 to P is used for all components of $\boldsymbol{\mathcal{A}}(P_0, P)$. In almost all applications, the place P_0 is thought of as fixed, whereas the place P may vary. For the purposes of computing the Abel map, both are treated in the same way, since obviously

$$
\boldsymbol{\mathcal{A}}(P_0, P) = \boldsymbol{\mathcal{A}}(P_0, Q) + \boldsymbol{\mathcal{A}}(Q, P) = -\boldsymbol{\mathcal{A}}(Q, P_0) + \boldsymbol{\mathcal{A}}(Q, P) , \tag{2.71}
$$

where Q is any place on Γ. We choose Q to be the place on the first sheet, above the base point a. All Abel map computations are split as in (2.71) with this choice of Q.

The input of the places P_0 and P is given in terms of Puiseux series. If P_0 and P are regular places, it suffices to specify an (x, y)-pair so that $f(x, y) = 0$. On the other hand, if, for instance, P is not a regular place, it needs to be specified by a Puiseux series of sufficiently high order in order to tell it apart from any other places with the same x-coordinate. Therefore, at least as many terms have to be used as necessary to specify the non-regular place as given by the option 0 in Maple's Puiseux command, see Sect. 2.3.

As in the previous section, the integrals of the holomorphic differentials reduce to integrals of the type

$$\int_0^1 \frac{P_i(\gamma(t), \tilde{\gamma}(y_0, t))}{\partial_y F(\gamma(t), \tilde{\gamma}(y_0, t))} \gamma'(t) \mathrm{d}t \ , \tag{2.72}$$

where this time $\gamma(t)$ is a part of a path from Q to P. This path consists of segments of the cycles c_k, $k = 1, \ldots, r$, for which the integration has already been done (allowing for the use of Maple's `remember` tables, dramatically increases the speed of the implementation of the algorithm), and new segments leading from a point on these cycles to the end point P. As before, $\tilde{\gamma}$ is used to denote the lift of γ to the appropriate sheet. Let us specify these paths in more detail. The paths consist of three main parts:

1. A path C_1, which is followed from Q to $\hat{Q}$, where $\hat{Q}$ lies above the base point on the same sheet as P. The places $P = (x_P, y_P)$ and $Q = (x_Q, y_Q)$ are said to lie on the same sheet if following the path constructed in Sect. 2.7 for the monodromy computation from the point x_Q to x_P leads y_Q to y_P. This first path C_1 connects two regular places, and there is no difficulty involved with using the numerical analytic continuation method, as outlined in Sect. 2.7. The only issue remaining is which path C_1 to follow. The path used is the shortest in a graph-theoretic sense: using the result from the monodromy algorithm, a table is made which tabulates which branch points can be used as gateways to go between which sheets. Since the Riemann surface is connected, it is possible to go from any sheet to any other sheet. The path C_1 is chosen so that the number of branch points to encircle is minimized.

2. A second path C_2 is followed from $\hat{Q}$ to $\hat{P}$, where $\hat{P}$ is the place closest (using the Euclidean distance) to P on a lift of the paths used on the x-Riemann sphere to the covering, see Fig. 2.9. The beginning and the endpoint of C_2 are regular places, and the numerical analytic continuation is used as before.

3. A third and last path C_3 is followed from $\hat{P}$ to P. This path can always be chosen as a straight-line path, which is what we do. By construction, this path does not pass close to any non-regular place (places above problem points or infinity), unless P is itself close to an irregular point. If P is not
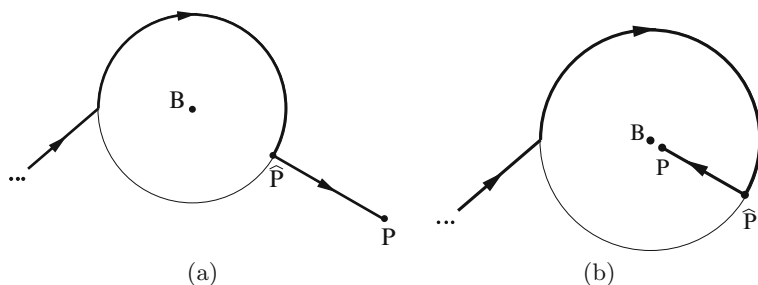
Fig. 2.9. Paths taken by the Abel transform to the place P. Depicted are lifts of the paths introduced for the monodromy algorithm to the appropriate sheet up to $\hat{P}$. From the $\hat{P}$ to P a straight-line path is used. For (a), the place P is far from any of the non-regular places, and numerical analytical continuation is used. For (b), the place P is too close to the non-regular place B, and a symbolic method using Puiseux expansions is employed

close to an irregular place, numerical analytic continuation may be used, as for the above two paths. If P is close to, or is an irregular place, then Puiseux series are used to expand the integrand in a power series of the local parameter t. The integral near the non-regular place is calculated symbolically, using this expansion method. We should remark that it was shown in [Pat07] that the radius of convergence of a Puiseux series around an irregular place is exactly the distance to the next closest irregular place. Once this symbolic method has allowed us to step away from the non-regular point sufficiently far, we again resort to numerical analytic continuation.

Some more remarks are in order about the symbolic integration steps. The integrands under consideration are holomorphic differentials, thus they are regular everywhere. Near a non-regular point, the singular terms are canceled symbolically, leaving us with a regular power series (truncated, of course) to integrate symbolically. The symbolic integration routine may be split in several smaller paths. The method works well in accordance with the above quoted convergence result, even in the case that P is a place at or near infinity. By the use of local parameters on the path, all integrals are proper integrals.

The Abel map is only defined modulo the period lattice of Γ. Thus, if the user wishes to check, validate or compare results of the calculation, it is necessary to have an additional command that allows us to reduce vectors modulo the period lattice, so as to obtain a unique representative inside the fundamental cell, i.e., on the Jacobian $J(\Gamma)$. Such a lattice reduction is easily implemented: we wish to write the vector $\boldsymbol{v} \in \mathbb{C}^g$ as

$$\boldsymbol{v} = [\boldsymbol{v}] + [[\boldsymbol{v}]] \,, \tag{2.73}$$

where $[\,\cdot\,]$ is a lattice vector, and $[[\,\cdot\,]]$ is a vector in the fundamental cell. We have

$$[\boldsymbol{v}] = \boldsymbol{M} + \hat{\boldsymbol{B}}\boldsymbol{N} , \tag{2.74}$$

for some $\boldsymbol{M}$, $\boldsymbol{N} \in \mathbb{Z}^g$. From the imaginary part of this equation, we easily find $\boldsymbol{N}$, after which $\boldsymbol{M}$ is found from the real part.

Example. A hyperelliptic curve of genus g may be written in Weierstrass form (see Appendices B and C) as

$$y^2 = P_{2g+1}(x), \tag{2.75}$$

where $P_{2g+1}(x)$ is a polynomial of degree $2g + 1$. It is known that the Abel map between any two branch points of a hyperelliptic curve is two torsion, i.e., twice the Abel map is a vector in the fundamental lattice $\Lambda(\Gamma)$ [Mum83]. We test this below for the curve

$$y^2 = (x^2 - 1)(x^2 - 4)(x^2 - 9)(x - 4) , \tag{2.76}$$

which has genus 3. The user may wish to refer to Sect. 2.3 for the syntax of the command `puiseux`, used below. As the starting place for the Abel map we choose the branch place with $x = -2$. The final place is the branch place at ∞. The command `ModPeriodLattice` is not available in Maple 11, but it, or a variant of it, will be available in Maple 12. The user can access the corresponding code at `http://www.amath.washington.edu/~bernard/papers.html`.

```
>#  load the algcurves package
>with(algcurves):
>#  define the algebraic curve
>f:=y^2-(x^2-1)(x^2-4)(x^2-9)(x-4):
>#  define the first place
>P1:=puiseux(f,x=-2,y,0,t)[1];
>#  define the second place
>P2:=puiseux(f,x=infinity,y,0,t)[1];
>#  we compute the Abel map from P1 to P2 with 10 digits of
>#  accuracy
>V:=AbelMap(f,x,y,P1,P2,t,10);
```

$$[.4782132267 - .6857777356\mathrm{i}, .04205771245 + .2852729945\mathrm{i},$$
$$.03629471563 - .2163228835\mathrm{i}]$$

```
>#  We compute the Riemann matrix B, to define the lattice.
>B:=periodmatrix(f,x,y,`Riemann`):
>#  Now we reduce. With the option `fraction` the command
>#  ModPeriodLattice
>#  returns the coefficients of the linear combination of
```

```
># lattice vectors that is equal to the lattice reduced
># vector.
>W:=ModPeriodLattice(2*V,B,'fraction');
```

$$\left[.99999922115566032, .879 \ 10^{-7}, .99999996924885282, .824 \ 10^{-7}, \right.$$
$$\left. .490957264234290476 \ 10^{-7}, .895170631038744930 \ 10^{-7}\right]$$

Up to small errors, these coefficients are all integers, implying that $2V$ is indeed a lattice vector.

Example. Recall from Chap. 1, that a divisor on a Riemann surface Γ is a formal sum of places with multiplicities. A divisor $\mathcal{D}$ is written as $\mathcal{D} = \sum_j p_j P_j$, where $p_j P_j$ denotes that the place P_j has multiplicity p_j. The degree of a divisor is the sum of its multiplicities, denoted $\deg \mathcal{D} = \sum_j p_j$. As an example, we compute the Abel map of the divisor of a meromorphic function on a Riemann surface, which has degree 0. By Abel's theorem, the resulting Abel map should be a point on the Jacobi lattice.

Consider the Riemann surface defined by

$$f(x, y) = y^8 + xy^5 + x^4 - x^6 \ . \tag{2.77}$$

This curve is not hyperelliptic, and has genus 8. We consider a meromorphic function y which has 6 zeros and 6 poles. The divisor of this functions can be written in the form (the formal sum of poles and zeros of the function)

$$D(y) = \left(-1 + \frac{t^5}{2}, t\right) + \left(1 + \frac{t^5}{2}, t\right) + \left(-t^3, t\right) + 3\left(t^5, -t^3\right)$$
$$-3\left(-\frac{1}{t^4}, -\frac{1}{t^3} + \frac{t^2}{8}\right) - 3\left(\frac{1}{t^4}, \frac{1}{t^3} + \frac{t^2}{8}\right) \ ; \tag{2.78}$$

we have used truncated Puiseux series to denote the different places in the divisor. Thus, t is a local parameter near the considered place. Below we define these points, and compute the Abel map of this divisor. Next, we reduce the resulting vector modulo the period lattice, to confirm Abel's theorem for this example.

```
># load the algcurves package
>with(algcurves):
># define the algebraic curve
>f:=y^8+x*y^5+x^4-x^6:
>genus(f,x,y);
```

$$8$$

```
># define the first place
>P[1]:=[x=-1+t^5/2,y=t]:
```

```
># define the second place
>P[2]:=[x=1+t^5/2,y=t]:
># define the third place
>P[3]:=[x=-t^3,y=t]:
># define the fourth place
>P[4]:=[x=t^5,y=-t^3]:
># define the fifth place
>P[5]:=[x=-1/t^4,y=-1/t^3+t^2/8]:
># define the sixth place
>P[6]:=[x=1/t^4,y=1/t^3-t^2/8]:
># define the multiplicities of all the places
>mult:=[1,1,1,3,-3,-3]:
># a starting point
>P0:=op(allvalues(puiseux(f,x=3,y,0,t))[1]);
```

$$P0 := [x = t + 3, y = \text{RootOf}(\_Z\,\hat{}\,8 + 3\_Z\,\hat{}\,5\text{-}648, \text{index} = 1)]$$

```
># Now we compute the Abel map of this divisor
>V:=add(mult[k]*AbelMap(f,x,y,P0,P[k],t,10));
```

$$
\begin{aligned}
V := [\ &-1.299153227 - 0.6624504705i, -0.2781898109 - 0.2041198002i, \\
&1.043210043 - 1.236099255i, 0.2796159734 + 0.4278560587i, \\
&0.2308962889 + 1.673495279i, 0.5429291623 - 1.575797812i, \\
&-1.300381962 + 0.6826256767i, 0.1436819475 + 0.0356601776i]
\end{aligned}
$$

```
># We reduce the vector V modulo the period lattice. First
># we compute the Riemann matrix B, to define the lattice.
>B:=periodmatrix(f,x,y,'Riemann'):
># Now we reduce.
>W:=ModPeriodLattice(V,B,'fraction');
```

$$
\begin{aligned}
[&0.9999998122, 0.9999998812, 0.9999999259, \\
&0.1429633247\ 10^{-6}, 0.9999994837, 0.9999999613, \\
&0.1218\ 10^{-6}, 0.5789289936\ 10^{-7}, 0.9999999395, \\
&0.9999998593, 0.9999999317, 0.9999997945, \\
&0.9999997974, 0.9999997890, 0.9999995188, 0.9999998646]
\end{aligned}
$$

Up to small errors, these numbers are all integers, implying that V is indeed a lattice vector.

2.12 Riemann Constant Vector of a Riemann Surface

Often, the Riemann constant vector is first encountered in the context of the Jacobi inversion problem, that is, the problem of finding a set of g places $P_1, \ldots, P_g$ for a given initial place P_0 on a Riemann surface Γ of genus g

such that $\sum_{i=1}^{g} \mathcal{A}(P_0, P_i) \equiv \boldsymbol{z}$ for a given vector $\boldsymbol{z} \in J(\Gamma)$, see [Dub81] (here '$\equiv$' denotes equal up to periods). Consequently the Riemann constant vector appears in all formulas determining finite-gap solutions of integrable equations, see [BBE$^+$94] for examples.

Before continuing, it is convenient to recall the definitions of the Riemann theta function, the m-th symmetric power of a Riemann surface and the divisor of an Abelian differential.

- The Riemann theta function (see Chap. 1) with parametric dependence on a $g \times g$ Riemann matrix $\hat{\boldsymbol{B}}$ (see Sect. 2.10) is given by

$$\theta : \boldsymbol{z} \mapsto \theta(\boldsymbol{z}|\hat{\boldsymbol{B}}) = \sum_{\boldsymbol{n} \in \mathbb{Z}^g} \exp\left\{2\pi\mathrm{i}\left(\frac{1}{2}\boldsymbol{n} \cdot \hat{\boldsymbol{B}}\boldsymbol{n} + \boldsymbol{z} \cdot \boldsymbol{n}\right)\right\} , \qquad (2.79)$$

  where $\boldsymbol{z} \in \mathbb{C}^g$. Next, we let Θ, known as the *theta divisor*, denote the subset of the Jacobian $J(\Gamma)$ such that $\theta(\boldsymbol{z}|\boldsymbol{B}) = 0$ for $\boldsymbol{z} \in \Theta$. Then the theta divisor is a complex $g - 1$ dimensional sub-manifold of $J(\Gamma)$ [FK92].
- A divisor $\mathcal{D} = \sum_j p_j P_j$ is called effective (or positive) if all p_j are positive. The set of all effective divisors of degree m on Γ is denoted $S^m\Gamma$, this is the m-th symmetric power of Γ.
- The divisor (ν) of an Abelian (or meromorphic) differential ν with zeros at the places $P_1, \ldots, P_m$ with multiplicities $p_1, \ldots, p_m$, and poles at the places $Q_1, \ldots, Q_n$ with multiplicities $q_1, \ldots, q_n$ is given by $(\nu) = \sum_{j=1}^{m} p_j P_j - \sum_{j=1}^{n} q_j Q_j$.

Let $\boldsymbol{z} = (z_1, \ldots, z_g) \in \mathbb{C}^g$, and assume an initial place P_0 is given. Consider the function $\phi : \Gamma \mapsto \mathbb{C}$ given by

$$\phi(P) = \theta(\mathcal{A}(P_0, P) - \boldsymbol{z} - \boldsymbol{K}_{P_0}) , \qquad (2.80)$$

where $\boldsymbol{K}_{P_0} = (K_1, \ldots, K_g)$ is defined componentwise by

$$K_i = \frac{1 + \boldsymbol{B}_{ii}}{2} - \sum_{j \neq i} \oint_{a_j} \left(\omega_j(P) \int_{P_0}^{P} \omega_i\right) . \qquad (2.81)$$

If ϕ is not identically zero on Γ, then it has g zeros $P_0, \ldots, P_g$ and, up to permutation, these zeroes uniquely solve the Jacobi inversion problem. This is the Riemann Vanishing Theorem [Dub81]. The vector $\boldsymbol{K}_{P_0}$ is called the Riemann constant vector with initial place P_0. The algorithm to compute the Riemann constant vector for an arbitrary place P_0 on a Riemann surface does not use formula (2.81), which is computationally too expensive. Instead, it relies on the two ideas described below.

- Given the divisor $\mathcal{D} = (\nu)$ of an Abelian differential ν and any initial place $P_0 \in \Gamma$, the Abel map of the divisor is such that [FK92]

$$-\mathcal{A}(P_0, \mathcal{D}) \equiv 2\boldsymbol{K}_{P_0} , \qquad (2.82)$$

where the Abel map $\mathbf{A}(P_0, \mathcal{D})$ of a divisor $\mathcal{D} = \sum_i p_i P_i$ is defined additively: $\mathbf{A}(P_0, \mathcal{D}) = \sum_i p_i \mathbf{A}(P_0, P_i)$. For convenience, denote by $\mathbb{H}_\Gamma$ the set of half lattice vectors in $J(\Gamma)$. That is,

$$\mathbb{H}_\Gamma = \left\{ \boldsymbol{h} \in J(\Gamma) : \boldsymbol{h} = \left[\!\left[\frac{1}{2}\boldsymbol{M} + \frac{1}{2}\boldsymbol{B}\,\boldsymbol{N} \right]\!\right], \quad \boldsymbol{M}, \boldsymbol{N} \in \mathbb{Z}^g \right\}, \qquad (2.83)$$

where $[\![\boldsymbol{z}]\!]$ is the vector $\boldsymbol{z} \in \mathbb{Z}^g$ reduced modulo the period lattice Λ. We denote the elements of $\mathbb{H}_\Gamma$ by $\boldsymbol{h}_i$ and assume $\boldsymbol{h}_1$ is the zero vector with $2g$ components. Using this notation, the equivalence relation (2.82) is rewritten as

$$-\frac{1}{2}\mathbf{A}(P_0, \mathcal{D}) + \boldsymbol{h}_i = \boldsymbol{K}_{P_0}, \qquad (2.84)$$

for an appropriate vector $\boldsymbol{h}_i \in \mathbb{H}_\Gamma$ chosen from the 2^{2g} elements of $\mathbb{H}_\Gamma$. Let us summarize: the above equation provides us with a finite number of possibilities for the Riemann constant vector. How do we select the correct one? The next paragraph provides a way to characterize the Riemann constant vector.

- Irrespective of the initial place P_0, the Riemann constant vector $\boldsymbol{K}_{P_0}$ is defined (see [FK92] and Chap. 1) via the theta divisor, i.e., the set of all $\boldsymbol{z} \in J(\Gamma)$ with $\theta(\boldsymbol{z}) = 0$ through the relation

$$\boldsymbol{z} \equiv \mathbf{A}(P_0, \mathcal{D}) + \boldsymbol{K}_{P_0}, \qquad (2.85)$$

with the divisor $\mathcal{D} \in S^{g-1}\Gamma$. Substituting $\mathcal{D} = (g-1)P_0$ in (2.85) demonstrates that $\theta(\boldsymbol{K}_{P_0}) = 0$ for all $P_0 \in \Gamma$.

Once the Riemann constant vector of any place P_0 on Γ is known, the Riemann constant vector of any other place P_0' may be computed using the formula

$$K_{P_0'} \equiv K_{P_0} - (g-1)\mathbf{A}(P_0, P_0'). \qquad (2.86)$$

Specifically, to compute $\boldsymbol{K}_{P_0}$ we first compute $\boldsymbol{K}_Q$, where, as before, Q is the place on the first sheet above the base point. Next, we compute the Abel map $\mathbf{A}(P_0, Q)$. Then the desired Riemann constant vector is a simple vector sum. The algorithm to compute the Riemann constant vector $\boldsymbol{\kappa}$ of $Q \in \Gamma$ is outlined below. The general idea is to use the fact that there is exactly one vector $\boldsymbol{h} \in \mathbb{H}_\Gamma$ such that $\theta(\boldsymbol{\kappa} + \boldsymbol{h} + \mathbf{A}(Q, \mathcal{D})) = 0$ for all $\mathcal{D} \in S^{g-1}\Gamma$. We use the following steps:

1. Compute the Riemann matrix associated with Γ as discussed in Sect. 2.10.
2. Calculate the divisor (ω) of one of the holomorphic (Abelian of the first kind) differentials ω from Sect. 2.9. To do this, consider the holomorphic differential ω and a place Q specified as a Puiseux expansion using the local coordinate t. The place Q is an element of the divisor (ω) with multiplicity q if near Q the differential ω has the representation $\omega_Q = t^q\, h(t)\mathrm{d}t$, where

$h(t)$ is locally holomorphic and $h(0) \neq 0$ [Gri89]. Such places occur only for a finite number of x-values, since a holomorphic differential has exactly $2g - 2$ zeros. Three groups of places are checked for membership in (ω):

(a) The intersection points of $P(x,y) = 0$ with $f(x,y) = 0$, where $\omega = P(x,y)\mathrm{d}x/\partial_y f(x,y)$. These are the obvious candidates for the zeros of ω. This is done by calculating the resultant (2.24) of $P(x,y)$ and $f(x,y)$ to eliminate y and to obtain a polynomial equation in x only. Using Puiseux expansions, places consisting of the roots of this equation and their corresponding y values are substituted in ω to determine their multiplicity.

(b) The places corresponding to the problem points defined in Sect. 2.7. Recall that the problem points include branch points, singular points, and the roots of $a_n(x) = 0$. These points may be zeros of ω, due to the presence of the differential $\mathrm{d}x$ in ω. As above, substitution of the Puiseux expansions at these places allows us to determine the multiplicity (possibly zero) of zeros of the Abelian differential ω.

(c) Places at infinity. These are treated in a different set of coordinates as usual, following from their description in terms of homogeneous coordinates. Their multiplicities are determined as above.

3. Compute the initial candidate for the Riemann constant vector, $\boldsymbol{\kappa}$, given by

$$\boldsymbol{\kappa} = \frac{1}{2}\boldsymbol{\mathcal{A}}(Q,(\omega)) + \boldsymbol{h}_1 = \frac{1}{2}\boldsymbol{\mathcal{A}}(Q,(\omega)) . \tag{2.87}$$

Using this first candidate, all other candidates are constructed as $\boldsymbol{\kappa} + \boldsymbol{h}_i$ for some $i \in \{2, \dots, 2^{2g}\}$.

4. Using the methods of [DHB$^+$04], we construct $T_\epsilon(\boldsymbol{z})$, an approximation for $\hat{\theta}(\boldsymbol{z}|\hat{\boldsymbol{B}})$ (the oscillatory part of the Riemann theta function, see [DHB$^+$04]) such that $|T_\epsilon(\boldsymbol{z}) - \hat{\theta}(\boldsymbol{z}|\hat{\boldsymbol{B}})| \leq \epsilon$.

5. For each of the 2^{2g} possible choices for $\boldsymbol{h}_i$, compute $\tau_i = |T_\epsilon(\boldsymbol{\kappa} + \boldsymbol{h}_i)|$, the approximate absolute value of the oscillatory part of the θ-function evaluated at the candidate Riemann constant vector associated with $\boldsymbol{h}_i$. By (2.85) and the theorem on the uniform approximation for theta functions from [DHB$^+$04], if $\tau > \epsilon$, the candidate is eliminated from the list of potential Riemann constant vectors.

   Note that ϵ in Step 4 is chosen to be fairly large (to minimize the evaluation time of T_ϵ), but sufficiently small to eliminate a relatively large number of candidates. This choice is made heuristically, as obtaining the statistics for arbitrary θ-function values needed for a better choice is computationally more expensive than evaluating T_ϵ a number of 2^{2g} times required for this part of the algorithm.

6. If Step 5 did not eliminate all but one candidate Riemann constant vector, further elimination is required. To this end we choose $g-1$ arbitrary places $P_1, \dots, P_{g-1} \in \Gamma$. A sequence $\mathcal{D}_1, \mathcal{D}_2, \dots$ of effective, degree $g-1$ divisors is formed from these places. If $\boldsymbol{h}_i$ is the correct half-lattice vector, then

by (2.84), $\theta(\boldsymbol{\kappa} + \boldsymbol{h}_i + \boldsymbol{\mathcal{A}}(Q, \boldsymbol{\mathcal{D}_j})) = 0$ for all $\mathcal{D}_j \in \mathcal{D}_1, \mathcal{D}_2, \ldots$. Thus, beginning with $j = 1$ and incrementing j as needed, we compute $\tau_i = |T_\epsilon(\boldsymbol{\kappa} + \boldsymbol{h}_i + \boldsymbol{\mathcal{A}}(Q, \mathcal{D}_j))|$ for all remaining candidates $\boldsymbol{\kappa} + \boldsymbol{h}_i$, eliminating those for which $\tau_i \geq \epsilon$. With each such check, the probability that there remain several $\boldsymbol{h} \in \mathbb{H}_\Gamma$ drops, as Θ is a $g - 1$ complex-dimensional sub-manifold of the g complex-dimensional manifold $J(\Gamma)$. In other words, the algorithm succeeds with probability 1. However, if several candidates are retained, the algorithm returns a corresponding error message. Otherwise the algorithm has found exactly one candidate $\boldsymbol{\kappa} + \boldsymbol{h}_i \in \Theta$: this is $\boldsymbol{\kappa} = \boldsymbol{K}_Q$.

The vector $\boldsymbol{K}_Q$ depends only on choices that are made algorithmically, namely the choice of homology basis and the base place Q (a place covering the base point). Permuting the holomorphic differentials basis induces the same permutation on the indices of $\boldsymbol{K}_Q$, $\boldsymbol{\mathcal{A}}$ and $\hat{\boldsymbol{B}}$. This is a trivial dependence as it is a mere reordering of the coordinates of $\mathbb{C}^g$, or alternatively, of $J(\Gamma)$.

The "algcurves" package of Maple 11 does not contain an implementation of the algorithm discussed here to compute the Riemann constant vector. However, such an implementation should be included in the release of Maple 12.

The following examples work with the `RiemannConstants` command as if it were a regular part of the "algcurves" package already.

Example. We compute the vector of Riemann constants for two places on the genus 2 curve defined by $y^3 + 2x^7 - x^3 y = 0$.

```
>with(algcurves):
># define the algebraic curve
>f:=y^3+2*x^7-x^3y:
># define the initial place
>P0:=puiseux(f,x=0,y,0,t)[1];
```

$$\left[x = t^2, y = t^3 \right]$$

```
># we compute the Riemann constant vector for P0
># asking for 5 digits of accuracy
>K:=RiemannConstants(f, x, y, P0, 5);
```

$$K := [.954915388\,10^{-1} - .2938926454\mathrm{i}, -.5000000019 + .5877852634\mathrm{i}]$$

```
># we compute the Riemann matrix B, to define the lattice
>B:=periodmatrix(f,x,y,'Riemann'):
># we compute the oscillatory part of the
># Riemann theta function evaluated at K; []denotes that no
># derivatives of the theta function are computed, .001 is
    the
># prescribed error estimate for the neglected terms in
># the theta series
>RiemannTheta(K, B, [], .001, output = list)[2];
```
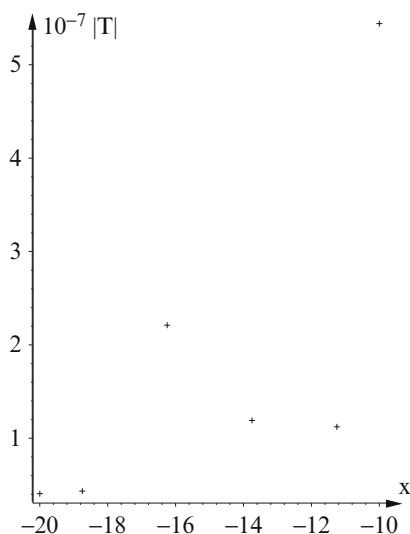
Fig. 2.10. The absolute value of the oscillatory part T_ϵ of the Riemann theta function evaluated at vectors $K0 + (g-1)\mathcal{A}(A_1, P_i)$ as a function of the x coordinate of P_i. The choice of the points P_i is discussed in the main text

$$.6372315\,10^{-7} - .1058378153\,10^{-7}\mathrm{i}$$

```
>#  RiemannConstants may also be called with the flag 'ZERO'
>#  which computes the Riemann constant vector of the
>#  place A_{1} on sheet one above the base point chosen by
    the
>#  monodromy procedure
>K0:=RiemannConstants(f, x, y, 'ZERO', 5);
```

$$K0 := [-.1300434055 - .4090318795\mathrm{i}, -.4799342464 + .4016561674\mathrm{i}]$$

```
>#  the oscillatory part of the Riemann theta function
>#  evaluated at K0
>RiemannTheta(K0, B, [], .001, output = list)[2];
```

$$-.9139985751\,10^{-6} - .1478028554\,10^{-5}\mathrm{i}$$

The fact that the absolute values of the oscillatory parts of the Riemann theta function computed in the previous example are small provides no verification that the correct Riemann constant vector has been obtained, since the algorithm chooses the candidates for the Riemann constant vector with exactly this property. To obtain an independent check, we need to verify that the difference, up to numerical error, between the Abel map of the $(g-1)$-th symmetric power and of the theta divisor is indeed equal to our choice for the

Riemann constant vector for a set of points on the Riemann surface. This is shown in Fig. 2.10. As both $S^{g-1}\Gamma$ and Θ are strictly lower dimensional sub-manifolds of $J(\Gamma)$, this demonstrates that the Riemann constant vector was chosen almost surely correct. An approximation of this offset at several arbitrarily chosen points on Γ is computed as follows: we compute a discrete set of points on the genus 2 Riemann surface Γ arising from $y^3 + 2x^7 - x^3y = 0$: we lift the regular points $(-20, -18.75, -16.25, -13.75, -11.25, -10)$, all on the arbitrarily chosen straight line from -20 to -10 in $\mathbb{C}$, to the places $P_1, \ldots, P_6$ on the first sheet. Next, we compute $V_i = K0 + (g-1)\mathcal{A}(base, P_i)$, where $base$ is the place on Γ chosen during the computation of the monodromy and $K0$ is the Riemann constant vector of $base$ computed in the previous example. In Fig. 2.10 we show the points $(x_i, |T(V_i)|)$, where x_i is the x-coordinate of place P_i and T is the approximate absolute value of the oscillatory part of the Riemann theta function. Small numerical error aside, the vectors V_i are in Θ, thus providing numerical confirmation of the correctness of $K0$.

Appendix

All of the algorithms discussed in the previous sections of this chapter are general in the sense that they apply to all compact connected Riemann surfaces with an exact representation of the coefficients in the defining equation for the algebraic curve. In this appendix, we discuss the use of a few algorithms that apply to restricted classes of algebraic curves and Riemann surfaces, such as elliptic and hyperelliptic surfaces. This appendix contains many examples, but no detailed explanation of the specifics of the algorithms.

1. Parameterizing a Plane Algebraic Curve of Genus Zero

If the genus of an algebraic curve is zero, then this curve can be parameterized in terms of rational functions [Gri89]. A method to construct such a parametrization was given by van Hoeij in [vH97]. This method is implemented as the `parametrization` command in the "algcurves" package. An example of its use is presented below.

Example. Consider the algebraic curve defined by

$$f = y^5 + 2y^4x - 4x^4 \ . \tag{2.88}$$

The genus of this curve is zero. We use the `parametrization` command to compute a rational parametrization of the algebraic curve in terms of a parameter t. If the genus of the algebraic curve is not zero, an error is returned.

```
>#  load the algcurves package
>with(algcurves):
>#  define the algebraic curve
```

```
>f:=y^5+2*y^4*x-4*x^4:
># calculate a rational parametrization for the
># algebraic curve defined by f using a parameter t
>parametrization(f,x,y,t);
```

$$\left[\frac{4}{t^4(2+t)}, \frac{4}{t^3(2+t)}\right]$$

2. When is an Algebraic Curve Hyperelliptic?

An algebraic curve of genus at least 2 is called hyperelliptic if there exists a holomorphic mapping of degree 2 from the curve into the extended complex plane [Gri89]. In practice, hyperelliptic curves stand out from other algebraic curves in the sense that many of their properties resemble those of elliptic curves, including how they may be represented: a hyperelliptic curve is birationally equivalent to a curve of the form

$$v^2 = P_{2g+1}(u) \;, \tag{2.89}$$

where P_{2g+1} is a polynomial of degree $2g + 1$. This is discussed in the next section. All curves of genus 2 are hyperelliptic [Gri89], but generically, curves of higher genus are not hyperelliptic. A theorem of Max Noether [Noe83] allows one to check when a plane algebraic curve is hyperelliptic, from the knowledge of its holomorphic differentials: let

$$\{f_1(x,y)\mathrm{d}x, \ldots, f_2(x,y)\mathrm{d}x\} \tag{2.90}$$

denote the set of holomorphic differentials on $\hat{\Gamma}$, defined by $f(x,y) = 0$. Next, one forms the quadratic combinations

$$\{f_i(x,y)f_j(x,y), \; i,j = 1, \ldots, g\} \;. \tag{2.91}$$

For a hyperelliptic algebraic curve, exactly $2g-1$ of these functions are linearly independent. For non-hyperelliptic curves, the number of linearly independent functions in the set (2.90) is greater than $2g-1$. Noether's theorem was used by van Hoeij to implement the "algcurves" command **is_hyperelliptic**, which determines whether a given plane algebraic curve is hyperelliptic or not.

Example. In this example, we use the is_hyperelliptic command to check whether three plane algebraic curves are hyperelliptic. The first curve has genus 2, thus is hyperelliptic. The next curve has genus 3, and is not hyperelliptic. The last curve has genus three, but is hyperelliptic.

```
># load the algcurves package
>with(algcurves):
># define the first algebraic curve
```

```
>f1:=y^3-2*x*y+x^4:
># define the second algebraic curve
>f2:=y^3-2*x*y+x^5:
># define the third algebraic curve
>f3:=y^9+3*x^2*y^6+3*x^4*y^3+x^6+y^2:
># the genus of the first curve
>genus(f1,x,y);
```

$$2$$

```
># thus, the curve is hyperelliptic
>is_hyperelliptic(f1,x,y);
```

$$\text{true}$$

```
># the genus of the second curve
>genus(f2,x,y);
```

$$3$$

```
># this curve is not hyperelliptic
>is_hyperelliptic(f2,x,y);
```

$$\text{false}$$

```
># the genus of the third curve
>genus(f3,x,y)
```

$$3$$

```
># this curve is, in fact, hyperelliptic
>is_hyperelliptic(f3,x,y);
```

$$\text{true}$$

3. The Weierstrass Form of a Hyperelliptic Algebraic Curve

If an algebraic curve is (hyper)elliptic, it is birationally equivalent to (2.89), which is known as the Weierstrass form of the hyperelliptic curve. An algorithm to construct the Weierstrass form for an elliptic curve was devised by van Hoeij [vH95], and later extended to hyperelliptic curves. A Maple implementation of this algorithm is available in the form of the `Weierstrassform` command in the "algcurves" package. We illustrate its use below.

Example. We use the `Weierstrassform` command to construct the Weierstrass form of the hyperelliptic plane algebraic curve defined by $f_3(x,y)$ in

the previous example. The Weierstrass form will be expressed in terms of two new coordinate functions u and v. These are rational functions of x and y. Their inverse $x(u,v)$ and $y(u,v)$ are also rational, and explicitly provided by the algorithm.

```
># load the algcurves package
>with(algcurves):
># define the algebraic curve
>f3:=y^9+3*x^2*y^6+3*x^4*y^3+x^6+y^2:
># the Weierstrass form
>wf:=Weierstrassform(f3,x,y,u,v):
>wf[1];
```

$$v^2 + 2 - 7*u - 35u^3 + 21u^2 + 35u^4 - 21u^5 + 7u^6 - u^7$$

```
>wf[2];                          # u(x,y)
```

$$\frac{y\left(x^2+y^3+1\right)}{y+x^4+2x^2y^3+y^6}$$

```
>wf[3];                          # v(x,y)
```

$$-\frac{x\left(x^2+y^3\right)}{y}$$

```
>wf[4];                          # x(u,v))
```

$$-(-1+u)v$$

```
>wf[5];                          # y(u,v)
```

$$1 - 3u + 3u^2 - u^3$$

Acknowledgements

References

[Abh90]   Abhyankar, S.S.: Algebraic geometry for scientists and engineers. Math-
             ematical Surveys and Monographs, vol. 35, American Mathematical
             Society, Providence, RI (1990)
[BBE⁺94]   Belokolos, E.D., Bobenko, A.I., Enol'skii, V.Z., Its, A.R., Matveev, V.B.:
             Algebro-geometric approach to nonlinear integrable problems. Springer
             Series in Nonlinear Dynamics. Springer, Berlin (1994)
[BK86]   Brieskorn, E., Knörrer, H.: Plane Algebraic Curves. Birkhäuser Verlag,
             Basel (1986)
[Bli66]   Bliss, G.A.: Algebraic Functions. Dover Publications Inc., New York
             (1966)
[Bob11]   Bobenko, A.I.: Introduction to compact Riemann surfaces. In: Bobenko,
             A.I., Klein, Ch. (eds.) Lecture Notes in Mathematics 2013, pp. 3–64.
             Springer, Berlin (2011)
[BT92]   Berry, K., Tretkoff, M.D.: The periodmatrix of macbeath's curve of genus
             seven. Contemp. Math. **136**, 31–40 (1992)
[DFN85]   Dubrovin, B.A., Fomenko, A.T., Novikov, S.P.: Modern geometry–
             methods and applications. Part I. Graduate Texts in Mathematics, vol.
             104. Springer, New York (1985)
[DHB⁺04]   Deconinck, B., Heil, M., Bobenko, A.I., van Hoeij, M., Schmies, M.: Com-
             puting Riemann theta functions. Math. Comput. **73**, 1417–1442 (2004)
[DP07a]   Deconinck, B., Patterson, M.S.: Computing the Abel map. Phys. D **237**,
             3214–3232 (2008)
[Dub81]   Dubrovin, B.A.: Theta functions and nonlinear equations. Russian Math.
             Surveys, **36**(2), 11–80 (1981)
[DvH01]   Deconinck, B., van Hoeij, M.: Computing Riemann matrices of algebraic
             curves. Phys. D, **152–153**, 28–46 (2001)
[FK92]   Farkas, H.M., Kra, I.: Riemann Surfaces, 2nd en. Springer, New York,
             (1992)
[Gri89]   Griffiths, P.: Introduction to algebraic curves. American Mathematical
             Society, Providence, RI (1989)
[Mn97]   Mñuk, M.: Computing adjoint curves. J. Symb. Comput. **23**, 229–240
             (1997)
[Mum83]   Mumford, D.: Tata lectures on theta. I, Progress in Mathematics, vol.
             28. Birkhäuser, Boston, MA (1983)
[Noe83]   Noether, M.: Rationale Ausführungen der Operationen in der Theorie
             der algebraischen Funktionen. Math. Ann. **23**, 311–358 (1883)
[Nov01]   Novikov, S.P. (ed.): Dynamical systems. IV, volume 4 of Encyclopaedia
             of Mathematical Sciences, vol. 4. Springer, Berlin (2001)
[Pat07]   Patterson, M.S.: Algebro-geometric algorithms for integrable systems.
             University of Washington Ph.D thesis (2007)
[Pot07]   Poteaux, A.: Computing monodromy groups defined by plane algebraic
             curves. Preprint, pp. 1–13. (2007)
[Rie90]   Riemann, G.B.: Gesammelte mathematische Werke, wissenschaftlicher
             Nachlass und Nachträge. Springer, Berlin (1990)
[Sie88]   Siegel, C.L.: Topics in complex function theory. Vol. I. Wiley, New York
             (1988)
[Spr57]   Springer, G.: Introduction to Riemann surfaces. Addison-Wesley Pub-
             lishing Company, Inc., Reading, Mass. (1957)

[TT84]   Tretkoff, C.L., Tretkoff, M.D.: Combinatorial group theory, Riemann sur-
             faces and differential equations. Contemp. Math. **33**, 467–517 (1984)
[vdW91]   van der Waerden, B.L.: Algebra, Vol. I. Springer, New York (1991)
[vH94]   van Hoeij, M.: An algorithm for computing an integral basis in an alge-
             braic function field. J. Symb. Comput. **18**, 353–363 (1994)
[vH95]   van Hoeij, M.: An algorithm for computing the Weierstrass normal form.
             In: ISSAC '95 Proceedings, pp. 90–95. (1995)
[vH97]   van Hoeij, M.: Rational parametrizations of algebraic curves using a
             canonical divisor. J. Symbolic Comput. **23**, 209–227 (1997)
[Wal62]   Walker, R.J.: Algebraic Curves. Dover Publications Inc., New York
             (1962)

3

Algebraic Curves and Riemann Surfaces in Matlab

Jörg Frauendiener[1,2] and Christian Klein[3]

[1] Department of Mathematics and Statistics, University of Otago,
   P.O. Box 56, Dunedin 9010, New Zealand
   `joergf@maths.otago.ac.nz`
[2] Centre of Mathematics for Applications, University of Oslo,
   P.O. Box 1053 Blindern, NO-0316 Oslo, Norway
[3] Institut de Mathématiques de Bourgogne,
   Université de Bourgogne,
   9 avenue Alain Savary,
   21078 Dijon Cedex, France
   `christian.klein@u-bourgogne.fr`

3.1 Introduction

In the previous chapter, a detailed description of the algorithms for the 'algcurves' package in Maple was presented. As discussed there, the package is able to handle general algebraic curves with coefficients given as exact arithmetic expressions, a restriction due to the use of exact integer arithmetic. Coefficients in terms of floating point numbers, i.e., the representation of decimal numbers of finite length on a computer, can in principle be handled, but the floating point numbers have to be converted to rational numbers. This can lead to technical difficulties in practice. One also faces limitations if one wants to study families of Riemann surfaces, where the coefficients in the algebraic equation defining the curve are floating point numbers depending on a set of parameters, i.e., if one wants to explore modular properties of Riemann surfaces as in the examples discussed below. An additional problem in this context can be computing time since the computation of the Riemann matrix uses the somewhat slow Maple integration routine. Thus, a more efficient computation of the Riemann matrix is interesting if one wants to study families of Riemann surfaces or higher genus examples which are computationally expensive.

Modular properties of Riemann surfaces are of interest in many fields of mathematics and physics. Numerical methods can be helpful to explore related questions and to visualize the results. Examples in this context are determinants of Laplacians on Riemann surfaces which appear for instance in conformal field theories, see [QS97] for an overview. Interesting related

questions are the existence of extremal points of the determinants and their global properties. A numerical study of these aspects for the determinant of the Laplacian in the Bergman metric on Riemann surfaces of genus 2 was presented in [KKK09]. The surfaces of genus 2 are known to be all hyperelliptic which simplifies the analysis, but the modular space has already six real dimensions. Thus, a numerical study of modular spaces requires efficient algorithms even in low genus.

The modular dependence of Riemann surfaces is also important in the asymptotic description of so-called dispersive shocks, highly oscillatory regions in solutions to purely dispersive equations such as the Korteweg-de Vries (KdV) and the nonlinear Schrödinger equation (NLS). These equations have almost periodic solutions in terms of multi-dimensional theta functions associated to hyperelliptic Riemann surfaces whose branch points are constant with respect to the physical coordinates. Since the dispersionless equations corresponding to KdV and NLS have shock solutions, the limit of small dispersion leads to rapidly modulated oscillations in the solutions in the vicinity of these shocks. According to Lax and Levermore [LL83], Venakides [Ven85] and Deift, Venakides and Zhou [DVZ97], the asymptotic description of the rapidly modulated oscillations in the dispersive shock is given by the exact solution to the KdV equation on a family of elliptic surfaces, where, however, the branch points depend on the physical coordinates via the Whitham equations [Whi66, Whi74]. A numerical implementation for these so-called single phase solutions was given in [GK07]. Multiphase solutions arising in the asymptotic description of solutions to initial data with several extrema are given in terms of hyperelliptic KdV solutions, see [GT02]. A numerical analysis of such cases would imply the use of an efficient code for families of hyperelliptic curves as given in [FK06]. In the asymptotic description of dispersive shocks for the focusing NLS equation, hyperelliptic curves appear generically, see [KMM03, TVZ04]. In the case of the Kadomtsev–Petviashvili (KP) equation [KP70], a completely integrable 2+1-dimensional generalization of the KdV equation, exact algebro-geometric solutions can be constructed on arbitrary compact Riemann surfaces, see e.g. [BBE+94]. It is unclear which surfaces appear in the asymptotic description of dispersive shocks in the KP equation as numerically studied in [KSM07]. Possibly modular properties of non-hyperelliptic surfaces will play a role in this context.

Families of hyperelliptic curves, where the branch points depend on the physical coordinates, also appear in exact solutions for the Ernst equation. This equation has many applications in mathematics such as the theory of Bianchi surfaces, and physics such as general relativity, see [KR05] for references. Hyperelliptic solutions to the Ernst equation were found by Korotkin [Kor89]. A numerical implementation of these solutions was given in [FK01, FK04]. The Einstein–Maxwell equations in the presence of two commuting Killing vectors are equivalent to the electro-magnetic Ernst equations. The latter have solutions on three-sheeted coverings of $\mathbb{C}P^1$ (which are in

general not hyperelliptic) with branch points depending on the physical coordinates, see [Kor89, Kle03].

To be able to study numerically modular properties of Riemann surfaces, an efficient implementation of the algorithms with floating point coefficients would therefore be helpful. Such an approach can use similar algorithms as a symbolic approach, but faces specific problems due to the inexact representation of the coefficients in the algebraic equations defining the curves. We present here a Matlab implementation which can basically handle the same tasks as the 'algcurves' package, but which uses the numerically optimal integration procedure, the Gauss quadrature. Matlab has access to symbolic computation by calling Maple, but this requires the presence of the latter and the Matlab Symbolic Math Toolbox. To obtain a standalone version and to allow for maximal efficiency, we do not use any symbolic computation here. To the best of our knowledge this is the first purely numerical approach to general algebraic curves [FK09]. Since the algorithms of the algcurves package were discussed in detail in the previous chapter, we will concentrate here on different approaches and on Matlab specific adaptions.

The chapter is organized as follows: In Sect. 3.2 we determine the critical points of an algebraic curve, i.e., branch points and singular points, via the `multroot` package. These points appear in our finite precision approach as zeros of a polynomial with inexact coefficients. Dealing with such polynomials is numerically a delicate problem. In the Maple implementation (see Chap. 2) this difficulty is avoided by the use of exact arithmetic. Here we use the Matlab package `multroot` which provides an efficient way to deal with zeros of polynomials with inexact coefficients. In Sect. 3.3 we compute the Puiseux expansions at the singular points via the Newton polygon. These expansions are used in Sect. 3.4 to determine a basis of the holomorphic one-forms. The monodromy of the algebraic curve is determined in Sect. 3.5 in a similar way as in Maple: the algebraic equation for the curve is solved at a set of points on contours avoiding the critical points. These points are those appearing in the numerical integration, the collocation points of the Gauss quadrature. The computation of the integrals of the holomorphic differentials is then only a matrix multiplication at negligible computational cost. A canonical basis of the homology is found in Sect. 3.6 via the Tretkoff–Tretkoff algorithm [TT84] as in Maple. The periods of the holomorphic 1-forms are computed for this basis. In Sect. 3.8 we discuss the numerical performance and convergence properties in dependence of the numerical resolution in the integration. Since the computational cost turns out to be mainly due to the solution of the algebraic equation on the collocation points, the algorithm is considerably more efficient in cases where the equation can be solved explicitly as for hyperelliptic curves. Since the latter appear in many applications, we present a code to deal with general hyperelliptic curves in Sect. 3.9. In Sect. 3.10 we use the characteristic quantities of the Riemann surface such as the Riemann matrix obtained above to compute multi-dimensional theta functions. This allows for an efficient computation of solutions to certain completely integrable equations as NLS, which we discuss as an example in Sect. 3.11.

3.2 Branch Points and Singular Points

All compact Riemann surfaces can be represented as compactifications of non-singular algebraic curves (see Chap. 1 [Bob11]). As in the previous chapters we consider plane algebraic curves C defined as a subset in $\mathbb{C}^2$, $C = \{(x, y) \in \mathbb{C}^2 | f(x, y) = 0)$, where $f(x, y)$ is an irreducible polynomial in x and y,

$$f(x, y) = \sum_{i=1}^{M} \sum_{j=1}^{N} a_{ij} x^i y^j = \sum_{j=1}^{N} a_j(x) y^j \ . \tag{3.1}$$

We assume that not all a_{iN} vanish and that N is thus the degree of the polynomial in y. The degree in x and y, i.e., the maximum of $i + j$ for non-vanishing a_{ij} is denoted by d.

   In this chapter we will always study the Riemann surface arising from solving (3.1) for y. In general position, for each x there are N distinct solutions y_n corresponding to the N sheets of the Riemann surface. At the points where $f_y(x, y)$ vanishes, there are less than N distinct solutions and thus less than N sheets. These points are either branch points or singularities. The points where $f(x, y) = 0$ and $f_y(x, y) = 0$ are given by the zeros of the resultant $R(x)$ of $Nf - f_y y$ and f_y, the discriminant of the curve. The resultant is given in terms of the $2N \times 2N$ Sylvester determinant; for the explicit form see (2.24) in Chap. 2.4 .

   The algebraic curve is completely characterized by the matrix a_{ij} in (3.1), which is one reason why a matrix-based language such as Matlab is convenient for a numerical treatment of algebraic curves. Each entry in the Sylvester determinant is one of the functions $a_j(x) = \sum_{i=1}^{M} a_{ij} x^i$ depending on x and thus by itself a vector of length M. Therefore, the computation of the determinant involves convolutions of these vectors which are known to be equivalent to products in Fourier space. To compute the resultant, we build the Sylvester determinant of the discrete Fourier transforms of the vectors $a_n = (a_{1n}, \ldots, a_{Mn})^T$. Each vector in this determinant is divided by N for numerical reasons. The determinant is obtained in Fourier space, and the resultant follows from this via an inverse Fourier transform.

   The roots of the resulting polynomial give the x coordinates of the points, where $f(x, y) = f_y(x, y) = 0$. Since, in contrast to Maple, we use finite precision arithmetic, rounding errors occur. We will thus round all numerical results to a certain number of digits which are limited by the machine precision in Matlab.[1] Typically we aim at a precision `Tol` which can be freely chosen between 10^{-10} and 10^{-14}.

---

[1] Matlab works with double precision, i.e., with 16 digits; thus, machine precision is typically limited to the order of 10^{-14} because of rounding errors.

Root finding in Matlab is possible via the `roots` function. It uses efficient algorithms to find the eigenvalues of the so-called companion matrix, i.e., the matrix which has the studied polynomial as the characteristic polynomial. The eigenvalues are determined to machine precision which does not mean, however, that the zeros of the polynomial with coefficients within roundoff error are determined with machine precision. Problems occur if there are multiple roots or roots which are almost identical. It is well known that the computation of multiple roots is a long standing numerical challenge, see for instance [Zen04] for references. The most common approaches in this context use multiprecision arithmetic, i.e., more than 16 digits, and need exact coefficients of the polynomials. However, if the coefficients of the polynomials are not exact, but obtained by truncating the floating point numbers, this will inhibit the identification of the correct multiple roots. Finite precision in the coefficients of the polynomial turns multiple roots into clusters of simple roots. Consider for example the case of the Klein curve, the curve of lowest genus with the maximal number of automorphisms, in the form

$$y^7 = x(x-1)^2 \ . \tag{3.2}$$

The resultant for this curve has the form $R(x) = x^6(x-1)^{12}$. After rounding, our procedure gives the correct coefficients of the polynomial up to machine precision, but instead of the root at 1 with multiplicity 12 `roots(R(x))` returns the following cluster of roots,

```
1.1053 + 0.0297i
1.1053 - 0.0297i
1.0736 + 0.0790i
1.0736 - 0.0790i
1.0224 + 0.1032i
1.0224 - 0.1032i
0.9686 + 0.0980i
0.9686 - 0.0980i
0.9264 + 0.0686i
0.9264 - 0.0686i
0.9037 + 0.0245i
0.9037 - 0.0245i,
```

a result which is obviously useless for our purposes.

This means that in our fully numerical approach to algebraic curves we need a reliable way to find the zeros of a polynomial with non-exact coefficients. Such a way exists in the form of Zeng's Matlab package `multroot`. As discussed in more detail in [Zen04], two algorithms are used by `multroot` to achieve this goal: The first algorithm identifies tentatively the multiplicity of the roots, the second uses a Newton iteration to determine the roots corresponding to this multiplicity structure to machine precision. The code

provides an estimation of the forward and backward error[2] and varies with the multiplicity structure to minimize the backward error. The `multroot` package is very efficient. For the above example of the Klein curve (3.2), it finds the two zeros 0 and 1 with multiplicity 6 and 12, respectively. Rounding is important in this context. The standard way to call `multroot` is with a precision of 10^{-10} of the coefficients, which is what we do. This can be changed if needed by hand, which is also possible for certain control parameters in the iteration as explained in the `multroot` [Zen04] documentation to which the reader is referred for details.

If the coefficients of the studied polynomials reach the order of 10^{10} or if the degree of the polynomials gets very high (of the order of 100), the restriction to machine precision in Matlab imposes obvious limitations on the possibility to identify the correct roots. This is typically the case for curves with singularities of high order. In these situations, which are beyond what we want to study here, the ratio of the estimated forward to backward error will be high, and the results for the roots will not be reliable. If this ratio is greater than 10^3, a warning will be given. The code will still try to compute the characteristic quantities of a Riemann surface, but will in general fail to produce correct results. In certain cases a modification of the input parameters of `multroot` will lead to the correct multiplicity of the roots. An alternative is to provide the correct roots of the resultant, for instance via a mixed symbolic and numerical approach, and to continue the computation with these (to this end one has to provide a vector with the zeros of the resultant and a vector with the singular points). The code will also produce a warning if the ratio of smallest to largest distance between two roots is smaller than 10^{-3} since this might lead to accuracy problems in the ensuing computation.

An approach to algebraic curves based on finite precision floating point numbers obviously faces limitations, but as we will show in the following, these restrictions are not severe. All singular points correspond to multiple roots of the resultant. We are mainly interested in the study of modular properties of generic Riemann surfaces of low genus, i.e., of curves which are regular or do not have singularities corresponding to zeros of very high multiplicity of the resultant. In these cases the purely numerical approach presented here works well and is considerably more efficient than mixed symbolic-numeric approaches.

Given the multiplicity of the roots of the resultant, the code determines the singular points, i.e., the points with $f(x,y) = f_x(x,y) = f_y(x,y) = 0$. All roots x_s with a multiplicity greater than one are tested in this context: the equation $f_y(x_s, y)$ is solved via `multroot` for y. For every root $y_s^{(n)}$ with $f(x_s, y_s^{(n)}) = 0$, it is checked whether $f_x(x_s, y_s^{(n)}) = 0$. All computations are

---

[2] As usual the forward error for the approximation of the value of a function $k(x)$ at some given point x via an approximate function $\tilde{k}(x)$ is defined as the difference $k(x) - \tilde{k}(x)$; the backward error is defined as the difference $\tilde{x} - x$, where $\tilde{x}$ is the value for which $k(\tilde{x}) = \tilde{k}(x)$.

carried out with the prescribed precision `Tol`, and the check whether a relation for a given root is satisfied is carried out with a precision $\mathtt{Tol} * 10^2$ to take care of a loss of accuracy due to rounding. In this way we find all finite branch points (the zeros of the resultant) and singularities unless `multroot` produced a warning.

To determine the singular behavior of the curve $f(x, y) = 0$ at infinity, we proceed similarly as the Maple package: we introduce homogeneous coordinates X, Y, Z via $x = X/Z$, $y = Y/Z$ in (3.1) and get

$$F(X, Y, Z) = Z^d f(X/Z, Y/Z) = 0 . \tag{3.3}$$

Infinite points of the algebraic curve are given by $Z = 0$, for the finite points one can choose $Z = 1$. Singular points at infinity satisfy $F_X(X, Y, 0) = F_Y(X, Y, 0) = F_Z(X, Y, 0) = 0$. We first check for such points with $Y \neq 0$ which implies we can put $Y = 1$ without loss of generality. The roots of $F_X(X, 1, 0) = 0$ are determined via `multroot`. It is then checked as above whether they also satisfy $F_Y(X, 1, 0) = 0$ and $F_Z(X, 1, 0) = 0$. This analysis identifies all singular points with $Y \neq 0$, but not the ones with $Y = 0$ and $X \neq 0$. In the latter case we can put $X = 1$ and check whether $F_X(1, 0, 0) = F_Y(1, 0, 0) = F_Z(1, 0, 0) = 0$. The singularities are given by the code in homogeneous coordinates in the form sing $= [X_s, Y_s, Z_s]$.

In what follows we will always consider the curve

$$f(x, y) = y^3 + 2x^3 y - x^7 = 0 , \tag{3.4}$$

which was already analyzed in the previous chapter as an example for the various aspects of the code, if necessary complemented by further curves. For (3.4) we find the finite branch points[3]

```
bpoints =
      -0.3197 - 0.9839i
       0.8370 - 0.6081i
      -1.0346
       0
       0.8370 + 0.6081i
      -0.3197 + 0.9839i
```

and two singularities,

```
sing =
         0     0     1     4
         0     1     0     9
```

corresponding to $x = y = 0$ and $Y = 1$, $X = Z = 0$. The last column corresponds to the delta invariant at the respective singularity, for a definition of which we refer to the previous chapter and a more detailed explanation below.

---

[3] For the ease of representation we only give 4 digits here though Matlab works internally with 16 digits.

3.3 Puiseux Expansions

To desingularize an algebraic curve, i.e., to obtain an atlas of local coordinates for the Riemann surface corresponding to the algebraic curve, we use series $y(x)$ with rational exponents in the vicinity of the singular point, just as in the previous chapter. These Puiseux expansions are calculated up to the order necessary to identify all sheets of the Riemann surface near the singularities. They are used as local coordinates in the vicinity of these points which will provide part of an atlas for the description of the Riemann surface as a smooth manifold. The procedure is analogous to the introduction of local coordinates at infinity for the example of hyperelliptic curves in Sect. 1.1.1.

We can restrict the analysis to singularities at $(0,0)$ for the following reason: For a singular point (x_s, y_s), we consider the curve $\tilde{f}(\tilde{x}, \tilde{y}) = 0$ obtained from $f(x, y) = 0$, where $\tilde{f}(\tilde{x}, \tilde{y}) = f(x_s + \tilde{x}, y_s + \tilde{y})$. The curve $\tilde{f}(\tilde{x}, \tilde{y}) = 0$ obviously has a singular point at $(0,0)$. At infinity we consider Puiseux expansions in the homogeneous coordinates with the same approach. For the following considerations we will drop the tilde and assume that $(0,0)$ is a singular point of the algebraic curve given by $f(x, y) = \sum_{n,m} a_{nm} x^n y^m = 0$. We write the Puiseux expansions in the form

$$x = t^r , \quad y = \alpha_1 t^{s_1}(1 + \alpha_2 t^{s_2}(1 + \alpha_3 t^{s_3}(1 + \ldots))) , \qquad (3.5)$$

where $r, s_1, s_2, \ldots \in \mathbb{N}$, and where $\alpha_i \in \mathbb{C}$ for $i = 1, 2, \ldots$. Let $y = 0$ be a zero of order m for the equation $f(0, y) = 0$. To identify all sheets in the vicinity of the singular point $(0,0)$, m inequivalent expansions of the form (3.5) are needed:

$$x = t^{r^{(n)}} , \quad y = \alpha_1^{(n)} t^{s_1^{(n)}}(1 + \alpha_2^{(n)} t^{s_2^{(n)}}(1 + \alpha_3^{(n)} t^{s_3^{(n)}}(1 + \ldots))) , \qquad (3.6)$$

$n = 0, 1, \ldots, m$, where $r^{(n)}, s_1^{(n)}, s_2^{(n)}, \ldots \in \mathbb{N}$, and where $\alpha_i^{(n)} \in \mathbb{C}$ for $i = 1, 2, \ldots$ and $n = 0, 1, \ldots, m$. We define the *singular part* of a Puiseux expansion as the part of the series up to the order where all sheets in the vicinity of the singularity are uniquely identified, i.e., the terms in (3.6) up to the $t^{s_i^{(n)}}$ with the smallest index i such that there are m distinct values for the corresponding $\alpha_i^{(n)}$.

In Maple one obtains the singular part by the command

```
puiseux(f,x=0,y,0,t).
```

Although our implementation is in principle suited to give arbitrary orders of the Puiseux expansion, we will only need the singular part to determine the holomorphic differentials on the Riemann surface. Therefore, we will not consider higher orders in the series. In the code, the expansion is done via the Newton polygon, the convex hull of the points (k, l) in $\mathbb{R}^2$ such that the coefficients a_{kl} from (3.1) do not vanish as explained in the previous chapter. For the Puiseux expansion we need only the part of the polygon between the

axes and lines with negative slope closest to them. This is conveniently done by treating the points with non-vanishing a_{kl} as points $z_j = k + il$ in the complex plane.

To construct the polygon, we start with the point z_{j_0} with smallest imaginary part among those with smallest real part. Then the code finds the next vertex of the polygon by considering the argument of the difference $z_j - z_{j_0}$; the minima of these values in $[-\pi/2, 0]$ gives the vertex. The procedure is iterated until the horizontal axis is reached or until there is no more vertex found. The slopes of these lines are equal to $r^{(n)}/s_1^{(n)}$ in (3.6). From these one obtains $r^{(n)}$ and $s_1^{(n)}$ uniquely by choosing them to be coprime. To obtain the values of $\alpha_1^{(n)}$, we substitute $x = t^{r^{(n)}}$ and $y = \alpha_1^{(n)} t^{s_1^{(n)}}$ in $f(x,y) = 0$. The lowest order terms in t must vanish in the resulting equation which leads to a polynomial relation for the $\alpha_1^{(n)}$. This relation is solved as in the previous section with `multroot`.

We are interested here only in the values of $\alpha_1^{(n)}$ which are non-zero. If the number of distinct non-zero $\alpha_1^{(n)}$ obtained in this way for all the edges of the part of the Newton polygon considered here is equal to m (the order of the zero at $y = 0$ in $f(x,y) = 0$), the singular part of the Puiseux expansion is identified. If not, we put

$$x = \hat{x}^{r^{(n)}}, \quad y = \alpha_1^{(n)} \hat{x}^{s_1^{(n)}} (1 + \hat{y}) \tag{3.7}$$

in $f(x,y) = 0$ and obtain the algebraic curve $\hat{f}(\hat{x}, \hat{y}) = 0$ which is again singular at $(0,0)$. With this curve we proceed as before to construct the Newton polygon and to find the Puiseux expansions of the form $\hat{x} = t^{\hat{r}^{(n)}}$ and $\hat{y} = \alpha_2^{(n)} t^{s_2^{(n)}} + \ldots$. The procedure is iterated until the singular part of the Puiseux expansion for the original curve $f(x,y) = 0$ is identified.

Remark 1. Duval [Duv89] gave an algorithm for rational Puiseux expansions, i.e, expansions with rational $\alpha_i^{(n)}$. Since we are here interested in an entirely numerical approach, rational Puiseux expansions do not offer an advantage even in cases where they are applicable. Notice that the exponents $r^{(n)}$ and $s_i^{(n)}$ are determined exactly nonetheless since they are integers. Accuracy problems appear when the algebraic curve has to be transformed in the course of the computation: first when the singularity is not at $(0,0)$, and second when one goes to higher order in the Puiseux expansions. In both cases binomial coefficients appear in the expansion of terms of the form $(x + x_s)^N$ which grow rapidly with N. Since we work with double precision, the unavoidable numerical errors in (x_s, y_s) and in the $\alpha_i^{(n)}$ require careful rounding: typically one loses a factor N in accuracy for each of the above transformations. This means one has to round roughly to the order `Tol` $* 10^s$, where s is the number of transformations performed. Obviously in a purely numerical double precision setting, the available precision of 16 digits thus will eventually limit the attainable accuracy for singularities of high order, at least once `Tol` $* 10^s$ is of

the order of 1. This is why the mixed symbolic-numeric approach to Puiseux expansions by Poteaux [Pot07] requires exact knowledge of the singularities and the coefficients of the curve and a multiprecision arithmetic. Such high order singularities are, however, not generic and beyond the scope of our approach. The rapid growth of the degree of the polynomial $\hat{f}(\hat{x}, \hat{y})$ obtained via successive transformations of the form (3.7) in $f(x, y) = 0$, and thus the size of the matrices $\hat{a}_{kl}$ in (3.1) corresponding to $\hat{f}(\hat{x}, \hat{y})$ on the other hand is of less importance, since the resulting matrices are sparse (which means they have mainly entries with value 0), and since Matlab provides efficient algorithms for sparse matrices.

The output (a variable called `PuiExp`) for the Puiseux expansions procedure is written in the form $[r^{(n)}, s_1^{(n)}, \alpha_1^{(n)}, s_2^{(n)}, \alpha_2^{(n)}, \ldots]$. For the example of the ramphoid cusp, $f(x, y) = (x^2 - x + 1)y^2 - 2x^2 y + x^4 = 0$, we obtain the singular part of the Puiseux expansion at $(0, 0)$ in the form

```
PuiExp =
        2       4       1       1      -1
        2       4       1       1       1
```

which coincides with the Maple result in the previous chapter. In contrast to there, we give also the $\alpha_i^{(n)}$ that differ only by a multiplication with a root of unity.

For the curve (3.4) we find

```
PuiExp{1} =
        2.0000          3.0000          0 + 1.4142i
        2.0000          3.0000          0 - 1.4142i
        1.0000          4.0000          0.5000
PuiExp{2} =
        4.0000          7.0000         -1.0000
        4.0000          7.0000          0 + 1.0000i
        4.0000          7.0000          0 - 1.0000i
        4.0000          7.0000          1.0000
```

where the matrix `PuiExp{1}` corresponds to the singularity at $(0, 0)$ ($[0, 0, 1]$) and the matrix `PuiExp{2}` to infinity ($[0, 1, 0]$).

3.4 Basis of the Holomorphic Differentials on the Riemann Surface

It is well known (see [BK86, Noe83] or the previous chapter) that the holomorphic differentials on the Riemann surface associated to an algebraic curve (3.1) can be written in the form

$$\omega_k = \frac{P_k(x, y)}{f_y(x, y)} \mathrm{d}x , \tag{3.8}$$

where the adjoint polynomials $P_k(x,y) = \sum_{i+j\leq d-3} c_{ij}^{(k)} x^i y^j$ are of degree at most $d-3$ in x and y. If the curve has no singular points, there are no further conditions on the P_k and, consequently, there are $g = (d-1)(d-2)/2$ linearly independent polynomials P_k. Since, as is well known, the dimension of the space of holomorphic 1-forms is equal to the genus g of the Riemann surface, the genus is $(d-1)(d-2)/2$ in this case.

If there are singular points, the set of which is denoted by S, there is a number δ_P – called the delta invariant – of further conditions on the P_k at a point $P \in S$ as a consequence of the holomorphicity of the differentials also at these points. The genus of the surface is given in this case by

$$g = \frac{1}{2}(d-1)(d-2) - \sum_{P\in S} \delta_P \ . \tag{3.9}$$

We determine these conditions by substituting the singular part of the m Puiseux expansions (3.6) at the singular points $P = (x_s, y_s)$ into (3.8). As described in the previous section this implies the transformation of both $f_y(x,y)$ and $P_k(x,y)$ to the coordinates $x = \tilde{x} + x_s$, $\tilde{y} + y_s$. In the denominator we determine the lowest power of t, denoted by n_D in the following.

If the singular part of the Puiseux expansion consists of one term only, the procedure is straightforward[4]: we get for the differentials in (3.8) in lowest order in t

$$\omega_k \sim \sum_{i+j\leq d-3} \left\{ \tilde{c}_{ij}^{(k)} t^{N_P(i,j)} + o\left(t^{N_P(i,j)} \right) \right\} dt \ , \tag{3.10}$$

where $N_P(i,j) = ri + s_1 j + r - 1 - n_D$ (r, s_1 as defined in (3.5)). Since the ω_k must be holomorphic in every coordinate chart, no negative powers in t can arise in (3.10) which implies that all coefficients in front of such terms must vanish. If a negative power $N_P(i,j)$ appears only once in an expansion, the corresponding $\tilde{c}_{ij}^{(k)} = 0$. If there are several $\tilde{c}_{ij}^{(k)}$ with the same value $N_P(i,j) < 0$, only a linear combination of them has to vanish. Transforming back to x and y, we obtain conditions on the coefficients $c_{ij}^{(k)}$. The number of linearly independent relations of this kind at a singularity is equal to its delta invariant. It is determined here simply by counting the conditions. For an alternative way to determine the delta-invariant at a given point from the Puiseux expansions alone see [Kir92] or the previous chapter.

If the singular part of the Puiseux expansion consists of several terms, higher order expansions of $P_k(x,y)$ and $f_y(x,y)$ in t have to be considered. To determine the lowest power of t, denoted by t^{n_D}, in $f_y(x,y)$ we use, if necessary several times, transformations of the form (3.7) as in the computation of the Puiseux expansions described in the previous section. For the polynomials $P_k(x,y)$ we get in a similar way

---

[4] For readability we omit the index (n) in (3.6) in the sequel; it is understood that the procedure described below has to be repeated for each of the m inequivalent Puiseux expansions.

$$P_k = \sum_{i+j\leq d-3} \sum_{l_1=0}^{j} \sum_{l_2=0}^{l_1} \ldots \sum_{l_{p-1}=0}^{l_{p-2}} \tilde{c}_{ij}^{(k)} t^{N_P(i,j,l_1,\ldots,l_{p-1})} \times$$

$$\alpha_1^j \alpha_2^{l_1} \alpha_3^{l_2} \ldots \alpha_p^{l_{p-1}} \binom{j}{l_1} \binom{l_1}{l_2} \ldots \binom{l_{p-2}}{l_{p-1}} ,$$

(3.11)

where the singular part of the Puiseux expansion (3.5) consists of p terms, and where the numbers $N_P(i,j,l_1,\ldots,l_{p-1}) = ri+js_1+l_1s_2+l_2s_3+\ldots+l_{p-1}s_p+r-1-n_D$ (r, $s_1,\ldots$ as defined in (3.5)) are stored as a $(p+1)$-dimensional array. For instance, for a singular part of the form $y = \alpha_1 t^{s_1}(1+\alpha_2 t^{s_2})$ we obtain in (3.10) powers of t with the exponents $N_P = ri + s_1 j + r - 1 - n_D + s_2 k$, $k = 0,\ldots j$ which is a 3-dimensional array in i, j and k. As above, negative powers must not appear due to the holomorphicity condition for the differentials. Thus, for a given exponent $N_P(i,j,l_1,\ldots,l_{p-1}) < 0$, the linear combination of the corresponding $\tilde{c}_{ij}^{(k)}$ must vanish. Thus, the array of exponents $N_P(i,j,l_1,\ldots,l_{p-1})$ in (3.11) also takes care of conditions for the holomorphicity of the differentials at the considered singularity due to higher order terms in the Puiseux expansions.

Singular points at infinity are treated in a completely analogous way after the transformation $x \to X/Z$ and $y \to Y/Z$ to homogeneous coordinates, which implies for (3.8)

$$\omega_k = \frac{Z^{d-3}P_k(X/Z,Y/Z)}{Z^{d-1}f_y(X/Z,Y/Z)} Z^2 \mathrm{d}(X/Z) = \frac{Z^{d-3}P_k(X/Z,Y/Z)}{Z^{d-1}f_y(X/Z,Y/Z)}(Z\mathrm{d}X - X\mathrm{d}Z) .$$

(3.12)

The powers of Z in the numerator and the denominator are chosen in a way that both are polynomials in X, Y and Z. With $X = X_s + \tilde{X}$ we get for (3.12)

$$\sum_{i+j\leq d-3} \sum_{l=0}^{i} c_{ij}^{(k)} \binom{i}{l} X_s^{i-l} \tilde{X}^l Y^j Z^{d-3-i-j} .$$

(3.13)

The Puiseux expansions can be used as above to determine the conditions on the $c_{ij}^{(k)}$.

To implement the conditions on the adjoint polynomials at the singularities in Matlab, we write the matrix $c_{ij}^{(k)}$ with $i + j \leq d - 3$ in a standard way as a vector $\mathbf{c}$ of length $(d-1)(d-2)/2$. The holomorphicity of (3.8) at the singular points implies relations of the form $H\mathbf{c} = 0$ where H is a $((d-1)(d-2)/2) \times \sum_{P\in S} \delta_P$ matrix. Each condition on $\mathbf{c}$ following from (3.10) or (3.11) gives a line in H. The first such condition found is stored as the first row of H. For each subsequent condition found, it is checked that this new condition is linearly independent of the already present ones in H. This is done in the following way: if the matrix H contains M linearly independent conditions on $\mathbf{c}$, the first M rows will be non-trivial, and H has rank M. The new condition will be tentatively added as row $M + 1$ in H, and it will be checked if the

resulting matrix has rank $M+1$. If not, the new condition is linearly dependent on the M conditions already stored in H, and line $M+1$ will be suppressed. At the end of this procedure, there will be $\sum_{P \in S} \delta_P$ non-trivial lines in this matrix. The holomorphic differentials correspond to the vectors $\mathbf{c}$ in the kernel of the matrix H. They are determined with the Matlab command *null*, where $null(\mathrm{H})$ provides an orthonormal basis for the null space of H. Notice that for reasons of numerical accuracy we do not look for a rational basis $\mathbf{c}$ of the kernel of H even in cases where such a basis exists. The polynomials P_k are stored in the form of matrices $c_{nm}^{(k)}$ where in Matlab convention $P_k(x,y) = \sum_{n,m=0}^{d-3} c_{nm}^{(k)} x^{d-3-n} y^{d-3-m}$, and where the first row/column has $n = 0/m = 0$. The code gives the matrices $c^{(k)}$ as $c\{1\}, \ldots, c\{g\}$, where g is the genus of the Riemann surface. For the curve (3.4), where d=7, we get

```
c{1} =
          0    0    0    0    0
          0    0    0    0    1
          0    0    0    0    0
          0    0    0    0    0
          0    0    0    0    0
c{2} =
          0    0    0    0    0
          0    0    0    0    0
          0    0    0    0    0
          0    0    0    1    0
          0    0    0    0    0
```

i.e., the polynomials $P_1 = xy$ and $P_2 = x^3$. Thus, the curve has genus 2.

3.5 Paths for the Computation of the Monodromies

To compute the monodromy group of a given Riemann surface, we proceed in a similar way as in the 'algcurves' package described in the previous chapter. In Sect. 3.2 we have determined the discriminant points, i.e., the branch points and singularities of a given algebraic curve, which are denoted by b_i, $i = 1, \ldots, N_c$. In this section we construct a set of generators for the fundamental group $\pi_1(\mathbb{C}P^1 \setminus \{b_i\}_{i=1}^{N_c})$: First we choose a base point a on $\mathbb{C}P^1 \setminus \{b_i\}_{i=1}^{N_c}$. Then we construct a set of contours Γ_i, $i = 1, \ldots, N_c$, i.e., closed paths in the base of the covering starting at the base point a and going around each of the finite discriminant points projected into the base. These contours have to generate the fundamental group of $\mathbb{C}P^1 \setminus \{b_i\}_{i=1}^{N_c}$ as discussed in Chap. 1, see Fig. 1.14. Numerical problems are to be expected if a contour Γ_i comes too close to one of the discriminant points or to points, where y is infinite on the algebraic curve, i.e., to one of the *problem points* P_j as defined in the previous chapter. Thus, it is necessary in the construction of the contours that all of them have a minimal distance from all problem points.

As in the previous chapter we determine the minimal distance ρ between any two problem points,

$$\rho = \min_{i \neq j} |P_i - P_j|$$

We choose a radius $R = \kappa\rho$, where $0 < \kappa < 0.5$ for circles around these discriminant points. For a better vectorization[5] of the code we use the same value of R for all discriminant points in contrast to the 'algcurves' package, where such a radius is determined for each of them. We typically work with values of κ between $1/3$ and $1/2.1$ (in Maple, the value $\kappa = 2/5$ is used). With this value for R we define a set of points on these circles,

$$C_i^\pm := b_i \pm R, \quad i = 1, \ldots, N_c,$$

which divide each circle into two half circles. The contours Γ_i, $i = 1, \ldots, N_c$, are built from these half circles and lines between the $C_i^\pm$.

The general procedure to construct the contours Γ_i is as follows: One of the $C_i^\pm$ is chosen to be the base point a. This point can be either, as in the 'algcurves' package, the $C_i^\pm$ with the smallest real part, or the $C_i^\pm$ closest to the arithmetic mean of the b_j, $j = 1, \ldots, N_c$. The latter is the choice here. The discriminant points are then reordered according to an ascending order of the arguments $\phi_i = \arg(b_i - a)$.[6] Let i_0 be the index of the discriminant point, such that a is one of the two points $C_{i_0}^\pm$. The positively oriented contour Γ_{i_0} is simply the circle around b_{i_0}, starting and ending at a.

The contours Γ_i for $i \neq i_0$ are constructed in the following way: one of the points $C_{i_0}^\pm$ and one of the $C_i^\pm$ are connected by a straight line in such a way that the distance between the line and b_i, b_{i_0} is maximal. Even if this connecting line does not touch any of the circles around the other branch points, it can enter the interior of the circles around b_i or b_{i_0} as can be seen in Fig. 3.1, where the paths are drawn for the curve (3.4). Such a connecting line comes closest to the branch points if the distance between it and b_i or b_{i_0} is equal to the minimal distance ρ, and if $|\Re(b_i - b_{i_0})| = R$. A simple calculation shows that the minimal distance between the above connecting line and one of the discriminant points is in this case $d_c := R\sqrt{1 - \kappa^2}$.

If one of the above connecting lines enters the interior of a circle around one of the remaining problem points P_j, the contour has to be deformed as in the Maple package: instead of the line between one of the $C_{i_0}^\pm$ and one of the $C_i^\pm$, two lines are considered between each pair of $C_{i_0}^\pm$ and $C_j^\pm$, and $C_j^\pm$ and $C_i^\pm$. This procedure is iterated until a contour is found that stays away from all problem points with minimal distance d_c. The result of this procedure for the curve (3.4) can be seen in Fig. 3.1.

---

[5] This denotes the simultaneous execution of similar commands by a computer.

[6] Since we use a fully numerical approach, rounding errors imply that there are in general no degeneracies of these arguments. Otherwise standard Matlab ordering is taken.
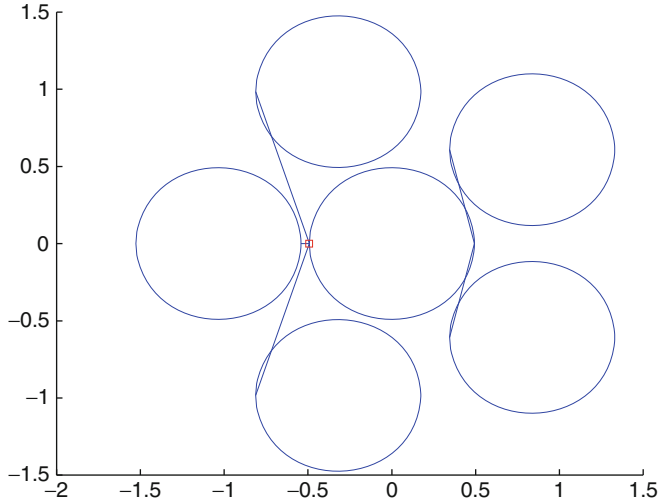
Fig. 3.1. Paths for the computation of the monodromies for the curve (3.4) with a radius of the circles around the discriminant points $R = 2.1 * \rho$, where ρ is the minimal distance between any two branch points. The base point is marked with a square

3.6 Computation of Monodromies and Periods

As shown in Sect. 1.2, an algebraic curve (3.1) defines an N-sheeted covering of the Riemann sphere. This covering can be characterized by the following data: branch points and permutations, which are called the monodromies of the covering. To compute them we lift the basis of $\pi_1(\mathbb{C}P^1 \setminus \{b_i\}_{i=1}^{N_c})$, the contours Γ_i, $i = 1, \ldots, N_c$, constructed in the previous section, to the covering.

Since by construction no branch point or singularity lies on the Γ_i, there are always N distinct roots y_n in $f(x, y) = 0$ for a given $x \in \Gamma_i$, $i = 1, \ldots, N_c$. The procedure is then similar to the one in the 'algcurves' package in Maple: At the base point $x = a$ we label the sheets and obtain a vector $\mathbf{y}(a) = (y_1(a), \ldots, y_N(a)) =: (A_1, \ldots, A_N)$ by solving $f(a, y) = 0$. If we start at a point A_k, $k = 1, \ldots, N$ on the covering, and consider the analytic continuation of the vector of roots $\mathbf{y}$ along one of the contours Γ_i, we will in general obtain a permutation of the components of the vector $\mathbf{y}$ back at the base points,

$$\sigma_i \mathbf{y} := (y_{\sigma_i(1)}(a), \ldots, y_{\sigma_i(N)}(a)) \tag{3.14}$$

The permutation σ_∞ associated to $x = \infty$ can be computed in the same way along a contour Γ_∞ with negative orientation surrounding all finite branch points, i.e., for which we have $\Gamma_1 \Gamma_2 \ldots \Gamma_{N_c} \Gamma_\infty = 1$. Alternatively it follows

from the permutations obtained for the finite discriminant points via the relation

$$\sigma_\infty \circ \sigma_{Nc} \circ \ldots \circ \sigma_1 = 1 \ . \tag{3.15}$$

The group generated by the σ_i is called the monodromy group of the covering.

The task is thus to numerically construct the analytic continuation of the vector $\mathbf{y}$ along the lifted contours Γ_i. Since we are interested in an efficient computation of the Riemann matrix, we do not separate the monodromy computation from the integration of the holomorphic differentials along these contours, but do both in one go. As will be seen in the next section, not all of these integrals are linearly independent. Our integration procedure will thus provide more integrals than actually needed. But the efficient vectorization algorithms in Matlab ensure that the computation of the additional integrals will not be time consuming. In addition, the possibility to check the validity of identities between the computed integrals will provide strong tests of the numerical results since the integrals are computed independently.

For the computation of the integrals of the form $\int_{-1}^{1} \mathcal{F}(x)\mathrm{d}x$ we use Gauss integration which is known to be numerically optimal, see for instance [Tre00] and references therein. The theoretical basis of Gauss(-Legendre) integration is an expansion of the integrand in Legendre polynomials by a *collocation method* on the *Legendre points* $\{x_l\}$, i.e., the zeroes of the Legendre polynomials $\mathcal{P}_n(x)$ for $|x| \leq 1$. This means that we approximate the function $\mathcal{F}(x)$ for $|x| \leq 1$ by a truncated series in Legendre polynomials: $\mathcal{F}(x) \sim \sum_{k=0}^{N_l} a_k \mathcal{P}_k(x)$, where the spectral coefficients a_k follow from imposing this approximation as an exact equation at the Legendre points x_l, i.e., $\mathcal{F}(x_l) = \sum_{k=0}^{N_l} a_k \mathcal{P}_k(x_l)$, $l = 0, \ldots, N_l$ (N_l is also called the number of *modes* in the computation). Consequently, we obtain

$$\int_{-1}^{1} \mathcal{F}(x)dx \sim \sum_{k=0}^{N_l} a_k \int_{-1}^{1} \mathcal{P}_k(x)\mathrm{d}x \ . \tag{3.16}$$

An expansion of a function with respect to a system of globally smooth functions on their domain is called a *(pseudo-)spectral method*. The computation of the spectral coefficients a_k by inverting the matrix $\mathcal{P}_k(x_l)$ and the integral of the Legendre polynomials in (3.16) can be combined in the so-called Legendre weights $\mathcal{L}_k$, with which (3.16) can be written in the form

$$\int_{-1}^{1} \mathcal{F}(x)\mathrm{d}x \sim \sum_{k=0}^{N_l} \mathcal{F}(x_k)\mathcal{L}_k \ . \tag{3.17}$$

Thus, for given function values $\mathcal{F}(x_k)$ at the Legendre points x_k and weights $\mathcal{L}_k$, the numerical approximation of the integral is just the computation of a scalar product. The Legendre points and weights can be conveniently determined in Matlab via Trefethen's code [Tre00, Tre]. They have to be computed only once and are then stored for later use in the numerical integrations.

It is known that the difference between a smooth function $\mathcal{F}$ and its spectral approximation decreases with N_l faster than any power of $1/N_l$, in practice exponentially with the number of modes N_l. Here we have to integrate functions of x and y on a set of contours where the functions are analytic, which guarantees an optimal efficiency of the method provided the radius R of the circles is not too small. Thus, we can reach machine precision typically with $N_l \leq 64$. The contours consist of lines and half circles each of which is mapped to the interval $[-1, 1]$, where we use Gauss integration. To reach machine precision, it is obviously necessary to know the integrand with this precision. Therefore, we cannot analytically continue the vector $\mathbf{y}$ as was done in Maple (see the previous chapter) for the monodromy computation by solving a first order differential equation (to reach machine precision the solution of a differential equation is not efficient, since too many steps would be needed). Instead we will solve the algebraic equation $f(x, y) = 0$ on each collocation point x_l. Since the Γ_i, $i = 1, \ldots, N_c$, by construction do not come close to branch points or singularities, no multiple roots will occur. Thus, we can use `roots` efficiently to determine $\mathbf{y}$. The analytic continuation is obtained by sorting the newly computed vector components according to minimal difference with the components at the previous collocation point.

Carrying out this procedure starting from a base point A_k along some contour Γ_i, $i = 1, \ldots, N_c$, one obtains the permutation by comparing the analytic continuation of $\mathbf{y}$ along Γ_i and $\mathbf{y}$. Since $\mathbf{y}$ is then known at the collocation points, the same holds for the holomorphic differentials there. The integrals of the holomorphic differentials along Γ_i are obtained via Gauss integration, and the results are stored in a $N \times N_c \times g$ array. The sum of integrals of a holomorphic differential over all contours with the same projection into the x-sphere must vanish. In practice this sum will not vanish because of numerical errors and thus gives an indication on the quality of the numerics. The code issues a warning if this sum is greater than the prescribed rounding tolerance `Tol`. The monodromies σ_i are stored in an $N \times N_c$-array. We then check which of the discriminant points are actually branch points, i.e., have non-trivial monodromy. The monodromy at infinity is computed via (3.15) from the monodromies at the finite branch points. It could be computed via the contour Γ_∞ as in Maple to provide an additional test, but this is not done here for reasons of numerical efficiency.

The base point used by the code is stored in the variable `base`, the vector $\mathbf{y}(a)$ indicating the labeling of the sheets in the variable `ybase`, the branch points in `bpoints`, and the monodromies in the variable `Mon`.

For the curve (3.4) the code produces the base point

```
base =
        -0.4926
ybase =
        -0.5031
         0.4736
         0.0296,
```

the branch points

```
bpoints =
     -1.0346
     -0.3197 - 0.9839i
      0.8370 - 0.6081i
            0
      0.8370 + 0.6081i
     -0.3197 + 0.9839i
          Inf
```

and the monodromies

```
Mon =
       1     3     1     2     1     3     2
       3     2     3     1     3     2     3
       2     1     2     3     2     1     1.
```
$$\text{(3.18)}$$

This example shows that going around the first branch point one ends up in the third sheet when starting in the second and vice versa, whereas sheet one is not affected.

Remark 2. The above procedure to compute monodromies and periods is insensitive to the accuracy with which the branch points are computed as long as the error in the branch points is much smaller than the radius of the circles around the points. For numerical accuracy of the periods, it is just important that the branch points are not close to the contours. Inaccuracies in the locations of the singular points will, however, affect the precision since they enter directly the regularity conditions on the holomorphic differentials and thus lead to numerical errors in the $c_{ij}^{(k)}$.

3.7 Homology of a Riemann Surface

The monodromies computed in the previous section provide the necessary information to determine a basis for the homology on a Riemann surface. We use as in the 'algcurves' package (see Chap. 2) the algorithm by Tretkoff and Tretkoff [TT84] to construct such a basis.

The first step in this construction is the identification of the points on the covering belonging to more than one sheet, i.e., the points, where the branching number defined in Sect. 1.3 is different from zero. To this end one has to identify the cycles[7] within the permutations in the monodromies computed in the previous section. This is simply done by determining for each

---

[7] We apologize for the dual use of the word cycle here, for a cycle in permutations and for a closed path; unfortunately cycle denotes different things in different parts of mathematics which are both relevant here.

discriminant point with non-trivial monodromy, i.e., each branch point, the sheets which are permuted whilst encircling this point. The permuted sheets form the cycles within the permutation. They are identified as follows: the monodromies are given as permutations of the vector $(1, 2, \ldots, N)$. For each permutation vector the code identifies the components which are not in the order $(1, 2, \ldots, N)$. For the first such component, it goes to the sheet indicated by this component, then to the next indicated by the component in the vectors there, until the starting point for the procedure is reached again. This identifies the first cycle. For the first vector in the example (3.18), the first permuted component corresponds to the second sheet. The 3 there indicates that going around this point in the second sheet, one ends up in the third. The third component of the permutation vector is a 2, the sheet where this cycle $(2, 3)$ started.

If not all permuted sheets appear in the first cycle identified in this way, the procedure is repeated for the remaining permuted sheets until all permutation cycles are determined. Each such cycle corresponds to one of the N_B ramification points on the covering and is labelled by B_i, $i = 1, \ldots, N_B$, where it is possible that several such points have the same projection onto the complex plane. From the number n_i of elements in the permutation cycle we obtain the branching number $\beta_i = n_i - 1$. The Riemann–Hurwitz formula (see Chap. 1) then allows the computation of the genus:

$$g = \frac{1}{2} \sum_{i=1}^{N_B} \beta_i + 1 - N \ . \tag{3.19}$$

Since the determination of the genus via monodromies is completely independent from the genus computation via the dimension of the space of the holomorphic 1-forms, this provides a strong test for the code. A failure in this test results in an error which typically indicates that the branch points and singularities were not correctly identified by `multroot`. For the curve (3.4) we find that all branch points on the covering connect exactly two sheets except for the one above infinity (3 sheets). The genus is thus 2 in accordance with the results for the holomorphic 1-form

We will briefly give the ingredients of the Tretkoff–Tretkoff algorithm used to determine the homology. This is just a planar version of the Tretkoff–Tretkoff tree constructed on the covering and discussed in Chap. 2. For details and proofs the reader is referred to [TT84]. The algorithm constructs a spanning tree connecting the points A_j on the covering starting from $\{A_1\}$ with the points $\{B_i\}$. We list below a set of rules to construct the tree that will consist of several branches:

1. Start with A_1 and connect A_1 to all B_i in the first sheet. The B_i have to be arranged on the tree with increasing index i. This leads to a first set of branches in the tree starting at A_1 and ending at the respective B_i.
2. Connect all B_i at the open branch ends to all A_j that can be reached directly from this B_i, except for those that are already present on the

considered branch. If several A_j can be reached in this way from one of the B_i, the A_j-ends have to be arranged in the tree in the order indicated by the corresponding permutation cycle.

3. Starting from the branch ends containing the B_i with smallest index i, terminate the branches at A_j which occur more than once on the tree.

4. Continue all not terminated branches to the B_k not yet on this branch that can be reached from the respective A_j. Arrange them in ascending order of the indices starting with the one following the index i of the last B_i in the considered branch. If index N_B is reached, one has to continue with 1.

5. Starting from the branch ends containing the B_i with smallest index i, terminate the branches at B_i which occur more than once on the tree.

6. Repeat steps 2.-5. until all branches are terminated.

In [TT84] it is proven that the resulting tree has $4g + 2N - 2$ branches. For the example of the monodromies (3.18) this procedure leads to the tree in Fig. 3.2.
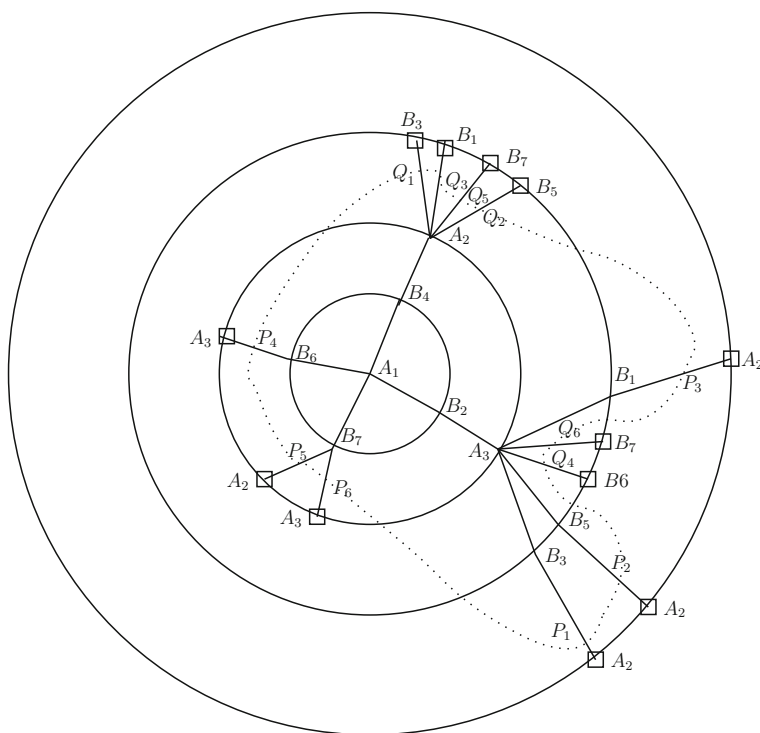
Fig. 3.2. Tretkoff–Tretkoff planar graph for the curve (3.4). The intersection numbers are obtained by following the *dashed cycle* as explained in the text

The Tretkoff–Tretkoff algorithm allows to identify non-trivial closed cycles on the Riemann surface and to compute intersection numbers between them. To this end one identifies the end piece $\overline{B_p A_q}$ of the planar graph (denoted by P_k), $k = 1, \ldots, 2g + N - 1$, with the end piece $\overline{A_q B_p}$ (denoted by Q_k) which leads to a closed cycle c_k on the surface. In total, one thus obtains $2g + N - 1$ cycles. Since the homology on a Riemann surface of genus g has dimension $2g$, the cycles cannot be all linearly independent. To find a canonical basis as defined in Chap. 1, one has to compute the intersection matrix K for the obtained $2g + N - 1$ cycles. This is straightforward to do from the planar graph: the intersection indices of the contours are replaced by intersection indices of the corresponding chords $[P_i, Q_i]$. Therefore, the intersection matrix is computed as follows: draw a closed contour in the planar graph going through all branch ends $\overline{B_p A_q}$ and $\overline{A_q B_p}$ (see for instance the dashed line in Fig. 3.2). To obtain the entries of the intersection matrix for the first cycle (the one corresponding to $[P_1, Q_1]$) one goes along this contour in positive direction from P_1 to Q_1. Each branch end P_i crossed on the way is counted as an intersection with value $+1$ of the first cycle with the ith, each end with Q_i as an intersection with value -1. It was shown in [TT84] that the resulting matrix has rank $2g$. For the example shown in Fig. 3.2 for the curve (3.4) we obtain the intersection matrix:

```
K =
        0    0    0    -1   -1   -1
        0    0    1    -1    0   -1
        0   -1    0     0   -1    0
        1    1    0     0    1    1
        1    0    1    -1    0    0
        1    1    0    -1    0    0.
```

This matrix can be transformed to the canonical form

$$\alpha \mathbf{K} \alpha^T = \begin{pmatrix} \mathbf{0}_g & \mathbf{I}_g & \mathbf{0}_{g,N-1} \\ -\mathbf{I}_g & \mathbf{0}_g & \mathbf{0}_{g,N-1} \\ \mathbf{0}_{N-1,g} & \mathbf{0}_{N-1,g} & \mathbf{0}_{N-1,N-1} \end{pmatrix} , \tag{3.20}$$

where α is a $(2g + N - 1) \times (2g + N - 1)$-matrix with integer entries and $\det \alpha = \pm 1$, $\mathbf{0}_g$ is the $g \times g$ zero matrix, $\mathbf{I}_g$ is the $g \times g$ identity matrix, and $\mathbf{0}_{i,j}$ the $i \times j$ zero matrix. The canonical basis of the homology of the surface is given by the cycles a_i and b_i:

$$a_i = \sum_{j=1}^{2g+N-1} \alpha_{ij} c_j , \quad b_i = \sum_{j=1}^{2g+N-1} \alpha_{i+g,j} c_j , \quad i = 1, \ldots, g , \tag{3.21}$$

where c_j are the $2g + N - 1$ closed contours obtained from the planar graph. The remaining cycles are homologous to zero,

$$0 = \sum_{j=1}^{2g+N-1} \alpha_{ij} c_j , \quad i = 2g + 1, \ldots, 2g + N - 1 . \tag{3.22}$$

For the curve (3.4), the code produces

```
acycle{1} =
        1    4    2    3    3    2    1
acycle{2} =
        1    4    2    1    3    2    1
bcycle{1} =
        1    6    3    2    1
bcycle{2} =
        2    3    3    2    3    5    2,
```

where `acycle{i}` corresponds to a_i, and `bcycle{i}` to b_i. These numbers are to be read in the following way: The numbers at odd positions in the cycle correspond to the indices j of A_j, $j = 1, \ldots, N$, the numbers at the even positions to the indices i of the B_i, $i = 1, \ldots, N_B$. In the above example, the cycle b_1 starts in the first sheet, goes around B_6 to end in the third sheet, then around B_2 to come back to the first sheet. The code can give more detailed information on the Tretkoff–Tretkoff tree and the cycles c_k, $k = 1, \ldots, 2g + N - 1$, as an option (it is stored in the variable `cycle` in the code tretkoffalg.m).

Relations (3.21) allow the computation of the periods of the holomorphic differentials from the integrals along the contours Γ_i used for the monodromy computation. The cycles c_k, $k = 1, \ldots, 2g+N-1$, are equivalent to a sequence of contours Γ_i. Thus, using (3.21) and the integrals of the holomorphic differentials along the contours Γ_i, we get the a- and b-periods of the holomorphic differentials, the matrices $\mathcal{A}$ and $\mathcal{B}$, respectively. The Riemann matrix $\mathbf{B}$ as defined in Chap. 1 is then given by

$$\mathbf{B} = \mathcal{A}^{-1}\mathcal{B}. \tag{3.23}$$

Since the Riemann matrix must be symmetric, the asymmetry of the computed matrix is a strong test for the numerical accuracy. A warning is reported if the asymmetry is greater than the prescribed tolerance. Similarly it is checked whether the periods along the cycles (3.22) homologous to zero vanish with the same accuracy. For the curve (3.4) the code finds the Riemann matrix

```
RieMat =
   0.3090 + 0.9511i    0.5000 - 0.3633i
   0.5000 - 0.3633i   -0.3090 + 0.9511i.
```

For a more compact representation we give only 4 digits here though 16 are available internally. The Matlab norm (the largest singular value[8]) of $\mathbf{B} - \mathbf{B}^T$

---

[8] The *singular-value decomposition* of an $m \times n$-matrix M with complex entries is given by $M = U\Sigma V^\dagger$; here U is an $m \times m$ unitary matrix, $V^\dagger$ denotes the conjugate transpose of V, an $n \times n$ unitary matrix, and the $m \times n$ matrix Σ is diagonal (as defined for a rectangular matrix); the non-negative numbers on the diagonal of Σ are called the *singular values* of M.

and the same norm of the periods along the cycles (3.22) are of the order of 10^{-7} with just 16 modes, and of the order of 10^{-15} with 64 modes. We will discuss the performance of the code in more detail in the next section.

3.8 Performance of the Code

As already mentioned, the exponential decrease of the error in the computation of the periods with the number N_l of Legendre polynomials is a general feature of spectral methods. The numerical error we will study here in more detail is defined as the maximum of the Matlab norm of the antisymmetric part of the numerically computed Riemann matrix and the same norm of the right hand sides of (3.22). The resulting variable is denoted by `err`. For the curve (3.4) we get the values for `err` shown in Fig. 3.3. The plot is typical for spectral methods: one can see the exponential decrease of the error (an essentially linear decrease in a log–log plot) and the saturation of the error once machine precision is reached, here at 10^{-14}.
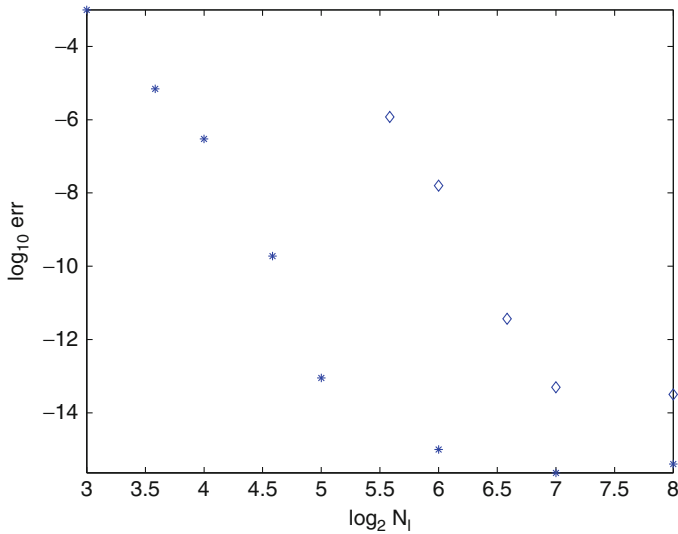
Fig. 3.3. Numerical error `err` as defined in the text for the curve (3.4) (*stars*) and the curve (3.24) (*diamonds*)

For the curve (3.4) machine precision is reached with just 32 polynomials. A more demanding test for the code is provided by the curve

$$f(x, y) = y^9 + 2x^2y^6 + 2x^4y^3 + x^6 + y^2 = 0, \tag{3.24}$$

which is a nine-sheeted genus 16 covering of the sphere with 42 finite branch points and two singular points $(0, 0, 1)$ and $(1,0,0)$. What makes this curve computationally demanding is the fact that the minimal distance between the branch points is just 0.018. The dependence of the error on the number of Legendre polynomials is shown in Fig. 3.3. It can be seen that machine precision is reached with just 128 polynomials.

It is difficult to compare timings in Matlab and Maple from a theoretical point of view since both are programming languages that can use both embedded and interpreted, i.e., not precompiled code. Thus, the found computing timings depend largely on how much a code makes use of precompiled commands. In addition the timings given by Maple and Matlab are strongly dependent on the used processor. But the timings have a practical value in the sense that they give an indication which kind of problems can be solved by the respective code on which timescales. The computation times given below have been obtained on a Macbook Pro with 1.8 GHz. The computation of the Riemann matrix for the curve (3.4) with 16 polynomials takes roughly 0.3 s in Matlab to reach $\text{err} = 3 * 10^{-7}$. On the same computer, the Maple 'algcurves' package takes roughly 13 s to achieve the same accuracy. To reach an error of the order of 10^{-13}, we need in Matlab 32 polynomials which takes roughly 0.5 s (Normally the code uses $N_l = 64$, but this can be changed by the user). The same precision can be reached in Maple by setting the variable `Digits` := 15. With this setting the computation takes roughly 35 s. Thus, the difference in computing time is more than an order of magnitude which implies that different sorts of problems can be studied in Matlab: curves of higher genus or families of curves to explore their modular properties. The computation of the Riemann matrix for the curve (3.24) takes for instance roughly 30 s with 64 polynomials ($\text{err} \approx 10^{-8}$).

It is interesting to know for which operations the computation time in Matlab is used. Again the above mentioned restrictions on the significance of Matlab timings apply, but here we are mainly interested in the practical aspect. In addition we used the vectorization algorithms in Matlab as much as possible to obtain an efficient code. For the Riemann matrix of the curve (3.4) computed with 64 polynomials we find that 67% of the time is used for the analytic continuation of $\mathbf{y}$ along the contours and the computation of the integrals. These 67% of the total computing time are distributed on the following tasks: 20% are used to solve the algebraic equation via `roots`. Almost 50% of the time are taken for the sorting of the found values for $\mathbf{y}(x_n)$ in order to provide minimal differences to $\mathbf{y}(x_{n-1})$, i.e., to obtain an analytic continuation of the sheets. The Gauss integration, which is just a matrix multiplication in this implementation, only takes negligible computation time. Other main contributions to the computing time are the identification of the branch points and singularities of the algebraic curve via `multroot` (12.7% of the total computing time) and the identification of the holomorphic differentials via Puiseux expansions (6.8%). The distribution of computing time to the different numerical tasks necessary to obtain the Riemann matrix for an algebraic curve

depends of course on the studied example. The above considerations indicate, however, where the main allocation of the computational resources is to be expected.

In the previous examples, the main numerical problems were related to the computation of the monodromies of the algebraic curve. Here difficulties arise if the branch points are 'very close' to each other, i.e., $\rho \ll 1$. If a curve has singularities where the singular part of the Puiseux expansion consists of many terms, rounding problems occur as mentioned in Sect. 3.3. For instance the curve

$$f(x,y) = ((y^3 + x^2)^2 + x^3 y^2)^2 + x^7 y^3 = 0 \qquad (3.25)$$

has a singularity at $(0,0,1)$, where the singular part of the Puiseux expansion consists of 3 terms. In this case the rounding errors in the Puiseux coefficients introduce errors in the conditions on the adjoint polynomials (the delta invariant is 43 at this point) and thus in the differentials. These errors are of the order of 10^{-5} which is also the value for the numerical error `err` in this case. The error does not get smaller if a higher number of Legendre polynomials and thus a higher numerical resolution is used since it is independent of the monodromy computation. Such non-generic singularities (which need high-order Puiseux expansions to be resolved) impose as expected limitations on the applicability of a purely numerical approach.

3.9 Hyperelliptic Surfaces

So far we have treated general algebraic curves within the limitations imposed by a fully numerical approach. In this section we will present a special code for the important subclass of hyperelliptic curves that has many applications in the theory of integrable systems.

In the previous section, the qualitative study of the distribution of computation time in the present approach to algebraic curves revealed that most of this time is needed to analytically continue the solutions $\mathbf{y}(x)$ of $f(x,y) = 0$, and to identify the critical points of the curve and the holomorphic differentials. Thus, an additional and decisive gain in speed is to be expected in cases, where the algebraic equation $f(x,y) = 0$ can be solved analytically. An important example of this kind are hyperelliptic curves, since they appear in the context of algebro-geometric solutions of various integrable equations such as KdV, NLS and Ernst equations. These have many applications in the theory of hydrodynamics, fiber optics and gravitation, see for instance [BBE+94, KR05] and references therein.

The equation for a hyperelliptic curve Σ_g of genus g can be written in the form

$$y^2 = \prod_{i=1}^{g+1}(x - E_i)(x - F_i) =: P_{2g+2}(x) , \quad E_i, F_i \in \mathbb{C} , \quad i = 1, \ldots, g+1 ,$$

$$(3.26)$$

if the curve is not branched at infinity, and as $y^2 = P_{2g+1}(x)$, where $P_{2g+1}(x)$ is a polynomial of degree $2g+1$ in x, if it is branched at infinity. A basis for the space of the holomorphic differentials is given by (see Chap. 1):

$$\nu = \left(\frac{\mathrm{d}x}{y}, \frac{x\mathrm{d}x}{y}, \ldots, \frac{x^{g-1}\mathrm{d}x}{y} \right) . \tag{3.27}$$

There is a standard way to choose a canonical basis for the homology of a hyperelliptic surface as follows: We introduce on Σ_g a canonical basis of cycles (a_k, b_k), $k = 1, \ldots, n$ as in Fig. 3.4. The cycle a_i encircles the cut $[E_{i+1}, F_{i+1}]$ for $i = 1, \ldots, g$ (if the curve is branched at infinity, we put $F_{g+1} = \infty$).

The cuts $[E_i, F_i]$, $i = 1, \ldots, g+1$ are chosen in a way not to cross each other. The branch points are supposed to be separated within the numerical resolution, i.e., the minimal distance between any two points should not be smaller than 10^{-14}. For general curves, the branch points had to be clearly separated, and the code gives a warning, if the minimal distance between branch points is smaller than 10^{-3}. For the hyperelliptic curves studied in this section, we explicitly allow for the fact that the branch points almost coincide pairwise, $|E_i - F_i| = 10^{-14}$ for any $i = 2, \ldots, g+1$. The limit $E_i \to F_i$, $i = 2, \ldots, g+1$ is known in the theory of algebro-geometric solutions to integrable equations as the *solitonic limit*. In this limit, the periods in the almost periodic solutions diverge and solitons appear. The canonical basis of the homology in Fig. 3.4 is adapted to this limit in the sense that the a-cycles surround the double points appearing in the solitonic limit.
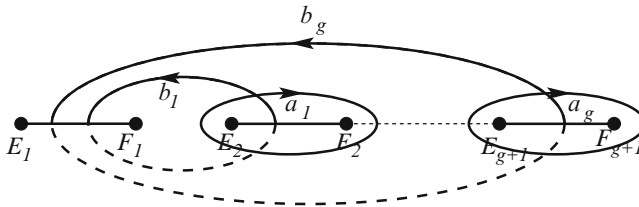
Fig. 3.4. Canonical cycles

For the computation, we use the fact (see e.g. [BBE+94]) that the periods of the holomorphic differentials can be expressed in terms of integrals along the cuts. For the a-periods, one has $\oint_{a_i} \nu_k = 2 \int_{E_{i+1}}^{F_{i+1}} \nu_k$, whereas the b-periods are sums of the integrals $-2 \int_{F_i}^{E_{i+1}} \nu_k$, $i, k = 1, \ldots, g,$. All these integrals are to be taken along the side of the cut in the upper sheet. From a numerical point of view, the disadvantage of an integration along the cut is that unavoidable numerical errors would lead to almost random sign changes of the root y in the integrals of (3.27). To overcome this problem, the integration path is taken parallel to the cut and displaced towards the upper sheet by some small distance δ, which is chosen to be of the order of the rounding error (10^{-14}).

Since δ is smaller than machine precision, the results will be numerically indistinguishable from the ones obtained by a direct integration along the cut. But the finite distance to the cut allows to effectively avoid unwanted sign changes of y due to numerical errors.

For the analytical continuation of y along the cycles in Fig. 3.4, we also use contours that almost coincide with the cuts, i.e., rectangles around the cuts with a distance δ to the cut. The advantage of this choice is that the cycles are geometrically simple, and that they do not come close to the other cuts. Thus, the cycle a_i is chosen as the rectangle with the sides $z = E_{i+1} + (F_{i+1} - E_{i+1})t \pm i\delta \exp(i\arg(F_{i+1} - E_{i+1}))$, $t \in [-\delta, 1 + \delta]$, $\delta \sim 10^{-14}$, which gives the two lines parallel to the cut at a distance δ to it, and the two lines connecting the neighboring end points of these lines. The b-cycles are built from analogous rectangles around $[F_i, E_{i+1}]$.

For the analytic continuation of y along these cycles, we fix a base point a near the branch point E_1 with smallest negative real part. At this point the sheets are labelled in the usual way, $y_{1,2} = \pm\sqrt{P_{2g+1}(a)}$ or $y_{1,2} = \pm\sqrt{P_{2g+2}(a)}$. We then determine this square root for x-values between a and $E_1 + \delta$. This is done for a vector $\mathbf{v} = (x_1, \ldots, x_{N_l})$, where $x_1 = a$ and $x_{N_l} = E_1 + \delta$ (for simplicity we use the same number of points as in the Gauss integration), which leads to a vector $\mathbf{u} = \sqrt{P_{2g+2}(\mathbf{v})}$ or $\mathbf{u} = \sqrt{P_{2g+1}(\mathbf{v})}$ in the upper sheet, where the square root is understood to be taken component-wise as in Matlab (this is done in a vectorized way). The built-in square root in Matlab is branched along the negative real axis. This implies that the computed $\mathbf{u}$ might change sign on the way from a to $E_1 + \delta$. The square root we are interested in is, however, only branched at the cuts $[E_i, F_i]$, $i = 1, \ldots, g+1$. To construct it from the computed Matlab root, we have to ensure that for each component u_n of $\mathbf{u}$ the absolute value of the difference to u_{n-1} is smaller than the one to $-u_{n-1}$, i.e., $|u_n + u_{n-1}| > |u_n - u_{n-1}|$. If this is not the case, this indicates a sign change in the Matlab root, and one has to change the sign of u_n. Notice that N_l has to be large enough to allow for a unique identification of the sheets in this way. The above procedure is then continued along the a- and b-cycles. The numerical precision is not very high for this procedure since we come close to the branch points, where y vanishes, but it is sufficient to determine the correct sign, which is the purpose of this procedure.

To compute the periods of the holomorphic differentials for the above canonical basis of the homology, we will again use Gauss integration. For an efficient use of this method, the integrands have to be smooth, which is not the case because the integration contour comes close to branch points where the integrands (3.27) proportional to $1/y$ have square root singularities. The situation is even worse close to the solitonic limit where the branch points almost coincide. The idea is to use substitutions in the period integrals leading to a smooth integrand. To determine the a-periods, we use for the cycle a_{i-1} the relation

$$x = \frac{E_i + F_i}{2} + \frac{F_i - E_i}{2}\cosh t , \quad i = 2, \ldots, g , \quad t \in [0, i\pi] . \tag{3.28}$$

The sign of y in the integrand (3.27) is fixed as described in the last paragraph. After the transformation $t = \mathrm{i}\pi(1 + l)/2$, $l \in [-1, 1]$, the integral is computed by Gauss quadrature. This also works in situations close to the solitonic limit.

To treat the b-periods in this case, we take care of the fact that $E_i \sim F_i$ in the solitonic limit. To obtain smooth integrands near E_i and F_i as well as E_{i+1} and F_{i+1}, we split the integral from F_i to E_{i+1} into two integrals from F_i to $(F_i + E_{i+1})/2$ and from $(F_i + E_{i+1})/2$ to E_{i+1}. In the former case we use the substitution

$$x = \frac{E_i + F_i}{2} + \frac{F_i - E_i}{2}\cosh t , \quad t \in \left[0, \operatorname{arcosh}\frac{E_{i+1} - E_i}{F_i - E_i}\right] , \qquad (3.29)$$

and in the latter

$$x = \frac{E_{i+1} + F_{i+1}}{2} + \frac{F_{i+1} - E_{i+1}}{2}\cosh t , \quad t \in \left[0, \operatorname{arcosh}\frac{F_i - F_{i+1}}{E_{i+1} - F_{i+1}}\right] .$$
$$(3.30)$$

These substitutions lead to a regular integrand even in situations close to the solitonic limit. After a linear transformation $t = \mathrm{i}\pi(1 + l)/2$, $l \in [-1, 1]$, the integrals are computed by Gauss quadrature.

The accuracy of the numerical method can be checked as before via the antisymmetric part of the computed Riemann matrix or the vanishing of integrals along trivial cycles. The exponential convergence of spectral methods is observed in this case as discussed in Sect. 3.8 up to minimal distances between the branch points of the order of 10^{-14} (see for instance [FK06] and the examples in Sect. 3.11, where at most 128 modes are used). Thus, the solitonic limit can be reached numerically with machine precision.

3.10 Theta Functions

Theta functions are a convenient tool to work with meromorphic functions on Riemann surfaces. We define them as an infinite series.

Definition 1. *Let $\mathbf{B}$ be a $g \times g$ Riemann matrix. The theta function with characteristic $[\mathbf{p}, \mathbf{q}]$ is defined as*

$$\Theta_{\mathbf{pq}}(\mathbf{z}, \mathbf{B}) = \sum_{\mathbf{N} \in \mathbb{Z}^g} \exp\left\{\mathrm{i}\pi\left\langle \mathbf{B}\left(\mathbf{N} + \mathbf{p}\right), \mathbf{N} + \mathbf{p}\right\rangle + 2\pi\mathrm{i}\left\langle \mathbf{z} + \mathbf{q}, \mathbf{N} + \mathbf{p}\right\rangle\right\} ,$$
$$(3.31)$$

with $\mathbf{z} \in \mathbb{C}^g$ and $\mathbf{p}, \mathbf{q} \in \mathbb{C}^g$, where $\langle \cdot, \cdot \rangle$ denotes the Euclidean scalar product $\langle \mathbf{N}, \mathbf{z}\rangle = \sum_{i=1}^{g} N_i z_i$.

The properties of the Riemann matrix ensure that the series converges absolutely and that the theta function is an entire function on $\mathbb{C}^g$. A characteristic is called *singular* if the corresponding theta function vanishes identically.

Of special importance are half-integer characteristics with $2\mathbf{p}, 2\mathbf{q} \in \mathbb{Z}^g$. A half-integer characteristic is called *even* if $4\langle \mathbf{p}, \mathbf{q} \rangle = 0$ mod 2 and *odd* otherwise. Theta functions with odd (even) characteristic are odd (even) functions of the argument $\mathbf{z}$. The theta function with characteristic is related to the Riemann theta function Θ, the theta function with zero characteristic $\Theta := \Theta_{\mathbf{00}}$, via

$$\Theta_{\mathbf{pq}}(\mathbf{z}, \mathbf{B}) = \Theta(\mathbf{z} + \mathbf{Bp} + \mathbf{q}) \exp \left\{ i\pi \langle \mathbf{Bp}, \mathbf{p} \rangle + 2\pi i \langle \mathbf{p}, \mathbf{z} + \mathbf{q} \rangle \right\} . \quad (3.32)$$

The theta function has the periodicity properties

$$\Theta_{\mathbf{pq}}(\mathbf{z} + \mathbf{e}_j) = e^{2\pi i p_j} \Theta_{\mathbf{pq}}(\mathbf{z}) , \quad \Theta_{\mathbf{pq}}(\mathbf{z} + \mathbf{Be}_j) = e^{-2\pi i(z_j + q_j) - i\pi B_{jj}} \Theta_{\mathbf{pq}}(\mathbf{z}) , \quad (3.33)$$

where $\mathbf{e}_j$ is a vector in $\mathbb{R}^g$ consisting of zeros except for a 1 in jth position. In the computation of the theta function we will always use the periodicity properties (3.33). This allows us to write an arbitrary vector $\mathbf{z} \in \mathbb{C}^g$ in the form $\mathbf{z} = \hat{\mathbf{z}} + \mathbf{N} + \mathbf{BM}$ with $\mathbf{N}, \mathbf{M} \in \mathbb{Z}^g$, where $\hat{\mathbf{z}}$ is a vector in the fundamental cell of the Jacobian, and to compute $\Theta(\hat{\mathbf{z}}, \mathbf{B})$ instead of $\Theta(\mathbf{z}, \mathbf{B})$ (they are identical up to an exponential factor). In the following we will always assume that z is in this fundamental cell.

The theta series (3.31) for the Riemann theta function (theta functions with characteristic follow from (3.32)) is approximated as the sum

$$\Theta(\mathbf{z}|\mathbf{B}) \approx \sum_{N_1 = -N_\theta}^{N_\theta} \ldots \sum_{N_g = -N_\theta}^{N_\theta} \exp \left\{ i\pi \langle \mathbf{BN}, \mathbf{N} \rangle + 2\pi i \langle \mathbf{z}, \mathbf{N} \rangle \right\} . \quad (3.34)$$

The value of N_θ is determined by the condition that terms in the series (3.31) for $n_i > N_\theta$, $i = 1, \ldots, g$ have absolute values strictly smaller than some threshold value ϵ which is typically taken to be of the order of 10^{-16}. To obtain an estimate for N_θ, we write

$$\mathbf{B} = \mathbf{X} + i\mathbf{Y} , \quad \mathbf{z} = \mathbf{x} + i\mathbf{y} , \quad (3.35)$$

where $\mathbf{X}, \mathbf{Y}, \mathbf{x}, \mathbf{y}$ are real. We can separate the terms in (3.34) into purely oscillatory terms with absolute value 1 and real exponentials,

$$\Theta(\mathbf{z}|\mathbf{B}) \approx \sum_{N_1 = -N_\theta}^{N_\theta} \ldots \sum_{N_g = -N_\theta}^{N_\theta} \exp \left\{ -\pi \langle \mathbf{YN}, \mathbf{N} \rangle - 2\pi \langle \mathbf{y}, \mathbf{N} \rangle \right\} \times F , \quad (3.36)$$

where $F = \exp \left\{ i\pi \langle \mathbf{XN}, \mathbf{N} \rangle + 2\pi i \langle \mathbf{x}, \mathbf{N} \rangle \right\}$ is a purely oscillatory factor. Since $\mathbf{B}$ is a Riemann matrix, $\mathbf{Y}$ is a real symmetric matrix with strictly positive eigenvalues, i.e., there exists a special orthogonal matrix O such that

$$O\mathbf{Y}O^t = \mathrm{diag}(\lambda_1, \ldots, \lambda_g) \quad (3.37)$$

with $0 < \lambda_1 \leq \ldots \leq \lambda_g$. Thus, we can write (3.36) in the form

$$\Theta(\mathbf{z}|\mathbf{B}) \approx \sum_{N_1=-N_\theta}^{N_\theta} \ldots \sum_{N_g=-N_\theta}^{N_\theta} \prod_{k=1}^{g} \exp\left\{-\pi(\lambda_k \tilde{N}_k^2 + 2\tilde{y}_k \tilde{N}_k)\right\} \times F , \quad (3.38)$$

where $\tilde{y} = Oy$ and $\tilde{\mathbf{N}} = O\mathbf{N}$. Then the condition on N_θ is that the absolute value of all terms with $|n_i| > N_\theta$ in (3.36) is strictly smaller than ϵ, i.e.,

$$\exp\left\{-\pi\lambda_1 N_\theta^2 \pm 2\pi\tilde{y}_1 N_\theta\right\} < \epsilon . \quad (3.39)$$

Since z is in the fundamental cell of the Jacobian, we can assume without loss of generality that $\tilde{y}_i \leq \lambda_i/2$. This and (3.38) implies for N_θ

$$N_\theta > \frac{1}{2} + \sqrt{\frac{1}{4} - \frac{\ln\epsilon}{\pi\lambda_1}} . \quad (3.40)$$

For a more sophisticated analysis of theta summations see [DHB+04]. In cases where the eigenvalues are such that $\lambda_g/\lambda_1 \gg 1$, a summation over a region in the $(n_1, \ldots, n_g)$-space delimited by an ellipse as in [DHB+04] rather than over a hypercube will be more efficient. The summation (3.38) over the hypercube has, however, the advantage that it can be implemented in Matlab for arbitrary genus whilst making full use of Matlab's vectorization algorithms outlined below. Thus, a summation over an ellipse would be only more efficient in terms of computation time for very extreme ratios of the eigenvalues of $\mathbf{Y}$. Instead of summing over an ellipse, in such a case we use a Matlab implementation [FK09] of the Siegel transformation from [DHB+04] to treat symplectically equivalent matrices $\mathbf{Y}$ with ratios of λ_g/λ_1 close to 1 and a smallest eigenvalue λ_1 of the order 1.

To compute the theta functions we make again use of Matlab's efficient way to handle matrices. We generate a g-dimensional array containing all $(2N_\theta + 1)^g$ possible index combinations and thus all components in the sum (3.34) which is then summed. To illustrate this we consider the simple example of genus 2 with $N_\theta = 2$. In this case, the summation indices are arranged in a $(2N_\theta + 1) \times (2N_\theta + 1)$-matrices. Each of these matrices (denoted by $\mathcal{N}_1$ and $\mathcal{N}_2$) contains $2N_\theta + 1$ copies of the vector $-(2N_\theta + 1), \ldots, 2N_\theta + 1$. The matrix $\mathcal{N}_2$ is the transposed matrix of $\mathcal{N}_1$. Explicitly, we have for $N_\theta = 2$

$$\mathcal{N}_1 = \begin{pmatrix} 2 & 2 & 2 & 2 & 2 \\ 1 & 1 & 1 & 1 & 1 \\ 0 & 0 & 0 & 0 & 0 \\ -1 & -1 & -1 & -1 & -1 \\ -2 & -2 & -2 & -2 & -2 \end{pmatrix} , \quad \mathcal{N}_2 = \begin{pmatrix} 2 & 1 & 0 & -1 & -2 \\ 2 & 1 & 0 & -1 & -2 \\ 2 & 1 & 0 & -1 & -2 \\ 2 & 1 & 0 & -1 & -2 \\ 2 & 1 & 0 & -1 & -2 \end{pmatrix} . \quad (3.41)$$

The terms in the sum (3.34) can thus be written in matrix form:

$$\exp\left\{ 2i\pi \left(\frac{1}{2}\mathcal{N}_1 \star \mathcal{N}_1 \mathbf{B}_{11} + \mathcal{N}_1 \star \mathcal{N}_2 \mathbf{B}_{12} + \frac{1}{2}\mathcal{N}_2 \star \mathcal{N}_2 \mathbf{B}_{22} \right. \right.$$
$$\left. \left. + \mathcal{N}_1 \star z_1 + \mathcal{N}_2 \star z_2 \right) \right\} , \quad (3.42)$$

where the operation $\mathcal{N}_1 \star \mathcal{N}_2$ denotes that each entry of $\mathcal{N}_1$ is multiplied with the corresponding entry of $\mathcal{N}_2$. Thus, the argument of exp in (3.42) is a $(2N_\theta + 1) \times (2N_\theta + 1)$-dimensional matrix. Furthermore, the exponential function is understood to act not on the matrix but on each of its entries individually, producing a matrix of the same size. The approximate value of the theta function is then obtained by summing up all the entries of the matrix (3.42).

The most time consuming operations in the computation of the theta functions are the determination of the bilinear terms in (3.42) involving the Riemann matrix. The limiting factor here is the size of the arrays which is limited to $2^{31} - 1$ components on a 32 bit computer.

3.11 Hyperelliptic Solutions to Nonlinear Schrödinger Equations

An important application of Riemann surfaces and theta functions are almost periodic solutions to completely integrable partial differential equations. As an example we will consider in this section solutions to the nonlinear Schrödinger equations (NLS) which are given in terms of multi-dimensional theta functions on hyperelliptic Riemann surfaces.

The focusing ($\rho = -1$) and defocusing ($\rho = 1$) NLS equations

$$\mathrm{i}\psi_t + \psi_{xx} - 2\rho|\psi|^2\psi = 0 \, , \quad x, t \in \mathbb{R}, \quad \psi \in \mathbb{C} \, , \qquad (3.43)$$

have important applications, for instance in nonlinear fiber optics and hydrodynamics. The complete integrability of the equations was shown by Zakharov and Shabat [ZS72]. Almost periodic solutions can be constructed on hyperelliptic Riemann surfaces, see [BBE+94] for further details and references. The hyperelliptic curves of genus g appearing in the context of the NLS equations are real, i.e., in the defining equation for the algebraic curve

$$y^2 = \prod_{i=1}^{g+1}(z - E_i)(z - F_i) =: z^{2g+2} - S_1 z^{2g+1} + z^{2g} S_2 + \dots \, , \qquad (3.44)$$

the branch points E_i and F_i are either all real (for the defocusing case) or pairwise complex conjugate, $E_i = \bar{F}_i$, $i = 1, \dots, g + 1$ (for the focusing case). The hyperelliptic solutions to the NLS equation can be written in the form

$$\psi(x, t) = A \frac{\theta(\mathrm{i}\mathbf{V}x + \mathrm{i}\mathbf{W}t - \mathbf{D} + \mathbf{r})}{\theta(\mathrm{i}\mathbf{V}x + \mathrm{i}\mathbf{W}t - \mathbf{D})} \exp(-\mathrm{i}Ex + \mathrm{i}Nt) \, ; \qquad (3.45)$$

here θ is the theta function associated to the curve (3.44), $\mathbf{D} \in \mathbb{C}^g$ is an arbitrary constant vector, $\mathbf{r} = \int_{\infty^-}^{\infty^+} \omega$, where ω is the vector of normalized ($\oint_{a_i} \omega_j = \delta_{ij}$, $i, j = 1, \dots, g$) holomorphic differentials, $A = C\sqrt{\omega_0}$ with C a complex constant, and the remaining quantities are defined via the integrals

of meromorphic differentials $d\Omega_i$ normalized by the condition of vanishing a-periods, and with single pole at infinity; the behavior of the integrals at infinity is given by the relations ($P \sim \infty^{\pm}$)

$$
\begin{aligned}
\Omega_1(P) &= \pm(x - E/2 + o(1)), \\
\Omega_2(P) &= \pm(2x^2 + N/2 + o(1)), \\
\Omega_3(P) &= \pm(\ln x - (1/2)\ln \omega_0 + o(1));
\end{aligned}
\tag{3.46}
$$

the vectors $\mathbf{V}$ and $\mathbf{W}$ are the b-periods of Ω_1 and Ω_2, respectively.

To be more specific we introduce the basis of the homology shown in Fig. 3.4 and choose $\Omega_i(E_1) = 0$, $i = 1, 2, 3$. The reality conditions imply that E, N and ω_0 are real in the focusing and defocusing case. In the latter case, ω_0 is positive, $\mathbf{B}$ is purely imaginary, and $\mathbf{V}$, $\mathbf{W}$ and $\mathbf{r}$ are real. We have $A = 2\sqrt{\omega_0}$ up to a complex phase and $\mathbf{D}$ purely imaginary (up to lattice vectors). In the focusing case ω_0 is negative, the vectors $\mathbf{V}$, $\mathbf{W}$ and the diagonal part of $\mathbf{B}$ are purely imaginary. Furthermore, we have for the non-diagonal entries of $\mathbf{B}$ that $\bar{B}_{ij} = B_{ij} + 1$, and $\bar{r}_i = r_i + 1$. This implies $A = 2\sqrt{-\omega_0}$ up to a complex phase and $\mathbf{D}$ purely imaginary (up to lattice vectors).

To get explicit expressions for $g \geq 2$, we write the holomorphic differentials in the form $\omega_i = \sum_{j=1}^{g} c_{ij}\nu_j$, $i = 1, \ldots, g$, where ν is given in (3.27), and $d\Omega_3 = x^g dx/y + \sum_{j=1}^{g} c_j^3 \nu_j$, which implies with the symmetric functions S_i defined in (3.44)

$$
V_i = 2c_{ig}, \quad W_i = 4\left(c_{i(g-1)} + c_{ig}\frac{S_1}{2}\right),
\tag{3.47}
$$

and

$$
E = S_1 + 2c_g^3, \quad N = -2\left(2c_{g-1}^3 + \frac{3}{4}S_1^2 - S_2 + S_1 c_g^3\right).
\tag{3.48}
$$

The formulae (3.47) and (3.48) also hold in the elliptic case, if we formally put quantities with index 0 equal to zero. For ω_0 we use the expression

$$
\omega_0 = \left(\frac{D_{\infty^+}\theta^*(0)}{2\theta^*(\mathbf{r})}\right)^2,
\tag{3.49}
$$

where θ^* is a theta function with an arbitrary non-singular odd characteristic, and where $D_P\Theta(z) := \sum_{i=1}^{g} \omega_i(P)\partial_{z_i}\Theta(z)$.

3.11.1 Solitonic Limit in the Defocusing Case

As already briefly mentioned in Sect. 3.9 (for details see for instance [BBE+94]), solitonic solutions can be obtained for many integrable equations from finite gap solutions by degenerating the Riemann surface as follows: for the defocusing case one starts (see [BBE+94]) with a surface with a real cut $[-\alpha, \alpha]$ (from $-\alpha$ via minus infinity to α). The remaining branch points

collapse to double points which are chosen to be in the interval $[-\alpha, \alpha]$. To obtain nontrivial solutions, the vector $\mathbf{D}$ has to contain half periods,

$$\mathbf{D}_i = \frac{1}{2}B_{ii} + 2\eta_i, \tag{3.50}$$

where η_i remains finite on the degenerate surface, but is otherwise arbitrary. If we choose $\Re\eta_i = 0$, the reality conditions for the defocusing case are satisfied. The resulting solitons do not tend to zero at infinity and are thus dark solitons, i.e., they represent dark regions propagating on a background of light. In the focusing case, the situation is more involved and will not be discussed here, see [BBE+94].

3.11.2 Examples for the Defocusing NLS

In the defocusing case, we consider solutions which lead to solitons in the degenerate case as described above. We show a typical genus 2 solution in Fig. 3.5 for the Riemann surface with branch points $-3, -2, -2 + \epsilon, 1, 1 + \epsilon, 3$ and $\epsilon = 1$; here and in the following we put $u = |\psi|^2$.
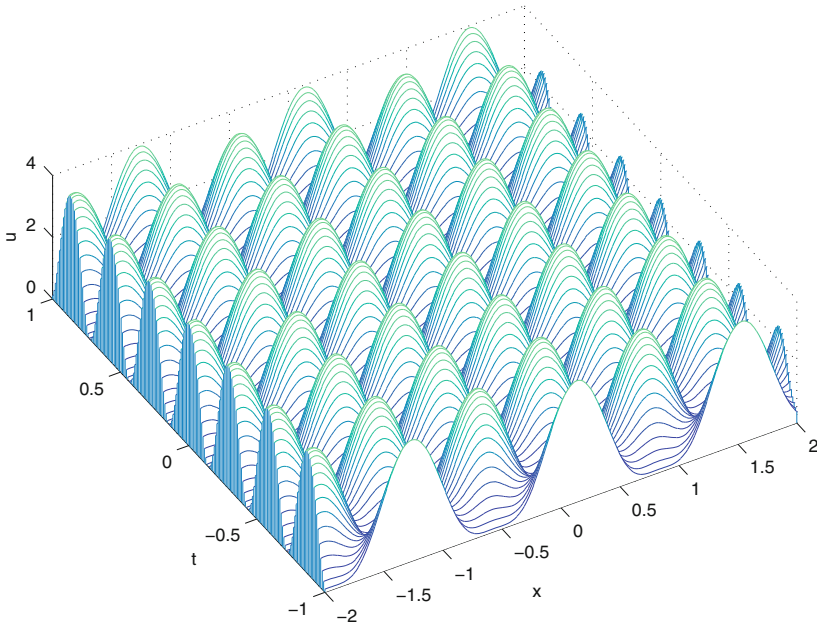
Fig. 3.5. Almost periodic solution to the defocusing NLS equation on a genus 2 surface

In the limit $\epsilon \to 0$ in this example one ends up with the 2-soliton solution which can be seen for $\epsilon = 10^{-14}$ in Fig. 3.6. Visibly the solution does not tend to zero for $x \to \infty$.
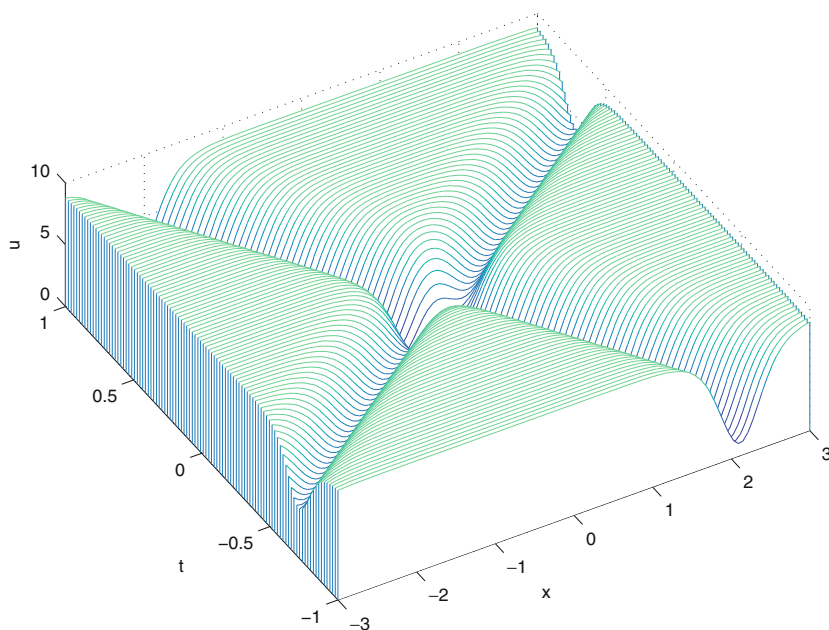
Fig. 3.6. Almost solitonic solution to the defocusing NLS equation on a genus 2 surface

A similar situation as in genus 2 is studied on a surface of genus 6 with branch points

$$-5, -3, -3 + \epsilon, -2, -2 + \epsilon, -1, -1 + \epsilon, 1, 1 + \epsilon, 2, 2 + \epsilon, 3, 3 + \epsilon, 5.$$

The corresponding solution for $\epsilon = 0.5$ can be seen in Fig. 3.7. The almost periodic character of the solution is obvious from the figure. By degenerating this surface ($\epsilon \to 0$) we obtain a 6-soliton solution which is shown for $\epsilon = 10^{-14}$ in Fig. 3.8.

3.11.3 Examples for the Focusing NLS

A typical example for genus 2 is shown in Fig. 3.9 on the surface with the branch points

$$-2 + i, -1 + i, 1 + i, -2 - i, -1 - i, 1 - i.$$

Similarly a genus 6 solution for the Riemann surface with branch points

$$-3 + i, -2 + i, -1 + i, i, 1 + i, 2 + i, 3 + i, -3 - i, -2 - i, -1 - i, -i, 1 - i, 2 - i, 3 - i$$

is shown in Fig. 3.10.
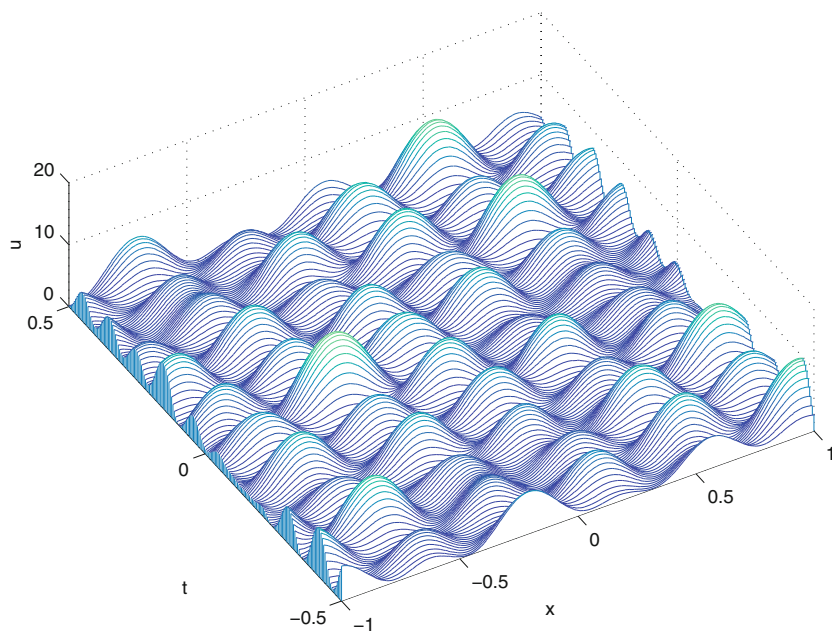
Fig. 3.7. Almost periodic solution to the defocusing NLS equation on a genus 6 surface
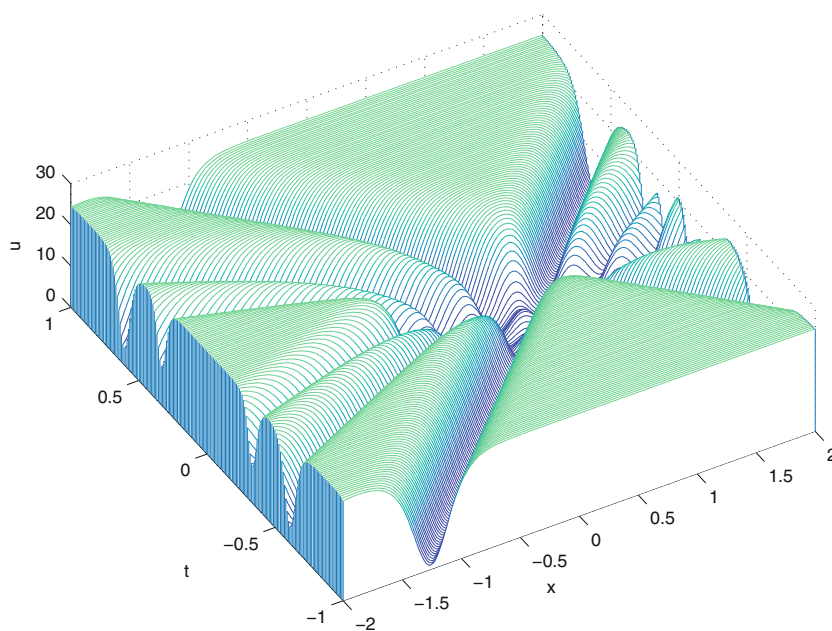
Fig. 3.8. Almost solitonic solution to the defocusing NLS equation on a genus 6 surface
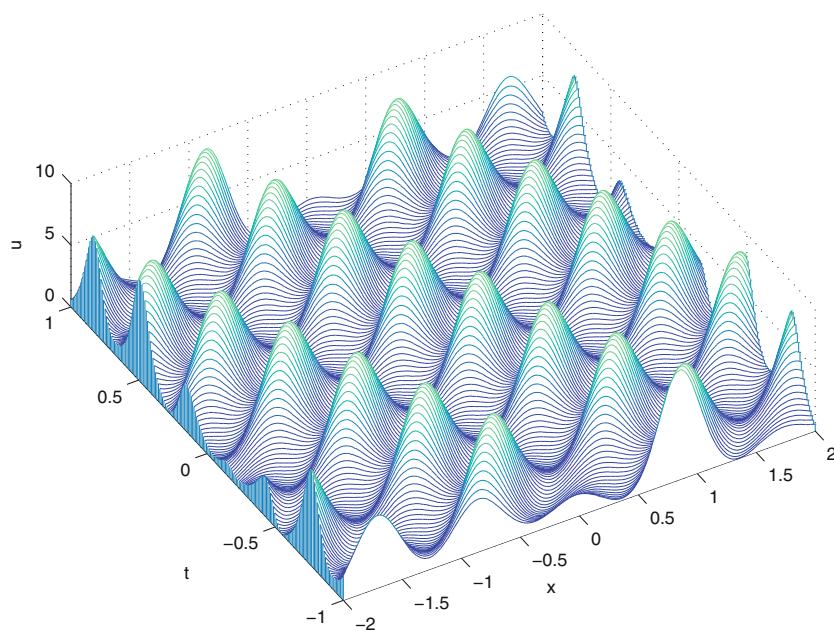
Fig. 3.9. Almost periodic solution to the focusing NLS equation on a genus 2 surface
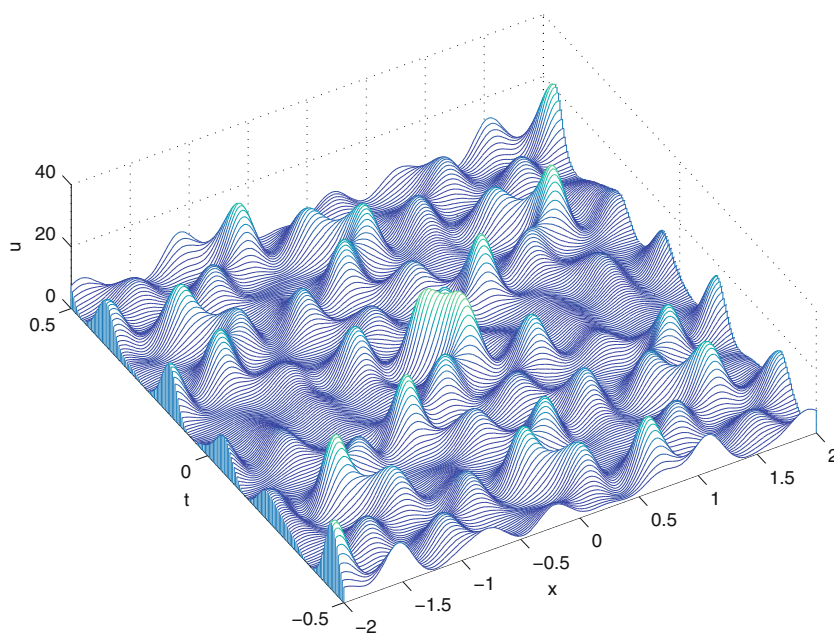
Fig. 3.10. Almost periodic solution to the focusing NLS equation on a genus 6 surface

Acknowledgement

References

[BBE+94]   Belokolos, E.D., Bobenko, A.I., Enolskii, V.Z., Its, A.R., Matveev, V.B.: Algebro-geometric approach to nonlinear integrable equations. Springer, Berlin (1994)

[BK86]   Brieskorn, E., Knörrer, H.: Plane algebraic curves. Birkhauser Verlag, Basel (1986)

[Bob11]   Bobenko, A.I.: Introduction to compact Riemann surfaces. In: Bobenko, A.I., Klein, Ch. (eds.) Lecture Notes in Mathematics 2013, pp. 3–64. Springer, Berlin (2011)

[DHB+04]   Deconinck, B., Heil, M., Bobenko, A.I., van Hoeij, M., Schmies, M.: Computing Riemann theta functions. Math. Comput. **73**, 1417–1442 (2004)

[DVZ97]   Deift, P., Venakides S., Zhou, X.: New result in small dispersion KdV by an extension of the steepest descent method for Riemann-Hilbert problems. IMRN **6**, 285–299 (1997)

[Duv89]   Duval, D.: Rational Puiseux Expansions. Compos. Math. **70**(2), 119–154 (1989)

[FK01]   Frauendiener, J., Klein, C.: On the exact treatment of stationary counter-rotating dust disks: Physical Properties. Phys. Rev. D **63**, 84025 (2001)

[FK04]   Frauendiener, J., Klein, C.: Hyperelliptic theta-functions and spectral methods. J. Comp. Appl. Math. **167**, 193 (2004)

[FK06]   Frauendiener, J., Klein, C.: Hyperelliptic theta-functions and spectral methods: KdV and KP solutions. Lett. Math. Phys. **76**, 249–267 (2006)

[FK09]   Frauendiener, J., Klein, C.: Computing with Algebraic Curves in Matlab, in preparation

[FK10]   Frauendiener, J., Klein, C.: Hyperelliptic Riemann surfaces in Matlab, in preparation

[GK07]   Grava, T., Klein, C.: Numerical solution of the small dispersion limit of Korteweg de Vries and Whitham equations. Comm. Pure Appl. Math. **60**, 1623–1664 (2007)

[GT02]   Grava, T., Tian, F.-R.: The generation, propagation, and extinction of multiphases in the KdV zero-dispersion limit. Comm. Pure Appl. Math. **55**(12), 1569–1639 (2002)

[KP70]   Kadomtsev, B.B., Petviashvili, V.I.: On the stability of solitary waves in weakly dispersing media. Sov. Phys. Dokl. **15**, 539–541 (1970)

[KMM03]   Kamvissis, S., McLaughlin, K.D.T.-R. Miller, P.D.: Semiclassical soliton ensembles for the focusing nonlinear Schrödinger equation. Annals of Mathematics Studies, vol. 154. Princeton University Press, Princeton, NJ (2003)

[Kir92]   Kirwan, F.: Complex Algebraic Curves. London Mathematical Society Student Texts, vol. 23. CUP, Cambridge (1992)

[Kle03]   Klein, C.: On explicit solutions to the stationary axisymmetric Einstein-Maxwell equations describing dust disks. Ann. Phys. (Leipzig) **12**, 599 (2003)

[KKK09]   Klein, C., Kokotov, A., Korotkin, D.: Extremal properties of the determinant of the Laplacian in the Bergman metric on the moduli space of genus two Riemann surfaces. Math. Zeitschr. **261**(1), 73–108 (2009)

[KR05]   Klein, C., Richter, O.: Ernst Equation and Riemann Surfaces. Lecture Notes in Physics, vol. 685. Springer, Berlin (2005)

[KSM07]   Klein, C., Sparber C., Markowich, P.: Numerical study of oscillatory regimes in the Kadomtsev-Petviashvili equation. J. Nonl. Sci. **17**(5), 429–470 (2007)

[Kor89]   Korotkin, D.A.: Finite-gap solutions of the stationary axially symmetric Einstein equation in vacuum. Theor. Math. Phys. **77**, 1018 (1989)

[LL83]   Lax, P.D., Levermore, C.D.: The small dispersion limit of the Korteweg de Vries equation, I,II,III. Comm. Pure Appl. Math. **36**, 253–290, 571–593, 809–830 (1983)

[Noe83]   Noether, M.: Rationale Ausführungen der Operationen in der Theorie der algebraischen Funktionen. Math. Ann. **23**, 311–358, (1883)

[Pot07]   Poteaux, A.: Computing Monodromy Groups defined by Plane Algebraic Curves. In: Proceedings of the 2007 International Workshop on Symbolic-numeric Computation. ACM, New-York, 36–45 (2007)

[QS97]   Quine, J.R., Sarnak, P. (eds.): Extremal Riemann surfaces. Contemporary Mathematics, vol. 201. AMS, Providence, RI (1997)

[TVZ04]   Tovbis, A., Venakides, S., Zhou, X.: On semiclassical (zero dispersion limit) solutions of the focusing nonlinear Schrödinger equation. Comm. Pure Appl. Math. **57** 877–985 (2004)

[Tre00]   Trefethen, L.N.: Spectral Methods in Matlab. SIAM, Philadelphia, PA (2000)

[TT84]   Tretkoff, C.L., Tretkoff, M.D.: Combinatorial group theory, Riemann surfaces and differential equations. Contemp. Math. **33**, 467–517 (1984)

[Ven85]   Venakides, V.: The zero dispersion limit of the Korteweg de Vries equation for initial potential with nontrivial reflection coefficient. Comm. Pure Appl. Math. **38**, 125–155 (1985)

[Whi66]   Whitham, G.B.: Nonlinear dispersive waves. SIAM J. App. Math. **14**, 956–958 (1966)

[Whi74]   Whitham, G.B.: Linear and nonlinear waves. Wiley, New York (1974)

[Tre]   www.comlab.ox.ac.uk/oucl/work/nick.trefethen

[ZS72]   Zakharov, V.E., Shabat, A.B.: Exact theory of two-dimensional self-focusing and one-dimensional self-modulation of waves in nonlinear media. Sov. Phys. JETP **34**, 62–69 (1972)

[Zen04]   Zeng, Z.: Computing multiple roots of inexact polynomials. Math. Comp. **74**, 869–903 (2004)

Part III Schottky Uniformization

Computing Poincaré Theta Series
for Schottky Groups

Markus Schmies

Institut für Mathematik,
Technische Universität Berlin,
Straße des 17. Juni 136, 10623 Berlin, Germany
`schmies@math.tu-berlin.de`

4.1 Introduction

Common numerical methods represent Riemann surfaces through algebraic curves, see Chaps. 2 and 3. This seems natural because algebraic curves can be used to define a Riemann surface, but this approach has some serious disadvantages: if one is interested in the corresponding Riemann surface only, one needs to factorize algebraic curves with respect to birational maps. This complicates the corresponding parameterization of Riemann surfaces. Moreover, a representation of a Riemann surfaces as a ramified multi-sheeted covering complicates the description of homology and integration paths, which leads to complex algorithms. Schottky uniformization (see Chap. 1) is an attractive alternative to describing Riemann surfaces in terms of algebraic curves.

A Schottky group is a free, finitely generated, discontinuous group G that is purely loxodromic, i.e., a Schottky group of rank N can always be generated by N loxodromic transformations $\sigma_1, \ldots, \sigma_N$. A classical theorem states that for any Riemann surface $\mathcal{R}$ there exists a Schottky group G such that $\mathcal{R}$ is conformally equivalent to the quotient Ω/G, where Ω denotes the set of discontinuity of G [For29]. The number N of generators of the Schottky group equals the genus of the associated Riemann surface. A loxodromic transformation σ_i is determined by its fixed points A_i and B_i and the loxodromic factor μ_i (see (1.96), we refer to [Bob11], Sect. 1.8 for more details on Schottky groups and uniformization). In other words, a Schottky group can be parameterized by the data

$$S = \{A_1, B_1, \mu_1, \ldots, A_N, B_N, \mu_N\} \ ,$$

which are fixed points and loxodromic factors of their generators $\sigma_1, \ldots, \sigma_N$. This provides a canonical way of parameterizing Riemann surfaces, which is good-natured in the sense that the characteristics of the geometry can easily

be preserved. This is unlike the situation in an algebraic curve representation where minor changes of its coefficients can change the nature of singularities or even the genus.

Finding the Schottky data for a given Riemann surface is an unsolved problem. Further it is also unknown how to evaluate whether a set of Schottky data yields a Riemann surface or not. But if all pairs of isometric circles of generators specified by the data lie outside each other then the Schottky data gives a Riemann surface. These Schottky groups are a special sub-class of so-called classical Schottky groups to which we refer as iso-classical. The numerics we present will be restricted to the iso-classical case.

Functions and differentials of the Riemann surface Ω/G are automorphic on Ω. This yields explicit representations for functions, differentials, and integrals in terms of Poincaré theta series. For example, normalized differentials of the first kind can be expressed as (-2)-dimensional Poincaré theta series:

$$\omega_n(z) = \sum_{\sigma \in G_n \backslash G} \left(\frac{1}{\sigma(z) - B_n} - \frac{1}{\sigma(z) - A_n} \right) d\sigma(z) . \tag{4.1}$$

If the series

$$\omega_n(z) = \sum_{\sigma \in G/G_n} \left(\frac{1}{z - \sigma(B_n)} - \frac{1}{z - \sigma(A_n)} \right) dz \tag{4.2}$$

are absolutely convergent, then they define holomorphic differentials normalized over a Schottky generic basis. Their integrals are then given by

$$\Omega_n(z) = \int_\infty^z \omega_n = \sum_{\sigma \in G/G_n} \log \frac{z - \sigma(B_n)}{z - \sigma(A_n)} . \tag{4.3}$$

The corresponding period matrix is given by

$$B_{nm} = \delta_{nm} \log \mu_n + \sum_{\sigma \in G_m \backslash G/G_n, \sigma \neq id} \log \{B_m, A_m, \sigma(B_n), \sigma(A_n)\} , \tag{4.4}$$

where the curly brackets indicate the cross-ratio

$$\{a, b, c, d\} = \frac{a - c}{a - d} \cdot \frac{b - d}{b - c} .$$

These series are the chief ingredient for any numerics regarding Riemann surfaces via Schottky groups but they do not necessarily converge in the general case. In fact, it is unknown whether an absolute convergent series exists for a given Riemann surface.

We developed sufficient a priori convergence criteria and error estimates which are given in terms of the Schottky uniformization data alone, and guarantees convergence for sufficiently small isometric circles. Such estimates have

been given first by Burnside [Bur92], see also [FK65, Bak97]. However, these authors considered only principle mathematical questions about the convergence. They used rather primitive estimates to show that for sufficiently small circles the series converge. Finding general convergence criteria remains an interesting open problem.

These estimates have been designed such that they can be evaluated efficiently as well as be seamlessly used in very effective pointwise evaluation algorithms which guarantees prescribed error bounds. We present these criteria, estimates and evaluation algorithms for the above Poincaré series and show results and benchmarks of numerically challenging examples.

4.2 Convergence Conditions

Let G be the free group generated by $\sigma_1, \ldots, \sigma_N \in G$. Each $\sigma \in G$ has a unique representation

$$\sigma = \sigma_{i_1}^{j_1} \ldots \sigma_{i_k}^{j_k}$$

with $j_l \in \{-1, 1\}$, $i_l \in \{1, \ldots, N\}$, and $j_l i_l \neq -j_{l+1} i_{l+1}$. Denote by

$$[\sigma] = [j_1 i_1, \ldots, j_k i_k]$$

the word of σ associated to the generators $\sigma_1, \ldots, \sigma_N$ and by

$$|\sigma| = k$$

its length. Denote further by G_n the subgroup generated by σ_n and define its cosets as:

$$G/G_n = \{\sigma \,|\, [\sigma] = [\ldots, r], |r| \neq n\}$$
$$G_n \backslash G = \{\sigma \,|\, [\sigma] = [s, \ldots], |s| \neq n\}$$
$$G_m \backslash G/G_n = \{\sigma \,|\, [\sigma] = [s, \ldots r], |s| \neq m \wedge |r| \neq n\} \ .$$

Let C_n (C'_n) be isometric circles of the iso-classical Schottky group G as in Sect. 1.8. We denote C_n and C'_n also by C_n^1 and C_n^{-1} respectively. Their open interior are denoted by D_n or D_n^1 and D'_n or D_n^{-1}. Note that

$$\sigma_m^i \left(\mathbb{C} \setminus \overline{D_m^i} \right) = D_m^{-i} \ ,$$

because Schottky groups map the outside of C_n onto the inside of C'_n. This yields

Lemma 4.2.1 *For* $\sigma_{(l)} = \sigma_{m_1}^{i_1} \cdot \ldots \cdot \sigma_{m_l}^{i_l} \in G$ *we have*

$$\sigma_{(l+1)} \left(\mathbb{C} \setminus \overline{D_{m_{l+1}}^{i_{l+1}}} \right) = \sigma_{(l)} \left(D_{m_{l+1}}^{-i_{l+1}} \right) \subset \sigma_{(l)} \left(\mathbb{C} \setminus \overline{D_{m_l}^{i_l}} \right) \ .$$

For σ with $[\sigma] = [im, \ldots]$ we have $\sigma(F) \subseteq D_m^{-i}$ which implies that for all $\sigma \in G_n \setminus G$ one has $\sigma(F) \cap D_n^{\pm 1} = \emptyset$, and $dist(\sigma(F), F) > 0$ for all $\sigma \in G$ with $|\sigma| > 1$. We now define constants measuring the displacement of the fundamental domain F under an element of the Schottky group. Let $\sigma \in G$ and define

$$
\begin{aligned}
k(P; \sigma) &= \min_{z \in F} |P - \sigma(z)| \\
K(P; \sigma) &= \max_{z \in F} |P - \sigma(z)| \ .
\end{aligned}
\tag{4.5}
$$

Let $\sigma_{(l)} = \sigma_{m_1}^{i_1} \cdot \ldots \cdot \sigma_{m_l}^{i_l} \in G$ and $P \notin D_{m_1}^{-i_1}$. We conclude that

$$
\begin{aligned}
0 \le k\left(P; \sigma_{(1)}\right) &< k\left(P; \sigma_{(2)}\right) < \ldots < \lim_{l \to \infty} k\left(P; \sigma_{(l)}\right) \\
\infty > K\left(P; \sigma_{(1)}\right) &> K\left(P; \sigma_{(2)}\right) > \ldots > \lim_{l \to \infty} K\left(P; \sigma_{(l)}\right) \ .
\end{aligned}
\tag{4.6}
$$

For iso-classical Schottky groups, the limits coincide, i.e.,

$$
\lim_{l \to \infty} k\left(P; \sigma_{(l)}\right) = \lim_{l \to \infty} K\left(P; \sigma_{(l)}\right) \ ,
\tag{4.7}
$$

which follows from the next lemma.

Lemma 4.2.2 *Let G be an iso-classical Schottky group and $\sigma_{(l)} = \sigma_{m_1}^{i_1} \cdot \ldots \cdot \sigma_{m_l}^{i_l} \in G$ be an infinite sequence. Then the depending sequence of sets $\sigma_{(l)}(F)$ contracts to a point.*

We will show that

$$
\left|\left(\sigma_{(l)}\right)'(z)\right| = \left|\left(\sigma_{m_1}^{i_1}\right)'\left(\sigma_{m_2}^{i_2} \cdot \ldots \cdot \sigma_{m_l}^{i_l}(z)\right)\right| \cdot \ldots \cdot \left|\left(\sigma_{m_{l-1}}^{i_{l-1}}\right)' \sigma_{m_l}^{i_l}(z)\right| \left|\left(\sigma_{m_l}^{i_l}\right)'(z)\right|
$$

vanishes in the limit. A computation shows that

$$
\left|\left(\sigma_n^i\right)'(z)\right| = \left(\frac{R_n}{|z - P_n^i|}\right)^2 \ ,
$$

where P_n^i is the center and R_n the radius of C_n^i. Therefore $\left|\sigma_n^i{}'(z)\right| < 1$ for all $z \notin \overline{D_n^i}$. For $\tau = \sigma_n^i \sigma$ we define:

$$
\theta(\tau) = \max_{z \in F} \left|\left(\sigma_n^i\right)'(\sigma(z))\right| = \max_{z \in F} \frac{R_n}{|\sigma(z) - P_n^i|} = \frac{R_n}{k(P_n^i; \sigma)} \ .
$$

Thus we have

$$
\left|\sigma_{(l)}'(z)\right| \le \theta^2\left(\sigma_{(l)}\right) \cdot \ldots \cdot \theta^2\left(\sigma_{(1)}\right) \ .
$$

which proves the claim because Lemma 4.2.1 guarantees that

$$
\theta\left(\sigma_{(l)}\right) < \theta\left(\sigma_{(l-1)}\right) < \ldots < \theta\left(\sigma_{(1)}\right) = 1 \ .
\tag{4.8}
$$

Now we can give a sufficient condition for the absolute convergence of series (4.3).

Theorem 4.2.3 *Let G be iso-classical Schottky group of rank N. If there exists an index l with*

$$2N - 1 < \theta_l^{-2}, \tag{4.9}$$

where $\theta_l = \max_{\sigma \in G, |\sigma| = l+1} \theta(\sigma)$, then the series (4.3) for the normalized integrals of the first kind are absolutely convergent.

Inequality (4.8) implies that the sequence of θ_l is strictly monotone, i.e.,

$$0 < \theta_\infty < \ldots < \theta_{l+1} < \theta_l < \ldots < \theta_0 = 1 \ .$$

If (4.9) holds for one index, it will also be true for all larger indices and for the limit as well. Let

$$G_n(\sigma) = \log \frac{z - \sigma(B_n)}{z - \sigma(A_n)}$$

denote a term of the infinite sum (4.3). Substituting $\log(z - w) = f(w)$ in $G_n(\sigma)$ yields

$$
\begin{aligned}
|G_n(\sigma)| &= |f(\sigma(B_n)) - f(\sigma(A_n))| \\
&\leq \max_{w \in \sigma(F)} |f'(w)| \cdot |\sigma(B_n) - \sigma(A_n)| \\
&= \frac{1}{k(z; \sigma)} |\sigma(B_n) - \sigma(A_n)| \ .
\end{aligned}
$$

Let $\sigma_{(l)} = \sigma_{m_l}^{i_l} \cdot \ldots \cdot \sigma_{m_1}^{i_1} \in G$ be an infinite sequence growing this time to the left. Then we have

$$\left| \sigma_{(l+1)}(z) - \sigma_{(l+1)}(w) \right| \leq \theta^2\left(\sigma_{(l+1)}\right) \left| \sigma_{(l)}(z) - \sigma_{(l)}(w) \right| \ ,$$

so that

$$\left| G_n\left(\sigma_{(l+k)}\right) \right| \leq \frac{\left| \sigma_{(l)}(B_n) - \sigma_{(l)}(A_n) \right|}{k\left(z; \sigma_{(l+k)}\right)} \theta_l^{2k} \ .$$

We would like to give a bound for $k\left(z; \sigma_{(l+k)}\right)$ (from below) by $k\left(z; \sigma_{(l)}\right)$, but we cannot directly take advantage of (4.6) because we need multiplications from the left for $\sigma_{(l)}$, but the estimates are for multiplications from the right. To address this we introduce

$$k(z; l) = \min_{\sigma \in G, |\sigma| = l} k(z; \sigma) \ ,$$

for which $k(z; l) < k(z; l+1)$ holds. Thus we have $k\left(z; \sigma_{(l+k)}\right) < k(z; l+k)$, which implies

$$\left| G_n\left(\sigma_{(l+k)}\right) \right| \leq \frac{\left| \sigma_{(l+k)}(B_n) - \sigma_{(l+k)}(A_n) \right|}{k(z; l+k)} \leq \frac{\left| \sigma_{(l)}(B_n) - \sigma_{(l)}(A_n) \right|}{k(z; l)} \theta_l^{2k} \ . \tag{4.10}$$

This implies the convergence of series (4.3), because G/G_n includes exactly $(2N - 2)(2N - 1)^l$ elements of length $l + 1$.

The inequality above will be essential when we develop a posteriori criteria for an evaluation algorithm in Sect. 4.4.

The proof of the convergence of the Poincaré theta series is done with a slightly different representation of the series (4.2). Let

$$H_n(z;\sigma) = \left(\frac{1}{\sigma(z) - B_n} - \frac{1}{\sigma(z) - A_n} \right) (\gamma_\sigma z + \delta_\sigma)^{-2}$$

where

$$\begin{pmatrix} \alpha_\sigma & \beta_\sigma \\ \gamma_\sigma & \delta_\sigma \end{pmatrix} \in PSL(2, \mathbb{C})$$

denotes the matrix representation of a linear fractional transformation σ. A short computation shows that for all $\sigma \in G$ we have

$$H(z;\sigma) = \frac{1}{z - \sigma^{-1}(B_n)} - \frac{1}{z - \sigma^{-1}(A_n)} , \qquad (4.11)$$

so that

$$\omega_n(z) = \sum_{\sigma \in G_n \backslash G} H_n(z;\sigma) \, dz , \qquad (4.12)$$

which is a (-2)-dimensional Poincaré theta series.

Theorem 4.2.4 *The theta series (4.12) corresponding to a Schottky group G are absolutely convergent iff*

$$\Gamma_n = \sum_{\sigma \in G_n \backslash G, \sigma \neq id} \frac{1}{|\gamma_\sigma|^2} < \infty . \qquad (4.13)$$

For genus $N = 1$ the coset $G_n \backslash G$ includes the identity only, therefore there is nothing to show. For $N > 1$ let $\sigma \in G_n \backslash G$. Since $\sigma^{-1}(\infty) = -\delta_\sigma/\gamma_\sigma$ we have

$$|\gamma_\sigma z + \delta_\sigma| = |z - \sigma^{-1}(\infty)| \, |\gamma_\sigma| ,$$

so that

$$\frac{l(\sigma, n)}{K(z;\sigma^{-1})^2} \frac{1}{|\gamma_\sigma|^2} \leq |H_n(z;\sigma)| \leq \frac{L(\sigma, n)}{k(z;\sigma^{-1})^2} \frac{1}{|\gamma_\sigma|^2} , \qquad (4.14)$$

where

$$l(\sigma, n) = \frac{|A_n - B_n|}{K(A_n;\sigma) K(B_n;\sigma)} \quad \text{and} \quad L(\sigma, n) = \frac{|A_n - B_n|}{k(A_n;\sigma) k(B_n;\sigma)} .$$

Because of (4.7) we can guarantee positive upper and lower bounds for all $|\sigma| > 1$, which proves the claim.

For $N > 1$, we have $G_n \setminus G \subset G = \cup_{n=1,\dots,N} G_n \setminus G$, so that

$$\Gamma_n < \Gamma < \sum_{n=1}^{N} \Gamma_n \qquad \text{with} \qquad \Gamma = \sum_{\sigma \in G, \sigma \neq id} \frac{1}{|\gamma_\sigma|^2} \,,$$

which implies that all ω_n, $n = 1, \dots, N$ converge absolutely iff $\Gamma < \infty$. This also holds for $N = 1$. Indeed, a simple estimation gives

$$\frac{1}{|\gamma_{\sigma^k}|^2} = \frac{|A - B|^2}{\left|1 - \sqrt{\mu^k}\right|^2} |\mu|^k \le \left(\frac{|A - B|}{1 - |\sqrt{\mu}|}\right)^2 |\mu|^k$$

and therefore

$$\Gamma < \left(\frac{|A - B|}{1 - |\sqrt{\mu}|}\right)^2 \frac{2|\mu|}{1 - |\mu|} < \infty \,.$$

Corollary 4.2.5 *All ω_n, $n = 1, \dots, N$ converge absolutely iff $\Gamma < \infty$.*

Another consequence of Theorem 4.2.4 is that if ω_n converges absolutely for one $z_0 \in F$, then it also converges for all $z \in F$. None of these results allow us to estimate any error or deliver a criterion that can be evaluated computationally. This is also true for the next lemma, but it shows the right direction.

Lemma 4.2.6 *For $\sigma \in G$ with $[\sigma] = [il, \dots, jr]$, denote*

$$\kappa_L(\sigma) = \left| \frac{\gamma_\sigma}{\gamma_{\sigma_l^{-j}\sigma}} \right| \qquad \text{and} \qquad \kappa_R(\sigma) = \left| \frac{\gamma_\sigma}{\gamma_{\sigma\sigma_r^{-i}}} \right| \,.$$

Then $\kappa_L(\sigma) = \kappa_R(\sigma^{-1})$, and if

$$2N - 1 < \kappa^2 \qquad \text{with} \qquad \kappa = \inf_{\sigma \in G, |\sigma| > 1} \kappa_{L/R}(\sigma),$$

then Γ is finite.

For any $\tilde{\kappa} < \kappa$, and hence also for all $\tilde{\kappa} \in \,]2N - 1, \kappa[$ there exists k_0 such that $\tilde{\kappa} < \kappa_{L/R}(\sigma)$ for all $\sigma \in G$ with $|\sigma| \ge k_0$, and thus for $\sigma_{(k)} = \sigma_{s_1}^{i_1} \cdot \dots \cdot \sigma_{s_k}^{i_k}$ we have

$$\left| \gamma_{\sigma_{(k)}\sigma} \right| = \left| \frac{\gamma_{\sigma_{(k)}\sigma}}{\gamma_{\sigma_{(k-1)}\sigma}} \right| \dots \left| \frac{\gamma_{\sigma_{(k_0+1)}\sigma}}{\gamma_{\sigma_{(k_0)}}} \right| \left| \gamma_{\sigma_{(k_0)}} \right| > \kappa^{k-k_0} \left| \gamma_{\sigma_{(k_0)}} \right| \,.$$

Because of the fact that there are exactly $2N(2N-1)^{k-1}$ transformations of length k, we have

$$\sum_{|\sigma| \ge k_0} \frac{1}{|\gamma_\sigma|^2} \le \sum_{|\sigma| \ge k_0} \frac{1}{\tilde{\kappa}^{2|\sigma|}} \le \frac{\tilde{\kappa}^{2k_0}}{\gamma_{k_0}^2} \frac{2N}{2N-1} \sum_{i=k_0}^{k} \left(\frac{2N-1}{\tilde{\kappa}^2}\right)^k$$

where $\gamma_n = \min_{|\sigma|=n} |\gamma_\sigma|$.

To obtain error estimates one has to control $\kappa_{L/R}$.

Lemma 4.2.7 *Let G be a Schottky group generated by $\sigma_1, \ldots, \sigma_N$ with fixed points A_n, B_n, $n = 1, \ldots, N$. For $\sigma \in G$ with $[\sigma] = [\ldots, ir]$ we have*

$$\kappa_R(\sigma) = \frac{\max_s \left| C_r^s + \frac{\delta_\tau}{\gamma_\tau} \right| \sqrt{|\mu_r^{is}|} - \left| C_r^{-s} + \frac{\delta_\tau}{\gamma_\tau} \right| \sqrt{|\mu_r^{-is}|}}{|A_r - B_r|} = \kappa_L(\sigma^{-1}) \quad (4.15)$$

with $C_r^1 = A_r, C_r^{-1} = B_r$ and $\tau = \sigma \sigma_r^{-i}$.

We have $\gamma_\sigma = \gamma_\tau \alpha_{\sigma_r^i} + \delta_\tau \gamma_{\sigma_r^i}$. Using the representation in terms of the Schottky data (1.96), one obtains

$$\begin{aligned}
\frac{\gamma_\sigma}{\gamma_\tau} &= \alpha_{\sigma_r^i} + \gamma_{\sigma_r^i} \frac{\delta_\tau}{\gamma_\tau} \\
&= \frac{1}{A_r - B_r} \left(A_r \sqrt{\mu_r^i} - B_r / \sqrt{\mu_r^i} + \left(\sqrt{\mu_r^i} - 1/\sqrt{\mu_r^i} \right) \frac{\delta_\tau}{\gamma_\tau} \right) \\
&= \frac{1}{A_r - B_r} \left(\left(A_r + \frac{\delta_\tau}{\gamma_\tau} \right) \sqrt{\mu_r^i} - \left(B_r + \frac{\delta_\tau}{\gamma_\tau} \right) \sqrt{\mu_r^{-i}} \right).
\end{aligned}$$

The fact that $\tau^{-1}(\infty) = -\delta_\tau / \gamma_\tau$ yields

$$k\left(C_r^s; \tau^{-1}\right) \leq \left| C_r^s + \frac{\delta_\tau}{\gamma_\tau} \right| \leq K\left(C_r^s; \tau^{-1}\right).$$

Let $\sigma = \tau \sigma_r^i$ with $|\sigma| > 0$. We let

$$\overline{\kappa_R}(\sigma) = \frac{1}{|A_r - B_r|} \left(k\left(C_r^{\tilde{s}}; \tau^{-1}\right) \sqrt{|\mu_r^{i\tilde{s}}|} - K\left(C_r^{-\tilde{s}}; \tau^{-1}\right) \sqrt{|\mu_r^{-i\tilde{s}}|} \right),$$

where $\tilde{s}$ takes the maximum in (4.15), e.g.

$$\kappa_R(\sigma) = \frac{1}{|A_r - B_r|} \left(\left| C_r^{\tilde{s}} + \frac{\delta_\tau}{\gamma_\tau} \right| \sqrt{|\mu_r^{i\tilde{s}}|} - \left| C_r^{-\tilde{s}} + \frac{\delta_\tau}{\gamma_\tau} \right| \sqrt{|\mu_r^{-i\tilde{s}}|} \right).$$

Note that $\overline{\kappa_R}(\sigma) < \kappa_R(\sigma)$.

Lemma 4.2.8 *Let G be an iso-classical Schottky group. Then for all $\epsilon > 0$ there exists n_ϵ such that*

$$\kappa_R(\sigma) - \overline{\kappa_R}(\sigma) < \epsilon \qquad \forall |\sigma| \geq n_\epsilon.$$

A computation yields

$$\kappa_R(\sigma) - \overline{\kappa_R}(\sigma) \leq \frac{\sqrt{|\mu_r^{i\tilde{s}}|} + \sqrt{|\mu_r^{-i\tilde{s}}|}}{|A_r - B_r|} diam\left(\tau^{-1}(F)\right),$$

which implies the claim along the lines of the proof of Lemma 4.2.2.

This leads to a result that allows us to check the condition $2N - 1 < \kappa^2$ by evaluating $\overline{\kappa_R}(\sigma)$ for finitely many transformations σ.

Lemma 4.2.9 *Let G be an iso-classical Schottky group and*

$$\kappa_n = \min_{|\sigma|=n} \overline{\kappa_R}(\sigma) \ .$$

Then $\kappa_n \leq \kappa_{|\sigma|} \leq \overline{\kappa_R}(\sigma) < \kappa_R(\sigma)$ for all $n \leq |\sigma|$, and we have

$$\kappa_1 < \ldots < \kappa_n < \ldots < \kappa_\infty = \kappa \ .$$

Let $\sigma = \sigma_l^j \tau \sigma_r^i$ with $|\sigma| = n+1$ and $\kappa_{n+1} = \overline{\kappa_R}(\sigma)$. Inequality (4.6) guarantees

$$k\left(C_r^{\tilde{s}}; \sigma\right) > k\left(C_r^{\tilde{s}}; \tau\sigma_r^i\right) \qquad \text{and} \qquad K\left(C_r^{\tilde{s}}; \sigma\right) < K\left(C_r^{\tilde{s}}; \tau\sigma_r^i\right) \ ,$$

so that

$$\kappa_n \leq \overline{\kappa_R}\left(\tau\sigma_r^i\right) < \overline{\kappa_R}(\sigma) = \kappa_{n+1} \ .$$

To prove that $\kappa_\infty = \kappa$, let $\sigma_{(n)}$ be a sequence satisfying $\kappa_n = \overline{\kappa_R}\left(\sigma_{(n)}\right)$ and $v_{(n)}$ one with the property

$$\kappa_R\left(v_{(n)}\right) = \min_{|\sigma|=n} \kappa_R(\sigma) \ .$$

Moreover $\lim_{n\to\infty} \kappa_R\left(v_{(n)}\right) = \kappa$ implies

$$\kappa_n = \overline{\kappa_R}\left(\sigma_{(n)}\right) \leq \overline{\kappa_R}\left(v_{(n)}\right) < \kappa_R\left(v_{(n)}\right) < \kappa + \epsilon \ ,$$

so that $\kappa_\infty \leq \kappa$. On the other hand, Lemma 4.2.8 guarantees that $\kappa_R\left(\sigma_{(l)}\right)$ and $\overline{\kappa_R}\left(\sigma_{(l)}\right)$ have the same limit and thus $\kappa \geq \lim_{n\to\infty} \kappa_R\left(\sigma_{(n)}\right) = \kappa$.

From the last result, Theorem 4.2.4, and Lemma 4.2.6 we obtain an evaluable criterion for the convergence of the Poincaré theta series giving normalized differentials of the first kind.

Theorem 4.2.10 *Let G be an iso-classical Schottky group of rank N. If there exists an index l with*

$$2N - 1 < \kappa_l^2 \ ,$$

then the series (2) giving normalized differentials of the first kind are absolutely convergent.

4.3 Error Estimates

Throughout this section, let G be always an iso-classical Schottky group. For a subset S of G/G_n, we approximate Ω_n by

$$\hat{\Omega}_n(z; S) = \sum_{\sigma \in S} G_n(\sigma) \ .$$

The corresponding error is

$$\varepsilon_{\Omega_n}(z; S) = \left| \Omega_n(z) - \hat{\Omega}_n(z; S) \right| .$$

Let $\sigma_{(l)} = \sigma_{n_l}^{i_l} \cdot \ldots \cdot \sigma_{n_1}^{i_1}$ be a leftward growing sequence in G/G_n i.e., $n_1 \neq n$. Then the proof of Theorem 4.2.3 provides estimates for G_n

$$\left| G_n\left(\sigma_{(l+k)}\right) \right| \le C_{\Omega_n}\left(z; \sigma_{(l+k)}\right) \le C_{\Omega_n}\left(z; \sigma_{(l)}\right) \theta_l^{2k} , \qquad (4.16)$$

with

$$C_{\Omega_n}(z; \sigma) = \frac{\left| \sigma(B_n) - \sigma(A_n) \right|}{k(z; |\sigma|)} .$$

Let $\sigma = \sigma_{n_k}^{i_k} \cdot \ldots \cdot \sigma_{n_1}^{i_1} \in G$. Then $\sigma_{(l)} = \sigma_{n_l}^{i_l} \cdot \ldots \cdot \sigma_{n_1}^{i_1}$, $l = 1, \ldots, k$ are called *suffixes* of σ. The identity element is a suffix of any group element. If a set S includes all the suffixes of its elements it is called *suffix closed*. The set of suffixes of a subset S of G is called *suffix closure* and denoted by $\overline{S}^s$. Relation (4.16) shows that the subset S of $G/G_n \subset G$ which is used for approximation should be suffix closed.

The *boundary* $\partial^s S$ of a suffix closed subset S, given by

$$\partial^s S = \left\{ \sigma \in S^{-1} \left| \overline{\{\sigma\}}^s \cap S^{-1} = \{\sigma\} \right. \right\} ,$$

has the property that for all $\sigma \in S^{-1}$ it includes exactly one element that is a suffix of σ. This enables a natural projection

$$\begin{aligned} \pi_S : \quad S^{-1} &\to \partial^s S \\ \sigma &\mapsto \partial^s S \cap \overline{\{\sigma\}}^s . \end{aligned}$$

The set $\pi_S^{-1}(\tau)$ consists of all $\sigma \in S^{-1}$ that have τ as suffix. The set

$$\pi_S^{-1}(\tau) = Cone^s(\tau) = \left\{ \sigma \in G \left| \tau \in \overline{\{\sigma\}}^s \right. \right\}$$

is called the *suffix cone*.

Corollary 4.3.1 *Let S be a suffix closed subset. Then we have*

$$S^{-1} = \dot{\cup}_{\sigma \in \partial^s S} Cone^s(\sigma) .$$

Lemma 4.3.2 *Let S be a suffix closed subset of G/G_n. If $2N - 1 < \theta_{|\tau|}^{-2}$ for all $\tau \in \partial^s S$, then*

$$\varepsilon_{\Omega_n}(z; S) = \left| \Omega_n(z) - \hat{\Omega}_n(z; S) \right| < \sum_{\tau \in \partial^s S} \hat{\varepsilon}_{\Omega_n}(z; \tau) = \hat{\varepsilon}_{\Omega_n}(z; S) ,$$

with $\hat{\varepsilon}_{\Omega_n}(z; \tau) = C_{\Omega_n}(z; \tau) R\left(\theta_{|\tau|}^2\right)$ and

$$R(q) = \sum_{\sigma \in Cone^s(\tau)} q^{|\sigma| - |\tau|} = (1 - (2N - 1) q)^{-1} .$$

We have

$$\left| \Omega_n \left(z \right) - \hat{\Omega}_n \left(z; S \right) \right| < \sum_{\sigma \in S^{-1}} \left| G_n \left(z; \sigma \right) \right| \ ,$$

so that in light of Corollary 4.3.1 we need to show

$$\sum_{\sigma \in Cone^s \left(\tau \right)} \left| G_n \left(z; \sigma \right) \right| < \hat{\varepsilon}_{\Omega_n} \left(z; \tau \right) \ .$$

Relation (4.16) yields

$$\sum_{\sigma \in Cone^s \left(\tau \right)} C_{\Omega_n} \left(z; \sigma \right) < C_{\Omega_n} \left(z; \tau \right) \sum_{\sigma \in Cone^s \left(\tau \right)} \theta_{|\tau|}^{2 \left(|\sigma| - |\tau| \right)} = \hat{\varepsilon}_{\Omega_n} \left(z; \tau \right) \ ,$$

because there are exactly $\left(2N - 1 \right)^k$ transformations in $Cone^s \left(\tau \right)$ of length $|\tau| + k$.

To approximate the elements of the period matrix B_{nm} by

$$\hat{B}_{nm} = \sum_{\sigma \in S} B_{nm} \left(\sigma \right) \ ,$$

let now S be a suffix closed subset of $G_m \setminus G/G_n$. The associated error will be defined like the one above and denoted by $\varepsilon_{B_{nm}} \left(S \right)$. Using the representation $B_{nm} \left(\sigma \right) = G_m \left(A_n \right) + G_m \left(B_n \right)$, we have in analogy to (4.9)

$$\left| B_{nm} \left(\sigma_{\left(l+k \right)} \right) \right| \le C_{B_{nm}} \left(\sigma_{\left(l+k \right)} \right) \le C_{B_{nm}} \left(\sigma_{\left(l \right)} \right) \theta_l^{2k} \ ,$$

with

$$C_{B_{nm}} \left(\sigma \right) = C_{\Omega_m} \left(A_n \right) + C_{\Omega_m} \left(B_n \right) \ .$$

Summing up the error is more difficult then before. We have

$$\varepsilon_{B_{nm}} \left(S \right) = \left| B_{nm} - \hat{B}_{nm} \left(S \right) \right| < \sum_{\sigma \in G_m \setminus G/G_n \setminus S} \left| B_{nm} \left(\sigma \right) \right| \ .$$

Since $S \subset G_m \setminus G/G_n = \left(G_m \setminus G \right) \cap \left(G/G_n \right)$, we get a simular result to Corollary 4.3.1:

$$\begin{aligned}
\left(G_m \setminus G/G_n \right) \setminus S &= \left(G_m \setminus G \right) \cap \left(\left(G/G_n \right) \setminus S \right) \\
&= \left(G_m \setminus G \right) \cap \dot{\cup}_{\sigma \in \partial^s S} Cone^s \left(\sigma \right) \\
&= \dot{\cup}_{\sigma \in \partial^s S} Cone_m^s \left(\sigma \right) ,
\end{aligned}$$

where $Cone_m^s \left(\sigma \right) = Cone^s \left(\sigma \right) \cap G_m \setminus G$. This yields furthermore

$$\varepsilon_{B_{nm}} \left(S \right) < \sum_{\tau \in \partial^s S} \sum_{\sigma \in Cone_m^s \left(\tau \right)} \left| B_{nm} \left(\sigma \right) \right| < \sum_{\tau \in \partial^s S} C_{B_{nm}} \left(\tau \right) \sum_{\sigma \in Cone_m^s \left(\tau \right)} \theta_{|\tau|}^{2 \left(|\sigma| - |\tau| \right)}$$

which leads to

Lemma 4.3.3 *Let S be a suffix closed subset of $G_m \setminus G/G_n$. If $2N - 1 < \theta_{|\tau|}^{-2}$ for all $\tau \in \partial^s S$, then*

$$\varepsilon_{B_{nm}}(S) = \left| B_{nm}(z) - \hat{B}_{nm}(S) \right| < \sum_{\tau \in \partial^s S} \hat{\varepsilon}_{\hat{B}_{nm}}(\tau) = \hat{\varepsilon}_{B_{nm}}(S)$$

with $\hat{\varepsilon}_{B_{nm}}(\tau) = C_{B_{nm}}(\tau) R_m(\tau; q)$ and

$$R_m(\sigma; q) = \sum_{\sigma \in Cone_m^s(\tau)} q^{|\sigma| - |\tau|} = (2N - 2) \frac{q}{1 + q} R(q) + \begin{cases} \frac{1}{1+q} & \sigma \in G_m \setminus G \\ 0 & otherwise \end{cases}$$

The derivation of expressions for $R_m(\tau; q)$ is lengthy but straight forward. We could have estimated $R_m(\tau; q)$ by $R(q)$, but we need the accuracy of Lemma 4.3.3. For slowly converging series where q almost equals $1/(2N - 1)$ we get an improvement by a factor of $1 - q$. For small q, i.e., for fast converging series, $R_m(\sigma; q)$ and $R(q)$ almost coincide for $\sigma \in G_m \setminus G$, but for $\sigma \notin G_m \setminus G$ $R_m(\sigma; q)$ gets small compared to $R(q)$.

In analogy to Ω_n we approximate ω_n by

$$\hat{\omega}_n(z; S) = \sum_{\sigma \in S} H_n\left(z; \sigma^{-1}\right) dz$$

and denote the associated error by $\varepsilon_{\omega_n}(z; S)$. The proof of Theorem 4.2.4 provides estimates for H_n. Relation (4.14) guarantees:

$$\left| H_n\left(z; \sigma^{-1}\right) \right| \leq \frac{L\left(\sigma^{-1}, n\right)}{k(z; \sigma)^2} \frac{1}{|\gamma_\sigma| 2} .$$

Let $\sigma_{(l)} = \sigma_{n_l}^{i_l} \cdot \ldots \cdot \sigma_{n_1}^{i_1}$ be a leftward growing sequence in G/G_n, i.e., $n_1 \neq n$. The definition of L and inequality (4.6) imply that $L\left(\sigma_{(l+k)}^{-1}\right) < L\left(\sigma_{(l)}^{-1}\right)$, which yields in combination with $k\left(z; \sigma_{(l+k)}\right) < k(z; l)$ and Lemma 4.2.9:

$$\left| H_n\left(z; \sigma_{(l+k)}^{-1}\right) \right| \leq C_{\omega_n}\left(z; \sigma_{(l+k)}\right) \leq C_{\omega_n}\left(z; \sigma_{(l)}\right) \kappa_l^{-2k} , \tag{4.17}$$

where $l > 1$,

$$C_{\omega_n}(z; \sigma) = \frac{L\left(\sigma^{-1}, n\right)}{k(z; |\sigma|)^2} \frac{1}{|\gamma_\sigma|^2} .$$

In analogy to Lemma 4.3.2, we conclude

Lemma 4.3.4 *Let S be a suffix closed a subset of G/G_n. If $2N - 1 < \kappa_{|\tau|}^2$ for all $\tau \in \partial^s S$, then*

$$\varepsilon_{\omega_n}(z; S) = |\omega_n(z) - \hat{\omega}_n(z; S)| < \sum_{\tau \in \partial^s S} \hat{\varepsilon}_{\omega_n}(z; \tau) = \hat{\varepsilon}_{\omega_n}(z; S)$$

with $\hat{\varepsilon}_{\omega_n}(z; \tau) = C_{\omega_n}(z; \tau) R\left(\tau; \kappa_{|\tau|}^{-2}\right)$.

The weak spot of our estimates is that we majorize $1/k\left(z;\sigma^{-1}\right)$ with $1/k\left(z;|\sigma|\right)$. This can be rather bad if the radii of the isometric circles differ significantly. To some exten this can be cured but at the cost of technical complications (compare [Sch05] pp. 30–37).

4.4 Evaluation Methods

Theorems 4.2.3 and 4.2.10 provide sufficient conditions for the convergence of the series for holomorphic differentials and integrals. Ω_n converges if

$$q_\infty^\Omega = (2N-1)\,\theta_\infty^2 < 1\;,\tag{4.18}$$

and ω_n converges if

$$q_\infty^\omega = (2N-1)\,\kappa_\infty^{-2} < 1\;.\tag{4.19}$$

The monotone series $(q_l^\star)$ converges very fast and experiments show that three terms suffice to extrapolate the limit with a high accuracy. Figure 4.1 shows the analysis of the convergence criteria (4.18) and (4.19) for several examples taken from the family of Riemann surfaces that are associated with constant mean curvature tori [Bob91]. These Schottky groups possess an anti-holomorphic involution in addition to the hyperelliptic one and are Fuchsian groups of the second kind (see Chap. 1), for which the convergence is known . All our examples of genus 2 are circle decomposable (see Chap. 1) which also implies the convergence. The examples show that our criteria can guarantee convergence for integrals, but at the same time fail for differentials. In all cases we have examined the integrals converge faster than the differentials. It is remarkable that the criteria can still guarantee convergence when the circles almost touch. The parameters (4.18) and (4.19) $q_\infty^\star$ are good indicators for the speed of convergence. For good numerical results these values should not be too close to 1. The first example in Fig. 4.1 describes the spectral curve (of genus 2) of the famous Wente torus having a threefold symmetry (see [Hei95, Bob08]). This is already at the limit of what we can handle with this method and thus a good candidate for test cases.

We need to determine a suffix closed subset $S_\star\left(z;\varepsilon\right)$ of G/G_n for a given accuracy $\varepsilon > 0$ such that $\varepsilon_\star\left(z;S_\star\left(z;\varepsilon\right)\right) < \varepsilon$. For efficiency reasons as well as for numerical stability the subset should be as small as possible.

Let G be an iso-classical Schottky group and l the smallest integer such that $q_l^\star < 1$. In order to use one of the Lemmas 4.3.2, 4.3.3, and 4.3.4, any suffix closed subset must contain all elements with a word length less than or equal to l. We denote the set of those elements with

$$S_n\left(l\right) = \left\{\sigma \in G/G_n\,||\sigma| \le l\right\}\;,$$

which is also a suffix closed subset.

A straightforward approach to determine a smallest suffix closed subset is the following

l	q_l^ω	q_l^Ω
1	-	1.5729726
2	2.1919203	0.6089423
3	0.7095799	0.6026912
4	0.7008699	0.5972790
5	0.6937671	0.5972347
6	0.6937057	0.5971962

l	q_l^ω	q_l^Ω
1	-	2.9883689
2	5.5728355	0.9239982
3	1.1721161	0.9228728
4	1.1678997	0.8975555
5	1.1295999	0.8975374
6	1.1295356	0.8971324

l	q_l^ω	q_l^Ω
1	-	2.4897787
2	6.5114680	1.1106899
3	1.6407322	1.0831381
4	1.5694645	1.0162737
5	1.4367818	1.0148276
6	1.4333759	1.0113023

l	q_l^ω	q_l^Ω
1	-	0.2075865
2	0.2221489	0.1390086
3	0.1452401	0.1379418
4	0.1440661	0.1378807
5	0.1439990	0.1378796
6	0.1439978	0.1378795

Fig. 4.1. Analysis of the convergence conditions (4.18) and (4.19) for several examples taken from the family of Riemann surfaces of genus 2 giving constant mean curvature tori. The first example is the Riemann surface of the Wente torus with threefold symmetry

Algorithm 4.4.1 *Let $\varepsilon > 0$, G an iso-classical Schottky group and l the smallest integer such that $q_l^\star < 1$:*
1. *Put $S_{(i=1)} = S_n(l)$.*
2. *If $\hat{\varepsilon}\left(z; S_{(i)}\right) < \varepsilon$, put $S_\star(z; \varepsilon) = S_{(i)}$ and finish.*
3. *Find $\sigma_{(i)} \in \partial^s S_{(i)}$ with $C_\star\left(z; \sigma_{(i)}\right) = \max_{\sigma \in \overline{S_{(i)}}} C_\star(z; \sigma)$.*
4. *Put $S_{(i+1)} = S_{(i)} \cup \left\{\sigma_{(i)}\right\}$.*
5. *Put $i = i + 1$ and continue with Step 2.*

The algorithm above is simple and gives the optimal result, but Step 3 makes it rather expensive. A different approach is inspired by the following property of the boundary of a suffix closed subset:

Corollary 4.4.2 *Let S be a suffix closed subset G/G_n. Then*

$$1 = \frac{2N - 1}{2N - 2} \sum_{\sigma \in \partial^s S} (2N - 1)^{-|\sigma|} .$$

Let $l = \max_{\sigma \in S} |\sigma|$. Then the boundary $\partial^s S_n(l) \subset S^{-1}$. $\pi_S^{-1}(\sigma)$ contains exactly $(2N - 1)^{l+1-|\sigma|}$ transformations of word length $l + 1$, i.e.,

$$\# \left(\pi_{S|\partial^s S_n(l)}^{-1}\right) = (2N - 1)^{l+1-|\sigma|} ,$$

which implies

$$1 = \frac{1}{(2N - 2)(2N - 1)^l} \sum_{\sigma \in \partial^s S_n(l)} 1$$

$$= \frac{1}{(2N - 2)(2N - 1)^l} \sum_{\sigma \in \partial^s S} \sum_{\hat{\sigma} \in \pi_{S|\partial^s S_n(l)}^{-1}} 1$$

$$= \frac{1}{(2N - 2)(2N - 1)^l} \sum_{\sigma \in \partial^s S} (2N - 1)^{l+1-|\sigma|} .$$

This property similar to a partition of 1 like yields the following

Algorithm 4.4.3 *Let $\varepsilon > 0$, G an iso-classical Schottky group and l the smallest integer such that $q_l^\star < 1$:*
1. *Put $S_{(i=1)} = S_n(l)$.*
2. *Put $\tilde{S}_{(i)} = \left\{\sigma \in \partial^s S_{(i)} \,\middle|\, \hat{\varepsilon}_\star(z; \sigma) > \frac{2N-1}{2N-2}(2N - 1)^{-|\sigma|} \varepsilon\right\}$.*
3. *If $\tilde{S}_{(i)} = \{\emptyset\}$, put $S_\star(z; \varepsilon) = S_{(i)}$ and finish.*
4. *Put $S_{(i+1)} = S_{(i)} \cup \tilde{S}_{(i)}$.*
5. *Put $i = i + 1$ and continue with Step 2.*
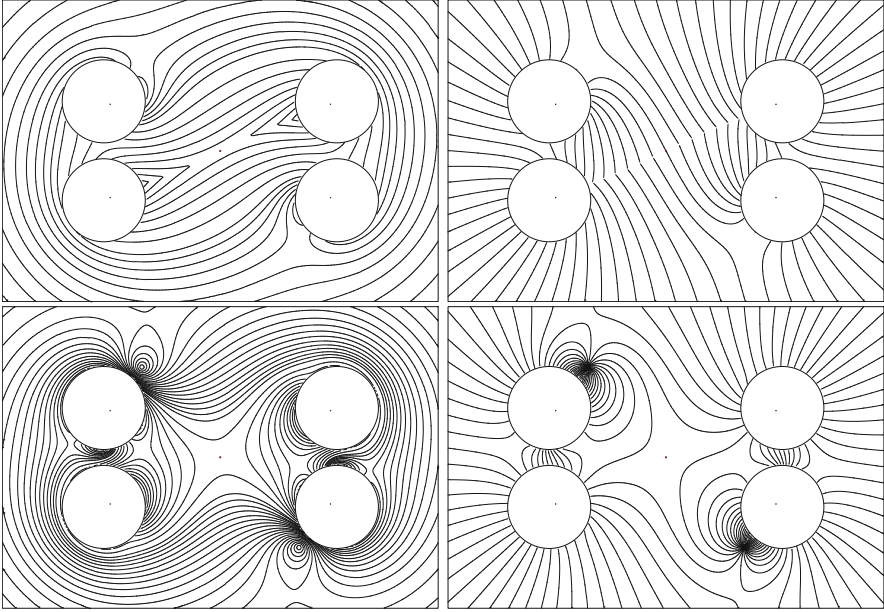
Fig. 4.2. Absolute (*left column*) and argument values (*right column*) of Ω_1(*top row*) and ω_1(*bottom row*) for the Wente torus with threefold symmetry

This method offers a good trade-off between the size of $S_\star(z;\varepsilon)$ on one hand and computational cost on the other.

In Step 2 of Algorithm 4.4.3 we stay for all $\sigma \in \partial^s S_{(i)} \setminus \tilde{S}_{(i)}$ below the threshold $\hat{\varepsilon}_\star(z;\sigma)$. We can therefore increase ε by

$$\frac{2N-1}{2N-2}(2N-1)^{-|\sigma|}\varepsilon - \hat{\varepsilon}_\star(z;\sigma)$$

after each test. We will refer to this optimized version as Algorithm 4.4.3*.

The crucial constants $C_\omega(z;\sigma)$ and $C_\Omega(z;\sigma)$ contain a computationally fairly inexpensive z-independent factor and an expensive z-dependent factor $k_{|\sigma|}(z)^{-p_\star}$, with $p = 1$ for Ω_n and B_{nm}, and $p = 2$ for ω_n. The complexity of the computation of $k_l(z)$ grows exponentially in l. Thus it is inevitable to replace $k_l(z)$ by $k_{\tilde{l}}(z)$ with a small $\tilde{l} = 1, 2, 3 \leq l$. This is negligible, because $k_l(z)$ converges very fast, particularly with respect to the fact that we earlier replaced $k(z;\sigma)$ by $k_{|\sigma|}(z)$. At this point we have reduced our evaluation methods to more or less elementary operations. Figure 4.2 shows plots, again for the Riemann surface of genus 2 describing the Wente torus with threefold symmetry, of the integral Ω_1 and of the differential ω_1 of first kind.

How rigorous are our estimates? We gave an estimate for the absolute value series. Let us denote them by $|\Omega|_n$ and $|\omega|_n$. Their approximation for a given suffix closed subset S of G/G_n is given by

$$\left|\hat{\Omega}\right|_n (z; S) = \sum_{\sigma \in S} |G_n (z; \sigma)| \quad \text{and}$$

$$|\hat{\omega}|_n (z; S) = \sum_{\sigma \in S} \left| H_n \left(z; \sigma^{-1} \right) \right| \ .$$

Plots of the defects $d_\star (z; \varepsilon) = |\star|_n (z) - |\widehat{\star}|_n (z; S_\star (z; \varepsilon))$ will reveal the results of our effort and show how rigorous our estimates are. To approximate the defect $d_\star (z; \varepsilon)$ we approximate $|\star|_n (z)$ by $|\widehat{\star}|_n (z; S_\star (z; \tilde{\varepsilon}))$, where $\tilde{\varepsilon}$ is significantly smaller than ε. For a relative error of 10% $\tilde{\varepsilon}$ should be 10 times smaller than the resulting minimum of $d_\star (z; \varepsilon)$.

The algorithm manages to keep the defect $d_{\Omega_1} \left(z; 10^{-3} \right)$ in the selected clipping in the range of $[1.5, 2.3] \cdot 10^{-4}$ and $d_{\omega_1} \left(z; 10^{-3} \right)$ in $[0.7, 2.3] \cdot 10^{-4}$.

The described algorithms are implemented in java and freely available as part of the JTEM (Java Tools for Experimental Mathematics, `http://www.math.tu-berlin.de/jtem/`) software project.

Acknowledgment

References

[Bak97] Baker, H.F.: Abelian functions. Abel's theorem and the allied theory of theta functions, Reprint of the 1897 original, xxxvi+684 pp. Cambridge University Press, Cambridge (1995)

[Bob91] Bobenko, A.I.: All constant mean curvature tori in R^3, S^3, H^3 in terms of theta-functions. Math. Ann. **290**, 209–245 (1991)

[Bob08] Bobenko, A.I.: Exploring Surfaces through Methods from the Theory of Integrable Systems: The Bonnet Problem, In: Surveys on Geometry and Integrable Systems. Advanced Studies in Pure Mathematics, vol. 51, pp. 1–51 (2008)

[Bob11] Bobenko, A.I.: Introduction to compact Riemann surfaces. In: Bobenko, A.I., Klein, Ch. (eds.) Lecture Notes in Mathematics 2013, pp. 3–64. Springer, Berlin (2011)

[Bur92] Burnside, W.: On a class of automorphic functions. Proc. Lond. Math. Soc. **23**, 49–88, 281–295 (1892)

[For29] Ford, L.R.: Automorphic Functions, vii+333 pp. McGraw-Hill, New York (1929)

[FK65]   Fricke, R., Klein, F.: Vorlesungen über die Theorie der automorphen Funktionen. Johnson Reprint Corp., New York; B.G. Teubner Verlagsgesellschaft, Stuttgart (1965), xiv+634 pp., xiv+668 pp.

[Hei95] Heil, M.: Numerical Tools for the study of finite gap solutions of integrable systems, PhD thesis, Technische Universität Berlin, 1995

[Sch05] Schmies, M.: Computational methods for Riemann surfaces and helicoids with handles, PhD thesis, Technische Universität Berlin, 2005, http://opus.kobv.de/tuberlin/volltexte/2005/1105/

5

Uniformizing Real Hyperelliptic M-Curves Using the Schottky–Klein Prime Function

Darren Crowdy and Jonathan S. Marshall

Department of Mathematics, Imperial College London, 180 Queen's Gate,
London, SW7 2AZ, United Kingdom
d.crowdy@imperial.ac.uk
jonathan.marshall@imperial.ac.uk

5.1 Introduction

It is a consequence of the uniformization theorem of Koebe and Poincaré that any smooth complex algebraic curve C of genus $g > 1$ is conformally equivalent to $\mathbb{H}/G_F$ where $\mathbb{H}$ is the upper-half complex plane and $G_F \in PSL_2(\mathbb{R})$ is a Fuchsian group. On the other hand, C is also known to be equivalent to Γ/G_S where Γ is some domain in the Riemann sphere and G_S is a Schottky group $G_S \in PSL_2(\mathbb{C})$ where the fundamental region associated with G_S is multiply connected.

   This paper is concerned with the matter of uniformizing real hyperelliptic M-curves of the form

$$y^2 = \prod_{j=1}^{2g+2} (x - e_j) \tag{5.1}$$

where the constants $\{e_j | j = 1, ..., 2g + 2\}$ are distinct real numbers. The curve (5.1) has genus g. Such a curve admits both an antiholomorphic involution given by

$$(x, y) \mapsto (\overline{x}, \overline{y}) \tag{5.2}$$

and a hyperelliptic involution given by

$$(x, y) \mapsto (x, -y) . \tag{5.3}$$

In Chap. 1 it was shown that hyperelliptic curves of this kind can be uniformized by Schottky groups of Fuchsian type (with essentially no difference between the two uniformizations described above), and this uniformization was performed there by representing the relevant mathematical objects in terms of Poincaré theta series (note also that, in his contribution to this book, M. Schmies develops a new algorithm for the calculation of Poincaré theta series and includes the relevant error estimates). The purpose of the

present chapter is to demonstrate an alternative approach using a special function called the *Schottky-Klein prime function* associated with the underlying Riemann surface.

The uniformization of algebraic curves is an old problem that has attracted the attention of many investigators. Some exact results are known for special curves, especially those with large groups of automorphisms (e.g. [Kul97]). There has been much recent attention, however, on the *numerical* uniformization problem. Buser and Silhol [BS01], for example, consider real hyperelliptic curves. They start with a compact Riemann surface given as the quotient of the Poincaré upper-half plane divided by the action of a Fuchsian group. They consider the hyperbolic $(2g + 2)$-gon associated with this group and compute the period matrix of the curve in terms of the conformal capacities of certain harmonic functions in this polygon. This is done numerically. Armed with this period matrix, they determine the algebraic equation of the hyperelliptic curve using theta characteristics. The numerical Schottky uniformization of hyperelliptic M-curves, as the topic arises in generating finite-gap solutions of integrable partial differential equations, has been solved in [BK87,Bob88] (the corresponding explicit uniformization map is presented in the monograph by Belokolos et al. [BBE+94] – see also Chap. 1 of this book [Bob11]). Schottky uniformizations, together with the associated software, of more general real Riemann surfaces are also discussed in [BK87,BBE+94].

Hidalgo [Hid01] and Hidalgo and Figueroa [Hid05] have presented a numerical approach to Schottky uniformization of algebraic curves. Hidalgo [Hid01] focusses on hyperelliptic M-curves (of, in principle, arbitrary genus) while Hidalgo and Figueroa [Hid05] consider maximally symmetric real curves of genus two. Having specified the a-cycles of the curve and certain corresponding circles in the Schottky uniformization domain, they exploit the fact that the holomorphic differentials on the universal cover as written down by Burnside [Bur92] are the lifting of the dual holomorphic 1-forms on the curve (with respect to the chosen a-cycles). By equating the period matrix computed both in the homology basis on the universal cover with the period matrix of the curve (either computed directly using the known basis of holomorphic 1-forms of the curve, or known from other considerations), a set of transcendental equations between the real parameters characterizing the uniformizing Schottky group and the branch points of the curve are derived. These can then be solved numerically.

The approach expounded here uses the Schottky–Klein prime function to construct an explicit conformal slit mapping from a fundamental region associated with a classical Schottky group to the region exterior to the slits (or branch cuts) of the curve (5.1). Semmler and Seppälä [SS95] and Seppälä [Sep04] have also presented a numerical algorithm to construct uniformizations of real hyperelliptic M-curves but they proceed in the opposite direction: their algorithm produces the group data from the branch point data by means of an iterative scheme, first proposed by Myrberg [Myr20], which "opens up" the slots (or cuts) between branch points to produce circles in the relevant uniformization domain.

5.2 The Schottky–Klein Prime Function

Let D_ζ be a multiply connected circular domain given as the unit ζ-disc with $M \geq 1$ smaller circular discs excised. Figure 5.1 shows an example with M = 2. For the particular application to the uniformization of real hyperelliptic curves (1) only Schottky circles with centres aligned along a common axis will be needed. The generators associated with such Schottky circles then generate a Schottky group of Fuchsian type.

The aim of this section is to define a special transcendental function, known as the *Schottky–Klein prime function*, associated with the domain D_ζ (or, strictly speaking, its Schottky double). First define M Möbius maps $\{\phi_j | j = 1, ..., M\}$ by insisting that $\overline{\zeta} = \phi_j(\zeta)$ on the circle C_j. That is, if C_j is defined by

$$|\zeta - \delta_j|^2 = (\zeta - \delta_j)(\overline{\zeta} - \overline{\delta_j}) = q_j^2 \tag{5.4}$$

then

$$\overline{\zeta} = \overline{\delta_j} + \frac{q_j^2}{\zeta - \delta_j} \tag{5.5}$$

so

$$\phi_j(\zeta) \equiv \overline{\delta_j} + \frac{q_j^2}{\zeta - \delta_j} . \tag{5.6}$$

Next, introduce the Möbius maps

$$\theta_j(\zeta) \equiv \overline{\phi}_j(\zeta^{-1}) = \delta_j + \frac{q_j^2 \zeta}{1 - \overline{\delta_j}\zeta} . \tag{5.7}$$
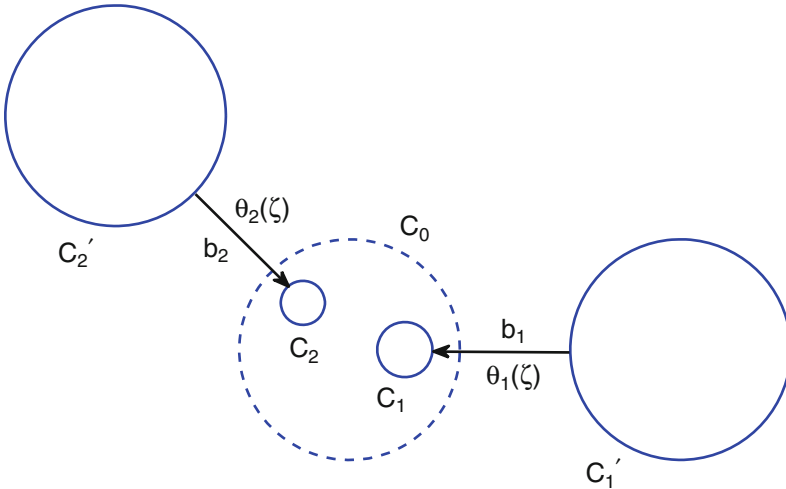
Fig. 5.1. Schematic illustrating the circles C_j and C_j' in a triply connected case ($M = 2$). Each of the two circles $\{C_j | j = 1, 2\}$ is an a-cycle. The two b-cycles are also indicated

Let C_j' be the circle obtained by reflection of the circle C_j in the unit circle $|\zeta| = 1$ (i.e. the circle obtained by the transformation $\zeta \mapsto 1/\bar{\zeta}$). These circles are depicted in Fig. 5.1. The unit circle is denoted by C_0. Referring back to the original curve (5.1), this (antiholomorphic) reflection of the region D_ζ to produce an identical copy, with the opposite conformal structure in $|\zeta| > 1$, effectively models the antiholomorphic involution (5.2) and allows us to uniformize the second sheet of the curve X.

It is easily verified that the image of the circle C_j' under the transformation θ_j is the circle C_j. In this way, θ_j identifies circle C_j' with circle C_j. Since the M circles $\{C_j | j = 1, ..., M\}$ are non-overlapping, so are the M circles $\{C_j' | j = 1, ..., M\}$. The (classical) *Schottky group* Θ is defined to be the infinite free group of mappings generated by compositions of the M basic Möbius maps $\{\theta_j | j = 1, ..., M\}$ and their inverses $\{\theta_j^{-1} | j = 1, ..., M\}$ and including the identity map.

Consider the (generally unbounded) region of the plane exterior to the $2M$ circles $\{C_j, C_j' | j = 1, ..., M\}$. Let this region be called F. F is known as the *fundamental region* associated with the Schottky group generated by the Möbius maps $\{\theta_j | j = 1, ..., M\}$ and their inverses. This is because the entire plane is tessellated with copies of this fundamental region obtained by mapping F by the elements of the Schottky group. This fundamental region can be understood as having two "halves" – the half that is inside the unit circle but exterior to the circles C_j is the domain D_ζ, the other half is the region outside the unit circle and exterior to the circles C_j'. This other half (or copy of D_ζ) is obtained by an (antiholomorphic) reflection of D_ζ in the unit circle C_0.

These two halves of F, one just a reflection through the unit circle of the other, can be viewed as a model of the two "sides" of a compact (symmetric) Riemann surface associated with D_ζ known as its *Schottky double*. The circles $\{C_j | j = 1, ..., M\}$ can be identified with the a-cycles of this compact Riemann surface (by identification, the circles $\{C_j' | j = 1, ..., M\}$ also correspond to a-cycles); any line joining identified points on C_j and C_j' can be identified with a b-cycle. There are clearly M such b-cycles. Figure 5.1 indicates these in the case M = 2.

Any compact Riemann surface of genus M also possesses exactly M holomorphic differentials [FK04] which we shall here denote $\{dv_j(\zeta) | j = 1, ..., M\}$. The functions $\{v_j(\zeta) | j = 1, ..., M\}$ are the *integrals of the first kind* and each is uniquely determined, up to an additive constant, by their periods around the a and b-cycles. These functions are analytic, but not single-valued, everywhere in F. Here we normalize the holomorphic differentials so that

$$\oint_{a_k} dv_j = \delta_{jk} \ , \quad \oint_{b_k} dv_j = \tau_{jk} \tag{5.8}$$

where τ_{jk} is the period matrix.

Armed with a normalized basis of a and b-cycles, the M integrals of the first kind and the Schottky group Θ, we have now set up all the necessary

machinery to be able to define the Schottky–Klein prime function. The following theorem is established in Hejhal [Hej72]:

Theorem 1. *There is a unique function $\tilde{X}(\zeta, \gamma)$ defined by the properties:*

(i) $\tilde{X}(\zeta, \gamma)$ *is analytic everywhere in F.*
(ii) *For $\gamma \in F$, $\tilde{X}(\zeta, \gamma)$ has a second-order zero at each of the points $\{\theta(\gamma) | \theta \in \Theta\}$.*
(iii) *For $\gamma \in F$,*

$$\lim_{\zeta \to \gamma} \frac{\tilde{X}(\zeta, \gamma)}{(\zeta - \gamma)^2} = 1 \ . \tag{5.9}$$

(iv) *For $j = 1, ..., M$,*

$$\tilde{X}(\theta_j(\zeta), \gamma) = \exp(-2\pi i(2(v_j(\zeta) - v_j(\gamma)) + \tau_{jj})) \frac{d\theta_j(\zeta)}{d\zeta} \tilde{X}(\zeta, \gamma) \ . \tag{5.10}$$

Hejhal [Hej72] then defines the *Klein prime function* $\omega(\zeta, \gamma)$ (or what we will call, following Baker [Bak97], the *Schottky–Klein prime function*) as the square root of this function, i.e.,

$$\omega(\zeta, \gamma) = (\tilde{X}(\zeta, \gamma))^{1/2} \tag{5.11}$$

where the branch of the square root is chosen so that $\omega(\zeta, \gamma)$ behaves like $(\zeta - \gamma)$ as $\zeta \to \gamma$.

There is a classical infinite product for the Schottky–Klein prime function [Bak97] described in the next section. It is known to converge for any Schottky group of Fuchsian type so this infinite product representation can be used in the uniformization problem of interest here. It is worth mentioning, however, that there are other ways to compute the Schottky–Klein prime function: for example, Crowdy and Marshall [CM07] have recently described a numerical algorithm for the computation of the Schottky–Klein prime function on the Schottky double of planar domains. The new method does not rely on a sum (or product) over a Schottky group (note that those authors do not prove convergence of the new method – further work is needed on this – but numerical evidence of convergence is provided). It is important to seek alternatives to infinite sum/product representations over Schottky groups because, from a numerical standpoint, the convergence of such representations can be very slow (especially as the genus of the curve gets large).

5.2.1 Infinite Product Formula

Following Baker [Bak97], an infinite product formula for the Schottky–Klein prime function is given by

$$\omega(\zeta, \gamma) = (\zeta - \gamma)\omega'(\zeta, \gamma) \tag{5.12}$$

where the function $\omega'(\zeta, \gamma)$ is

$$\omega'(\zeta, \gamma) = \prod_{\theta_i \in \Theta''} \frac{(\theta_i(\zeta) - \gamma)(\theta_i(\gamma) - \zeta)}{(\theta_i(\zeta) - \zeta)(\theta_i(\gamma) - \gamma)} \ . \tag{5.13}$$

This product is over all mappings in a set Θ'' which is used to denote the Schottky group Θ excluding the identity map and all inverse maps. This means that if a term associated with the mapping θ_i is included in the product, then the term corresponding to θ_i^{-1} must be omitted. The function $\omega(\zeta, \gamma)$ is single-valued on the whole ζ-plane, has a simple zero at γ and all points equivalent to γ under the mappings of the group Θ. The prime notation is not used here to denote differentiation.

Infinite product formulae for the period matrices are also available. When $k \neq j$,

$$\tau_{jk} = \frac{1}{2\pi i} \log \left[\prod_{\psi \in {}_k\Theta_j} \left(\frac{\psi(\mathcal{B}_j) - \mathcal{B}_k}{\psi(\mathcal{B}_j) - \mathcal{A}_k} \right) \left(\frac{\psi(\mathcal{A}_j) - \mathcal{A}_k}{\psi(\mathcal{A}_j) - \mathcal{B}_k} \right) \right] \tag{5.14}$$

where $\mathcal{A}_k, \mathcal{B}_k$ are the two fixed points of the mapping θ_k and the product is now taken over all elements in the set ${}_k\Theta_j$ which denotes all elements of Θ which, written as a composition of the M generating maps, do not have any power of the generator θ_k on the left end or any power of θ_j on the right end. We note that the following identities hold for each generator of the Schottky group:

$$\frac{\theta_j(\zeta) - \mathcal{B}_j}{\theta_j(\zeta) - \mathcal{A}_j} = \mu_j e^{i\kappa_j} \frac{\zeta - \mathcal{B}_j}{\zeta - \mathcal{A}_j} \ , \quad j = 1, ..., M \tag{5.15}$$

for some real parameters $\{\mu_j, \kappa_j | j = 1, ..., M\}$. Given these parameters, we can also write the diagonal terms of the period matrix for any $k = 1, ..., M$:

$$\tau_{kk} = \frac{1}{2\pi i} \log \left[\mu_k e^{i\kappa_k} \prod_{\psi \in {}_k\Theta_k''} \left[\left(\frac{\psi(\mathcal{B}_k) - \mathcal{B}_k}{\psi(\mathcal{B}_k) - \mathcal{A}_k} \right) \left(\frac{\psi(\mathcal{A}_k) - \mathcal{A}_k}{\psi(\mathcal{A}_k) - \mathcal{B}_k} \right) \right]^2 \right] \ . \tag{5.16}$$

Finally, for the symmetric Schottky groups considered in this paper, it is also possible to demonstrate that the Schottky–Klein prime function satisfies the relation

$$\overline{\omega}(\zeta^{-1}, \gamma^{-1}) = -\frac{1}{\zeta\gamma} \omega(\zeta, \gamma) \ . \tag{5.17}$$

This identity is established, based on use of the infinite product formula (5.12) and (5.13), in an appendix to Crowdy and Marshall [CM05] and the reader is referred there for additional details.

5.3 Slit Mappings

We now pick a circular region D_ζ consisting of the unit disc with M smaller circles excised all of which are centered on the real axis. Next, consider the sequence of conformal mappings from D_ζ in a complex ζ-plane to a complex z-plane given by:

$$\zeta_1(\zeta) = -\frac{\omega(\zeta,1)}{\omega(\zeta,-1)}, \qquad \zeta_2(\zeta_1) = \frac{1-\zeta_1}{1+\zeta_1}, \qquad z(\zeta_2) = \frac{1}{2}\left(\zeta_2^{-1} + \zeta_2\right). \quad (5.18)$$

$\omega(\zeta,.)$ is the Schottky–Klein prime function associated with D_ζ. Figure 5.2 illustrates this composition of mappings in the case $M = 3$. By the end of the composition the half of D_ζ in the lower half-plane is mapped to an upper-half plane exterior to a collection of slits along the real axis. The only non-trivial component of this sequence is the initial mapping to the ζ_1-plane. However,
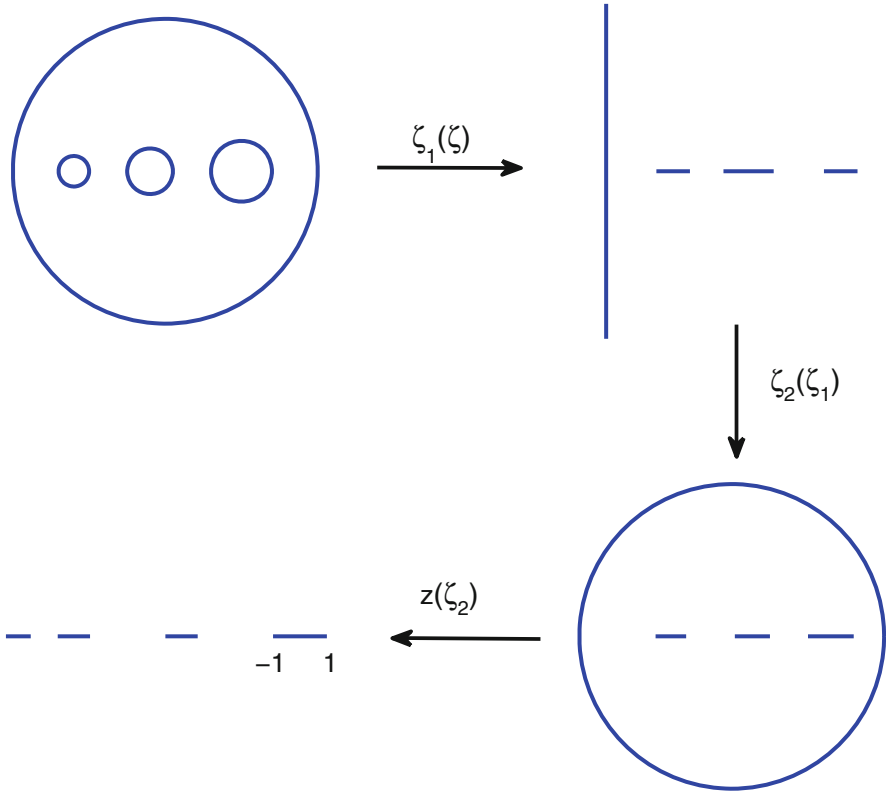
Fig. 5.2. Composition of mappings (5.18) leading to a slit map (5.19) from the interior of D_ζ to the unbounded region in a z-plane exterior to $M + 1$ slits on the real axis (the case $M = 3$ is shown)

by making use of the two relations (5.10) and (5.17) satisfied by the prime function, it is a straightforward exercise to show that $\overline{\zeta_1(\zeta)} = \zeta_1(\zeta)$ when ζ is on a circle C_j for $j = 1, ..., M$. This means that all circles $\{C_j | j = 1, ..., M\}$ map to intervals on the real ζ_1 axis, as indicated in the genus-3 case in Fig. 5.2. It is also easy to make use of (5.17) to show that C_0 maps to the imaginary ζ_1-axis.

The final composed map $z(\zeta)$ takes the simple functional form

$$z(\zeta) = \frac{\omega^2(\zeta, -1) + \omega^2(\zeta, 1)}{\omega^2(\zeta, -1) - \omega^2(\zeta, 1)}. \tag{5.19}$$

$z(\zeta)$ maps D_ζ onto the region consisting of the entire complex plane exterior to four slits on the real axis, where the image of the unit circle is the slit with endpoints ± 1.

To determine the real parameters $\{\delta_j, q_j | j = 1, ..., M\}$ we make use of a system of real equations arising from the fact that the branch points of the curve $\{e_j | j = 3, ..., 2g\}$ are the images of the points where the inner circles of D_ζ intersect the real axis (and, now, we have set $M = g$). This system of transcendental equations must be solved for the group parameters if the branch points of the curve are given. The Schottky group associated with D_ζ provides a Schottky uniformization of the hyperelliptic curve X. On the other hand, if the uniformizing Schottky group is given, then a direct evaluation of the conformal map $z(\zeta)$ (using the given group data to construct the prime function) at the relevant points immediately produces the branch point data for the curve.

5.4 Numerical Examples

In this section, we find the uniformizing Schottky groups of some example hyperelliptic curves. Since our construction is trivial in one direction (i.e., that of finding the algebraic curve given the group data), we concentrate on constructing the group data given the branch points of a hyperelliptic curve. This direction is only slightly more complicated because the solution of a finite transcendental system of equations needs to be found. We encountered no difficulty, however, in all the following examples, using a Newton iteration scheme to generate the solution.

5.4.1 Comparison with a Myrberg Iteration Scheme

A check on the new method can be found by comparing it with an independent method. In §6 of [SS95], Semmler and Seppälä consider examples of genus-2 hyperelliptic curves corresponding to (5.1) where

$$e_1 = 8, \quad e_2 = 6, \quad e_3 = 1/k, \quad e_4 = -1/k, \quad e_5 = -6, \quad e_6 = -8 \tag{5.20}$$

where $1 \leq k \leq 9$ is an integer. Their circular domains are slightly different to those we have considered: we obtain theirs from ours by simply inverting, via the mapping $\zeta \mapsto \zeta^{-1}$, in C_0 and then re-scaling by a real constant. Owing to the symmetry of the distribution of the points (5.20), such circular domains are reflectionally symmetric in the imaginary axis. Label the points in the right half plane where these circles intersect the real axis as p_1, p_2 and p_3. Semmler and Seppälä [SS95] have computed these points for $1 \leq k \leq 9$. The values are recorded in Table 2 of [SS95]. In Table 5.1, we present the values of these points as computed using the alternative method described above. For comparison, the values found by Semmler and Seppälä [SS95] are given in brackets. Our computations have been made using truncations, to level 5, of the infinite product defining the Schottky–Klein prime function. Excellent agreement is obtained.

Table 5.1. A reproduction of Table 2 of [SS95] obtained using the new method. The values obtained in [SS95] are included in brackets

k	p_1	p_2	p_3
1	0.50530 (0.50530)	6.4418 (6.4418)	7.4484 (7.4484)
2	0.25261 (0.25261)	6.4716 (6.4715)	7.4742 (7.4741)
3	0.16840 (0.16840)	6.4770 (6.4770)	7.4789 (7.4789)
4	0.12630 (0.12630)	6.4790 (6.4789)	7.4806 (7.4805)
5	0.10104 (0.10104)	6.4799 (6.4798)	7.4814 (7.4813)
6	0.084199 (0.084199)	6.4803 (6.4803)	7.4818 (7.4817)
7	0.072170 (0.072170)	6.4806 (6.4806)	7.4820 (7.4820)
8	0.063149 (0.063149)	6.4808 (6.4808)	7.4822 (7.4821)
9	0.056132 (0.056132)	6.4809 (6.4809)	7.4822 (7.4822)

5.4.2 A Genus-3 Example

Suppose we have the genus-3 curve

$$y^2 = \prod_{n=1}^{8} (x - n) \,. \tag{5.21}$$

Numerically we find the Schottky domain which, under (5.19), maps onto the slit domain where three of the branch points have been normalized, by a preliminary Möbius mapping, to be at ± 1 and 20 (we pick these values arbitrarily). For $i = 1, 2, 3$ we find the center and radius of the circle C_i in the interior of the unit circle to be (reported here correct to 6 decimal places):

$$\begin{aligned}
\delta_1 &= 0.122809, & q_1 &= 0.017780, \\
\delta_2 &= 0.054921, & q_2 &= 0.004353, \\
\delta_3 &= 0.032974, & q_3 &= 0.001903.
\end{aligned} \tag{5.22}$$

5.4.3 A Genus-4 Example

Now consider instead the genus-4 curve

$$y^2 = \prod_{n=1}^{10} (x - n) \ . \tag{5.23}$$

Again, we numerically compute the Schottky domain which, under (5.19), maps onto the slit domain transformed so that three of the branch points are at ± 1 and 20. For $i = 1, ..., 4$ we find the center and radius of the circle C_i in the interior of the unit circle to be (reported here correct to 4 decimal places):

$$
\begin{aligned}
\delta_1 &= 0.1317 \ , \quad q_1 = 0.0177 \ , \\
\delta_2 &= 0.0639 \ , \quad q_2 = 0.0044 \ , \\
\delta_3 &= 0.0419 \ , \quad q_3 = 0.0019 \ , \\
\delta_4 &= 0.0311 \ , \quad q_4 = 0.0010 \ .
\end{aligned}
\tag{5.24}
$$

5.5 Discussion

This paper has presented a simple numerical method for uniformizing a real hyperelliptic M-curve. The method makes use of the simple conformal map

$$z(\zeta) = \frac{\omega^2(\zeta, -1) + \omega^2(\zeta, 1)}{\omega^2(\zeta, -1) - \omega^2(\zeta, 1)} \ , \tag{5.25}$$

where $\omega(\zeta, .)$ is the Schottky–Klein prime function associated with the relevant uniformizing groups.

While there are many others ways to treat the particular uniformization problem considered here, consideration of the Schottky–Klein prime function is a novel ingredient in the present method that we wish to emphasize. It is an important mathematical object associated with any compact Riemann surface, and it can facilitate the solution of other problems of conformal mapping and uniformization. For example, in terms of it, it is possible to derive a rather compact extension of the classical Schwarz–Christoffel formula to give conformal mappings from multiply connected circular regions to arbitrary multiply connected polygonal regions [Cro05, Cro07].

References

[Bak97]   Baker, H.F.: Abelian functions: Abel's theorem and the allied theory of theta functions, Cambridge University Press, Cambridge (1897)

[BBE+94] Belokolos, E.D., Bobenko, A.I., Enol'skii, V.Z., Its, A.R., Matveev, V.B.: Algebro-geometric approach to nonlinear integrable equations. Springer, Berlin (1994)

[BK87]   Bobenko, A.I., Kubensky, D.A.: Qualitative analysis and calculations of the finite-gap solutions of the KdV equation. An automorphic approach. Teor. Mat. Fiz. **72**(3), 352–360 (1987)

[Bob88]   Bobenko, A.I.: Schottky uniformization and finite gap integration. Sov. Math. Dokl. **36**(1), 38–43 (1988)

[Bob11]   Bobenko, A.I.: Introduction to compact Riemann surfaces. In: Bobenko, A.I., Klein, Ch. (eds.) Lecture Notes in Mathematics 2013, pp. 3–64. Springer, Berlin (2011)

[Bur92]   Burnside, W.: On a class of automorphic functions. Proc. Lond. Math. Soc. **23**, 49–88 (1892)

[BS01]   Buser, P., Silhol, R.: Geodesics, periods, and equations of real hyperelliptic curves. Duke Math. J. **108**(2), 211–250 (2001)

[CM07]   Crowdy, D.G., Marshall, J.S.: Computing the Schottky-Klein prime function on the Schottky double of planar domains. Comput. Methods Funct. Theory **7**(1), 293–308 (2007)

[CM05]   Crowdy, D.G., Marshall, J.S.: Analytical formulae for the Kirchhoff-Routh path function in multiply connected domains. Proc. R. Soc. A, **461**, 2477–2501 (2005)

[Cro05]   Crowdy, D.G.: The Schwarz-Christoffel mapping to bounded multiply connected polygonal domains. Proc. R. Soc. A **461**, 2653–2678 (2005)

[Cro07]   Crowdy, D.G.: Schwarz-Christoffel mappings to unbounded multiply connected polygonal regions. Math. Proc. Camb. Phil. Soc. **142**, 319–339 (2007)

[FK04]   Karkas, H., Kra, I.: Riemann surfaces. Springer, Berlin (2004)

[Hej72]   Hejhal, D.A.: Theta functions, kernel functions, and abelian integrals, Memoirs of the American Mathematical Society, vol. 129. American Mathematical Society, Providence (1972)

[Hid01]   Hidalgo, R.A.: Numerical uniformization of hyperelliptic M-symmetric Riemann surfaces. Proyecciones **20**(3), 351–365 (2001)

[Hid05]   Hidalgo, R.A., Figueroa, J.: Numerical Schottky uniformizations, Geometriae Dedicata. **111**, 125–157 (2005)

[Kul97]   Kulkarni, R.S.: Riemann surfaces admitting large automorphism groups. In: Quine, J.R., Sarnak, P. (eds.) Extremal Riemann surfaces. Contemporary Mathematics, vol. 201. AMS, Providence (1997)

[Myr20]   Myrberg, P.J.: Uber die numerische Ausfuhrung der Uniformisierung. Acta Soc. Sci. Fenn. **XLVIII**(7), 1–53 (1920)

[SS95]   Semmler, K-D., Seppälä, M.: Numerical uniformization of hyperelliptic curves. Proc. ISSAC 95 (1995)

[Sep04]   Seppälä, M.: Myrberg's numerical uniformization of hyperelliptic curves, Ann. Acad. Sci. Fenn. **29**, 3–20 (2004)

6

Numerical Schottky Uniformizations: Myrberg's Opening Process

Rubén A. Hidalgo[1] and Mika Seppälä[2]

[1] Departamento de Matemáticas, Universidad Técnica Federico Santa María, Valparaíso, Chile
   `ruben.hidalgo@usm.cl`
[2] Department of Mathematics, Florida State University, USA
   and Department of Mathematics and Statistics, University of Helsinki, Finland
   `mika.seppala@fsu.edu`

6.1 Introduction

It is well known that a closed Riemann surface may be described by different kind of objects; for instance, by algebraic curves, Fuchsian groups, Schottky groups, Riemann period matrices, etc. In general, if one knows explicitly one of these presentations, it is a very hard problem to provide the others in an explicit way. In the 1920s, Myrberg [Myr16] proposed an algorithm which permits to approximate numerically a Schottky uniformization of a hyperelliptic Riemann surface once an explicit hyperelliptic curve presentation is given. The convergence of such a method was discussed by Semmler and Seppälä [SS95] in 1995 for the case that the hyperelliptic Riemann surface admits a maximal symmetry, that is, an anticonformal involution with the maximal number $(g + 1)$ (where g denotes the genus of the surface) of connected components of fixed points. In [Sep04] the convergence was shown using a normal family argument. This normal family argument applies also to the general case, and will be used, in this paper, to show the convergence of the algorithm in the general case.

The goal of the paper [Sep04] was to approximate a Fuchsian uniformization of a Riemann surface given as an algebraic curve. The method presented there applied to real hyperelliptic curves with real branch points. Yuri Lebedev [Leb08] is presently working on computational problems regarding Riemann surfaces. He has developed an OpenMath library with the particular aim of providing the computational infrastructure making implementations of Myrberg's algorithm possible.

6.1.1 Hyperelliptic Riemann Surfaces

A closed Riemann surface S of genus $g \geq 2$ is called *hyperelliptic* if it admits a conformal involution $j : S \to S$ with exactly $2(g + 1)$ fixed points, called the *hyperelliptic involution*; equivalently, there is a two-fold branched covering $\pi : S \to \widehat{\mathbb{C}}$. Let us consider the projection under π of the set of fixed points of j, say $\mathcal{B} = \{a_1, ..., a_{2g+2}\} \subset \widehat{\mathbb{C}}$. The conformal class of S is uniquely determined by $\mathcal{B}$ and it is defined by the algebraic curve

$$y^2 = (x - a_1) \cdots (x - a_{2(g+1)}) .$$

Any set $\mathcal{A} \subset \widehat{\mathbb{C}}$ of cardinality $2(g + 1)$ is the branch locus for some two-fold branched covering of some hyperelliptic Riemann surface, and $\mathcal{A}$ defines the same conformal class of S if and only if it is the image under a Möbius transformation of $\mathcal{B}$.

As the hyperelliptic involution j is unique [FK92], the group of conformal and anticonformal automorphisms of S induces a finite group of (extended) Möbius transformations that coincides with the group of (extended) Möbius transformations preserving the set $\mathcal{B}$.

6.1.2 Kleinian Groups

A *Kleinian group* is a discrete subgroup of $\mathrm{PSL}(2, \mathbb{C})$, which we identify as the group of conformal automorphisms of the Riemann sphere $\widehat{\mathbb{C}}$. Every Kleinian group G decomposes $\widehat{\mathbb{C}}$ into two disjoint sets; *the limit set $\Lambda = \Lambda(G)$*, and its complement, *the regular set (or region of discontinuity) $\Omega = \Omega(G)$*.

If G is finitely generated and if there is an invariant component $\Delta \subset \Omega(G)$, then we say that the pair (Δ, G) is a *function group*. If, moreover, G acts freely on Δ, then we say that (Δ, G) is a *freely acting function group*.

If (Δ, G) is a function group, then $S = \Delta/G$ is an *analytically finite Riemann orbifold* [Ahl64, Ber67], that is a closed Riemann orbifold with a finite number of so called conical points. The complement of these conical points is an ordinary Riemann surface.

In the case that (Δ, G) is a freely acting function group, S has no conical points, that is, it is an analytically finite Riemann surface. If $P : \Delta \to S$ is a regular branched covering induced by the action of G, then we say that the triple $(\Delta, G, P : \Delta \to S)$ is an *uniformization* of S.

The existence of uniformizations is a consequence of uniformization theorem. Classical examples of uniformizations are provided by Fuchsian groups of the first kind G acting on the hyperbolic plane $\mathbb{H}^2$; called *Fuchsian uniformizations*. Other examples are the *Schottky uniformizations* whose definition is recalled below.

6.1.3 Schottky Groups

A *Schottky group of rank g* is a Kleinian group G generated by loxodromic transformations, say $A_1, \ldots, A_g$, so that there are $2g$ disjoint simple loops, $C_1, C_1', \ldots, C_g, C_g'$, bounding a common domain D in the extended complex plane $\widehat{\mathbb{C}}$, where $A_i(C_i) = C_i'$, and $A_i(D) \cap D = \emptyset$, $i = 1, \ldots, p$. The transformations $A_1, ..., A_g$ are called a *set of Schottky generators* of G and the collection of loops $C_1, C_1', ..., C_g, C_g'$ is called a *fundamental set of loops* of G. In [Chu68] V. Chuckrow has shown that every set of free generators of a Schottky group is in fact a set of Schottky generators.

If G is a Schottky group of rank g, then $\Lambda(G)$ is empty for $g = 0$, two points for $g = 1$ and a Cantor set for $g \geq 2$. The quotient $\Omega(G)/G$ turns out to be a closed Riemann surface of genus g. The triple $(G, \Omega(G), P : \Omega(G) \to S)$ is called a *Schottky uniformization of S*. The Retrosection Theorem [Ber75, Kle83, Koe10] asserts that every closed Riemann surface of genus g may be uniformized by a Schottky group of rank g.

6.1.4 Classical Schottky Groups

By a *circle* in the Riemann sphere $\widehat{\mathbb{C}}$ we mean either an Euclidean circle in the complex plane or the union of the point at infinity with an Euclidean line. If we may choose a fundamental set of loops for a Schottky group G consisting of circles of $\widehat{\mathbb{C}}$, then we say that G is a *classical Schottky group* and that $(G, \Omega(G), P : \Omega(G) \to S)$ is a *classical Schottky uniformization of S*.

The existence of non-classical Schottky groups is due to Marden [Mar74] and an explicit example is due to Yamamoto [Yam91]. In [HM06] there is a theoretical construction of non-classical Schottky groups in every genera.

Conjecture 1. Every closed Riemann surface may be uniformized by a classical Schottky group.

Conjecture 1 has been proved for (a) Riemann surfaces admitting an anticonformal involution with fixed points, see for instance [Bob87, Koe10, Mas97, Sep04], and (b) Riemann surfaces with a collection of g homologically independent simple closed geodesics sufficiently short, as a consequence of the Round Modulus Theorem due to C. McMullen in [McM94].

6.1.5 Whittaker Groups

A *Whittaker group of rank g* is a Kleinian group $\widehat{G}$ generated by $(g+1)$ elliptic elements of order 2, say $E_1, ..., E_{g+1}$, so that there is a collection of pairwise disjoint simple closed curves, say $C_1, ..., C_{g+1}$, so that all of them bound a common domain $\mathcal{D}$ of connectivity $(g + 1)$ and so that E_j permutes the two topological discs bounded by C_j. The set of generators $E_1, ..., E_{g+1}$ is called a *set of Whittaker generators* and the collection of loops $C_1, ..., C_{g+1}$ is called

a *fundamental set of loops*. Both fixed points of E_j belong to C_j and $\mathcal{D}$ is a fundamental domain for $\widehat{G}$. As consequence of the Klein–Maskit's combination theorems, every elliptic element of $\widehat{G}$ is conjugate to some E_j in $\widehat{G}$. This, in particular, permits to see that every set of free generators, by elements of order 2, of a Whittaker group is a Whittaker set of generators. The quotient $R = \Omega(\widehat{G})/\widehat{G}$ is the Riemann sphere with exactly $2(g + 1)$ conical points of order 2. Let us denote by $Q : \Omega(\widehat{G}) \to R$ the natural regular branched covering map with $\widehat{G}$ as covering group. The triple $(\Omega(\widehat{G}), \widehat{G}, Q : \Omega(\widehat{G}) \to R)$ is called a *Whittaker uniformization of R*. Let us denote by $p_j, q_j \in C_j$ both fixed points of E_j. Then, on R we have a collection of pairwise disjoint simple arcs $\gamma_j = Q(C_j)$ connecting the two points $Q(p_j)$ and $Q(q_j)$, for $j = 1, .., g+1$. We say that the collection of arcs $\gamma_1, ..., \gamma_{g+1}$ is a *set of Whittaker fundamental arcs for $\widehat{G}$*.

Lemma 1. *If we start with a Riemann orbifold R given by the Riemann sphere with exactly $2(g + 1)$ conical points of order 2, say a_1, $b_1, ..., a_{g+1}$ and b_{g+1}, and a set of pairwise disjoint simple arcs, say $\gamma_1, ..., \gamma_{g+1}$, so that γ_j connects a_j with b_j, then there is a Whittaker uniformization $(\Omega(\widehat{G}), \widehat{G}, Q : \Omega(\widehat{G}) \to R)$ so that the loops $\gamma_1, ..., \gamma_{g+1}$ form a set of Whittaker fundamental arcs for $\widehat{G}$.*

Proof. This is consequence of quasiconformal deformation theory [Ber75] (this was also observed by L. Keen in [Kee80]). □

Lemma 2. *Let us consider two Whittaker uniformizations, say $(\Omega(\widehat{G}_1), \widehat{G}_1, Q_1 : \Omega(\widehat{G}_1) \to R)$ and $(\Omega(\widehat{G}_2), \widehat{G}_2, Q_2 : \Omega(\widehat{G}_2) \to R)$, both of them defining the same set of Whittaker fundamental arcs on R. Then, there is a Möbius transformation A so that $\widehat{G}_2 = A\widehat{G}_1 A^{-1}$ and $Q_2 = Q_1 A^{-1}$.*

Proof. The hypothesis asserts that there is a fundamental set of loops $C_1^j, ..., C_{g+1}^j$, with respect to a fundamental set of generators $E_1^j, ..., E_{g+1}^j$ for $\widehat{G}_j$, for $j = 1, 2$, so that $Q_1(C_k^1) = Q_2(C_k^2)$, for $k = 1, ..., g + 1$. We may construct a homeomorphism $A : \Omega(\widehat{G}_1) \to \Omega(\widehat{G}_2)$ satisfying $AE_k^1 = E_k^2 A$, for $k = 1, ..., g+1$, and $Q_2 = Q_1 A^{-1}$. As Q_j is locally conformal homeomorphism (except at the fixed points of the elliptic transformations), we also have that A is a conformal homeomorphism. As the region of discontinuity of a Schottky group is of type O_{AD} (that is, it admits no holomorphic function with finite Dirichlet norm (see [AS60, p. 241])), then the region of discontinuity of $\widehat{G}_1$ is also of type O_{AD} (as it is the region of discontinuity of the associated hyperelliptic Schottky group). It follows from this (see [AS60, p. 200]) that every conformal map from $\Omega(\widehat{G}_1)$ into the extended complex plane is fractionally linear, in particular, A is a Möbius transformation. □

6.1.6 Classical Whittaker Groups

If we may choose a set of fundamental loops consisting of circles for a Whittaker group $\widehat{G}$, then we say that $\widehat{G}$ is a *classical Whittaker group* and that $(\widehat{G}, \Omega(\widehat{G}), P : \Omega(\widehat{G}) \to S)$ is a *classical Whittaker uniformization of S*.

Conjecture 2. Every Riemann orbifold given by the Riemann sphere and an even number of conical points of order two may be uniformized by a classical Whittaker group.

6.1.7 Hyperelliptic Schottky Groups

If $\widehat{G} = \langle E_1, ..., E_{g+1} \rangle$ is a Whittaker group of rank g, then the elements $A_1 = E_{g+1}E_1, A_2 = E_{g+1}E_2, ..., A_g = E_{g+1}E_g$ are Schottky generators of a Schottky group G of rank g; the unique index two torsion free subgroup of $\widehat{G}$. We say that G is a *hyperelliptic Schottky group*. If $C_1, ..., C_{g+1}$ is a fundamental set of loops for $\widehat{G}$ associated to the Whittaker set of generators $E_1, ..., E_{g+1}$, then the collection $C_1, C_1' = E_{g+1}(C_1), ..., C_g, C_g' = E_{g+1}(C_g)$, defines a standard fundamental set of loops of G with respect to the generators $A_1, ..., A_g$. As G has index two in $\widehat{G}$, they have the same region of discontinuity, say Ω. If $g \geq 2$ and we set $\Omega/G = S$ and $\Omega/\widehat{G} = R$, then S is a hyperelliptic Riemann surface; each involution E_j induces the hyperelliptic involution j and $R = S/\langle j \rangle$. If we denote by $P : \Omega \to \widehat{\mathbb{C}}$ a branched covering with $\widehat{G}$ as cover group and denote by $Q : \Omega \to S$ a covering with G as cover group, then we have a two-fold branched covering $\pi : S \to \widehat{\mathbb{C}}$ so that $\pi Q = P$. In this way, the projection of the $2(g+1)$ fixed points of the $E_0, ..., E_g$, is exactly the branch locus of π.

It was noted by L. Keen in [Kee80] that every Schottky group of rank 2 is a hyperelliptic one. In fact, if G is a Schottky group of rank 2, say freely generated by A and B, then $E_3 = AB - BA$, $E_1 = E_3A$ and $E_2 = E_3B$ are elliptic elements of order two. Moreover, the elements E_1, E_2, E_3 are a Whittaker set of generators of a Whittaker group $\widehat{G}$ whose index two torsion free subgroup is G. Moreover, L. Keen observed the following.

Theorem 1. *[Kee80] Every hyperelliptic Riemann surface may be uniformized by a hyperelliptic Schottky group.*

Remark 1. If Conjecture 2 holds, then Conjecture 1 also holds at the level of hyperelliptic Riemann surfaces using hyperelliptic Schottky groups.

6.1.8 Numerical Uniformization Problem

Let us consider a non-singular plane algebraic curve C defined by an affine polynomial equation $P(x, y) = 0$. Then, by compactifying it and by a process of desingularization, there is a closed Riemann surface S_C defined by C.

The *numerical uniformization* problem of C is to find an uniformization $(\Delta, G, P : \Delta \to S_C)$ in an explicit way.

Explicit constructions for uniformizations have been difficult to find in spite of huge efforts to solve this problem. Burnside [Bur93] provided the first explicit uniformization in a special case. Buser and Silhol [BS01] (see also [GSST98, Sil01]) have developed methods that allow one to find a Fuchsian group uniformizing a given real hyperelliptic curve. They are able to compute equations for certain surfaces having given geometric properties. Buser has further studied differetial geometric methods to calculate lengths of closed geodesics curves on a given hyperelliptic curve. Also, given a classical Schottky group, methods due to Burnside [Bur92] permit to compute algebraic curves and Riemann period matrices for the corresponding Riemann surface. These methods have been applied in [BBE+94, Bob87, HF05]

The second author [Sep04] has used Myrberg's algortithm to find Schottky groups that uniformize a given (real) hyperelliptic Riemann surface. In this paper we recall Myrberg's process in the general situation in order to approximate numerically Schottky uniformizations of hyperelliptic Riemann surfaces and prove the convergence of it.

6.2 Some Basic Facts

Lemma 3. *Let us consider any two branched regular coverings $\pi_1, \pi_2 : \widehat{\mathbb{C}} \to \widehat{\mathbb{C}}$, both with covering group $G = \langle E \rangle$, where E is a Möbius transformation of order two. Then, there is a Möbius transformation A so that $\pi_2 = A\pi_1$.*

Proof. Let p, q be the fixed points of E. Set $a = \pi_1(p)$, $b = \pi_1(q)$, $c = \pi_2(p)$ and $d = \pi_2(q)$. We may define $A(a) = c$ and $A(b) = d$. If $z \notin \{a, b\}$, then $\pi_1^{-1}(z) = \{u, v\}$ so that $v = E(u)$. In this way, we may define $A(z) = \pi_2(u)$. It is clear that A is well defined homeomorphism of the Riemann sphere so that $A\pi_1 = \pi_2$. Since π_j are locally conformal homeomorphisms in the complement of $\{p, q\}$, A is a Möbius transformation.   □

6.2.1 Opening Arcs

By a *simple arc* we mean the image of a homeomorphic embedding $\alpha : [0, 1] \to \widehat{\mathbb{C}}$.

Let L be a simple arc, say parametrized by the homeomorphic embedding $\alpha : [0, 1] \to \widehat{\mathbb{C}}$, that is, $L = \alpha([0, 1])$. Set $p = \alpha(0)$ and $q = \alpha(1)$. Let us fix three different points $a, b, c \in \widehat{\mathbb{C}} - L$.

As a consequence of Lemma 1 there is a Whittaker uniformization $(\widehat{G} = \langle E_L \rangle, \widehat{\mathbb{C}}, Q_L : \widehat{\mathbb{C}} \to R)$, where R is the orbifold provided by the Riemann sphere and whose conical points are p and q (both of order two) and there is a simple loop Γ_L, containing both fixed points of the conformal involution

E_L, bounding two discs which are permuted by E_L, say D_L and D_L^*, and $L = Q_L(\Gamma_L)$. By composing Q_L at the right by a suitable Möbius transformation, we may also assume $\{a, b, c\} \subset D_L$ and $Q_L(x) = x$ for $x \in \{a, b, c\}$. The above Whittaker uniformization is uniquely determined by this normalization for Q_L.

The conformal homeomorphism $\Phi_L = Q_L^{-1} : \widehat{\mathbb{C}} - L \to D_L$ satisfies the following properties:

(1) $\Phi_L(a) = a, \Phi_L(b) = b$ and $\Phi_L(c) = c$
(2) $\Phi_L^{-1} : D_L \to \widehat{\mathbb{C}} - L$ extends continuously to a map
      $Q_L : \overline{D_L} = D_L \cup \Gamma_L \to \widehat{\mathbb{C}}$ with $Q_L(x) = Q_L(y)$ if and only if $y = E_L(x)$
      for every pair of points $x, y \in \Gamma_L$, and $\Phi_L^{-1}(\Gamma_L) = L$.

Lemma 4. *The map Φ_L is uniquely determined by the normalization (1).*

Proof. Assume we have another conformal homeomorphism $\Psi : \widehat{\mathbb{C}} - L \to D$, where D is a Jordan disc on the Riemann sphere (say bounded by the simple loop Υ) with $\{a, b, c\} \subset D$, so that $\Psi(x) = x$ for $x \in \{a, b, c\}$, and that there is an elliptic Möbius transformation F of order two that permutes both discs bounded by Υ, such that $\Psi^{-1}(x) = \Psi^{-1}(y)$ if and only if $y = F(x)$ for every pair of points $x, y \in \Upsilon$. The map $\eta = \Phi_L \Psi^{-1} : D \to D_L$ is a conformal homeomorphism that fixes three different points and which can be extended to a homeomorphism of the Riemann sphere satisfying the condition $E_L \eta F = \eta$. Clearly, η is the restriction of a Möbius transformation that fixes three different points, so it is the identity. $\square$

As a consequence, D_L and E_L are also uniquely determined by the arc L and the normalization (1). We call Φ_L the *opening map of L normalized at the points a, b and c* or just *opening map of L* if the choice of the points a, b and c is clear.

6.2.2 Explicit Form of the Opening Map Φ_L

Let us consider a Möbius transformation T so that $T(p) = 0$ and $T(q) = \infty$ (for instance $T(z) = (z - p)/(z - q)$). We have that $T(L)$ is a simple arc connecting 0 with ∞.

Let us consider $\pi : \widehat{\mathbb{C}} \to \widehat{\mathbb{C}}$ defined by $\pi(z) = z^2$. By lifting the simple arc $T(L)$ under π, we obtain a simple loop $\widehat{L}$, through 0 and ∞, which is invariant under the Möbius transformation $E(z) = -z$. Choose one of the two discs bounded by $\widehat{L}$, say D, and consider the branch of $\sqrt{z} : \widehat{\mathbb{C}} \to D$. Using this branch, we compute $\sqrt{T(a)}, \sqrt{T(b)}, \sqrt{T(c)} \in D$. Let L be the Möbius transformation satisfying $L(\sqrt{T(a)}) = a$, $L(\sqrt{T(b)}) = b$ and $L(\sqrt{T(c)}) = c$. Since, by Lemma 4, Φ_L is unique under the normalization of fixing a, b and c, we have the following.

Lemma 5.

$$\Phi_L(z) = \frac{AF(z) + B}{CF(z) + D} \ ,$$

where

$$A = ab\left(F(a) - F(b)\right) + bc\left(F(b) - F(c)\right) + ac\left(F(c) - F(a)\right) \ ,$$

$$B = abF(c)\left(F(b) - F(a)\right) + bcF(a)\left(F(c) - F(b)\right) + acF(b)\left(F(a) - F(c)\right) \ ,$$

$$C = a\left(F(c) - F(b)\right) + b\left(F(a) - F(c)\right) + c\left(F(b) - F(a)\right) \ ,$$

$$D = aF(a)\left(F(b) - F(c)\right) + bF(b)\left(F(c) - F(a)\right) + cF(c)\left(F(a) - F(b)\right)$$

$$F(z) = \sqrt{\frac{z - p}{z - q}} \ .$$

6.3 Myrberg's Opening Process

In this section we explain Myrberg's algorithm [Myr20] and provide a proof of its convergence (see Theorem 2).

6.3.1 Starting Point

Let us consider a collection of $\gamma = g + 1$ (where $g \geq 2$) pairwise disjoint simple arcs, say $L_1, ..., L_\gamma$. Set $S = \widehat{\mathbb{C}} - (L_1 \cup \cdots \cup L_\gamma)$ and choose three different points on S, say $a, b, c \in S$.

Let R be the Riemann orbifold given by the Riemann sphere with conical points at the 2γ end points of the above simple arcs L_j, each one with order 2.

As a consequence of Lemmas 1 and 2, there is a unique Whittaker uniformization

$$(\widehat{G}, \Omega, Q : \Omega \to R) \ ,$$

for which $L_1, ..., L_\gamma$ is a Whittaker fundamental set of arcs, and Q is normalized by the rule $Q(a) = a, Q(b) = b$ and $Q(c) = c$.

In this way, there is a collection of pairwise disjoint simple loops, say $C_1, ..., C_\gamma \subset \Omega$, all of them bounding a common domain $\mathcal{D} \subset \Omega$ of connectivity 2γ (a fundamental domain for $\widehat{G}$), and there are elliptic Möbius transformation of order two, say $E_1, ..., E_\gamma$, so that $E_j(C_j) = C_j$, $E_j(\mathcal{D}) \cap \mathcal{D} = \emptyset$, $Q(C_j) = L_j$, for all $j = 1, .., \gamma$, and $\widehat{G} = \langle E_1, ..., E_\gamma \rangle$.

Let us consider the inverse $\Psi = Q^{-1} : S \to \mathcal{D}$, which is a conformal homeomorphism. Below, we construct a sequence of conformal homeomorphisms $\psi_n : S \to \mathcal{D}_n \subset \widehat{\mathbb{C}}$, where each ψ_n is the composition of certain opening maps, whose limit is Ψ.

6.3.2 Special Chain of Subgroups

We call $E_1, ..., E_\gamma$ the *first generation elements* of $\widehat{G}$. For each $k \in \{1, 2, ...\}$ and $i_1, ..., i_k, i_{k+1} \in \{1, 2, ..., \gamma\}$ so that $i_1 \neq i_2 \neq \cdots \neq i_{k-1} \neq i_k \neq i_{k+1}$, we call any of the elements of the form $E_{i_1} E_{i_2} \cdots E_{i_{k-1}} E_{i_k} E_{i_{k+1}} E_{i_k} E_{i_{k-1}} \cdots E_{i_2} E_{i_1}$ an $(k+1)$-*generation element* of $\widehat{G}$.

A sequence of subgroups $\widehat{G}_n < \widehat{G}$ is called *admissible* if the following holds

(1) $\widehat{G}_0 = \widehat{G}$
(2) $\widehat{G}_{j+1} \lhd \widehat{G}_j$ of index two
(3) $\widehat{G}_{j+1}$ is obtained by elimination of an element of $\widehat{G}_j$ of lowest generation

Example 1. Let $\gamma = 3$ and $\widehat{G} = \langle E_1, E_2, E_3 \rangle$. The first four terms for an admissible sequence are the following ones.

$$\widehat{G}_0 = \langle E_1, E_2, E_3 \rangle \,,$$

$$\widehat{G}_1 = \langle E_2, E_3, E_1 E_2 E_1, E_1 E_3 E_1 \rangle \,,$$

$$\widehat{G}_2 = \langle E_3, E_1 E_2 E_1, E_1 E_3 E_1, E_2 E_3 E_2, E_2 E_1 E_2 E_1 E_2, E_2 E_1 E_3 E_1 E_2 \rangle \,,$$

$$\widehat{G}_3 = \langle E_1 E_2 E_1, E_1 E_3 E_1, E_2 E_3 E_2, E_2 E_1 E_2 E_1 E_2, E_2 E_1 E_3 E_1 E_2, E_3 E_1 E_2 E_1 E_3,$$

$$E_3 E_1 E_3 E_1 E_3, E_3 E_2 E_3 E_2 E_3, E_3 E_2 E_1 E_2 E_1 E_2 E_3, E_3 E_2 E_1 E_3 E_1 E_2 E_3 \rangle \,.$$

Let us consider an admissible sequence of subgroups $\widehat{G}_n < \widehat{G}$. By construction, $\widehat{G}_n$ has index 2^n in $\widehat{G}$, in particular, each $\widehat{G}_n$ has the same region of discontinuity Ω. It follows the existence of a regular branched covering map

$$\eta_n : \Omega \to R_n \,,$$

where R_n is the Riemann sphere with a finite collection of conical points of order two, whose covering group is $\widehat{G}_n$ with $\eta_n(a) = a$, $\eta_n(b) = b$, $\eta_n(c) = c$ and a (not necessarily regular) covering $Q_n : \widehat{\mathbb{C}} \to R$ so that $Q = Q_n \eta_n$ (see Fig. 6.1). In particular, $Q_n(a) = a$, $Q_n(b) = b$ and $Q_n(c) = c$.

Set $\mathcal{D}_n = \eta_n(\mathcal{D})$. It follows from the construction that $Q_n : \mathcal{D}_n \to S$ is a conformal homeomorphism. We denote by $\psi_n : S \to \mathcal{D}_n$ the inverse.

The following is a simple consequence of the above construction and the fact that $\bigcap_{j=1}^\infty \widehat{G}_n = \{I\}$, where (G_n) is any admissible sequence in the Whittaker group $\widehat{G}$.

6.3.3 Convergence

Theorem 2. *The sequence η_n converges locally uniformly to the identity map and the sequence ψ_n converges locally uniformly to $\Psi : S \to \mathcal{D}$.*

Proof. Normality of the family. Let us consider the collection of points $R \subset \Omega$ obtained by the union of the G-orbits of the points a, b and c. Set $\Omega_R = \Omega - R$ and let us consider the collection of holomorphic maps η_j restricted to Ω_R. The images of Ω_R under each η_j misses the three points a, b and c. By Montel's theorem $\eta_j : \Omega_R \to \mathbb{C}$ is a normal family. Unfortunately, this is not enough to ensure $\eta_j : \Omega \to \mathbb{C}$ to be a normal family.

Let us consider any fundamental domain D for G so that in its interior D^0 are contained points $a_D \in D^0$ in the G-orbit of a, $b_D \in D^0$ in the G-orbit of b and $c_D \in D^0$ in the G-orbit of c. Consider the family of restrictions $\eta_j : D^0 \to \widehat{\mathbb{C}}$. Clearly, $\eta_j(a_D) = 0$, $\eta_j(b_D) = 1$ and $\eta_j(c_D) = \infty$. It follows from Theorem 2.1 in [Leh86] that $\eta_j : D^0 \to \widehat{\mathbb{C}}$ is a normal family.

If $D_1, ..., D_n$ are fundamental domains for G, so that the interior D_k^0 of D_k always contains a point in the G-orbit of a, b and c, then the previous ensures that $\eta_j : D_k^0 \to \widehat{\mathbb{C}}$ is a normal family. It follows that $\eta_j : \cup_{k=1}^n D_k^0 \to \widehat{\mathbb{C}}$ is a normal family.

As Ω is a countable union of interiors of fundamental domains as above, we may construct a family of open domains $R_1 \subset R_2 \subset \cdots \subset \Omega$ so that $\cup_{k=1}^\infty R_k = \Omega$ and $\eta_j : R_k \to \widehat{\mathbb{C}}$ is a normal family, for each k.

For any subsequence of $\eta_j : \Omega \to \widehat{\mathbb{C}}$, we can find a subsequence of $\eta_j : R_1 \to \widehat{\mathbb{C}}$ that converges locally uniformly. Now, there is such a subsequence whose restriction to R_2 converges locally uniformly. We then consider such a new subsequence and restrict it to R_3 and continue inductively such a process. We use the diagonal method to obtain a subsequence converging locally uniformly on all Ω.

Limit mappings of subsequences. Let us choose any subsequence $\eta_{j_k} : \Omega \to \widehat{\mathbb{C}}$ that converges locally uniformly to the conformal map $\eta_\infty : \Omega \to \widehat{\mathbb{C}}$.

As $\eta_j(a) = a$, $\eta_j(b) = b$ and $\eta_j(c) = c$, it follows that $\eta_\infty(a) = a$, $\eta_\infty(b) = b$ and $\eta_\infty(c) = c$, in particular, η_∞ is a non-constant conformal mapping.

As $G_{j+1} \triangleleft G_j$ and $\cap_{j=0}^\infty G_j = \{I\}$, we may construct fundamental domains D_j for G_j so that $D_j \subset D_{j+1}$ and $\cup_{j=1}^\infty D_j = \Omega$. Let us denote by D_j^0 the interior of D_j.

Clearly, for each $j \geq k$, η_j restricted to D_k^0 is an injective conformal mapping.

The convergent subsequence of injective conformal mappings $\eta_{j_k} : D_k^0 \to \widehat{\mathbb{C}}$ converges uniformly to $\eta_\infty : D_k^0 \to \widehat{\mathbb{C}}$, which is either constant or injective. As we know the last to be non-constant, we obtain that $\eta_\infty : \Omega \to \widehat{\mathbb{C}}$ is a locally injective conformal map, that is, a local homeomorphism onto its image.

Let $\gamma \in G$. As $\cap_{j=0}^\infty G_j = \{I\}$, there is some j_0 so that $\gamma \notin G_j$, for $j \geq j_0$. It follows that η_∞ is globally injective on all Ω.

As Ω is also the region of discontinuity of a Schottky group, which is a domain of class O_{AD} (that is, it admits no holomorphic function with finite Dirichlet norm (see [AS60, p. 241]). It follows from this (see [AS60, p. 200]) that any one-to-one conformal map on Ω is necessarily the restriction of a Möbius transformation. In particular, η_∞ is the restriction of a Möbius transformation. As it fixes three different points, $\eta_\infty = I$ (identity map).

Convergence of all the family. Since any subsequence of (η_j) has a convergent subsequence, the above asserts that the complete sequence converges locally uniformly to the identity map. Now, as $Q = Q_j\eta_j$, it follows that (ψ_j) converges locally uniformly to Ψ.

6.3.4 Slots Generation

Myrberg's opening process permits to see that each ψ_n can be seen as a composition of opening mappings of arcs. We use the points a, b, c to normalize each opening map, that is, each opening map is assumed to fix these three points. As in [Sep04], we call the arcs $L_1, ..., L_\gamma$ the *first generation slots*.

We consider the opening map $\Phi_{L_1} : \widehat{\mathbb{C}} - L_1 \to D_{L_1} = \widehat{\mathbb{C}} - \overline{D^*_{L_1}}$ and the Möbius transformation E_{L_1} of order two. We have that E_{L_1} has both fixed points on the boundary loop $C_{L_1} = \partial\overline{D_{L_1}}$ and permutes D_{L_1} with $D^*_{L_1}$.

The arcs $\Phi_{L_1}(L_2), ..., \Phi_{L_1}(L_\gamma)$ are *first generation slots*, and $E_{L_1}(\Phi_{L_1}(L_2)), ..., E_{L_1}(\Phi_{L_1}(L_\gamma))$ are called *second generation slots*.

We now choose any of the new first generation slots to proceed as done with L_1. For instance, if we choose the arc $L = \Phi_{L_1}(L_2)$, then we consider the opening map ϕ_L defined on the complement of L onto a disc $D_L = \widehat{\mathbb{C}} - \overline{D^*_L}$. We have again a Möbius transformation of order two, say E_L, with both fixed points on the boundary loop $\partial\overline{D_L}$ and permutes D_L with D^*_L. The arcs

$$\Phi_L(\Phi_{L_1}(L_3)), \ldots, \Phi_L(\Phi_{L_1}(L_\gamma))$$

are still *first generation slots.*

The arcs

$$\Phi_L(E_{L_1}(\Phi_{L_1}(L_2))), \ldots, \Phi_L(E_{L_1}(\Phi_{L_1}(L_\gamma)))$$

and

$$E_L(\Phi_L(\Phi_{L_1}(L_3))), \ldots, E_L(\Phi_L(\Phi_{L_1}(L_\gamma)))$$

are *second generation slots*) and

$$E_L(\Phi_L(E_{L_1}(\Phi_{L_1}(L_2)))), \ldots, E_L(\Phi_L(E_{L_1}(\Phi_{L_1}(L_\gamma))))$$

are called *third generation slots*).

We continue the process until all first generations slots have been opened and new higher generation slots have been formed. In this way, when opening slots, one forms iteratively new slots which are divided into generations. Order these slots by generation and within a generation. Continue with opening the slots in the order we have chosen above. Iterating this procedure we get a sequence of conformal mappings $\Phi_1, \Phi_2, \ldots$. These mappings are simply the various opening mappings.

6.3.5 Final Steps

The chosen order for the opening slot process produces in a natural way an admissible sequence $\widehat{G}_n$ so that

$$\psi_n = \Phi_n \Phi_{n-1} \cdots \Phi_2 \Phi_1 : S \to \widehat{\mathbb{C}} \ .$$

The region $\Psi_n(S)$ is a domain bounded by $(g+1)$ pairwise disjoint simple loops, say $C_{1,n}, ..., C_{\gamma,n}$, contained in some region $\Omega_n \subset \widehat{\mathbb{C}}$. We also have conformal homeomorphisms of Ω_n, each one of order two (not necessarily Möbius transformations), say $E_{1,n}^*, ..., E_{\gamma,n}^*$, so that $E_{j,n}^*$ keeps invariant the loop $C_{j,n}$, permutes the two components $\Omega_n - C_{j,n}$ and has exactly two fixed points on $C_{j,n}$. As a consequence of Theorem 2, the homeomorphism $E_{j,n}^*$ converges to the Möbius transformation $E_j \in \widehat{G}$.

Let us consider the unique Möbius transformations of order two $E_{1,n}, ..., E_{\gamma,n}$ so that $E_{j,n}$ has as fixed points the two fixed points of $E_{j,n}^*$. Set

$$G_n = \langle E_{1,n}, ..., E_{\gamma,n} \rangle$$

The above asserts that the sequence of groups (G_n) converges to the Whittaker group $\widehat{G}$.

Remark 2. Above we have described Myrberg's algorithm and also proved its convergence. This algorithm permits to approximate numerically a Schottky uniformization of a hyperelliptic Riemann surfaces

$$y^2 = (x - a_1) \cdots (x - a_{2g+2}) \ ,$$

where $a_1, ..., a_{2g+2} \in \mathbb{C}$ are different points. In the case that each $a_j \in \mathbb{R}$, already considered in [Sep04], the limit Schottky group is a classical one. In the general case, the limit Schottky group may not be a classical one.

6.4 Genus Two Riemann Surfaces

Every closed Riemann surface of genus two S can be described by a plane algebraic curve

$$y^2 = x(x - 1)(x - \lambda_1)(x - \lambda_2)(x - \lambda_3) \tag{6.1}$$

where $\lambda_j \in \mathbb{C} - \{0, 1\}$ and $\lambda_j \neq \lambda_k$ for $j \neq k$.

Starting from an algebraic curve of type (6.1), Myrberg's opening process permits to obtain a numerical algorithm to construct Schottky groups uniformizing "very close" surfaces, that is, algebraic curves of the form

$$y^2 = x(x - 1)(x - \lambda_{1,n})(x - \lambda_{2,n})(x - \lambda_{3,n})$$

with $\lim_{n \to \infty} \lambda_{j,n} = \lambda_j$ (see for instance [Sep04] for the case when all $\lambda_j \in \mathbb{R}$).

Yuri Lebedev [Leb08] and John George are currently working on implementations of this algorithm.
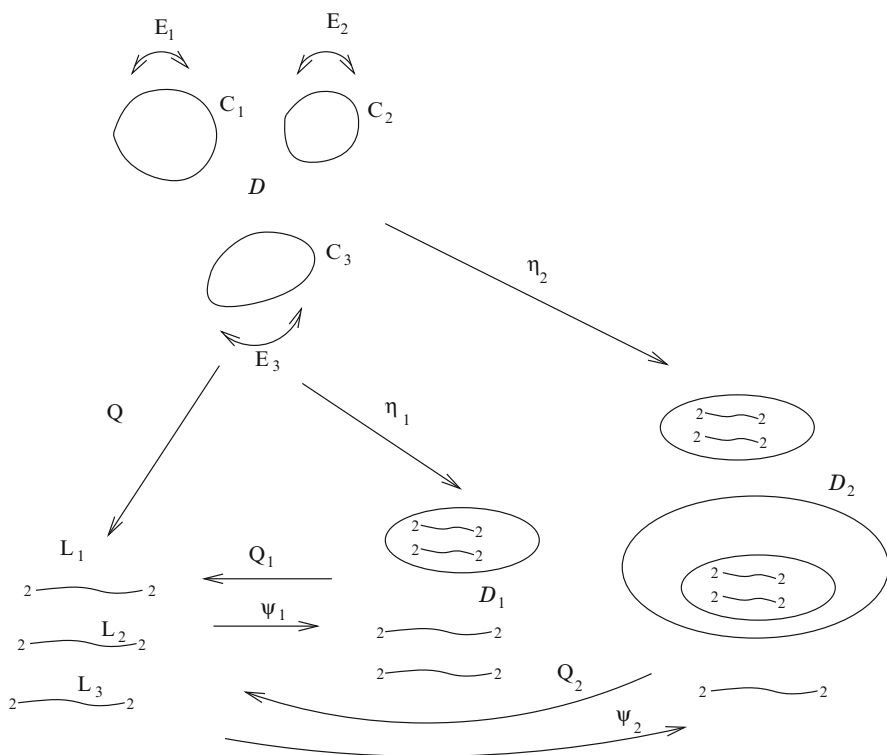
Fig. 6.1. $\widehat{G}_n$ for $n = 0, 1, 2$

Remark 3. Given a Fuchsian uniformization of a genus two Riemann surface, a numerical method to obtain the algebraic curve has been done in [BS01, GSST98, Sil01]. Similarly, in [Bob87, BBE+94, HF05, Sep94] algebraic curves in terms of classical Schottky groups are obtained.

Acknowledgment

References

[AS60]   Ahlfors, L., Sario, L.: Riemann Surfaces. Princeton Mathematical Series **26**. Princeton University Press, Princeton, N.J. (1960)

[Ahl64]   Ahlfors, L.: Finitely generated Kleinian groups. Am. J. Math. **86**, 413–429 (1964)

[BBE+94] Belokolos, E.D., Bobenko, A.I., Enol'ski, V.Z., Its, A.R., Matveev, V.B.: Algebro-geometric approach to nonlinear integrable equations. Springer Series in Nonlinear Dynamics. Springer, Berlin (1994)

[Ber75] Bers, L.: Automorphic forms for Schottky groups. Adv. Math. **16**, 332–361 (1975)

[Ber67] Bers, L.: On the Ahlfors' finiteness theorem. Am. Math. J. **89** (4), 1078–1082 (1967)

[Bob87] Bobenko, A.I.: Schottky uniformization and finite-gap integration, Soviet Math. Dokl. **36**, No. 1, 38–42 (1988) (transl. from Russian: Dokl. Akad. Nauk SSSR, 295, No. 2 (1987))

[Bur93] Burnside, W.: Note on the equation $y^2 = x(x^4 - 1)$. Proc. Lond. Math. Soc. (1) **24**, 17–20 (1893)

[Bur92] Burnside, W.: On a class of Automorphic Functions. Proc. Lond. Math. Soc. **23**, 49–88 (1892)

[BS01] Buser, P., Silhol, R.: Geodesic, Periods and Equations of Real Hyperelliptic Curves. Duke Math. J. **108**, 211–250 (2001)

[Chu68] Chuckrow, V.: On Schottky groups with applications to Kleinian groups. Ann. Math. **88**, 47–61 (1968)

[FK92] Farkas, H., Kra, I.: Riemann Surfaces. Second edition. Graduate Texts in Mathematics **71**. Springer, New York (1992)

[GSST98] Gianni, P., Seppälä, M., Silhol, R., Trager, B.: Riemann surfaces, plane algebraic curves and their period matrices. J. Symbolic Comput. **26**, 789–803 (1998)

[HM06] Hidalgo, R.A., Maskit, B.: On neoclassical Schottky groups. Trans. AMS. **358**, 4765–4792 (2006)

[HF05] Hidalgo, R.A., Figueroa, J.: Numerical Schottky uniformizations. Geometriae Dedicata **111**, 125–157 (2005)

[Kee80] Keen, L.: On Hyperelliptic Schottky groups. Ann. Acad. Sci. Fenn. Ser. A.I. Math. **5** (1), 165–174 (1980)

[Kle83] Klein, F.: Neue Beiträge zur Riemann'schen Funktionentheorie. Math. Ann. **21**, 141–218 (1883)

[Koe10] Koebe, P.: Über die Uniformisierung der Algebraischen Kurven II. Math. Ann. **69**, 1–81 (1910)

[Leb08] Lebedev, Y.: OpenMath Library for Computing on Riemann Surfaces. Ph. D. Thesis, Florida State University (2008). http://etd.lib.fsu.edu/theses/available/etd-11102008-184256/unrestricted/LebedevYDissertation.pdf

[Leh86] Lehto, O.: Univalent Functions and Teichmüller Spaces. GTM, vol. **109**, Springer, New York (1986)

[Mar74] Marden, A.: Schottky groups and circles. In: Contributions to Analysis, pp. 273–278. Academic, New York and London (1974)

[Mas97] Maskit, B.: Remarks on m-symmetric Riemann surfaces. Contemp. Math. **211**, 433–445 (1997)

[McM94] McMullen, C.: Complex Dynamics and Renormalization. Annals of Mathematical Studies, vol. 135. Princeton University Press, Princeton (1984)

[Myr20] Myrberg, J.P.: Über die Numerische Ausführung der Uniformisierung. Acta Soc. Scie. Fenn. **XLVIII**(7), 1–53 (1920)

[SS95] Semmler, K.-D. and Seppälä, M.: Numerical uniformization of hyperelliptic curves. In: Proceedings of ISSAC 1995 (1995)

[Sep04]   Seppälä, M.: Myrberg's numerical uniformization of hyperelliptic curves.
          Ann. Acad. Scie. Fenn. Math. **29**, 3–20 (2004)
[Sep94]   Seppälä, M.: Computation of period matrices of real algebraic curves.
          Discrete Comput. Geom. **11**, 65–81 (1994)
[Sil01]   Silhol, R.: Hyperbolic lego and algebraic curves in genus 2 and 3. Con-
          temporary Math. **311**. Complex Manifolds and Hyperbolic Geometry,
          313–334 (2001)
[Yam91]   Yamamoto, H..: An example of a non-classical Schottky group. Duke
          Math. J. **63**, 193–197 (1991)

Part IV Discrete Surfaces

7

Period Matrices of Polyhedral Surfaces

Alexander I. Bobenko[1], Christian Mercat[2], and Markus Schmies[1]

[1] Institut für Mathematik, Technische Universität Berlin, Strasse des 17. Juni 136, 10623 Berlin, Germany, `bobenko, schmies@math.tu-berlin.de`
[2] I3M c.c. 51, Université Montpellier 2, F-34095 Montpellier cedex 5, France, `mercat@math.univ-montp2.fr`

7.1 Introduction

Finding a conformal parameterization for a surface and computing its period matrix is a classical problem which is useful in a lot of contexts, from statistical mechanics to computer graphics.

The 2D-Ising model [Mer01,CSM02,CSM03] for example can be realized on a cellular decomposition of a surface whose edges are decorated by interaction constants, understood as a discrete conformal structure. In certain configurations, called critical temperature, the model exhibits conformal invariance properties in the thermodynamical limit and certain statistical expectations become discrete holomorphic at the finite level. The computation of the period matrix of higher genus surfaces built from the rectangular and triangular lattices from discrete Riemann theory has been addressed in the cited papers by Costa-Santos and McCoy.

Global conformal parameterization of a surface is important in computer graphics [JWYG04,DMA02,BCGB08,TACSD06,KSS06,War06,SSP08] in issues such as texture mapping of a flat picture onto a curved surface in $\mathbb{R}^3$. When the texture is recognized by the user as a natural texture known as featuring round grains, these features should be preserved when mapped onto the surface, mainly because any shear of circles into ellipses is going to be wrongly interpreted as suggesting depth increase. Characterizing a surface by a few numbers is as well a desired feature in computer graphics, for problems like pattern recognition. Computing numerically the period matrix of a surface has been addressed in [JWYG04].

This chapter uses the general framework of the theory of discrete Riemann surfaces [Fer44,Duf68,Mer01,BMS05] and the computation of period matrices within this framework (based on theorems and not only numerical analogies). Other approaches have emerged recently [GN07,DN03,Kis08]. We focus here on the computation of period matrices within this framework (based on theorems and not only numerical analogies).

We start with some surfaces with known period matrices and compute numerically their discrete period matrices, at different levels of refinement. In particular, some genus two surfaces made up of squares and the Wente torus are considered. We observe numerically good convergence properties. Moreover, we compute the yet unknown period matrix of the Lawson surface, identify it numerically as one of the tested surfaces, which allows us to conjecture their conformal equivalence, and finally to prove it.

7.2 Discrete Conformal Structure

Consider a polyhedral surface in $\mathbb{R}^3$. It has a unique Delaunay tessellation, generically a triangulation [BS07]. That is to say each face is associated with a circumcircle drawn on the surface and this disk contains no other vertices than the ones on its boundary. Let's call Γ the graph of this cellular decomposition, Γ_0 its vertices, Γ_1 its edges and complete it into a cellular decomposition with Γ_2 the set of triangles. Each edge $(x, x') = e \in \Gamma_1$ is adjacent to a pair of triangles, associated with two circumcenters y, y'. The ratio of the (intrinsic) distances between the circumcenters and the length of the (orthogonal) edge e is called $\rho(e)$. It is the celebrated cotan formula [PP93].

$$\rho = \frac{|y' - y|}{|x' - x|}$$
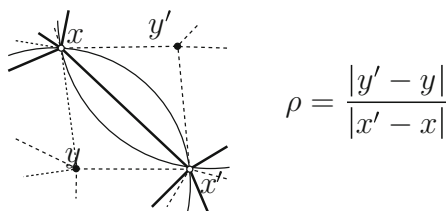
Fig. 7.1. The ratio of the intrinsic lengths of the diagonals is the cotan weight

Following [Mer01], we call these data of a graph Γ, whose edges are equipped with a positive real number, a *discrete conformal structure.* A discrete Riemann surface is a conformal equivalence class of surfaces with the same discrete conformal structure. It leads to a theory of discrete Riemann surfaces and discrete analytic functions, developed in [Fer44, Duf68, Mer01, Mer04, Mer07, BMS05, DKT08], that shares a lot of features with the continuous theory, and these features are recovered in a proper refinement limit. We are going to summarize these results (Fig. 7.1).

In our examples, the extrinsic triangulations are Delaunay. That is to say the triangulations come from the embedding in $\mathbb{R}^3$ and the edges $(x, x') \in \Gamma_1$ of the triangulation are the edges of the polyhedral surface in $\mathbb{R}^3$. On the other hand, the geodesic connecting the circumcenters y and y' on the surface is not an interval of a straight line and its length is generically greater than the distance $||y - y'||$ in $\mathbb{R}^3$. The latter gives a more naive definition of ρ and is

easier to compute. We will call it *extrinsic*, because in contrast to the *intrinsic* ρ, it depends on the embedding of the surface in $\mathbb{R}^3$ and is not preserved by isometries. For surfaces which are refined and flat enough, the difference between extrinsic and intrinsic distances is not large. We compare numerically the two ways to compute ρ. The conclusion is that, in the examples we tested, the intrinsic distance is marginally better, see Sect. 7.4.2.

The circumcenters and their adjacencies define a 3-valent abstract (locally planar) graph, dual to the graph of the surface, that we call Γ^*, with vertices $\Gamma_0^* = \Gamma_2$, edges $\Gamma_1^* \simeq \Gamma_1$. We equip the edge $(y, y') = e^* \in \Gamma_1^*$, dual to the primal edge $e \in \Gamma_1$, with the positive real constant $\rho(e^*) = 1/\rho(e)$. We define $\Lambda := \Gamma \oplus \Gamma^*$ the *double* graph, with vertices $\Lambda_0 = \Gamma_0 \sqcup \Gamma_0^*$ and edges $\Lambda_1 = \Gamma_1 \sqcup \Gamma_1^*$. Each pair of dual edges $e, e^* \in \Lambda_1$, $e = (x, x') \in \Gamma_1$, $e^* = (y, y') \in \Gamma_1^*$, is seen as the diagonals of a quadrilateral (x, y, x', y'), composing a quad-graph $\Diamond$, with vertices $\Diamond_0 = \Lambda_0$, edges $\Diamond_1$ composed of couples (x, y) and faces $\Diamond_2$ composed of quadrilaterals (x, y, x', y').

The Hodge star, which in the continuous theory is defined by $*(f \, dx + g \, dy) = -g \, dx + f \, dy$, is in the discrete case the duality transformation multiplied by the conformal structure:

$$\int_{e^*} * \alpha := \rho(e) \int_e \alpha \tag{7.1}$$

A 1-form $\alpha \in C^1(\Lambda)$ is *of type* $(1,0)$ if and only if, for each quadrilateral $(x, y, x', y') \in \Diamond_2$, $\int_{(y,y')} \alpha = i \, \rho(x, x') \int_{(x,x')} \alpha$, that is to say if $*\alpha = -i \, \alpha$. Similarly forms of type $(0,1)$ are defined by $*\alpha = +i \, \alpha$. A form is *holomorphic*, respectively *anti-holomorphic*, if it is closed and of type $(1,0)$, respectively of type $(0,1)$. A function $f : \Lambda_0 \to \mathbb{C}$ is holomorphic iff $d_\Lambda f$ is.

We define a wedge product for 1-forms living either on edges $\Diamond_1$ or on their diagonals Λ_1, as a 2-form living on faces $\Diamond_2$. The formula for the latter is:

$$\iint_{(x,y,x',y')} \alpha \wedge \beta := \frac{1}{2} \left(\int_{(x,x')} \alpha \int_{(y,y')} \beta - \int_{(y,y')} \alpha \int_{(x,x')} \beta \right) \tag{7.2}$$

The exterior derivative d is a derivation for the wedge product, for functions f, g and a 1-form α:

$$d(fg) = f \, dg + g \, df \,, \qquad\qquad d(f\alpha) = df \wedge \alpha + f \, d\alpha \,.$$

Together with the Hodge star, they give rise, in the compact case, to the usual scalar product on 1-forms:

$$(\alpha, \beta) := \iint_{\Diamond_2} \alpha \wedge *\bar{\beta} = (*\alpha, *\beta) = \overline{(\beta, \alpha)} = \frac{1}{2} \sum_{e \in \Lambda_1} \rho(e) \int_e \alpha \int_e \bar{\beta} \tag{7.3}$$

The adjoint $d^* = -*d*$ of the coboundary d allows to define the discrete Laplacian $\Delta = d^* d + d d^*$, whose kernel are the harmonic forms and functions. It reads, for a function at a vertex $x \in \Lambda_0$ with neighbours $x' \sim x$:

$$(\Delta f)(x) = \sum_{x' \sim x} \rho(x, x')\left(f(x) - f(x')\right) .$$

Hodge theorem: The two $\pm$i-eigenspaces decompose the space of 1-forms, especially the space of harmonic forms, into an orthogonal direct sum. Types are interchanged by conjugation: $\alpha \in C^{(1,0)}(\Lambda) \Leftrightarrow \overline{\alpha} \in C^{(0,1)}(\Lambda)$ therefore

$$(\alpha, \beta) = (\pi_{(1,0)}\alpha, \pi_{(1,0)}\beta) + (\pi_{(0,1)}\alpha, \pi_{(0,1)}\beta)$$

where the projections on $(1,0)$ and $(0,1)$ spaces are

$$\pi_{(1,0)} = \frac{1}{2}(\mathrm{Id} + \mathrm{i}*) , \qquad \pi_{(0,1)} = \frac{1}{2}(\mathrm{Id} - \mathrm{i}*) .$$

The harmonic forms of type $(1,0)$ are the *holomorphic* forms, the harmonic forms of type $(0,1)$ are the *anti-holomorphic* forms.

The L^2 norm of the 1-form $\mathrm{d}f$, called the Dirichlet energy of the function f, is the average of the usual Dirichlet energies on each independent graph

$$E_D(f) := \|\mathrm{d}f\|^2 = (\mathrm{d}f, \mathrm{d}f) = \frac{1}{2} \sum_{(x,x') \in \Lambda_1} \rho(x, x') \left|f(x') - f(x)\right|^2 \qquad (7.4)$$

$$= \frac{E_D(f|_\Gamma) + E_D(f|_{\Gamma^*})}{2} .$$

The conformal energy of a map measures its conformality defect, relating these two harmonic functions. A conformal map fulfills the Cauchy–Riemann equation

$$* \, \mathrm{d}f = -\mathrm{i} \, \mathrm{d}f . \qquad (7.5)$$

Therefore a quadratic energy whose null functions are the holomorphic ones is

$$E_C(f) := \frac{1}{2}\|\mathrm{d}f - \mathrm{i}*\mathrm{d}f\|^2 . \qquad (7.6)$$

It is related to the Dirichlet energy through the same formula as in the continuous case:

$$E_C(f) = \frac{1}{2}(\mathrm{d}f - \mathrm{i}*\mathrm{d}f, \mathrm{d}f - \mathrm{i}*\mathrm{d}f)$$

$$= \frac{1}{2}\|\mathrm{d}f\|^2 + \frac{1}{2}\|-\mathrm{i}*\mathrm{d}f\|^2 + \mathrm{Re}(\mathrm{d}f, -\mathrm{i}*\mathrm{d}f)$$

$$= \|\mathrm{d}f\|^2 + \mathrm{Im} \iint_{\Diamond_2} \mathrm{d}f \wedge \overline{\mathrm{d}f}$$

$$= E_D(f) - 2\mathcal{A}(f) , \qquad (7.7)$$

where the area of the image of the map f in the complex plane has the same formulae (the second one meaningful on a simply connected domain)

$$\mathcal{A}(f) = \frac{\mathrm{i}}{2} \iint_{\Diamond_2} \mathrm{d}f \wedge \overline{\mathrm{d}f} = \frac{\mathrm{i}}{4} \oint_{\partial \Diamond_2} f \, \overline{\mathrm{d}f} - \overline{f} \, \mathrm{d}f \qquad (7.8)$$

as in the continuous case. For a face $(x, y, x', y') \in \Diamond_2$, the algebraic area of the oriented quadrilateral $\left(f(x), f(x'), f(y), f(y') \right)$ is given by

$$\iint\limits_{(x,y,x',y')} \mathrm{d}f \wedge \overline{\mathrm{d}f} = \mathrm{i} \operatorname{Im} \left((f(x') - f(x))\overline{(f(y') - f(y))} \right)$$
$$= -2\mathrm{i}\mathcal{A}\left(f(x), f(x'), f(y), f(y') \right) .$$

When a holomorphic reference map $z : \Lambda_0 \to \mathbb{C}$ is chosen, a holomorphic (resp. anti-holomorphic) 1-form $\mathrm{d}f$ is, locally on each pair of dual diagonals, proportional to $\mathrm{d}z$, resp. $\mathrm{d}\bar{z}$, so that the decomposition of the exterior derivative into holomorphic and anti-holomorphic parts yields $\mathrm{d}f \wedge \overline{\mathrm{d}f} = \left(|\partial f|^2 + |\bar{\partial} f|^2 \right) \mathrm{d}z \wedge \mathrm{d}\bar{z}$ where the derivatives naturally live on faces and are not to be mixed up with the boundary operator ∂.

7.3 Algorithm

The theory described above is straightforward to implement. The most sensitive part is based on a minimizer procedure which finds the minimum of the Dirichlet energy for a discrete Riemann surface, given some boundary conditions. Here is the crude algorithm that we are going to detail.

The *intersection number* $\gamma \circ \gamma'$ between two loops γ and γ' on a surface counts their algebraic number of crossings. It is a homotopy invariant and has a clear discrete counterpart.

A *canonical dissection* $\aleph$ is a normalized homotopy basis of a quad-graph $\Diamond(S)$, that is to say, a set $(\aleph_k)_{1 \leq k \leq 2g}$ of loops $\aleph_k \in \ker \partial$ such that the intersection numbers verify, for $1 \leq k, \ell \leq g$,

$$\aleph_k \circ \aleph_\ell = 0, \quad \aleph_{k+g} \circ \aleph_{\ell+g} = 0, \quad \aleph_k \circ \aleph_{\ell+g} = \delta_{k,\ell} . \tag{7.9}$$

The situation is again doubled and a loop $\aleph_k$ is pushed on the graph Γ to the cycle $\aleph_k^\Gamma$ and on its dual Γ^* to $\aleph_k^{\Gamma^*}$. See [Mer07] for more details.

Basis of holomorphic forms and the period matrix (of a discrete Riemann surface S)

- Find a normalized (7.9) homotopy basis $\aleph$ of $\Diamond(S)$ and compute $\aleph_k^\Gamma$ and $\aleph_k^{\Gamma^*}$
- Compute the real discrete harmonic forms ω_k on Γ such that $\oint_\gamma \omega_k = \gamma \circ \aleph_k^\Gamma$
- Compute the dual discrete forms $*\omega_k$ on Γ^*, check $*\omega_k$ is discrete harmonic on Γ^*
- Compute its periods $(\oint_{\aleph_\ell^{\Gamma^*}} *\omega_k)_{k,\ell}$ on Γ^*
- Do likewise for the analogous discrete harmonic forms ω_k^* on Γ^*
- Find the basis of holomorphic forms (ζ_k) normalized by

$$\oint_{\aleph_\ell^\Gamma} \zeta_k = \delta_{k,\ell}, \quad \oint_{\aleph_\ell^{\Gamma^*}} \zeta_k = 0, \ 1 \leq k, \ell \leq g.$$

This can be done by some linear algebra $(\zeta) = R(\mathrm{Id} + \mathrm{i}*)(\omega)$ (R is a rectangular complex matrix)

- Define the period matrix of Γ, $\Pi_{k,\ell} := \oint_{\aleph_{g+\ell}^{\Gamma*}} \zeta_k + \oint_{\aleph_{g+\ell}^{\Gamma}} \zeta_k$ for $1 \le \ell, k \le g$
- Do likewise for ζ_k^* normalized by

$$\oint_{\aleph_\ell^{\Gamma*}} \zeta_k^* = \delta_{k,\ell}, \quad \oint_{\aleph_\ell^{\Gamma}} \zeta_k^* = 0, \ 1 \le k, \ell \le g$$

- Define the period matrix of Γ^*, $\Pi_{k,\ell}^* := \oint_{\aleph_{g+\ell}^{\Gamma}} \zeta_k^* + \oint_{\aleph_{g+\ell}^{\Gamma*}} \zeta_k^*$
- Define the period matrix as the half-sum

$$\frac{1}{2}(\Pi + \Pi^*).$$

Finding a normalized homotopy basis of a connected cellular decomposition is performed by several well known algorithms. The way we did it is to select a root vertex and grow from there a spanning tree, by computing the vertices at combinatorial distance d from the root and linking each one of them to a unique vertex at distance $d-1$, already in the tree. Repeat until no vertices are left.

Then we inflate this tree into a polygonal fundamental domain by adding faces one by one to the domain, keeping it simply connected: We recursively add all the faces which have only one edge not in the domain. We stop when all the remaining faces have at least two edges not in the domain (see Fig. 7.2).
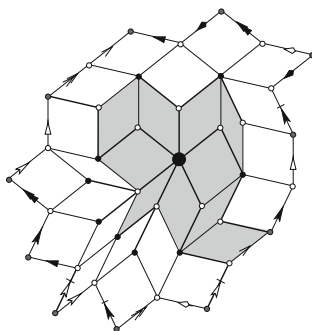
Fig. 7.2. A maximal spanning tree and its first inflation step

Then we pick one edge (one of the closest to the root) as defining the first element of our homotopy basis: adding this edge to the fundamental domain yields a non simply connected cellular decomposition and the spanning tree gives us a rooted cycle of this homotopy type going down the tree to the root. It is (one of) the combinatorially shortest in its (rooted) homology class. We add faces recursively in a similar way until we can no go further. Then we choose a new homotopy basis element, and so on until every face is closed

(see Fig. 7.3). At the end we have a homotopy basis. We compute later on the intersection numbers in order to normalize the basis.
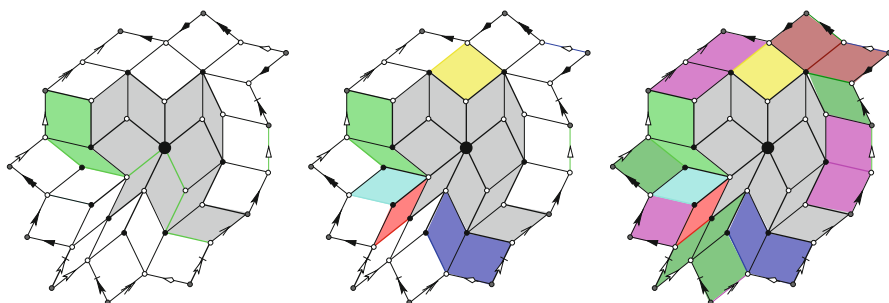
Fig. 7.3. A homotopy class is associated with an edge linking two sides of the polygon. Here a genus 4 example

We compute the unique real harmonic form η associated with each cycle $\aleph$ such that $\oint_\gamma \eta = \gamma \circ \aleph$. This is done by a minimizing procedure which finds the unique harmonic function f on the graph Γ, split along $\aleph$, whose vertices are duplicated, which is zero at the root and increases by one when going across $\aleph$. This is done by linking the values at the duplicated vertices, in effect yielding a harmonic function on the universal cover of Γ. The harmonic 1-form df does not depend on the chosen root nor on the representative $\aleph$ in its homology class.

7.4 Numerics
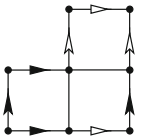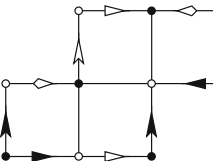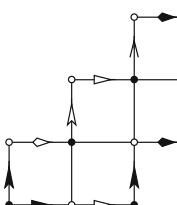
We begun with testing discrete surfaces of known moduli in order to investigate the quality of the numerics and the robustness of the method. We purposely chose to stick with raw *double* 15-digits numbers and a linear algebra library which is fast but not particularly accurate. In order to be able to compare period matrices, we used a Siegel reduction algorithm [DHB$^+$04] to map them by a modular transformation to the same canonical form.

7.4.1 Surfaces Tiled by Squares

Robert Silhol supplied us with sets of surfaces tiled by squares for which the period matrices are known [Sil06, Sil01, BS01, RGA97]. There are translation and half-translation surfaces: In these surfaces, each horizontal side is glued to a horizontal side, a vertical to a vertical, and the identification between edges of the fundamental polygon are translations for translation surfaces and translations followed by a half-twist for half-translations. The discrete conformal structure for these surfaces is very simple: the combinatorics is given by the gluing conditions and the conformal parameter $\rho \equiv 1$ is constant.

The genus one examples are not interesting because this 1-form is then the unique holomorphic form and there is nothing to compute (the algorithm does give back this known result). Genus 2 examples are non trivial because a second holomorphic form has to be computed.

The translation surfaces are particularly adapted because the discrete 1-form read off the picture is already a discrete holomorphic form. Therefore the computations are accurate even for a small number of squares. Finer squares only blur the result with numerical noise. For half-translation surfaces this is not the case, a continuous limit has to be taken in order to get a better approximation.

Surface & Period matrix	Numerical analysis	
$\Omega_1 = \frac{i}{3}\begin{pmatrix} 5 & -4 \\ -4 & 5 \end{pmatrix}$	#vertices	$\|\Omega_D - \Omega_1\|_\infty$
	25	$1.13 \cdot 10^{-8}$
	106	$3.38 \cdot 10^{-8}$
	430	$4.75 \cdot 10^{-8}$
	1726	$1.42 \cdot 10^{-7}$
	6928	$1.35 \cdot 10^{-6}$
$\Omega_2 = \frac{1}{3}\begin{pmatrix} -2+\sqrt{8}i & 1-\sqrt{2}i \\ 1-\sqrt{2}i & -2+\sqrt{8}i \end{pmatrix}$	#vertices	$\|\Omega_D - \Omega_2\|_\infty$
	14	$3.40 \cdot 10^{-2}$
	62	$9.51 \cdot 10^{-3}$
	254	$2.44 \cdot 10^{-3}$
	1022	$6.12 \cdot 10^{-4}$
	4096	$1.53 \cdot 10^{-4}$
$\Omega_3 = \frac{i}{\sqrt{3}}\begin{pmatrix} 2 & -1 \\ -1 & 2 \end{pmatrix}$	#vertices	$\|\Omega_D - \Omega_3\|_\infty$
	22	$3.40 \cdot 10^{-3}$
	94	$9.51 \cdot 10^{-3}$
	382	$2.44 \cdot 10^{-4}$
	1534	$6.12 \cdot 10^{-5}$
	6142	$1.53 \cdot 10^{-6}$

Using 15 digits numbers, the theoretical numerical accuracy is limited to 8 digits because our energy is quadratic therefore half of the digits are lost. Using an arbitrary precision toolbox or Cholesky decomposition in order to solve the linear system would allow for better results but this is not the point here.

7.4.2 Wente Torus

For a first test of the numerics on a an immersed surface in $\mathbb{R}^3$ our choice is the famous CMC-torus discovered by Wente [Wen86] for which an explicit immersion formula exists in terms of theta functions [Abr87, Wal89, Bob91]. The modulus of the rhombic Wente torus is known [Hei96] to be equal to:

$$\tau_w \approx 0.41300\ldots + 0.91073\ldots i \approx \exp(i1.145045\ldots) .$$

Grid : 10×10 Grid : 20×20

Grid : 40×40 Grid : 80×80
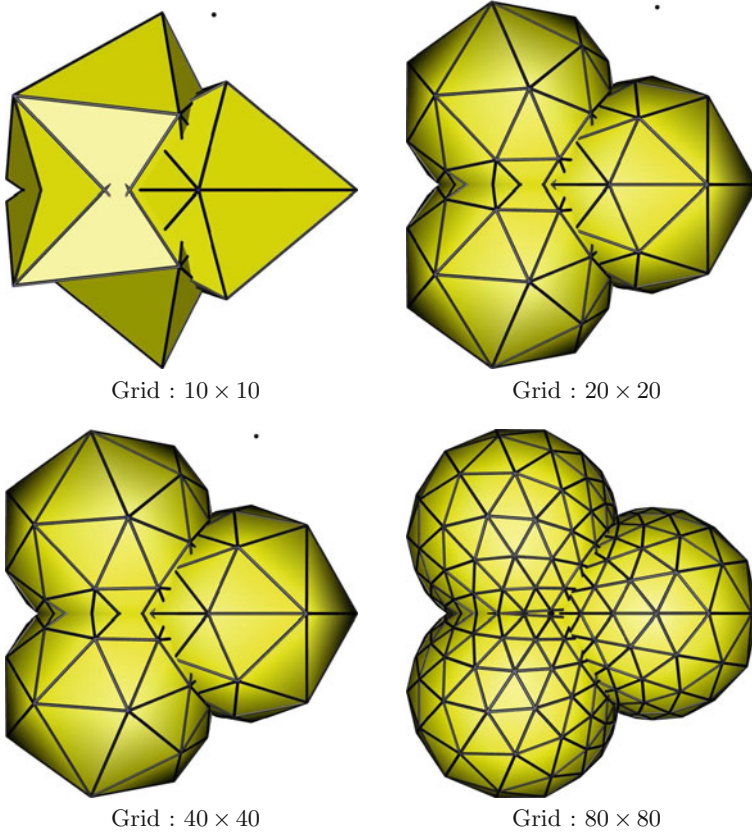
Fig. 7.4. Regular Delaunay triangulations of the Wente torus

We compute several regular discretizations of the Wente torus (Fig. 7.4) and generate discrete conformal structures using ρ_{ex} that are imposed by the extrinsic Euclidean metric of $\mathbb{R}^3$ as well as ρ_{in} which are given by the intrinsic flat metric of the surface. For a sequence of finer discretizations of a smooth immersion, the two sets of numbers come closer and closer. For these discrete conformal structures we compute again the moduli which we denote by τ_{ex} and τ_{im} and compare them with τ_w from above:

Grid	$\|\tau_{\mathrm{in}} - \tau_w\|$	$\|\tau_{\mathrm{ex}} - \tau_w\|$
10×10	$5.69 \cdot 10^{-3}$	$5.00 \cdot 10^{-3}$
20×20	$2.00 \cdot 10^{-3}$	$5.93 \cdot 10^{-3}$
40×40	$5.11 \cdot 10^{-4}$	$1.85 \cdot 10^{-3}$
80×80	$2.41 \cdot 10^{-4}$	$6.00 \cdot 10^{-4}$

For the lowest resolution the accuracy of τ_{ex} is slightly better then the one of τ_{in}. For all other the discrete conformal structures with the intrinsically generated ρ_{in} yields significant higher accuracy.

7.4.3 Lawson Surface

<div align="center">1162 vertices   2498 vertices</div>
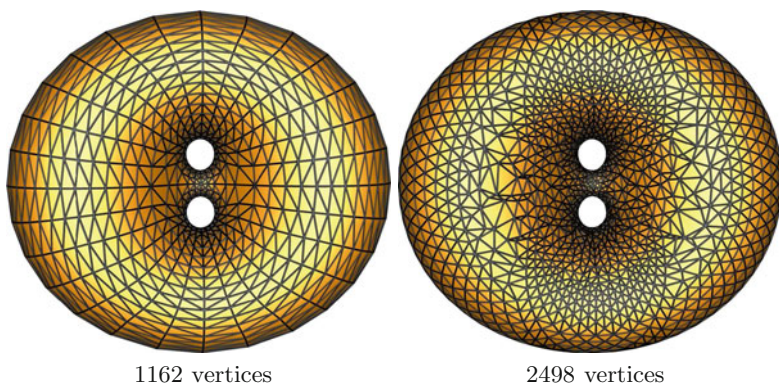
Fig. 7.5. Delaunay triangulations of the Lawson surface

Finally we apply our method to compute the period matrix of Lawson's genus 2 minimal surface in $\mathbb{S}^3$ [Law70]. Konrad Polthier [GBP96] supplied us with several resolutions of the surface which are generated by a coarsening and mesh beautifying process of a very fine approximation of the Lawson surface (Fig. 7.5). Our numerical analysis gives evidence that the period matrix of the Lawson surface is

$$\Omega_l = \frac{i}{\sqrt{3}} \begin{pmatrix} 2 & -1 \\ -1 & 2 \end{pmatrix}$$

which equals the period matrix Ω_3 of the third example from Sect. 7.4.1. Once conjectured that these two surfaces are conformally equivalent, it is a matter of checking that the symmetry group of the Lawson genus two surface yields indeed this period matrix, which was done, without prior connection, in [BBM85]. An explicit conformal mapping of the surfaces can be found manually: The genus 2 Lawson surface exhibits by construction four points with an order six symmetry and six points of order four, which decomposes the surface into 24 conformally equivalent triangles, of angles $\frac{\pi}{6}$, $\frac{\pi}{2}$, $\frac{\pi}{2}$. Therefore an algebraic equation for the Lawson surface is $y^2 = x^6 - 1$, with six branch points at the roots of unity. The correspondence between the points in the square picture of the surface and the double sheeted cover of the complex plane is done in Fig. 7.6. In particular the center of the six squares are sent to

$$y^2 = x^6 - 1$$
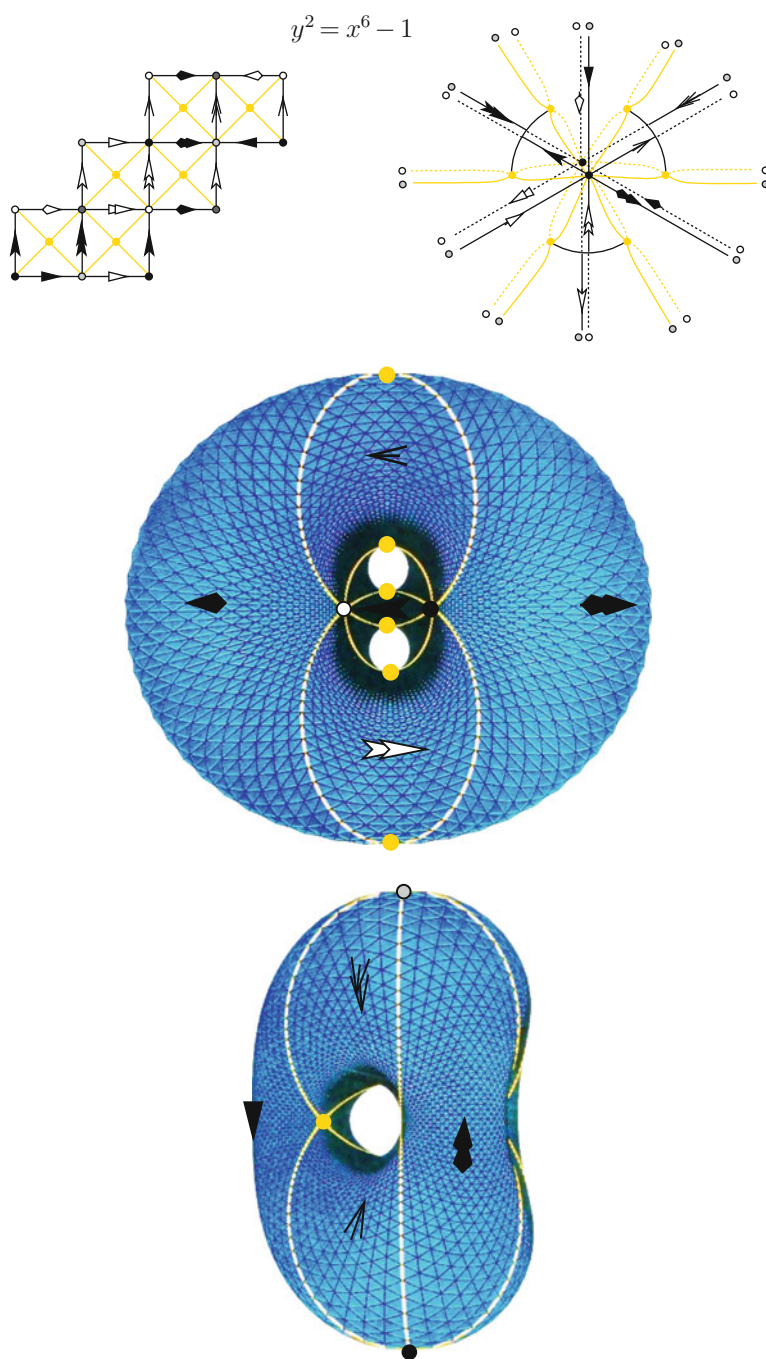
Fig. 7.6. The Lawson surface is conformally equivalent to a surface made of squares

the branch points, the vertices are sent to the two copies of 0 (black and dark gray) and ∞ (white and light gray), the squares are sent to double sheeted 2-gons corresponding to a sextant.

Similarly to Sect. 7.4.2 we compute the period matrices Ω_{ex} and Ω_{in} for different resolutions utilizing weights imposed by the extrinsic and intrinsic metric and compare the results with our conjectured period matrix for the Lawson surface Ω_l:

#vertices	$\|\Omega_{\mathrm{in}} - \Omega_l\|_\infty$	$\|\Omega_{\mathrm{ex}} - \Omega_l\|_\infty$
1162	$1.68 \cdot 10^{-3}$	$1.68 \cdot 10^{-3}$
2498	$3.01 \cdot 10^{-3}$	$3.20 \cdot 10^{-3}$
10090	$8.55 \cdot 10^{-3}$	$8.56 \cdot 10^{-3}$

Our first observation is that the matrices Ω_{ex} and Ω_{in} almost coincide. Hence the method for computing the ρ seems to have only little influence on this result (compare also Sect. 7.4.2). Further we see that figures of the higher resolution surface, i.e., with 2498 and 10090 vertices are worse than the coarsest one with 1162 vertices. The mesh beautifying process was most successful on the coarsest triangulation of the Lawson surface (Fig. 7.5). The quality of the mesh has a significant impact on the accuracy of our computation: One can see that the triangles on the coarsest example are of even shapes with comparable side lengths, while the finer resolution contains thin triangles with small angles. The convergence speed proven in [Mer01] and used in [Mer07] for period matrices is governed by this smallest angles, accounting for the poor result. Therefore for this method to be applicable, the data should be well suited. It is not enough to have very refined data if the triangles themselves are not of a good shape. A further impediment to the method is the fact that the triangulation should be Delaunay. If it is not, it can be repaired by the algorithm described in [FSSB07].

Acknowledgment

References

[Abr87]   Abresch, U.: Constant mean curvature tori in terms of elliptic functions. J. Reine Angew. Math. **374**, 169–192 (1987)

[BBM85]   Babich, M.V., Bobenko, A.I., Matveev, V.B.: Solution of nonlinear equations, integrable by the inverse problem method, in Jacobi theta-functions and the symmetry of algebraic curves. Izv. Akad. Nauk SSSR Ser. Mat. **49**(3), 511–529 (1985)

[BCGB08]   Ben-Chen, M., Gotsman, C., Bunin, G.: Conformal flattening by curvature prescription and metric scaling. In: Computer Graphics Forum, vol. 27(2). Proceedings of the Eurographics (2008)

[BMS05]   Bobenko, A.I., Mercat, C., Suris, Y.B.: Linear and nonlinear theories of discrete analytic functions. Integrable structure and isomonodromic Green's function. J. Reine Angew. Math. **583**, 117–161 (2005)

[Bob91]   Bobenko, A.I.: All constant mean curvature tori in $\mathbf{R}^3$, S^3, H^3 in terms of theta-functions. Math. Ann. **290**(2), 209–245 (1991)

[BS07]   Bobenko, A.I., Springborn, B.A.: A discrete Laplace-Beltrami operator for simplicial surfaces. Discrete Comput. Geom. **38**(4), 740–756 (2007)

[BS01]   Buser, P., Silhol, R.: Geodesics, periods, and equations of real hyperelliptic curves. Duke Math. J. **108**(2), 211–250 (2001)

[CSM02]   Costa-Santos, R., McCoy, B.M.: Dimers and the critical Ising model on lattices of genus > 1. Nucl. Phys. B **623**(3), 439–473 (2002)

[CSM03]   Costa-Santos, R., McCoy, B.M.: Finite size corrections for the Ising model on higher genus triangular lattices. J. Statist. Phys. **112**(5–6), 889–920 (2003)

[DHB$^+$04] Deconinck, B., Heil, M., Bobenko, A.I., van Hoeij, M., Schmies, M.: Computing Riemann theta functions. Math. Comput. **73**(247), 1417–1442 (2004)

[DKT08]   Desbrun, M., Kanso, E., Tong, Y.: Discrete differential forms for computational modeling. In: Bobenko, A.I., Schröder, P., Sullivan, J.M., Ziegler, G.M. (eds.) Discrete Differential Geometry, Oberwolfach Seminars, vol. 38, pp. 287–323. Birkhäuser, Basel (2008)

[DMA02]   Desbrun, M., Meyer, M., Alliez, P.: Intrinsic parameterizations of surface meshes. Computer Graphics Forum, **21**, 209–218. Proc. Eurographics (2002)

[Duf68]   Duffin, R.J.: Potential theory on a rhombic lattice. J. Combin. Theory, **5**, 258–272 (1968)

[DN03]   Dynnikov, I.A., Novikov, S.P.: Geometry of the triangle equation on two-manifolds. Mosc. Math. J. **3**(2), 419–438 (2003)

[Fer44]   Ferrand, J.: Fonctions préharmoniques et fonctions préholomorphes. Bull. Sci. Math. (2), **68**, 152–180 (1944)

[FSSB07]   Fisher, M., Springborn, B., Schröder, P., Bobenko, A.I.: An algorithm for the construction of intrinsic Delaunay triangulations with applications to digital geometry processing. Computing, **81**(2–3), 199–213 (2007)

[GN07]   Grinevich, P.G., Novikov, R.G.: The Cauchy kernel for the Novikov-Dynnikov DN-discrete complex analysis in triangular lattices. Russ. Math. Surv. **62**(4), 799–801 (2007)

[GBP96]   Grosse-Brauckmann, K., Polthier, K.: Numerical examples of compact surfaces of constant mean curvature. In: Chow, B., Gulliver, R., Levy, S., Sullivan, J. (eds.) Elliptic and parabolic methods in geometry, pp. 23–46, A K Peters, Wellesley (1996)

[Hei96]   Heil, M.: Numerical tools for the study of finite gap solutions of integrable systems. PhD thesis, TU Berlin (1995)

[JWYG04]   Jin, M., Wang, Y., Yau, S.-T., Gu, X.: Optimal global conformal surface parameterization. In: VIS '04: Proceedings of the conference on Visualization '04 (2004)

[KSS06]   Kharevych, L., Springborn, B., Schröder, P.: Discrete conformal mappings via circle patterns. ACM Trans. Graph. **25**(2), 412–438 (2006)

[Kis08]   Kiselman, C.: Functions on discrete sets holomorphic in the sense of Ferrand, or monodiffric functions of the second kind. Sci. China Ser. A **51**(4), 604–619 (2008)

[Law70]   Lawson, H.B. Jr.: Complete minimal surfaces in S^3. Ann. Math. (2), **92**, 335–374 (1970)

[Mer01]   Mercat, C.: Discrete Riemann surfaces and the Ising model. Comm. Math. Phys. **218**(1), 177–216 (2001)

[Mer04]   Mercat, C.: Exponentials form a basis of discrete holomorphic functions on a compact. Bull. Soc. Math. France **132**(2), 305–326 (2004)

[Mer07]   Mercat, C.: Discrete Riemann surfaces. In: Papadopoulos, A. (ed) Handbook of Teichmüller Theory, vol. I, IRMA Lect. Math. Theor. Phys., **11**, 541–575. Eur. Math. Soc., Zürich (2007)

[PP93]   Pinkall, U., Polthier, K.: Computing discrete minimal surfaces and their conjugates. Experiment. Math. **2**(1), 15–36 (1993)

[RGA97]   Rodríguez, R.E., González-Aguilera, V.: Fermat's quartic curve, Klein's curve and the tetrahedron. In: Quine, J.R., Sarnak, P. (eds.) Extremal Riemann surfaces. Contemporary Mathematics, **201**. AMS, Providence, RI (1997)

[Sil01]   Silhol, R.: Period matrices and the Schottky problem. In: Topics on Riemann surfaces and Fuchsian groups (Madrid, 1998), volume 287 of London Math. Soc. Lecture Note Ser., **287**, 155–163. Cambridge University Press, Cambridge (2001)

[Sil06]   Silhol, R.: Genus 2 translation surfaces with an order 4 automorphism. In: The geometry of Riemann surfaces and abelian varieties. Contemp. Math., **397**, 207–213. Amer. Math. Soc., Providence, RI (2006)

[SSP08]   Springborn, B., Schröder, P., Pinkall, U.: Conformal equivalence of triangle meshes. SIGGRAPH '08: ACM SIGGRAPH 2008 papers, 1–11. ACM, New York (2008)

[TACSD06] Tong, Y., Alliez, P., Cohen-Steiner, D., Desbrun, M.: Designing quadrangulations with discrete harmonic forms. In: Sheffer, A., Polthier, K. (eds.) Symposium on Geometry Processing, 201–210, Cagliari, Sardinia, Italy (2006) Eurographics Association

[Wal89]   Walter, R.: Constant mean curvature tori with spherical curvature lines in non-Euclidean geometry. Manuscripta Math. **63**(3), 343–363 (1989)

[War06]   Wardetzky, M.: Discrete Differential Operators on Polyhedral Surfaces – Convergence and Approximation. PhD thesis, FU Berlin (2006)

[Wen86]   Wente, H.C.: Counterexample to a conjecture of H. Hopf. Pac. J. Math. **121**(1), 193–243 (1986)

8

On the Spectral Theory of the Laplacian on Compact Polyhedral Surfaces of Arbitrary Genus

Alexey Kokotov

Department of Mathematics and Statistics, Concordia University,
1455 de Maisonneuve Blvd. West, Montreal, Quebec, H3G 1M8 Canada,
`alexey@mathstat.concordia.ca`

8.1 Introduction

There are several well-known ways to introduce a compact Riemann surface which are also discussed in the present volume, e.g., via algebraic equations or by means of some uniformization theorem, where the surface is introduced as the quotient of the upper half-plane over the action of a Fuchsian group. In this chapter we consider a less popular approach which is at the same time, perhaps, the most elementary: one can simply consider the boundary of a connected (but, generally, not simply connected) polyhedron in three dimensional Euclidean space. This is a polyhedral surface which carries the structure of a complex manifold (the corresponding system of holomorphic local parameters is obvious for all points except the vertices; near a vertex one should introduce the local parameter $\zeta = z^{2\pi/\alpha}$, where α is the sum of the angles adjacent to the vertex). In this way the Riemann surface arises together with a conformal metric; this metric is flat and has conical singularities at the vertices. Instead of a polyhedron one can also start from some abstract simplicial complex, thinking of a polyhedral surface as glued from plane triangles.

The present chapter is devoted to the spectral theory of the Laplacian on such surfaces. The main goal is to study the determinant of the Laplacian (acting in the trivial line bundle over the surface) as a functional on the space of Riemann surfaces with conformal flat conical metrics (polyhedral surfaces). The similar question for *smooth* conformal metrics and arbitrary holomorphic bundles was very popular in the eighties and early nineties being motivated by string theory. The determinants of Laplacians in flat singular metrics are much less studied: among the very few appropriate references we mention [DP89], where the determinant of the Laplacian in a conical metric was defined via some special regularization of the diverging Liouville integral,

and the question about the relation of such a definition with the spectrum of the Laplacian remained open, and two papers [Kin93, AS94] dealing with flat conical metrics on the Riemann sphere.

In [KK09] (see also [KK04]) the determinant of the Laplacian was studied as a functional

$$\mathcal{H}_g(k_1, \dots, k_M) \ni (\mathcal{X}, \omega) \mapsto \det \Delta^{|\omega|^2}$$

on the space $\mathcal{H}_g(k_1, \dots, k_M)$ of equivalence classes of pairs $(\mathcal{X}, \omega)$, where $\mathcal{X}$ is a compact Riemann surface of genus g and ω is a holomorphic one-form (an Abelian differential) with M zeros of multiplicities $k_1, \dots, k_M$. Here $\det \Delta^{|\omega|^2}$ stands for the determinant of the Laplacian in the flat metric $|\omega|^2$ having conical singularities at the zeros of ω. The flat conical metric $|\omega|^2$ considered in [KK09] is very special: the divisor of the conical points of this metric is not arbitrary (it should be the canonical one, i.e., coincide with the divisor of a holomorphic one-form), and the conical angles at the conical points are integer multiples of 2π. Later in [KK07] this restrictive condition has been eliminated in the case of polyhedral surfaces of genus one.

In the present chapter we generalize the results of [KK09] and [KK07] to the case of polyhedral surfaces of an arbitrary genus. Moreover, we give a short and self-contained survey of some basic facts from the spectral theory of the Laplacian on flat surfaces with conical points. In particular, we discuss the theory of self-adjoint extensions of this Laplacian and study the asymptotics of the corresponding heat kernel.

8.2 Flat Conical Metrics on Surfaces

Following [Tro86] and [KK07], we discuss here flat conical metrics on compact Riemann surfaces of an arbitrary genus.

8.2.1 Troyanov's Theorem

Let $\sum_{k=1}^{N} b_k P_k$ be a generalized (i.e., the coefficients b_k are not necessary integers) divisor on a compact Riemann surface $\mathcal{X}$ of genus g. Let also $\sum_{k=1}^{N} b_k = 2g - 2$. Then, according to Troyanov's theorem (see [Tro86]), there exists a (unique up to a rescaling) conformal (i.e., giving rise to a complex structure which coincides with that of $\mathcal{X}$) flat metric $\mathbf{m}$ on $\mathcal{X}$ which is smooth in $\mathcal{X} \setminus \{P_1, \dots, P_N\}$ and has simple singularities of order b_k at P_k. The latter means that in a vicinity of P_k the metric $\mathbf{m}$ can be represented in the form

$$\mathbf{m} = \mathrm{e}^{u(z,\bar{z})} |z|^{2b_k} |\mathrm{d}z|^2 , \tag{8.1}$$

where z is a conformal coordinate and u is a smooth real-valued function. In particular, if the conical angle $\beta_k = 2\pi(b_k + 1)$ satisfies $\beta_k > -1$, the point P_k is conical with this angle. Here we construct the metric $\mathbf{m}$ explicitly, giving an effective proof of Troyanov's theorem (cf. [KK07]).

Fix a canonical basis of cycles on $\mathcal{X}$ (we assume that $g \geq 1$, the case $g = 0$ is trivial) and let $E(P,Q)$ be the prime-form (see [Fay73]). Then for any divisor $\mathcal{D} = r_1 Q_1 + \ldots r_m Q_M - s_1 R_1 - \cdots - s_N R_N$ of degree zero on $\mathcal{X}$ (here the coefficients r_k, s_k are positive integers) the meromorphic differential

$$\omega_{\mathcal{D}} = \mathrm{d}_z \log \frac{\prod_{k=1}^{M} E^{r_k}(z, Q_k)}{\prod_{k=1}^{N} E^{s_k}(z, R_k)}$$

is holomorphic outside $\mathcal{D}$ and has first order poles at the points of $\mathcal{D}$ with residues r_k at Q_k and $-s_k$ at R_k. Since the prime-form is single-valued along the **a**-cycles, all **a**-periods of the differential $\omega_{\mathcal{D}}$ vanish.

Let $\{v_\alpha\}_{\alpha=1}^{g}$ be the basis of holomorphic differentials normalized by $\int_{a_\alpha} v_\beta = \delta_{\alpha\beta}$ and $\mathbb{B}$ the corresponding matrix of **b**-periods. Then all **a**- and **b**-periods of the meromorphic differential

$$\Omega_{\mathcal{D}} = \omega_{\mathcal{D}} - 2\pi\mathrm{i} \sum_{\alpha,\beta=1}^{g} ((\Im\mathbb{B})^{-1})_{\alpha\beta} \Im \left(\int_{s_1 R_1 + \ldots s_N R_N}^{r_1 Q_1 + \ldots r_M Q_M} v_\beta \right) v_\alpha$$

are purely imaginary (see [Fay73], p. 4).

Obviously, the differentials $\omega_{\mathcal{D}}$ and $\Omega_{\mathcal{D}}$ have the same structure of poles: their difference is a holomorphic 1-form.

Choose a base-point P_0 on $\mathcal{X}$ and introduce the following quantity

$$\mathcal{F}_{\mathcal{D}}(P) = \exp \int_{P_0}^{P} \Omega_{\mathcal{D}} \,.$$

Clearly, $\mathcal{F}_{\mathcal{D}}$ is a meromorphic section of some *unitary* flat line bundle over $\mathcal{X}$, the divisor of this section coincides with $\mathcal{D}$.

Now we are ready to construct the metric **m**. Choose any holomorphic differential w on $\mathcal{X}$ with, say, only simple zeros $S_1, \ldots, S_{2g-2}$. Then one can set $\mathbf{m} = |u|^2$, where

$$u(P) = w(P)\mathcal{F}_{(2g-2)S_0 - S_1 - \ldots S_{2g-2}}(P) \prod_{k=1}^{N} [\mathcal{F}_{P_k - S_0}(P)]^{b_k} \,, \qquad (8.2)$$

and S_0 is an arbitrary point.

Notice that in the case $g = 1$ the second factor in (8.2) is absent and the remaining part is nonsingular at the point S_0.

8.2.2 Distinguished Local Parameter

In a vicinity of a conical point the flat metric (8.1) takes the form

$$\mathbf{m} = |h(z)|^2 |z|^{2b} |\mathrm{d}z|^2$$

with some holomorphic function h such that $h(0) \neq 0$. It is easy to show (see, e. g., [Tro86], Proposition 2) that there exists a holomorphic change of variable $z = z(x)$ such that in the local parameter x

$$\mathbf{m} = |x|^{2b}|\mathrm{d}x|^2 .$$

We shall call the parameter x (unique up to a constant factor c, $|c| = 1$) *distinguished*. In case $b > -1$ the existence of the distinguished parameter means that in a vicinity of a conical point the surface $\mathcal{X}$ is isometric to the standard cone with conical angle $\beta = 2\pi(b+1)$.

8.2.3 Euclidean Polyhedral Surfaces

In [Tro86] it is proved that any compact Riemann surface with flat conformal conical metric admits a proper triangulation (i.e., each conical point is a vertex of some triangle of the triangulation). This means that any compact Riemann surface with a flat conical metric is a *Euclidean polyhedral surface* (see [Bob11]), i.e., can be glued from Euclidean triangles. On the other hand as it is explained in [Bob11] any compact Euclidean oriented polyhedral surface gives rise to a Riemann surface with a flat conical metric. Therefore, from now on we do not discern compact Euclidean polyhedral surfaces and Riemann surfaces with flat conical metrics.

8.3 Laplacians on Polyhedral Surfaces: Basic Facts

Without claiming originality we give here a short self-contained survey of some basic facts from the spectral theory of Laplacian on compact polyhedral surfaces. We start with recalling the (slightly modified) Carslaw construction (1909) of the heat kernel on a cone, then we describe the set of self-adjoint extensions of a conical Laplacian (these results are complementary to Kondratjev's study [Kon67] of elliptic equations on conical manifolds and are well-known, being in the folklore since the sixties of the last century; their generalization to the case of Laplacians acting on p-forms can be found in [Moo99]). Finally, we establish the precise heat asymptotics for the Friedrichs extension of the Laplacian on a compact polyhedral surface. It should be noted that more general results on the heat asymptotics for Laplacians acting on p-forms on piecewise flat pseudomanifolds can be found in [Che83].

8.3.1 The Heat Kernel on the Infinite Cone

We start from the standard heat kernel

$$H_{2\pi}(x, y; t) = \frac{1}{4\pi t} \exp\{-(x - y) \cdot (x - y)/4t\} \tag{8.3}$$

in the space $\mathbb{R}^2$ which we consider as the cone with conical angle 2π. Introducing the polar coordinates (r, θ) and (ρ, ψ) in the x and y-planes, one can rewrite (8.3) as the contour integral

$$H_{2\pi}(x, y; t) =$$

$$\frac{1}{16\pi^2 it} \exp\{-(r^2 + \rho^2)/4t\} \int_{C_{\theta,\psi}} \exp\{r\rho \cos(\alpha - \theta)/2t\} \cot \frac{\alpha - \psi}{2} \, d\alpha \ , \quad (8.4)$$

where $C_{\theta,\psi}$ denotes the union of a small positively oriented circle centered at $\alpha = \psi$ and the two vertical lines, $l_1 = (\theta - \pi - i\infty, \theta - \pi + i\infty)$ and $l_2 = (\theta + \pi + i\infty, \theta + \pi - i\infty)$, having mutually opposite orientations.

To prove (8.4) one has to notice that

(1) $\Re \cos(\alpha - \theta) < 0$ in vicinities of the lines l_1 and l_2 and, therefore, the integrals over these lines converge.

(2) The integrals over the lines cancel due to the 2π-periodicity of the integrand and the remaining integral over the circle coincides with (8.3) due to the Cauchy Theorem.

Observe that one can deform the contour $C_{\theta,\psi}$ into the union, A_θ, of two contours lying in the open domains $\{\theta - \pi < \Re \alpha < \theta + \pi, \ \Im \alpha > 0\}$ and $\{\theta - \pi < \Re \alpha < \theta + \pi, \ \Im \alpha < 0\}$ respectively, the first contour goes from $\theta + \pi + i\infty$ to $\theta - \pi + i\infty$, the second one goes from $\theta - \pi - i\infty$ to $\theta + \pi - i\infty$. This leads to the following representation for the heat kernel $H_{2\pi}$:

$$H_{2\pi}(x, y; t) =$$

$$\frac{1}{16\pi^2 it} \exp\{-(r^2 + \rho^2)/4t\} \int_{A_\theta} \exp\{r\rho \cos(\alpha - \theta)/2t\} \cot \frac{\alpha - \psi}{2} \, d\alpha \ . \quad (8.5)$$

The latter representation admits a natural generalization to the case of the cone C_β with conical angle β, $0 < \beta < +\infty$. Notice here that in case $0 < \beta \leq 2\pi$ the cone C_β is isometric to the surface $z_3 = \sqrt{(\frac{4\pi^2}{\beta^2} - 1)(z_1^2 + z_2^2)}$.

Namely, introducing the polar coordinates on C_β, we see that the following expression represents the heat kernel on C_β:

$$H_\beta(r, \theta, \rho, \psi; t) =$$

$$\frac{1}{8\pi\beta it} \exp\{-(r^2 + \rho^2)/4t\} \int_{A_\theta} \exp\{r\rho \cos(\alpha - \theta)/2t\} \cot \frac{\pi(\alpha - \psi)}{\beta} \, d\alpha \ . \quad (8.6)$$

Clearly, expression (8.6) is symmetric with respect to (r, θ) and (ρ, ψ) and is β-periodic with respect to the angle variables θ, ψ. Moreover, it satisfies the heat equation on C_β. Therefore, to verify that H_β is in fact the heat kernel on C_β it remains to show that $H_\beta(\cdot, y, t) \longrightarrow \delta(\cdot - y)$ as $t \to 0+$. To this end deform the contour A_ψ into the union of the lines l_1 and l_2 and (possibly many) small circles centered at the poles of $\cot \frac{\pi(\cdot - \psi)}{\beta}$ in the strip $\theta - \pi < \Re \alpha < \theta + \pi$. The integrals over all the components of this union except the circle centered at $\alpha = \psi$ vanish in the limit as $t \to 0+$, whereas the integral over the latter circle coincides with $H_{2\pi}$.

The Heat Asymptotics Near the Vertex

Proposition 1. *Let $R > 0$ and $C_\beta(R) = \{x \in C_\beta : \mathrm{dist}(x, \mathcal{O}) < R\}$. Let also dx denote the area element on C_β. Then for some $\epsilon > 0$*

$$\int_{C_\beta(R)} H_\beta(x, x; t)\, dx = \frac{1}{4\pi t}\mathrm{Area}(C_\beta(R)) + \frac{1}{12}\left(\frac{2\pi}{\beta} - \frac{\beta}{2\pi}\right) + O(e^{-\epsilon/t}) \quad (8.7)$$

as $t \to 0+$.

Proof (cf. [Fur94], p. 1433). Make in (8.6) the change of variable $\gamma = \alpha - \psi$ and deform the contour $A_{\theta-\psi}$ into the contour $\Gamma^-_{\theta-\psi} \cup \Gamma^+_{\theta-\psi} \cup \{|\gamma| = \delta\}$, where the oriented curve $\Gamma^-_{\theta-\psi}$ goes from $\theta-\psi-\pi-i\infty$ to $\theta-\psi-\pi+i\infty$ and intersects the real axis at $\gamma = -\delta$, the oriented curve $\Gamma^+_{\theta-\psi}$ goes from $\theta - \psi + \pi + i\infty$ to $\theta - \psi + \pi - i\infty$ and intersects the real axis at $\gamma = \delta$, the circle $\{|\gamma| = \delta\}$ is positively oriented and δ is a small positive number. Calculating the integral over the circle $\{|\gamma| = \delta\}$ via the Cauchy Theorem, we get

$$H_\beta(x, y; t) - H_{2\pi}(x, y; t) =$$

$$\frac{1}{8\pi\beta i t} \exp\{-(r^2 + \rho^2)/4t\} \int_{\Gamma^-_{\theta-\psi} \cup \Gamma^+_{\theta-\psi}} \exp\{r\rho\cos(\gamma + \psi - \theta)/2t\} \cot\frac{\pi\gamma}{\beta}\, d\gamma \tag{8.8}$$

and

$$\int_{C_\beta(R)} \left(H_\beta(x, x; t) - \frac{1}{4\pi t}\right) dx =$$

$$\frac{1}{8\pi i t} \int_0^R dr\, r \int_{\Gamma^-_0 \cup \Gamma^+_0} \exp\{-\frac{r^2\sin^2(\gamma/2)}{t}\} \cot\frac{\pi\gamma}{\beta}\, d\gamma. \tag{8.9}$$

The integration over r can be done explicitly and the right hand side of (8.9) reduces to

$$\frac{1}{16\pi i} \int_{\Gamma^-_0 \cup \Gamma^+_0} \frac{\cot(\frac{\pi\gamma}{\beta})}{\sin^2(\gamma/2)}\, d\gamma + O(e^{-\epsilon/t}). \tag{8.10}$$

(One can assume that $\Re\sin^2(\gamma/2)$ is positive and separated from zero when $\gamma \in \Gamma^-_0 \cup \Gamma^+_0$.) The contour of integration in (8.10) can be changed for a negatively oriented circle centered at $\gamma = 0$. Since $\mathrm{Res}(\frac{\cot(\frac{\pi\gamma}{\beta})}{\sin^2(\gamma/2)}, \gamma = 0) = \frac{2}{3}(\frac{\beta}{2\pi} - \frac{2\pi}{\beta})$, we arrive at (8.7).

Remark 1. The Laplacian Δ corresponding to the flat conical metric $(d\rho)^2 + r^2(d\theta)^2, 0 \le \theta \le \beta$ on C_β with domain $C_0^\infty(C_\beta \setminus \mathcal{O})$ has infinitely many self-adjoint extensions. Analyzing the asymptotics of (8.6) near the vertex $\mathcal{O}$, one can show that for any $y \in C_\beta$ and $t > 0$ the function $H_\beta(\cdot, y; t)$ belongs to the domain of the Friedrichs extension Δ_F of Δ and does not belong to

the domain of any other extension. Moreover, using a Hankel transform, it is possible to get an explicit spectral representation of Δ_F (this operator has an absolutely continuous spectrum of infinite multiplicity) and to show that the Schwartz kernel of the operator $e^{t\Delta_F}$ coincides with $H_\beta(\cdot,\cdot;t)$ (see, e.g., [Tay97] formula (8.8.30) together with [Car10], p. 370.)

8.3.2 Heat Asymptotics for Compact Polyhedral Surfaces

Self-Adjoint Extensions of a Conical Laplacian

Let $\mathcal{X}$ be a compact polyhedral surface with vertices (conical points) $P_1, \ldots, P_N$. The Laplacian Δ corresponding to the natural flat conical metric on $\mathcal{X}$ with domain $C_0^\infty(\mathcal{X} \setminus \{P_1, \ldots, P_N\})$ (we remind the reader that the Riemannian manifold $\mathcal{X}$ is smooth everywhere except the vertices) is not essentially self-adjoint and one has to fix one of its self-adjoint extensions. We are to discuss now the choice of a self-adjoint extension.

This choice is defined by the prescription of some particular asymptotical behavior near the conical points to functions from the domain of the Laplacian; it is sufficient to consider a surface with only one conical point P of the conical angle β. More precisely, assume that $\mathcal{X}$ is smooth everywhere except the point P and that some vicinity of P is isometric to a vicinity of the vertex $\mathcal{O}$ of the standard cone C_β (of course, now the metric on $\mathcal{X}$ no more can be flat everywhere in $\mathcal{X} \setminus P$ unless the genus g of $\mathcal{X}$ is greater than one and $\beta = 2\pi(2g - 1)$).

For $k \in \mathbb{N}_0$ introduce the functions $V_\pm^k$ on C_β by

$$V_\pm^k(r, \theta) = r^{\pm \frac{2\pi k}{\beta}} \exp\{i \tfrac{2\pi k\theta}{\beta}\} \; ; \quad k > 0 \,,$$
$$V_+^0 = 1 \,, \quad V_-^0 = \log r \,.$$

Clearly, these functions are formal solutions to the homogeneous problem $\Delta u = 0$ on C_β. Notice that the functions V_-^k grow near the vertex but are still square integrable in its vicinity if $k < \frac{\beta}{2\pi}$.

Let $\mathcal{D}_{\min}$ denote the graph closure of $C_0^\infty(\mathcal{X} \setminus P)$, i.e.,

$$U \in \mathcal{D}_{\min} \Leftrightarrow \exists u_m \in C_0^\infty(\mathcal{X} \setminus P), W \in L_2(\mathcal{X}) : u_m \to U \text{and } \Delta u_m \to W \text{ in } L_2(\mathcal{X}) \,.$$

Define the space $H_\delta^2(C_\beta)$ as the closure of $C_0^\infty(C_\beta \setminus \mathcal{O})$ with respect to the norm

$$||u; H_\delta^2(C_\beta)||^2 = \sum_{|\alpha| \leq 2} \int_{C_\beta} r^{2(\delta - 2 + |\alpha|)} |D_x^\alpha u(x)|^2 \mathrm{d}x.$$

Then for any $\delta \in \mathbb{R}$ such that $\delta - 1 \neq \frac{2\pi k}{\beta}, k \in \mathbb{Z}$ one has the a priori estimate

$$||u; H_\delta^2(C_\beta)|| \leq c ||\Delta u; H_\delta^0(C_\beta)|| \tag{8.11}$$

for any $u \in C_0^\infty(C_\beta \setminus \mathcal{O})$ and some constant c being independent of u (see, e.g., [NP92], Chap. 2).

It follows from Sobolev's imbedding theorem that for functions from $u \in H_\delta^2(C_\beta)$ one has the point-wise estimate

$$r^{\delta-1}|u(r,\theta)| \le c\|u; H_\delta^2(C_\beta)\| . \tag{8.12}$$

Applying estimates (8.11) and (8.12) with $\delta = 0$, we see that functions u from $\mathcal{D}_{\min}$ must obey the asymptotics $u(r,\theta) = O(r)$ as $r \to 0$.

Now the description of the set of all self-adjoint extensions of Δ looks as follows. Let χ be a smooth function on $\mathcal{X}$ which is equal to 1 near the vertex P and such that in a vicinity of the support of χ one has that $\mathcal{X}$ is isometric to C_β. Denote by $\mathfrak{M}$ the linear subspace of $L_2(\mathcal{X})$ spanned by the functions $\chi V_\pm^k$ with $0 \le k < \frac{\beta}{2\pi}$. The dimension, $2d$, of $\mathfrak{M}$ is even. To get a self-adjoint extension of Δ one chooses a subspace $\mathfrak{N}$ of $\mathfrak{M}$ of dimension d such that

$$(\Delta u, v)_{L_2(\mathcal{X})} - (u, \Delta v)_{L_2(\mathcal{X})} = \lim_{\epsilon \to 0+} \oint_{r=\epsilon} \left(u \frac{\partial v}{\partial r} - v \frac{\partial u}{\partial r} \right) \mathrm{d}s = 0$$

for any $u, v \in \mathfrak{N}$, where $\mathrm{d}s$ is the length element on the circle $r = \epsilon$. To any such subspace $\mathfrak{N}$ there corresponds a self-adjoint extension $\Delta_{\mathfrak{N}}$ of Δ with domain $\mathfrak{N} + \mathcal{D}_{\min}$.

The extension corresponding to the subspace $\mathfrak{N}$ spanned by the functions χV_+^k, $0 \le k < \frac{\beta}{2\pi}$ coincides with the Friedrichs extension of Δ. The functions from the domain of the Friedrichs extension are bounded near the vertex.

From now on we denote by Δ the Friedrichs extension of the Laplacian on the polyhedral surface $\mathcal{X}$; other extensions will not be considered here.

Heat Asymptotics

Theorem 1. *Let $\mathcal{X}$ be a compact polyhedral surface with vertices $P_1, \ldots, P_N$ of conical angles $\beta_1, \ldots, \beta_N$. Let Δ be the Friedrichs extension of the Laplacian defined on functions from $C_0^\infty(\mathcal{X} \setminus \{P_1, \ldots, P_N\})$. Then*

1. *The spectrum of the operator Δ is discrete, all the eigenvalues of Δ have finite multiplicity.*
2. *Let $\mathcal{H}(x, y; t)$ be the heat kernel for Δ. Then for some $\epsilon > 0$*

$$\mathrm{Tr}\, e^{t\Delta} = \int_{\mathcal{X}} \mathcal{H}(x, x; t)\, \mathrm{d}x = \frac{\mathrm{Area}(\mathcal{X})}{4\pi t} + \frac{1}{12} \sum_{k=1}^{N} \left\{ \frac{2\pi}{\beta_k} - \frac{\beta_k}{2\pi} \right\} + O(e^{-\epsilon/t}), \tag{8.13}$$

as $t \to 0+$.
3. *The counting function, $N(\lambda)$, of the spectrum of Δ obeys the asymptotics $N(\lambda) = O(\lambda)$ as $\lambda \to +\infty$.*

Proof. (1) The proof of the first statement is a standard exercise (cf. [Kin93]). We indicate only the main idea leaving the details to the reader. Introduce the closure, $H^1(\mathcal{X})$, of $C_0^\infty(\mathcal{X} \setminus \{P_1, \ldots, P_N\}$ with respect to the norm $|||u||| = ||u; L_2|| + ||\nabla u; L_2||$. It is sufficient to prove that any bounded set S in $H^1(\mathcal{X})$ is precompact in the L_2-topology (this will imply the compactness of the self-adjoint operator $(I - \Delta)^{-1}$). Moreover, one can assume that the supports of functions from S belong to a small ball B centered at a conical point P. Now to prove the precompactness of S it is sufficient to make use of the expansion with respect to eigenfunctions of the Dirichlet problem in B and the diagonal process.

(2) Let $\mathcal{X} = \cup_{j=0}^N K_j$, where K_j, $j = 1, \ldots, N$ is a neighborhood of the conical point P_j which is isometric to $C_{\beta_j}(R)$ with some $R > 0$, and $K_0 = \mathcal{X} \setminus \cup_{j=1}^N K_j$.

Let also $K_j^{\epsilon_1} \supset K_j$ and $K_j^{\epsilon_1}$ be isometric to $C_{\beta_j}(R + \epsilon_1)$ with some $\epsilon_1 > 0$ and $j = 1, \ldots, N$.

Fixing $t > 0$ and $x, y \in K_j$ with $j > 0$, one has

$$\int_0^t ds \int_{K_j^{\epsilon_1}} (\psi\{\Delta_z - \partial_s\}\phi - \phi\{\Delta_z + \partial_s\}\psi) \, dz = \tag{8.14}$$

$$\int_0^t ds \int_{\partial K_j^{\epsilon_1}} \left(\phi\frac{\partial\psi}{\partial n} - \psi\frac{\partial\phi}{\partial n}\right) dl(z) - \int_{K_j^{\epsilon_1}} (\phi(z,t)\psi(z,t) - \phi(z,0)\psi(z,0)) \, dz$$
$$\tag{8.15}$$

with $\phi(z,t) = \mathcal{H}(z,y;t) - H_{\beta_j}(z,y;t)$ and $\psi(z,t) = H_{\beta_j}(z,x;t-s)$. (Here it is important that we are working with the heat kernel of the Friedrichs extension of the Laplacian, for other extensions the heat kernel has growing terms in the asymptotics near the vertex and the right hand side of (8.14) gets extra terms.) Therefore,

$$H_{\beta_j}(x,y;t) - \mathcal{H}(x,y;t) =$$

$$\int_0^t ds \int_{\partial K_j^{\epsilon_1}} \left(\mathcal{H}(y,z;s)\frac{\partial H_{\beta_j}(x,z;t-s)}{\partial n(z)} - H_{\beta_j}(z,x;t-s)\frac{\partial \mathcal{H}(z,y;s)}{\partial n(z)}\right) dl(z)$$

$$= O(e^{-\epsilon_2/t})$$

with some $\epsilon_2 > 0$ as $t \to 0+$ uniformly with respect to $x, y \in K_j$. This implies that

$$\int_{K_j} \mathcal{H}(x,x;t)dx = \int_{K_j} H_{\beta_j}(x,x;t)dx + O(e^{-\epsilon_2/t}) . \tag{8.16}$$

Since the metric on $\mathcal{X}$ is flat in a vicinity of K_0, one has the asymptotics

$$\int_{K_0} \mathcal{H}(x,x;t)dx = \frac{\text{Area}(K_0)}{4\pi t} + O(e^{-\epsilon_3/t})$$

with some $\epsilon_3 > 0$ (cf. [MS67]). Now (8.13) follows from (8.7).

(3) The third statement of the theorem follows from the second one due to the standard Tauberian arguments.

8.4 Determinant of the Laplacian: Analytic Surgery and Polyakov-Type Formulas

Theorem 1 opens a way to define the determinant, $\det \Delta$, of the Laplacian on a compact polyhedral surface via the standard Ray–Singer regularization. Namely introduce the operator ζ-function

$$\zeta_\Delta(s) = \sum_{\lambda_k > 0} \frac{1}{\lambda_k^s} \ , \tag{8.17}$$

where the summation goes over all strictly positive eigenvalues λ_k of the operator $-\Delta$ (counting multiplicities). Due to the third statement of Theorem 1, the function ζ_Δ is holomorphic in the half-plane $\{\Re s > 1\}$. Moreover, due to the equality

$$\zeta_\Delta(s) = \frac{1}{\Gamma(s)} \int_0^\infty \left\{ \operatorname{Tr} e^{t\Delta} - 1 \right\} t^{s-1} \, dt \tag{8.18}$$

and the asymptotics (8.13), one has the equality

$$\zeta_\Delta(s) = \frac{1}{\Gamma(s)} \left\{ \frac{\operatorname{Area}(\mathcal{X})}{4\pi(s-1)} + \left[\frac{1}{12} \sum_{k=1}^N \left\{ \frac{2\pi}{\beta_k} - \frac{\beta_k}{2\pi} \right\} - 1 \right] \frac{1}{s} + e(s) \right\} \ , \tag{8.19}$$

where $e(s)$ is an entire function. Thus, ζ_Δ is regular at $s = 0$ and one can define the ζ-regularized determinant of the Laplacian via usual ζ-regularization (cf. [Ray73]):

$$\det \Delta := \exp\{-\zeta'_\Delta(0)\} \, . \tag{8.20}$$

Moreover, (8.19) and the relation $\sum_{k=1}^N b_k = 2g - 2$; $b_k = \frac{\beta_k}{2\pi} - 1$ yield

$$\zeta_\Delta(0) = \frac{1}{12} \sum_{k=1}^N \left\{ \frac{2\pi}{\beta_k} - \frac{\beta_k}{2\pi} \right\} - 1 = \left(\frac{\chi(\mathcal{X})}{6} - 1 \right) + \frac{1}{12} \sum_{k=1}^N \left\{ \frac{2\pi}{\beta_k} + \frac{\beta_k}{2\pi} - 2 \right\} \, , \tag{8.21}$$

where $\chi(\mathcal{X}) = 2 - 2g$ is the Euler characteristics of $\mathcal{X}$.

It should be noted that the term $\frac{\chi(\mathcal{X})}{6} - 1$ at the right hand side of (8.21) coincides with the value at zero of the operator ζ-function of the Laplacian corresponding to an arbitrary *smooth* metric on $\mathcal{X}$ (see, e. g., [OPS88], p. 155).

Let $\mathbf{m}$ and $\tilde{\mathbf{m}} = \kappa \mathbf{m}$, $\kappa > 0$ be two homothetic flat metrics with the same conical points with conical angles $\beta_1, \dots, \beta_N$. Then (8.17), (8.20) and (8.21) imply the following *rescaling property* of the conical Laplacian:

$$\det \Delta^{\tilde{\mathbf{m}}} = \kappa^{-\left(\frac{\chi(\mathcal{X})}{6} - 1 \right) - \frac{1}{12} \sum_{k=1}^N \left\{ \frac{2\pi}{\beta_k} + \frac{\beta_k}{2\pi} - 2 \right\}} \det \Delta^{\mathbf{m}} \, . \tag{8.22}$$

8.4.1 Analytic Surgery

Let $\mathbf{m}$ be an arbitrary smooth metric on $\mathcal{X}$ and denote by $\Delta^{\mathbf{m}}$ the corresponding Laplacian. Consider N nonoverlapping connected and simply connected domains $D_1, \ldots, D_N \subset \mathcal{X}$ bounded by closed curves $\gamma_1, \ldots, \gamma_N$ and introduce also the domain $\Sigma = \mathcal{X} \setminus \cup_{k=1}^N D_k$ and the contour $\Gamma = \cup_{k=1}^N \gamma_k$.

Define *the Neumann jump operator* $R : C^\infty(\Gamma) \to C^\infty(\Gamma)$ by

$$R(f)|_{\gamma_k} = \partial_\nu (V_k^- - V_k^+) \,,$$

where ν is the outward normal to $\gamma_k = \partial D_k$, the functions V_k^- and V^+ are the solutions of the boundary value problems $\Delta^{\mathbf{m}} V_k^- = 0$ in D_k, $V^-|_{\partial D_k} = f$ and $\Delta^{\mathbf{m}} V^+ = 0$ in Σ, $V^+|_\Gamma = f$. The Neumann jump operator is an elliptic pseudodifferential operator of order 1, and it is known that one can define its determinant via the standard ζ-regularization.

In what follows it is crucial that the Neumann jump operator does not change if we vary the metric within the same conformal class.

Let $(\Delta^{\mathbf{m}}|D_k)$ and $(\Delta^{\mathbf{m}}|\Sigma)$ be the operators of the Dirichlet boundary problem for $\Delta^{\mathbf{m}}$ in domains D_k and Σ respectively, the determinants of these operators also can be defined via ζ-regularization.

Due to Theorem B^* from [BFK92], we have

$$\det \Delta^{\mathbf{m}} = \left\{ \prod_{k=1}^N \det(\Delta^{\mathbf{m}}|D_k) \right\} \det(\Delta^{\mathbf{m}}|\Sigma) \det R \left\{ \text{Area}(\mathcal{X}, \mathbf{m}) \right\} \left\{ l(\Gamma) \right\}^{-1} \,,$$

$$(8.23)$$

where $l(\Gamma)$ is the length of the contour Γ in the metric $\mathbf{m}$

Remark 2. We have excluded the zero modes of an operator from the definition of its determinant, so we are using the same notation $\det A$ for the determinants of operators A with and without zero modes. In [BFK92] the determinant of an operator A with zero modes is always equal to zero, and what we call here $\det A$ is called the modified determinant in [BFK92] and denoted there by $\det^* A$.

An analogous statement holds for the flat conical metric. Namely let $\mathcal{X}$ be a compact polyhedral surface with vertices $P_1, \ldots, P_N$ and g be a corresponding flat metric with conical singularities. Choose the domains D_k, $k = 1, \ldots, N$ being (open) nonoverlapping disks centered at P_k and let $(\Delta|D_k)$ be the Friedrichs extension of the Laplacian with domain $C_0^\infty(D_k \setminus P_k)$ in $L_2(D_k)$. Then formula (8.23) is still valid with $\Delta^{\mathbf{m}} = \Delta$ (cf. [KK04] or the recent paper [LMP07] for a more general result).

8.4.2 Polyakov's Formula

We state this result in the form given in ([Fay92], p. 62). Let $\mathbf{m}_1 = \rho_1^{-2}(z, \bar{z})\widehat{\mathrm{d}z}$, where $\widehat{\mathrm{d}z} = \frac{\mathrm{d}z \wedge \overline{\mathrm{d}z}}{-2\mathrm{i}} = \mathrm{d}x \wedge \mathrm{d}y$, and $\mathbf{m}_2 = \rho_2^{-2}(z, \bar{z})\widehat{\mathrm{d}z}$ be two *smooth*

conformal metrics on $\mathcal{X}$ and let $\det \Delta^{\mathbf{m}_1}$ and $\det \Delta^{\mathbf{m}_2}$ be the determinants of the corresponding Laplacians (defined via the standard Ray–Singer regularization). Then

$$\frac{\det \Delta^{\mathbf{m}_2}}{\det \Delta^{\mathbf{m}_1}} = \frac{\text{Area}(\mathcal{X}, \mathbf{m}_2)}{\text{Area}(\mathcal{X}, \mathbf{m}_1)} \exp \left\{ \frac{1}{3\pi} \int_{\mathcal{X}} \log \frac{\rho_2}{\rho_1} \partial^2_{z\bar{z}} \log(\rho_2 \rho_1) \widehat{dz} \right\} . \qquad (8.24)$$

8.4.3 Analog of Polyakov's Formula for a Pair of Flat Conical Metrics

Proposition 2. *Let $a_1, \ldots, a_N$ and $b_1, \ldots, b_M$ be real numbers which are greater than -1 and satisfy $a_1 + \cdots + a_N = b_1 + \cdots + b_M = 2g - 2$. Let also T be a connected C^1-manifold and let*

$$T \ni t \mapsto \mathbf{m}_1(t), \quad T \ni t \mapsto \mathbf{m}_2(t)$$

be two C^1-families of flat conical metrics on $\mathcal{X}$ such that

1. *For any $t \in T$ the metrics $\mathbf{m}_1(t)$ and $\mathbf{m}_2(t)$ define the same conformal structure on $\mathcal{X}$*
2. *$\mathbf{m}_1(t)$ has conical singularities at $P_1(t), \ldots, P_N(t) \in \mathcal{X}$ with conical angles $2\pi(a_1 + 1), \ldots, 2\pi(a_N + 1)$*
3. *$\mathbf{m}_2(t)$ has conical singularities at $Q_1(t), \ldots, Q_M(t) \in L$ with conical angles $2\pi(b_1 + 1), \ldots, 2\pi(b_M + 1)$*
4. *For any $t \in T$ the sets $\{P_1(t), \ldots, P_N(t)\}$ and $\{Q_1(t), \ldots, Q_M(t)\}$ do not intersect*

Let x_k be distinguished local parameter for $\mathbf{m}_1$ near P_k and y_l be distinguished local parameter for $\mathbf{m}_2$ near Q_l (we omit the argument t).

Introduce the functions f_k, g_l and the complex numbers $\mathbf{f_k}$, $\mathbf{g_l}$ by

$$\mathbf{m}_2 = |f_k(x_k)|^2 |dx_k|^2 \quad near \ \ P_k; \qquad \mathbf{f_k} := f_k(0) ,$$

$$\mathbf{m}_1 = |g_l(y_l)|^2 |dy_l|^2 \quad near \ \ Q_l; \qquad \mathbf{g_l} := g_l(0) .$$

Then the following equality holds

$$\frac{\det \Delta^{\mathbf{m}_1}}{\det \Delta^{\mathbf{m}_2}} = C \, \frac{\text{Area}(\mathcal{X}, \mathbf{m}_1)}{\text{Area}(\mathcal{X}, \mathbf{m}_2)} \, \frac{\prod_{l=1}^{M} |\mathbf{g_l}|^{b_l/6}}{\prod_{k=1}^{N} |\mathbf{f_k}|^{a_k/6}} , \qquad (8.25)$$

where the constant C is independent of $t \in T$.

Proof. Take $\epsilon > 0$ and introduce the disks $D_k(\epsilon)$, $k = 1, \ldots, M + N$ centered at the points $P_1, \ldots, P_N, Q_1, \ldots, Q_M$; $D_k(\epsilon) = \{|x_k| \leq \epsilon\}$ for $k = 1, \ldots, N$ and $D_{N+l} = \{|y_l| \leq \epsilon\}$ for $l = 1, \ldots, M$. Let $h_k : \mathbb{R}_+ \to \mathbb{R}$, $k = 1, \ldots, N + M$ be smooth positive functions such that

1.

$$\int_0^1 h_k^2(r)r\mathrm{d}r = \begin{cases} \int_0^1 r^{2a_k+1}\mathrm{d}r = \frac{1}{2a_k+2}, & \text{if } k=1,\ldots,N \\ \int_0^1 r^{2b_l+1}\mathrm{d}r = \frac{1}{2b_l+2}, & \text{if } k=N+l,\ l=1,\ldots,M \end{cases}$$

2.

$$h_k(r) = \begin{cases} r^{a_k} & \text{for } r \geq 1 \text{ if } k=1,\ldots,N \\ r^{b_l} & \text{for } r \geq 1 \text{ if } k=N+l,\ l=1,\ldots,M \end{cases}$$

Define two families of *smooth* metrics $\mathbf{m}_1^\epsilon$, $\mathbf{m}_2^\epsilon$ on $\mathcal{X}$ via

$$\mathbf{m}_1^\epsilon(z) = \begin{cases} \epsilon^{2a_k} h_k^2(|x_k|/\epsilon)|\mathrm{d}x_k|^2, & z \in D_k(\epsilon), \quad k=1,\ldots,N \\ \mathbf{m}(z), & z \in \mathcal{X} \setminus \cup_{k=1}^N D_k(\epsilon), \end{cases}$$

$$\mathbf{m}_2^\epsilon(z) = \begin{cases} \epsilon^{2b_l} h_{N+l}^2(|y_l|/\epsilon)|\mathrm{d}y_l|^2, & z \in D_{N+l}(\epsilon), \quad l=1,\ldots,M \\ \mathbf{m}(z), & z \in \mathcal{X} \setminus \cup_{l=1}^M D_{N+l}(\epsilon). \end{cases}$$

The metrics $\mathbf{m}_{1,2}^\epsilon$ converge to $\mathbf{m}_{1,2}$ as $\epsilon \to 0$ and

$$\mathrm{Area}(\mathcal{X}, \mathbf{m}_{1,2}^\epsilon) = \mathrm{Area}(\mathcal{X}, \mathbf{m}_{1,2}).$$

Lemma 1. *Let ∂_t be the differentiation with respect to one of the coordinates on T and let $\det\Delta^{\mathbf{m}_{1,2}^\epsilon}$ be the standard ζ-regularized determinant of the Laplacian corresponding to the smooth metric $\mathbf{m}_{1,2}^\epsilon$. Then*

$$\partial_t \log \det\Delta^{\mathbf{m}_{1,2}} = \partial_t \log \det\Delta^{\mathbf{m}_{1,2}^\epsilon}. \tag{8.26}$$

To establish the lemma consider for definiteness the pair $\mathbf{m}_1$ and $\mathbf{m}_1(\epsilon)$. Due to the analytic surgery formulas from Sect. 8.4.1 one has

$$\det\Delta^{\mathbf{m}_1} = \left\{ \prod_{k=1}^N \det(\Delta^{\mathbf{m}_1}|D_k(\epsilon)) \right\} \det(\Delta^{\mathbf{m}_1}|\Sigma) \det R \left\{ \mathrm{Area}(\mathcal{X}, \mathbf{m}_1) \right\} \left\{ l(\Gamma) \right\}^{-1}, \tag{8.27}$$

$$\det\Delta^{\mathbf{m}_1^\epsilon} = \left\{ \prod_{k=1}^N \det(\Delta^{\mathbf{m}_1^\epsilon}|D_k(\epsilon)) \right\} \det(\Delta^{\mathbf{m}_1^\epsilon}|\Sigma) \det R \left\{ \mathrm{Area}(\mathcal{X}, \mathbf{m}_1^\epsilon) \right\} \left\{ l(\Gamma) \right\}^{-1}, \tag{8.28}$$

with $\Sigma = \mathcal{X} \setminus \cup_{k=1}^N D_k(\epsilon)$.

Notice that the variations of the logarithms of the first factors in the right hand sides of (8.27) and (8.28) vanish (these factors are independent of t) whereas the variations of the logarithms of all the remaining factors coincide. This leads to (8.26).

By virtue of Lemma 1 one has the relation

$$\partial_t \left\{ \log \frac{\det\varDelta^{\mathbf{m}_1}}{\mathrm{Area}(\mathcal{X}, \mathbf{m}_1)} - \log \frac{\det\varDelta^{\mathbf{m}_2}}{\mathrm{Area}(\mathcal{X}, \mathbf{m}_2)} \right\} =$$

$$\partial_t \left\{ \log \frac{\det\varDelta^{\mathbf{m}_1^\epsilon}}{\mathrm{Area}(\mathcal{X}, \mathbf{m}_1^\epsilon)} - \log \frac{\det\varDelta^{\mathbf{m}_2^\epsilon}}{\mathrm{Area}(\mathcal{X}, \mathbf{m}_2^\epsilon)} \right\} . \tag{8.29}$$

By virtue of Polyakov's formula the r.h.s. of (8.29) can be rewritten as

$$\sum_{k=1}^{N} \frac{1}{3\pi} \partial_t \int_{D_k(\epsilon)} (\log H_k)_{x_k \bar{x}_k} \log |f_k| \widehat{\mathrm{d}x_k} -$$

$$\sum_{l=1}^{M} \frac{1}{3\pi} \partial_t \int_{D_{N+l}(\epsilon)} (\log H_{N+l})_{y_l \bar{y}_l} \log |g_l| \widehat{\mathrm{d}y_l} , \tag{8.30}$$

where $H_k(x_k) = \epsilon^{-a_k} h_k^{-1}(|x_k|/\epsilon)$, $k = 1, \ldots, N$ and $H_{N+l}(y_l) = \epsilon^{-b_l} h_{N+l}^{-1}(|y_l|/\epsilon)$, $l = 1, \ldots, M$. Notice that for $k = 1, \ldots, N$ the function H_k coincides with $|x_k|^{-a_k}$ in a vicinity of the circle $\{|x_k| = \epsilon\}$ and the Green formula implies that

$$\int_{D_k(\epsilon)} (\log H_k)_{x_k \bar{x}_k} \log |f_k| \widehat{\mathrm{d}w_k} = \frac{\mathrm{i}}{2} \left\{ \oint_{|x_k|=\epsilon} (\log |x_k|^{-a_k})_{\bar{x}_k} \log |f_k| \mathrm{d}\bar{x}_k + \right.$$

$$\left. + \oint_{|x_k|=\epsilon} \log |x_k|^{-a_k} (\log |f_k|)_{x_k} \mathrm{d}x_k + \int_{D_k(\epsilon)} (\log |f_k|)_{x_k \bar{x}_k} \log H_k \mathrm{d}x_k \wedge \mathrm{d}\bar{x}_k \right\}$$

and, therefore,

$$\partial_t \int_{D_k(\epsilon)} (\log H_k)_{x_k \bar{x}_k} \log |f_k| \widehat{\mathrm{d}x_k} = -\frac{a_k \pi}{2} \partial_t \log |\mathbf{f}_k| + o(1) \tag{8.31}$$

as $\epsilon \to 0$. Analogously

$$\partial_t \int_{D_{N+l}(\epsilon)} (\log H_{N+l})_{y_l \bar{y}_l} \log |g_l| \widehat{\mathrm{d}y_l} = -\frac{b_l \pi}{2} \partial_t \log |\mathbf{g}_l| + o(1) \tag{8.32}$$

as $\epsilon \to 0$.

Formula (8.25) follows from (8.29), (8.31) and (8.32). $\square$

8.4.4 Lemma on Three Polyhedra

For any metric $\mathbf{m}$ on $\mathcal{X}$ denote by $Q(\mathbf{m})$ the ratio $\det \varDelta^{\mathbf{m}}/\mathrm{Area}(\mathcal{X}, \mathbf{m})$.

Consider three families of flat conical metrics $\mathbf{l}(t) \sim \mathbf{m}(t) \sim \mathbf{n}(t)$ on $\mathcal{X}$ (here $\sim$ means conformal equivalence), where the metric $\mathbf{l}(t)$ has conical points $P_1(t), \ldots, P_L(t)$ with conical angles $2\pi(a_1 + 1), \ldots, 2\pi(a_L + 1)$,

the metric $\mathbf{m}(t)$ has conical points $Q_1(t),\ldots,Q_M(t)$ with conical angles $2\pi(b_1 + 1),\ldots,2\pi(b_M + 1)$ and the metric $\mathbf{n}(t)$ has conical points $R_1(t),\ldots,$ $R_N(t)$ with conical angles $2\pi(c_1 + 1),\ldots,2\pi(c_N + 1)$.

Let x_k be the distinguished local parameter for $\mathbf{l}(t)$ near $P_k(t)$ and let $\mathbf{m}(t) = |f_k(x_k)|^2|dx_k|^2$ and $\mathbf{n}(t) = |g_k(x_k)|^2|dx_k|^2$ near $P_k(t)$. Let ξ be an arbitrary conformal local coordinate in a vicinity of the point $P_k(t)$. Then one has $\mathbf{m} = |f(\xi)|^2|d\xi|^2$ and $\mathbf{n} = |g(\xi)|^2|d\xi|^2$ with some holomorphic functions f and g and the ratio

$$\frac{\mathbf{m}(t)}{\mathbf{n}(t)}(P_k(t)) := \frac{|f(0)|^2}{|g(0)|^2}$$

is independent of the choice of the conformal local coordinate. In particular it coincides with the ratio $|f_k(0)|^2/|g_k(0)|^2$.

From Proposition 2, one gets the relation

$$1 = \left\{ \frac{Q(\mathbf{l}(t))}{Q(\mathbf{m}(t))} \frac{Q(\mathbf{m}(t))}{Q(\mathbf{n}(t))} \frac{Q(\mathbf{n}(t))}{Q(\mathbf{l}(t))} \right\}^{-12} =$$

$$\mathrm{C} \prod_{i=1}^{N} \left[\frac{\mathbf{l}(t)}{\mathbf{m}(t)}(R_i(t)) \right]^{c_i} \prod_{j=1}^{L} \left[\frac{\mathbf{m}(t)}{\mathbf{n}(t)}(P_j(t)) \right]^{a_j} \prod_{k=1}^{M} \left[\frac{\mathbf{n}(t)}{\mathbf{l}(t)}(Q_k(t)) \right]^{b_k}, \quad (8.33)$$

where the constant C is independent of t.

From the following statement (which we call *the lemma on three polyhedra*) one can see that the constant C in (8.33) is equal to 1.

Lemma 2. *Let $\mathcal{X}$ be a compact Riemann surface and let $\mathbf{l}$, $\mathbf{m}$ and $\mathbf{n}$ be three conformal flat conical metrics on $\mathcal{X}$. Suppose that the metric $\mathbf{l}$ has conical points $P_1,\ldots,P_L$ with conical angles $2\pi(a_1 + 1),\ldots,2\pi(a_L + 1)$, the metric $\mathbf{m}$ has conical points $Q_1,\ldots,Q_M$ with conical angles $2\pi(b_1 + 1),\ldots,$ $2\pi(b_M + 1)$ and the metric $\mathbf{n}$ has conical points $R_1,\ldots,R_N$ with conical angles $2\pi(c_1 + 1),\ldots,2\pi(c_N + 1)$. (All the points P_l, Q_m, R_n are supposed to be distinct.) Then one has the relation*

$$\prod_{i=1}^{N} \left[\frac{\mathbf{l}}{\mathbf{m}}(R_i) \right]^{c_i} \prod_{j=1}^{L} \left[\frac{\mathbf{m}}{\mathbf{n}}(P_j) \right]^{a_j} \prod_{k=1}^{M} \left[\frac{\mathbf{n}}{\mathbf{l}}(Q_k) \right]^{b_k} = 1. \quad (8.34)$$

Proof. When all three metrics $\mathbf{l}$, $\mathbf{m}$ and $\mathbf{n}$ have trivial holonomy, i.e., one has $\mathbf{l} = |\omega_1|^2$, $\mathbf{m} = |\omega_2|^2$ and $\mathbf{n} = |\omega_3|^2$ with some holomorphic one-forms ω_1, ω_2 and ω_3, relation (8.34) is an immediate consequence of the Weil reciprocity law (see [GH78], §2.3). In the general case the statement reduces to an analog of the Weil reciprocity law for harmonic functions with isolated singularities. $\square$

8.5 Polyhedral Tori

Here we establish a formula for the determinant of the Laplacian on a polyhedral torus, i.e., a Riemann surface of genus one with flat conical metric. We do this by comparing this determinant with the determinant of the Laplacian

corresponding to the smooth flat metric on the same torus. For the latter Laplacian the spectrum is easy to find and the determinant is explicitly known (it is given by the Ray–Singer formula stated below).

In this section $\mathcal{X}$ is an elliptic ($g = 1$) curve and it is assumed that $\mathcal{X}$ is the quotient of the complex plane $\mathbb{C}$ by the lattice generated by 1 and σ, where $\Im\sigma > 0$. The differential dz on $\mathbb{C}$ gives rise to a holomorphic differential v_0 on $\mathcal{X}$ with periods 1 and σ.

Ray–Singer Formula

Let Δ be the Laplacian on $\mathcal{X}$ corresponding to the flat smooth metric $|v_0|^2$. The following formula for $\det\Delta$ was proved in [Ray73]:

$$\det\Delta = C|\Im\sigma|^2|\eta(\sigma)|^4 , \qquad (8.35)$$

where C is a σ-independent constant and η is the Dedekind eta-function.

8.5.1 Determinant of the Laplacian on a Polyhedral Torus

Let $\sum_{k=1}^{N} b_k P_k$ be a generalized divisor on $\mathcal{X}$ with $\sum_{k=1}^{N} b_k = 0$ and assume that $b_k > -1$ for all k. Let $\mathbf{m}$ be a flat conical metric corresponding to this divisor via Troyanov's theorem. Clearly, it has a finite area and is defined uniquely when this area is fixed. Fixing numbers $b_1, \ldots, b_N > -1$ such that $\sum_{k=1}^{N} b_k = 0$, we define the space $\mathcal{M}(b_1, \ldots, b_N)$ as the moduli space of pairs $(\mathcal{X}, \mathbf{m})$, where $\mathcal{X}$ is an elliptic curve and $\mathbf{m}$ is a flat conformal metric on $\mathcal{X}$ having N conical singularities with conical angles $2\pi(b_k + 1)$, $k = 1, \ldots, N$. The space $\mathcal{M}(b_1, \ldots, b_N)$ is a connected orbifold of real dimension $2N + 3$.

We are going to give an explicit formula for the function

$$\mathcal{M}(\beta_1, \ldots, \beta_N) \ni (\mathcal{X}, \mathbf{m}) \mapsto \det\Delta^{\mathbf{m}} .$$

Write the normalized holomorphic differential v_0 on the elliptic curve $\mathcal{X}$ in the distinguished local parameter x_k near the conical point P_k ($k = 1, \ldots, N$) as

$$v_0 = f_k(x_k)dx_k$$

and define

$$\mathbf{f}_k := f_k(x_k)|_{x_k=0}, \ \ k = 1, \ldots, N . \qquad (8.36)$$

Theorem 2. *The following formula holds true*

$$\det\Delta^{\mathbf{m}} = C|\Im\sigma| \operatorname{Area}(\mathcal{X}, \mathbf{m}) |\eta(\sigma)|^4 \prod_{k=1}^{N} |\mathbf{f}_k|^{-b_k/6} , \qquad (8.37)$$

where C is a constant depending only on $b_1, \ldots, b_N$.

Proof. The theorem immediately follows from (8.35) and (8.25).

8.6 Polyhedral Surfaces of Higher Genus

Here we generalize the results of the previous section to the case of polyhedral surfaces of an arbitrary genus. Among all polyhedral surfaces of genus $g \geq 1$ we distinguish *flat surfaces with trivial holonomy*. In our calculation of the determinant of the Laplacian, it is this class of surfaces which plays the role of the smooth flat tori in genus one. For flat surfaces with trivial holonomy we find an explicit expression for the determinant of the Laplacian which generalizes the Ray–Singer formula (8.35) for smooth flat tori. As we did in genus one, comparing two determinants of the Laplacians by means of Proposition 2, we derive a formula for the determinant of the Laplacian on a general polyhedral surface.

8.6.1 Flat Surfaces with Trivial Holonomy and Moduli Spaces of Holomorphic Differentials on Riemann Surfaces

We follow [KZ03] and Zorich's survey [Zor06]. Outside the vertices a Euclidean polyhedral surface $\mathcal{X}$ is locally isometric to a Euclidean plane and one can define the parallel transport along paths on the punctured surface $\mathcal{X} \setminus \{P_1, \ldots, P_N\}$. The parallel transport along a homotopically nontrivial loop in $\mathcal{X} \setminus \{P_1, \ldots, P_N\}$ is generally nontrivial. If, e.g., a small loop encircles a conical point P_k with conical angle β_k, then a tangent vector to $\mathcal{X}$ turns by β_k after the parallel transport along this loop.

A Euclidean polyhedral surface $\mathcal{X}$ is called *a surface with trivial holonomy* if the parallel transport along any loop in $\mathcal{X} \setminus \{P_1, \ldots, P_N\}$ does not change tangent vectors to $\mathcal{X}$.

All conical points of a surface with trivial holonomy must have conical angles which are integer multiples of 2π.

A flat conical metric g on a compact real oriented two-dimensional manifold $\mathcal{X}$ equips $\mathcal{X}$ with the structure of a compact Riemann surface, if this metric has trivial holonomy then it necessarily has the form $g = |w|^2$, where w is a holomorphic differential on the Riemann surface $\mathcal{X}$ (see [Zor06]). The holomorphic differential w has zeros at the conical points of the metric g. The multiplicity of the zero at the point P_m with the conical angle $2\pi(k_m + 1)$ is equal to k_m.[1]

The holomorphic differential w is defined up to a unitary complex factor. This ambiguity can be avoided if the surface $\mathcal{X}$ is provided with a distinguished

---

[1] There exist polyhedral surfaces with nontrivial holonomy whose conical angles are all integer multiples of 2π. To construct an example take a compact Riemann surface $\mathcal{X}$ of genus $g > 1$ and choose $2g - 2$ points $P_1, \ldots, P_{2g-2}$ on $\mathcal{X}$ in such a way that the divisor $P_1 + \cdots + P_{2g-2}$ is not in the canonical class. Consider the flat conical conformal metric **m** corresponding to the divisor $P_1 + \cdots + P_{2g-2}$ according to the Troyanov theorem. This metric must have nontrivial holonomy and all its conical angles are equal to 4π.

direction (see [Zor06]), and it is assumed that w is real along this distinguished direction. In what follows we always assume that surfaces with trivial holonomy are provided with such a direction.

Thus, to a Euclidean polyhedral surface of genus g with trivial holonomy we put into correspondence a pair $(\mathcal{X}, w)$, where $\mathcal{X}$ is a compact Riemann surface and ω is a holomorphic differential on this surface. This means that we get an element of *the moduli space*, $\mathcal{H}_g$, *of holomorphic differentials over Riemann surfaces of genus g* (see [KZ03]).

The space $\mathcal{H}_g$ is stratified according to the multiplicities of zeros of w.

Denote by $\mathcal{H}_g(k_1, \ldots, k_M)$ the stratum of $\mathcal{H}_g$, consisting of differentials w which have M zeros on $\mathcal{X}$ of multiplicities $(k_1, \ldots, k_M)$. Denote the zeros of w by $P_1, \ldots, P_M$; then the divisor of the differential w is given by $(w) = \sum_{m=1}^{M} k_m P_m$. Let us choose a canonical basis of cycles (a_α, b_α) on the Riemann surface $\mathcal{X}$ and cut $\mathcal{X}$ along these cycles starting at the same point to get the fundamental polygon $\hat{\mathcal{X}}$. Inside $\hat{\mathcal{X}}$ we choose $M-1$ (homology classes of) paths l_m on $\mathcal{X} \setminus (w)$ connecting the zero P_1 with other zeros P_m of w, $m = 2, \ldots, M$. Then the local coordinates on $\mathcal{H}_g(k_1, \ldots, k_M)$ can be chosen as follows [KZ97]:

$$A_\alpha := \oint_{a_\alpha} w \ , \quad B_\alpha := \oint_{b_\alpha} w \ , \quad z_m := \int_{l_m} w \ , \quad \alpha = 1, \ldots, g; \ m = 2, \ldots, M \ .$$

$$(8.38)$$

The area of the surface $\mathcal{X}$ in the metric $|w|^2$ can be expressed in terms of these coordinates as follows:

$$\text{Area}(\mathcal{X}, |w|^2) = \Im \sum_{\alpha=1}^{g} A_\alpha \bar{B}_\alpha \ .$$

If all zeros of w are simple, we have $M = 2g - 2$; therefore, the dimension of the highest stratum $\mathcal{H}_g(1, \ldots, 1)$ equals $4g - 3$.

The Abelian integral $z(P) = \int_{P_1}^{P} w$ provides a local coordinate in a neighborhood of any point $P \in \mathcal{X}$ except the zeros $P_1, \ldots, P_M$. In a neighborhood of P_m the local coordinate can be chosen to be $(z(P) - z_m)^{1/(k_m+1)}$.

Remark 3. The following construction helps to visualize these coordinates in the case of the highest stratum $H_g(1, \ldots, 1)$.

Consider g parallelograms $\Pi_1, \ldots, \Pi_g$ in the complex plane with coordinate z having the sides $(A_1, B_1), \ldots, (A_g, B_g)$. Provide these parallelograms with a system of cuts

$$[0, z_2], \quad [z_3, z_4], \quad \ldots, \quad [z_{2g-3}, z_{2g-2}]$$

(each cut should be repeated on two different parallelograms). Identifying opposite sides of the parallelograms and gluing the obtained g tori along the cuts, we get a compact Riemann surface $\mathcal{X}$ of genus g. Moreover, the differential dz on the complex plane gives rise to a holomorphic differential

w on $\mathcal{X}$ which has $2g - 2$ zeros at the ends of the cuts. Thus, we get a point $(\mathcal{X}, w)$ from $\mathcal{H}_g(1, \ldots, 1)$. It can be shown that any generic point of $\mathcal{H}_g(1, \ldots, 1)$ can be obtained via this construction; more sophisticated gluing is required to represent points of other strata, or non generic points of the stratum $\mathcal{H}_g(1, \ldots, 1)$.

To shorten the notations it is convenient to consider the coordinates A_α, B_α, z_m altogether. Namely, in the sequel we shall denote them by ζ_k, $k = 1, \ldots, 2g + M - 1$, where

$$\zeta_\alpha := A_\alpha \ , \quad \zeta_{g+\alpha} := B_\alpha \ , \quad \alpha = 1, \ldots, g \ , \quad \zeta_{2g+m} := z_{m+1} \ , \quad m = 1, \ldots, M-1 \ . \tag{8.39}$$

Let us also introduce corresponding cycles s_k, $k = 1, \ldots, 2g + M - 1$, as follows:

$$s_\alpha = -b_\alpha \ , \quad s_{g+\alpha} = a_\alpha \ , \quad \alpha = 1, \ldots, g \ ; \tag{8.40}$$

the cycle s_{2g+m}, $m = 1, \ldots, M - 1$ is defined to be the small circle with positive orientation around the point P_{m+1}.

Variational Formulas on the Spaces of Holomorphic Differentials

In the previous section we introduced the coordinates on the space of surfaces with trivial holonomy and fixed the type of conical singularities. Here we study the behavior of basic objects on these surfaces under the change of the coordinates. In particular, we derive variational formulas of Rauch type for the matrix of **b**-periods of the underlying Riemann surfaces. We also give variational formulas for the Green function, individual eigenvalues, and the determinant of the Laplacian on these surfaces.

Rauch formulas on the spaces of holomorphic differentials. For any compact Riemann surface $\mathcal{X}$ we introduce the prime-form $E(P, Q)$ and the canonical meromorphic bidifferential

$$\mathbf{w}(P, Q) = \mathrm{d}_P \mathrm{d}_Q \log E(P, Q) \tag{8.41}$$

(see [Fay92]). The bidifferential $\mathbf{w}(P, Q)$ has the following local behavior as $P \to Q$:

$$\mathbf{w}(P, Q) = \left(\frac{1}{(x(P) - x(Q))^2} + \frac{1}{6} S_B(x(P)) + o(1) \right) \mathrm{d}x(P) \mathrm{d}x(Q) \ , \quad (8.42)$$

where $x(P)$ is a local parameter. The term $S_B(x(P))$ is a projective connection which is called *the Bergman projective connection* (see [Fay92]).

Denote by $v_\alpha(P)$ the basis of holomorphic 1-forms on $\mathcal{X}$ normalized by $\int_{a_\alpha} v_\beta = \delta_{\alpha\beta}$.

The matrix of **b**-periods of the surface $\mathcal{X}$ is given by $\mathbf{B}_{\alpha\beta} := \oint_{b_\alpha} v_\beta$.

Proposition 3. *(see [KK09]) Let a pair $(\mathcal{X}, w)$ belong to the space $\mathcal{H}_g(k_1, \ldots, k_M)$. Under variations of the coordinates on $\mathcal{H}_g(k_1, \ldots, k_M)$ the normalized holomorphic differentials and the matrix of $\mathbf{b}$-periods of the surface $\mathcal{X}$ behave as follows:*

$$\left.\frac{\partial v_\alpha(P)}{\partial \zeta_k}\right|_{z(P)} = \frac{1}{2\pi i} \oint_{s_k} \frac{v_\alpha(Q)\mathbf{w}(P,Q)}{w(Q)}, \qquad (8.43)$$

$$\frac{\partial \mathbf{B}_{\alpha\beta}}{\partial \zeta_k} = \oint_{s_k} \frac{v_\alpha v_\beta}{w}, \qquad (8.44)$$

where $k = 1, \ldots, 2g + M - 1$; we assume that the local coordinate $z(P) = \int_{P_1}^{P} w$ is kept constant under differentiation.

   Variation of the resolvent kernel and eigenvalues. For a pair $(\mathcal{X}, w)$ from $\mathcal{H}_g(k_1, \ldots, k_M)$ introduce the Laplacian $\Delta := \Delta^{|w|^2}$ in the flat conical metric $|w|^2$ on $\mathcal{X}$ (recall that we always deal with the Friedrichs extensions). The corresponding resolvent kernel $G(P, Q; \lambda)$, $\lambda \in \mathbb{C} \setminus \mathrm{sp}(\Delta)$

- Satisfies $(\Delta_P - \lambda)G(P, Q; \lambda) = (\Delta_Q - \lambda)G(P, Q; \lambda) = 0$ outside the diagonal $\{P = Q\}$
- Is bounded near the conical points, i.e., for any $P \in \mathcal{X} \setminus \{P_1, \ldots, P_M\}$

$$G(P, Q; \lambda) = O(1)$$

   as $Q \to P_k$, $k = 1, \ldots, M$
- Obeys the asymptotics

$$G(P, Q; \lambda) = \frac{1}{2\pi} \log |x(P) - x(Q)| + O(1)$$

   as $P \to Q$, where $x(\cdot)$ is an arbitrary (holomorphic) local parameter near P

The following proposition is an analog of the classical Hadamard formula for the variation of the Green function of the Dirichlet problem in a plane domain.

Proposition 4. *The following variational formulas for the resolvent kernel $G(P, Q; \lambda)$ hold:*

$$\frac{\partial G(P, Q; \lambda)}{\partial A_\alpha} = 2i \int_{\mathbf{b}_\alpha} \omega(P, Q; \lambda), \qquad (8.45)$$

$$\frac{\partial G(P, Q; \lambda)}{\partial B_\alpha} = -2i \int_{\mathbf{a}_\alpha} \omega(P, Q; \lambda), \qquad (8.46)$$

where

$$\omega(P, Q; \lambda) = G(P, z; \lambda)G_{z\bar{z}}(Q, z; \lambda)\overline{dz} + G_z(P, z; \lambda)G_z(Q, z; \lambda)dz$$

is a closed 1-*form and* $\alpha = 1, \dots, g$;

$$\frac{\partial G(P, Q; \lambda)}{\partial z_m} = -2\mathrm{i} \lim_{\epsilon \to 0} \oint_{|z - z_m| = \epsilon} G_z(z, P; \lambda) G_z(z, Q; \lambda) \mathrm{d}z \,, \qquad (8.47)$$

where $m = 2, \dots, M$. *It is assumed that the coordinates* $z(P)$ *and* $z(Q)$ *are kept constant under variation of the moduli* A_α, B_α, z_m.

Remark 4. One can combine the formulas (8.45-8.47) into a single formula:

$$\frac{\partial G(P, Q; \lambda)}{\partial \zeta_k} =$$

$$-2\mathrm{i} \left\{ \int_{s_k} \frac{G(R, P; \lambda) \partial_R \overline{\partial_R} G(R, Q; \lambda) + \partial_R G(R, P; \lambda) \partial_R G(R, Q; \lambda)}{w(R)} \right\} \,, \quad (8.48)$$

where $k=1, \dots, 2g+M-1$.

Proof. We start with the following integral representation of a solution u to the homogeneous equation $\Delta u - \lambda u = 0$ inside the fundamental polygon $\hat{\mathcal{X}}$:

$$u(\xi, \bar{\xi}) = -2\mathrm{i} \int_{\partial \hat{\mathcal{X}}} G(z, \bar{z}, \xi, \bar{\xi}; \lambda) u_{\bar{z}}(z, \bar{z}) \mathrm{d}\bar{z} + G_z(z, \bar{z}, \xi, \bar{\xi}; \lambda) u(z, \bar{z}) \mathrm{d}z \,. \quad (8.49)$$

Cutting the surface $\mathcal{X}$ along the basic cycles, we notice that the function $\dot{G}(P, \, \cdot \, ; \lambda) = \frac{\partial G(P, \, \cdot \, ; \lambda)}{\partial B_\beta}$ is a solution to the homogeneous equation $\Delta u - \lambda u = 0$ inside the fundamental polygon (the singularity of $G(P, Q; \lambda)$ at $Q = P$ disappears after differentiation) and that the functions $\dot{G}(P, \, \cdot \, ; \lambda)$ and $\dot{G}_{\bar{z}}(P, \, \cdot \, ; \lambda)$ have the jumps $G_z(P, \, \cdot \, ; \lambda)$ and $G_{z\bar{z}}(P, \, \cdot \, ; \lambda)$ on the cycle $\mathbf{a}_\beta$. Applying (8.49) with $u = \dot{G}(P, \, \cdot \, ; \lambda)$, we get (8.46). Formula (8.45) can be proved in the same manner.

The relation $\mathrm{d}\omega(P, Q; \lambda) = 0$ immediately follows from the equality $G_{z\bar{z}}(z, \bar{z}, P; \lambda) = \frac{\lambda}{4} G(z, \bar{z}, P; \lambda)$.

Let us prove (8.47). From now on we assume for simplicity that $k_m = 1$, where k_m is the multiplicity of the zero P_m of the holomorphic differential w.

Applying Green's formula (8.49) to the domain $\hat{\mathcal{X}} \setminus \{|z - z_m| < \epsilon\}$ and $u = \dot{G} = \frac{\partial G}{\partial z_m}$, one gets

$$\dot{G}(P, Q; \lambda) =$$

$$2\mathrm{i} \lim_{\epsilon \to 0} \oint_{|z - z_m| = \epsilon} \dot{G}_{\bar{z}}(z, \bar{z}, Q; \lambda) G(z, \bar{z}, P; \lambda) \mathrm{d}\bar{z} + \dot{G}(z, \bar{z}, Q; \lambda) G_z(z, \bar{z}, P; \lambda) \mathrm{d}z \,.$$
$$(8.50)$$

Observe that the function $x_m \mapsto G(x_m, \bar{x}_m, P; \lambda)$ (defined in a small neighborhood of the point $x_m = 0$) is a bounded solution to the elliptic equation

$$\frac{\partial^2 G(x_m, \bar{x}_m, P; \lambda)}{\partial x_m \partial \bar{x}_m} - \lambda |x_m|^2 G(x_m, \bar{x}_m, P; \lambda) = 0$$

with real analytic coefficients and, therefore, is real analytic near $x_m = 0$.

From now on we write x instead of $x_m = \sqrt{z - z_m}$. Differentiating the expansion

$$G(x, \bar{x}, P; \lambda) = a_0(P, \lambda) + a_1(P, \lambda)x + a_2(P, \lambda)\bar{x} + a_3(P, \lambda)x\bar{x} + \dots \quad (8.51)$$

with respect to z_m, z and $\bar{z}$, one gets the asymptotics

$$\dot{G}(z, \bar{z}, Q; \lambda) = -\frac{a_1(Q, \lambda)}{2x} + O(1) , \quad (8.52)$$

$$\dot{G}_{\bar{z}}(z, \bar{z}, Q; \lambda) = \frac{\dot{a}_2(Q, \lambda)}{2\bar{x}} - \frac{a_3(Q, \lambda)}{4x\bar{x}} + O(1) , \quad (8.53)$$

$$G_z(z, \bar{z}, P; \lambda) = \frac{a_1(P, \lambda)}{2x} + O(1) . \quad (8.54)$$

Substituting (8.52), (8.53) and (8.54) into (8.50), we get the relation

$$\dot{G}(P, Q, \lambda) = 2\pi a_1(P, \lambda)a_1(Q, \lambda) .$$

On the other hand, calculation of the right hand side of formula (8.47) via (8.54) leads to the same result. $\square$

Now we give a variation formula for an eigenvalue of the Laplacian on a flat surface with trivial holonomy.

Proposition 5. *Let λ be an eigenvalue of Δ (for simplicity we assume it to have multiplicity one) and let ϕ be the corresponding normalized eigenfunction. Then*

$$\frac{\partial \lambda}{\partial \zeta_k} = 2\mathrm{i} \int_{s_k} \left(\frac{(\partial\phi)^2}{w} + \frac{1}{4}\lambda\phi^2\bar{w} \right) , \quad (8.55)$$

where $k = 1, \dots, 2g + M - 1$.

Proof. For brevity we give the proof only for the case $k = g + 1, \dots, 2g$. One has

$$\iint_{\hat{L}} \phi\dot{\phi} = \frac{1}{\lambda} \iint_{\hat{\mathcal{X}}} \Delta\phi\,\dot{\phi} = \frac{1}{\lambda} \left\{ 2\mathrm{i} \int_{\partial\hat{\mathcal{X}}} (\phi_{\bar{z}}\dot{\phi}\mathrm{d}\bar{z} + \phi\dot{\phi}_z\,\mathrm{d}z) + \iint_{\hat{\mathcal{X}}} \phi(\lambda\phi)^{\cdot} \right\} =$$

$$\frac{1}{\lambda} \left\{ 2\mathrm{i} \int_{\mathbf{a}_\beta} (\phi_{\bar{z}}\phi_z\,\mathrm{d}\bar{z} + \phi\phi_{zz}\,\mathrm{d}z) + \dot{\lambda} + \lambda \iint_{\hat{\mathcal{X}}} \phi\dot{\phi} \right\} .$$

This implies (8.55) after integration by parts (one has to make use of the relation $\mathrm{d}(\phi\phi_z) = \phi_z^2\mathrm{d}z + \phi\phi_{zz}\mathrm{d}z + \phi_{\bar{z}}\phi_z\mathrm{d}\bar{z} + \frac{1}{4}\lambda\phi^2\mathrm{d}\bar{z}$). $\square$

Variation of the determinant of the Laplacian. For simplicity we consider only flat surfaces with trivial holonomy having $2g - 2$ conical points with conical angles 4π. The proof of the following proposition can be found in [KK09].

Proposition 6. *Let* $(\mathcal{X}, w) \in \mathcal{H}_g(1, \ldots, 1)$. *Introduce the notation*

$$\mathbb{Q}(\mathcal{X}, |w|^2) := \left\{ \frac{\det \Delta^{|w|^2}}{\mathrm{Area}(\mathcal{X}, |w|^2) \det \Im \mathbf{B}} \right\}, \tag{8.56}$$

where $\mathbf{B}$ *is the matrix of* $\mathbf{b}$*-periods of the surface* $\mathcal{X}$ *and* $\mathrm{Area}(\mathcal{X}, |w|^2)$ *denotes the area of* $\mathcal{X}$ *in the metric* $|w|^2$.

The following variational formulas hold

$$\frac{\partial \log \mathbb{Q}(\mathcal{X}, |w|^2)}{\partial \zeta_k} = -\frac{1}{12\pi \mathrm{i}} \oint_{s_k} \frac{S_B - S_w}{w}, \tag{8.57}$$

where $k = 1, \ldots, 4g - 3$; S_B *is the Bergman projective connection,* S_w *is the projective connection given by the Schwarzian derivative* $\left\{ \int^P w, x(P) \right\}$; $S_B - S_w$ *is a meromorphic quadratic differential with poles of second order at the zeroes* P_m *of* w.

An Explicit Formula for the Determinant of the Laplacian on a Flat Surface with Trivial Holonomy

We start with recalling the properties of the prime form $E(P, Q)$ (see [Fay73, Fay92], some of these properties were already used in our proof of the Troyanov theorem above).

- The prime form $E(P, Q)$ is an antisymmetric $-1/2$-differential with respect to both P and Q
- Under tracing of Q along the cycle $\mathbf{a}_\alpha$ the prime-form remains invariant; under the tracing along $\mathbf{b}_\alpha$ it gains the factor

$$\exp \left(-\pi \mathrm{i} \mathbf{B}_{\alpha\alpha} - 2\pi \mathrm{i} \int_P^Q v_\alpha \right). \tag{8.58}$$

- On the diagonal $Q \to P$ the prime-form has first order zero with the following asymptotics:

$$E(x(P), x(Q)) \sqrt{\mathrm{d}x(P)} \sqrt{\mathrm{d}x(Q)} =$$

$$(x(Q) - x(P)) \left(1 - \frac{1}{12} S_B(x(P))(x(Q) - x(P))^2 + O((x(Q) - x(P))^3) \right), \tag{8.59}$$

where S_B is the Bergman projective connection and $x(P)$ is an arbitrary local parameter.

The next object we shall need is the vector of Riemann constants:

$$K_\alpha^P = \frac{1}{2} + \frac{1}{2} \mathbf{B}_{\alpha\alpha} - \sum_{\beta=1, \beta \neq \alpha}^{g} \oint_{\mathbf{a}_\beta} \left(v_\beta \int_P^x v_\alpha \right) \tag{8.60}$$

where the interior integral is taken along a path which does not intersect $\partial \widehat{\mathcal{X}}$.

In what follows the pivotal role is played by the holomorphic multivalued $g(1-g)/2$-differential on $\mathcal{X}$

$$\mathcal{C}(P) = \frac{1}{\mathcal{W}[v_1, \ldots, v_g](P)} \sum_{\alpha_1, \ldots, \alpha_g=1}^{g} \frac{\partial^g \Theta(K^P)}{\partial z_{\alpha_1} \ldots \partial z_{\alpha_g}} v_{\alpha_1} \ldots v_{\alpha_g}(P), \qquad (8.61)$$

where Θ is the theta function of the Riemann surface $\mathcal{X}$,

$$\mathcal{W}(P) := \det_{1 \leq \alpha, \beta \leq g} \| v_\beta^{(\alpha-1)}(P) \| \qquad (8.62)$$

is the Wronskian determinant of holomorphic differentials at the point P.

The differential $\mathcal{C}$ has multipliers 1 and $\exp\{-\pi\mathrm{i}(g-1)^2 \mathbf{B}_{\alpha\alpha} - 2\pi\mathrm{i}(g-1) K_\alpha^P\}$ along basic cycles $\mathbf{a}_\alpha$ and $\mathbf{b}_\alpha$, respectively.

In what follows we shall often treat tensor objects like $E(P, Q)$, $\mathcal{C}(P)$, etc. as scalar functions of one of the arguments (or both). This makes sense after fixing the local system of coordinates, which is usually taken to be $z(Q) = \int^Q w$. In particular, the expression "the value of the tensor T at the point Q in local parameter $z(Q)$" denotes the value of the scalar $Tw^{-\alpha}$ at the point Q, where α is the tensor weight of $T(Q)$.

The following proposition was proved in [KK09].

Proposition 7. *Consider the highest stratum $\mathcal{H}_g(1, \ldots, 1)$ of the space $\mathcal{H}_g$ containing Abelian differentials w with simple zeros.*

Let us choose the fundamental polygon $\hat{\mathcal{X}}$ such that $\mathcal{A}_P((w)) + 2K^P = 0$, where $\mathcal{A}_P$ is the Abel map with the initial point P. Consider the following expression

$$\tau(\mathcal{X}, w) = \mathcal{F}^{2/3} \prod_{\substack{m,l=1 \\ m<l}}^{2g-2} [E(Q_m, Q_l)]^{1/6}, \qquad (8.63)$$

where the quantity

$$\mathcal{F} := [w(P)]^{\frac{g-1}{2}} \mathcal{C}(P) \prod_{m=1}^{2g-2} [E(P, Q_m)]^{\frac{(1-g)}{2}} \qquad (8.64)$$

does not depend on P; all prime-forms are evaluated at the zeroes Q_m of the differential w in the distinguished local parameters $x_m(P) = \left(\int_{Q_m}^P w\right)^{1/2}$. Then

$$\frac{\partial \log \tau}{\partial \zeta_k} = -\frac{1}{12\pi\mathrm{i}} \oint_{s_k} \frac{S_B - S_w}{w}, \qquad (8.65)$$

where $k = 1, \ldots, 4g-3$.

The following Theorem immediately follows from Propositions 6 and 7. It can be considered as a natural generalization of the Ray–Singer formula (8.35) to the higher genus case.

Theorem 3. *Let a pair $(\mathcal{X}, w)$ be a point of the space $\mathcal{H}_g(1, \ldots, 1)$. Then the determinant of the Laplacian $\Delta^{|w|^2}$ is given by the following expression*

$$\det \Delta^{|w|^2} = C \; \text{Area}(\mathcal{X}, |w|^2) \det \Im \mathbf{B} \; |\tau(\mathcal{X}, w)|^2 \;, \tag{8.66}$$

where the constant C is independent of a point of $\mathcal{H}_g(1, \ldots, 1)$. Here $\tau(\mathcal{X}, w)$ is given by (8.63).

8.6.2 Determinant of the Laplacian on an Arbitrary Polyhedral Surface of Genus $g > 1$

Let $b_1, \ldots, b_N$ be real numbers such that $b_k > -1$ and $b_1 + \cdots + b_N = 2g - 2$. Denote by $\mathcal{M}_g(b_1, \ldots, b_N)$ the moduli space of pairs $(\mathcal{X}, \mathbf{m})$, where $\mathcal{X}$ is a compact Riemann surface of genus $g > 1$ and $\mathbf{m}$ is a flat conformal conical metric on $\mathcal{X}$ having N conical points with conical angles $2\pi(b_1 + 1), \ldots, 2\pi(b_N + 1)$. The space $\mathcal{M}_g(b_1, \ldots, b_N)$ is a (real) orbifold of (real) dimension $6g + 2N - 5$. Let w be a holomorphic differential with $2g - 2$ simple zeroes on $\mathcal{X}$. Assume also that the set of conical points of the metric $\mathbf{m}$ and the set of zeros of the differential w do not intersect.

Let $P_1, \ldots, P_N$ be the conical points of $\mathbf{m}$ and let $Q_1, \ldots, Q_{2g-2}$ be the zeroes of w. Let x_k be a distinguished local parameter for $\mathbf{m}$ near P_k and y_l be a distinguished local parameter for w near Q_l. Introduce the functions f_k, g_l and the complex numbers $\mathbf{f_k}$, $\mathbf{g_l}$ by

$$|w|^2 = |f_k(x_k)|^2 |dx_k|^2 \quad \text{near} \quad P_k \;; \qquad \mathbf{f_k} := f_k(0),$$

$$\mathbf{m} = |g_l(y_l)|^2 |dy_l|^2 \quad \text{near} \quad Q_l \;; \qquad \mathbf{g_l} := g_l(0) \;.$$

Then from (8.25) and (8.66) and the lemma on three polyhedra from §4.4 one obtains the relation

$$\det \Delta^{\mathbf{m}} = C \text{Area}(\mathcal{X}, \mathbf{m}) \det \Im \mathbf{B} \; |\tau(\mathcal{X}, w)|^2 \frac{\prod_{l=1}^{2g-2} |\mathbf{g_l}|^{1/6}}{\prod_{k=1}^{N} |\mathbf{f_k}|^{b_k/6}} \;, \tag{8.67}$$

where the constant C depends only on $b_1, \ldots, b_N$ (and neither the differential w nor the point $(\mathcal{X}, \mathbf{m}) \in \mathcal{M}_g(b_1, \ldots, b_N)$) and $\tau(\mathcal{X}, w)$ is given by (8.63).

Acknowledgements

References

[AS94] Aurell, E., Salomonson, P.: Further Results on Functional Determinants of Laplacians in Simplicial Complexes, hep-th/9405140

[Bob11] Bobenko, A.I.: Introduction to compact Riemann surfaces. In: Bobenko, A.I., Klein, Ch. (eds.) Lecture Notes in Mathematics 2013, pp. 3–64. Springer, Berlin (2011)

[BFK92] Burghelea, D., Friedlander, L., Kappeler, T.: Meyer-Vietoris type formula for determinants of elliptic differential operators. J. Funct. Anal. **107**, 34–65 (1992)

[Car10] Carslaw, H.S.: The Green's function for a wedge of any angle, and other problems in the conduction of heat. Proc. Lond. Math. Soc. **8**, 365–374 (1910)

[Che83] Cheeger, J.: Spectral geometry of singular Riemannian spaces. J. Diff. Geom. **18**, 575–657 (1983)

[DP89] D'Hoker, E., Phong, D.H.: Functional determinants on Mandelstam diagrams. Comm. Math. Phys. **124**, 629–645 (1989)

[Fay73] Fay, J.D.: Theta-functions on Riemann surfaces. Lect. Notes in Math., vol. 352. Springer, Berlin (1973)

[Fay92] Fay, J.D.: Kernel functions, analytic torsion, and moduli spaces. Memoir. AMS **464** (1992)

[Fur94] Fursaev, D.V.: The heat-kernel expansion on a cone and quantum fields near cosmic strings. Class. Quant. Grav. **11**, 1431–1443 (1994)

[GH78] Griffiths, P., Harris, J.: Principles of Algebraic Geometry. Wiley, New York (1978)

[Kin93] King, h.K.: Determinants of Laplacians on the space of conical metrics on the sphere. Trans. AMS **339**, 525–536 (1993)

[KK07] Klochko, Y., Kokotov, A.: Genus one polyhedral surfaces, spaces of quadratic differentials on tori and determinants of Laplacians. Manuscripta Math. **122**, 195–216 (2007)

[KK04] Kokotov, A., Korotkin, D.: Tau-functions on the spaces of Abelian and quadratic differentials and determinants of Laplacians in Strebel metrics of finite volume, preprint of the Max-Planck Institute for Mathematics in the Science, Leipzig, 46/2004; math.SP/0405042

[Kok07] Kokotov, A.: Preprint (127) of Max-Planck-Institut für Mathematik in Bonn (2007)

[KK09] Kokotov, A., Korotkin, D.: Tau-functions on spaces of Abelian differentials and higher genus generalization of Ray-Singer formula. J. Differ. Geom. **82**, 35–100 (2009)

[Kon67] Kondratjev, V.: Boundary value problems for elliptic equations in domains with conical and angle points. Proc. Moscow Math. Soc. **16**, 219–292 (1967)

[KZ03] Kontsevich, M., Zorich, A.: Connected components of the moduli spaces of holomorphic differentials with prescribed singularities. Invent. Math. **153**, 631–678 (2003)

[KZ97] Kontsevitch, M., Zorich A.: Lyapunov exponents and Hodge theory, hep-th/9701164

[LMP07] Loya, P., McDonald, P., Park, J.: Zeta regularized determinants for conic manifolds. J. Funct. Anal. **242**(1), 195–229 (2007)

[MS67]   McKean, H.P., Singer, I.M.: Curvature and the eigenvalues of the Laplacian. J. Diff. Geom. **1**, 43–69 (1967)

[Moo99] Mooers, E.: Heat kernel asymptotics on manifolds with conic singularities. J. D'Analyse Mathématique, **78**, 1–36 (1999)

[NP92]   Nazarov, S., Plamenevskii, B.: Elliptic boundary value problems in domains with piece-wise smooth boundary, Moscow, "Nauka" (1992)

[OPS88] Osgood, B., Phillips, R., Sarnak, P.: Extremals of determinants of laplacian. J. Funct. Anal. **80**(1), 148–211 (1988)

[Ray73] Ray D.B., Singer I.M.: Analytic torsion for complex manifolds. Ann. Math. **98**(1), 154–177 (1973)

[Tay97] Taylor, M.: Partial Differential Equations, vol. 2. Springer, New York (1996) (Appl. Math. Sci., **116**)

[Tro86] Troyanov, M.: Les surfaces euclidiennes à singularités coniques. L'Enseignement Mathématique, **32**, 79–94 (1986)

[Zor06] Zorich, A.: Flat Surfaces. In Cartier, P., Julia, B., Moussa, P., Vanhove, P. (eds.) Frontiers in Number theory, Physics and Geometry. Vol. 1: On random matrices, zeta functions, and dynamical systems, pp. 439–586. Springer, Berlin (2006)

Index

Lecture Notes in Mathematics

For information about earlier volumes
please contact your bookseller or Springer
LNM Online archive: springerlink.com

Vol. 1867: J. Sneyd (Ed.), Tutorials in Mathematical Biosciences II. Mathematical Modeling of Calcium Dynamics and Signal Transduction. (2005)

Vol. 1868: J. Jorgenson, S. Lang, $Pos_n(R)$ and Eisenstein Series. (2005)

Vol. 1869: A. Dembo, T. Funaki, Lectures on Probability Theory and Statistics. Ecole d'Eté de Probabilités de Saint-Flour XXXIII-2003. Editor: J. Picard (2005)

Vol. 1870: V.I. Gurariy, W. Lusky, Geometry of Mntz Spaces and Related Questions. (2005)

Vol. 1871: P. Constantin, G. Gallavotti, A.V. Kazhikhov, Y. Meyer, S. Ukai, Mathematical Foundation of Turbulent Viscous Flows, Martina Franca, Italy, 2003. Editors: M. Cannone, T. Miyakawa (2006)

Vol. 1872: A. Friedman (Ed.), Tutorials in Mathematical Biosciences III. Cell Cycle, Proliferation, and Cancer (2006)

Vol. 1873: R. Mansuy, M. Yor, Random Times and Enlargements of Filtrations in a Brownian Setting (2006)

Vol. 1874: M. Yor, M. Émery (Eds.), In Memoriam Paul-Andr Meyer - Sminaire de Probabilits XXXIX (2006)

Vol. 1875: J. Pitman, Combinatorial Stochastic Processes. Ecole d'Et de Probabilits de Saint-Flour XXXII-2002. Editor: J. Picard (2006)

Vol. 1876: H. Herrlich, Axiom of Choice (2006)

Vol. 1877: J. Steuding, Value Distributions of L-Functions (2007)

Vol. 1878: R. Cerf, The Wulff Crystal in Ising and Percolation Models, Ecole d'Et de Probabilités de Saint-Flour XXXIV-2004. Editor: Jean Picard (2006)

Vol. 1879: G. Slade, The Lace Expansion and its Applications, Ecole d'Et de Probabilits de Saint-Flour XXXIV-2004. Editor: Jean Picard (2006)

Vol. 1880: S. Attal, A. Joye, C.-A. Pillet, Open Quantum Systems I, The Hamiltonian Approach (2006)

Vol. 1881: S. Attal, A. Joye, C.-A. Pillet, Open Quantum Systems II, The Markovian Approach (2006)

Vol. 1882: S. Attal, A. Joye, C.-A. Pillet, Open Quantum Systems III, Recent Developments (2006)

Vol. 1883: W. Van Assche, F. Marcellàn (Eds.), Orthogonal Polynomials and Special Functions, Computation and Application (2006)

Vol. 1884: N. Hayashi, E.I. Kaikina, P.I. Naumkin, I.A. Shishmarev, Asymptotics for Dissipative Nonlinear Equations (2006)

Vol. 1885: A. Telcs, The Art of Random Walks (2006)

Vol. 1886: S. Takamura, Splitting Deformations of Degenerations of Complex Curves (2006)

Vol. 1887: K. Habermann, L. Habermann, Introduction to Symplectic Dirac Operators (2006)

Vol. 1888: J. van der Hoeven, Transseries and Real Differential Algebra (2006)

Vol. 1889: G. Osipenko, Dynamical Systems, Graphs, and Algorithms (2006)

Vol. 1890: M. Bunge, J. Funk, Singular Coverings of Toposes (2006)

Vol. 1891: J.B. Friedlander, D.R. Heath-Brown, H. Iwaniec, J. Kaczorowski, Analytic Number Theory, Cetraro, Italy, 2002. Editors: A. Perelli, C. Viola (2006)

Vol. 1892: A. Baddeley, I. Bárány, R. Schneider, W. Weil, Stochastic Geometry, Martina Franca, Italy, 2004. Editor: W. Weil (2007)

Vol. 1893: H. Hanßmann, Local and Semi-Local Bifurcations in Hamiltonian Dynamical Systems, Results and Examples (2007)

Vol. 1894: C.W. Groetsch, Stable Approximate Evaluation of Unbounded Operators (2007)

Vol. 1895: L. Molnár, Selected Preserver Problems on Algebraic Structures of Linear Operators and on Function Spaces (2007)

Vol. 1896: P. Massart, Concentration Inequalities and Model Selection, Ecole d'Été de Probabilités de Saint-Flour XXXIII-2003. Editor: J. Picard (2007)

Vol. 1897: R. Doney, Fluctuation Theory for Lévy Processes, Ecole d'Été de Probabilités de Saint-Flour XXXV-2005. Editor: J. Picard (2007)

Vol. 1898: H.R. Beyer, Beyond Partial Differential Equations, On linear and Quasi-Linear Abstract Hyperbolic Evolution Equations (2007)

Vol. 1899: Séminaire de Probabilités XL. Editors: C. Donati-Martin, M. Émery, A. Rouault, C. Stricker (2007)

Vol. 1900: E. Bolthausen, A. Bovier (Eds.), Spin Glasses (2007)

Vol. 1901: O. Wittenberg, Intersections de deux quadriques et pinceaux de courbes de genre 1, Intersections of Two Quadrics and Pencils of Curves of Genus 1 (2007)

Vol. 1902: A. Isaev, Lectures on the Automorphism Groups of Kobayashi-Hyperbolic Manifolds (2007)

Vol. 1903: G. Kresin, V. Maz'ya, Sharp Real-Part Theorems (2007)

Vol. 1904: P. Giesl, Construction of Global Lyapunov Functions Using Radial Basis Functions (2007)

Vol. 1905: C. Prévôt, M. Röckner, A Concise Course on Stochastic Partial Differential Equations (2007)

Vol. 1906: T. Schuster, The Method of Approximate Inverse: Theory and Applications (2007)

Vol. 1907: M. Rasmussen, Attractivity and Bifurcation for Nonautonomous Dynamical Systems (2007)

Vol. 1908: T.J. Lyons, M. Caruana, T. Lévy, Differential Equations Driven by Rough Paths, Ecole d'Été de Probabilités de Saint-Flour XXXIV-2004 (2007)

Vol. 1909: H. Akiyoshi, M. Sakuma, M. Wada, Y. Yamashita, Punctured Torus Groups and 2-Bridge Knot Groups (I) (2007)

Vol. 1910: V.D. Milman, G. Schechtman (Eds.), Geometric Aspects of Functional Analysis. Israel Seminar 2004-2005 (2007)

Vol. 1911: A. Bressan, D. Serre, M. Williams, K. Zumbrun, Hyperbolic Systems of Balance Laws. Cetraro, Italy 2003. Editor: P. Marcati (2007)

Vol. 1912: V. Berinde, Iterative Approximation of Fixed Points (2007)

Vol. 1913: J.E. Marsden, G. Misiołek, J.-P. Ortega, M. Perlmutter, T.S. Ratiu, Hamiltonian Reduction by Stages (2007)

Vol. 1914: G. Kutyniok, Affine Density in Wavelet Analysis (2007)

Vol. 1915: T. Bıyıkoğlu, J. Leydold, P.F. Stadler, Laplacian Eigenvectors of Graphs. Perron-Frobenius and Faber-Krahn Type Theorems (2007)

Vol. 1916: C. Villani, F. Rezakhanlou, Entropy Methods for the Boltzmann Equation. Editors: F. Golse, S. Olla (2008)

Vol. 1917: I. Veselić, Existence and Regularity Properties of the Integrated Density of States of Random Schrdinger (2008)

Vol. 1918: B. Roberts, R. Schmidt, Local Newforms for GSp(4) (2007)

Vol. 1919: R.A. Carmona, I. Ekeland, A. Kohatsu-Higa, J.-M. Lasry, P.-L. Lions, H. Pham, E. Taflin, Paris-Princeton Lectures on Mathematical Finance 2004. Editors: R.A. Carmona, E. inlar, I. Ekeland, E. Jouini, J.A. Scheinkman, N. Touzi (2007)

Vol. 1971: L. Saint-Raymond, Hydrodynamic Limits of the Boltzmann Equation (2009)

Vol. 1972: T. Mochizuki, Donaldson Type Invariants for Algebraic Surfaces (2009)

Vol. 1973: M.A. Berger, L.H. Kauffmann, B. Khesin, H.K. Moffatt, R.L. Ricca, De W. Sumners, Lectures on Topological Fluid Mechanics. Cetraro, Italy 2001. Editor: R.L. Ricca (2009)

Vol. 1974: F. den Hollander, Random Polymers: École d'Été de Probabilités de Saint-Flour XXXVII – 2007 (2009)

Vol. 1975: J.C. Rohde, Cyclic Coverings, Calabi-Yau Manifolds and Complex Multiplication (2009)

Vol. 1976: N. Ginoux, The Dirac Spectrum (2009)

Vol. 1977: M.J. Gursky, E. Lanconelli, A. Malchiodi, G. Tarantello, X.-J. Wang, P.C. Yang, Geometric Analysis and PDEs. Cetraro, Italy 2001. Editors: A. Ambrosetti, S.-Y.A. Chang, A. Malchiodi (2009)

Vol. 1978: M. Qian, J.-S. Xie, S. Zhu, Smooth Ergodic Theory for Endomorphisms (2009)

Vol. 1979: C. Donati-Martin, M. Émery, A. Rouault, C. Stricker (Eds.), Séminaire de Probablitiés XLII (2009)

Vol. 1980: P. Graczyk, A. Stos (Eds.), Potential Analysis of Stable Processes and its Extensions (2009)

Vol. 1981: M. Chlouveraki, Blocks and Families for Cyclotomic Hecke Algebras (2009)

Vol. 1982: N. Privault, Stochastic Analysis in Discrete and Continuous Settings. With Normal Martingales (2009)

Vol. 1983: H. Ammari (Ed.), Mathematical Modeling in Biomedical Imaging I. Electrical and Ultrasound Tomographies, Anomaly Detection, and Brain Imaging (2009)

Vol. 1984: V. Caselles, P. Monasse, Geometric Description of Images as Topographic Maps (2010)

Vol. 1985: T. Linß, Layer-Adapted Meshes for Reaction-Convection-Diffusion Problems (2010)

Vol. 1986: J.-P. Antoine, C. Trapani, Partial Inner Product Spaces. Theory and Applications (2009)

Vol. 1987: J.-P. Brasselet, J. Seade, T. Suwa, Vector Fields on Singular Varieties (2010)

Vol. 1988: M. Broué, Introduction to Complex Reflection Groups and Their Braid Groups (2010)

Vol. 1989: I.M. Bomze, V. Demyanov, Nonlinear Optimization. Cetraro, Italy 2007. Editors: G. di Pillo, F. Schoen (2010)

Vol. 1990: S. Bouc, Biset Functors for Finite Groups (2010)

Vol. 1991: F. Gazzola, H.-C. Grunau, G. Sweers, Polyharmonic Boundary Value Problems (2010)

Vol. 1992: A. Parmeggiani, Spectral Theory of Non-Commutative Harmonic Oscillators: An Introduction (2010)

Vol. 1993: P. Dodos, Banach Spaces and Descriptive Set Theory: Selected Topics (2010)

Vol. 1994: A. Baricz, Generalized Bessel Functions of the First Kind (2010)

Vol. 1995: A.Y. Khapalov, Controllability of Partial Differential Equations Governed by Multiplicative Controls (2010)

Vol. 1996: T. Lorenz, Mutational Analysis. A Joint Framework for Cauchy Problems *In* and *Beyond* Vector Spaces (2010)

Vol. 1997: M. Banagl, Intersection Spaces, Spatial Homology Truncation, and String Theory (2010)

Vol. 1998: M. Abate, E. Bedford, M. Brunella, T.-C. Dinh, D. Schleicher, N. Sibony, Holomorphic Dynamical Systems. Cetraro, Italy 2008. Editors: G. Gentili, J. Guenot, G. Patrizio (2010)

Vol. 1999: H. Schoutens, The Use of Ultraproducts in Commutative Algebra (2010)

Vol. 2000: H. Yserentant, Regularity and Approximability of Electronic Wave Functions (2010)

Vol. 2001: T. Duquesne, O. Reichmann, K.-i. Sato, C. Schwab, Lévy Matters I. Editors: O.E. Barndorff-Nielson, J. Bertoin, J. Jacod, C. Klüppelberg (2010)

Vol. 2002: C. Pötzsche, Geometric Theory of Discrete Nonautonomous Dynamical Systems (2010)

Vol. 2003: A. Cousin, S. Crépey, O. Guéant, D. Hobson, M. Jeanblanc, J.-M. Lasry, J.-P. Laurent, P.-L. Lions, P. Tankov, Paris-Princeton Lectures on Mathematical Finance 2010. Editors: R.A. Carmona, E. Cinlar, I. Ekeland, E. Jouini, J.A. Scheinkman, N. Touzi (2010)

Vol. 2004: K. Diethelm, The Analysis of Fractional Differential Equations (2010)

Vol. 2005: W. Yuan, W. Sickel, D. Yang, Morrey and Campanato Meet Besov, Lizorkin and Triebel (2011)

Vol. 2006: C. Donati-Martin, A. Lejay, W. Rouault (Eds.), Séminaire de Probabilités XLIII (2011)

Vol. 2007: E. Bujalance, F.J. Cirre, J.M. Gamboa, G. Gromadzki, Symmetries of Compact Riemann Surfaces (2010)

Vol. 2008: P.F. Baum, G. Cortiñas, R. Meyer, R. Sánchez-García, M. Schlichting, B. Toën, Topics in Algebraic and Topological K-Theory. Editor: G. Cortiñas (2011)

Vol. 2009: J.-L. Colliot-Thélène, P.S. Dyer, P. Vojta, Arithmetic Geometry. Cetraro, Italy 2007. Editors: P. Corvaja, C. Gasbarri (2011)

Vol. 2010: A. Farina, A. Klar, R.M.M. Mattheij, A. Mikelić, N. Siedow, Mathematical Models in the Manufacturing of Glass. Cetraro, Italy 2008. Editor: A. Fasano (2011)

Vol. 2011: B. Andrews, C. Hopper, The Ricci Flow in Riemannian Geometry, A Complete Proof of the Differentiable 1/4-Pinching Sphere Theorem (2011)

Vol. 2012: A Etheridge, Some Mathematical Models from Population Genetics. École d'Été de Probabilités de Saint-Flour XXXIX-2009 (2011)

Vol. 2013: A.I. Bobenko, C. Klein (Eds.), Computational Approach to Riemann Surfaces (2011)

Recent Reprints and New Editions

Vol. 1702: J. Ma, J. Yong, Forward-Backward Stochastic Differential Equations and their Applications. 1999 – Corr. 3rd printing (2007)

Vol. 830: J.A. Green, Polynomial Representations of GL_n, with an Appendix on Schensted Correspondence and Littelmann Paths by K. Erdmann, J.A. Green and M. Schoker 1980 – 2nd corr. and augmented edition (2007)

Vol. 1693: S. Simons, From Hahn-Banach to Monotonicity (Minimax and Monotonicity 1998) – 2nd exp. edition (2008)

Vol. 470: R.E. Bowen, Equilibrium States and the Ergodic Theory of Anosov Diffeomorphisms. With a preface by D. Ruelle. Edited by J.-R. Chazottes. 1975 – 2nd rev. edition (2008)

Vol. 523: S.A. Albeverio, R.J. Høegh-Krohn, S. Mazzucchi, Mathematical Theory of Feynman Path Integral. 1976 – 2nd corr. and enlarged edition (2008)

Vol. 1764: A. Cannas da Silva, Lectures on Symplectic Geometry 2001 – Corr. 2nd printing (2008)

LECTURE NOTES IN MATHEMATICS

Editorial Policy (for Multi-Author Publications: Summer Schools/Intensive Courses)

1. Lecture Notes aim to report new developments in all areas of mathematics and their applications - quickly, informally and at a high level. Mathematical texts analysing new developments in modelling and numerical simulation are welcome. Manuscripts should be reasonably self-contained and rounded off. Thus they may, and often will, present not only results of the author but also related work by other people. They should provide sufficient motivation, examples and applications. There should also be an introduction making the text comprehensible to a wider audience. This clearly distinguishes Lecture Notes from journal articles or technical reports which normally are very concise. Articles intended for a journal but too long to be accepted by most journals, usually do not have this "lecture notes" character.

2. In general SUMMER SCHOOLS and other similar INTENSIVE COURSES are held to present mathematical topics that are close to the frontiers of recent research to an audience at the beginning or intermediate graduate level, who may want to continue with this area of work, for a thesis or later. This makes demands on the didactic aspects of the presentation. Because the subjects of such schools are advanced, there often exists no textbook, and so ideally, the publication resulting from such a school could be a first approximation to such a textbook. Usually several authors are involved in the writing, so it is not always simple to obtain a unified approach to the presentation.

   For prospective publication in LNM, the resulting manuscript should not be just a collection of course notes, each of which has been developed by an individual author with little or no co-ordination with the others, and with little or no common concept. The subject matter should dictate the structure of the book, and the authorship of each part or chapter should take secondary importance. Of course the choice of authors is crucial to the quality of the material at the school and in the book, and the intention here is not to belittle their impact, but simply to say that the book should be planned to be written by these authors jointly, and not just assembled as a result of what these authors happen to submit.

   This represents considerable preparatory work (as it is imperative to ensure that the authors know these criteria before they invest work on a manuscript), and also considerable editing work afterwards, to get the book into final shape. Still it is the form that holds the most promise of a successful book that will be used by its intended audience, rather than yet another volume of proceedings for the library shelf.

3. Manuscripts should be submitted either online at www.editorialmanager.com/lnm/ to Springer's mathematics editorial, or to one of the series editors. Volume editors are expected to arrange for the refereeing, to the usual scientific standards, of the individual contributions. If the resulting reports can be forwarded to us (series editors or Springer) this is very helpful. If no reports are forwarded or if other questions remain unclear in respect of homogeneity etc, the series editors may wish to consult external referees for an overall evaluation of the volume. A final decision to publish can be made only on the basis of the complete manuscript; however a preliminary decision can be based on a pre-final or incomplete manuscript. The strict minimum amount of material that will be considered should include a detailed outline describing the planned contents of each chapter.

   Volume editors and authors should be aware that incomplete or insufficiently close to final manuscripts almost always result in longer evaluation times. They should also be aware that parallel submission of their manuscript to another publisher while under consideration for LNM will in general lead to immediate rejection.

4. Manuscripts should in general be submitted in English. Final manuscripts should contain at least 100 pages of mathematical text and should always include
   – a general table of contents;
   – an informative introduction, with adequate motivation and perhaps some historical remarks: it should be accessible to a reader not intimately familiar with the topic treated;
   – a global subject index: as a rule this is genuinely helpful for the reader.

   Lecture Notes volumes are, as a rule, printed digitally from the authors' files. We strongly recommend that all contributions in a volume be written in the same LaTeX version, preferably LaTeX2e. To ensure best results, authors are asked to use the LaTeX2e style files available from Springer's web-server at

   ftp://ftp.springer.de/pub/tex/latex/svmonot1/ (for monographs) and
   ftp://ftp.springer.de/pub/tex/latex/svmultt1/ (for summer schools/tutorials).

   Additional technical instructions are available on request from: lnm@springer.com.

5. Careful preparation of the manuscripts will help keep production time short besides ensuring satisfactory appearance of the finished book in print and online. After acceptance of the manuscript authors will be asked to prepare the final LaTeX source files and also the corresponding dvi-, pdf- or zipped ps-file. The LaTeX source files are essential for producing the full-text online version of the book. For the existing online volumes of LNM see: http://www.springerlink.com/openurl.asp?genre=journal&issn=0075-8434.

   The actual production of a Lecture Notes volume takes approximately 12 weeks.

6. Volume editors receive a total of 50 free copies of their volume to be shared with the authors, but no royalties. They and the authors are entitled to a discount of 33.3% on the price of Springer books purchased for their personal use, if ordering directly from Springer.

7. Commitment to publish is made by letter of intent rather than by signing a formal contract. Springer-Verlag secures the copyright for each volume. Authors are free to reuse material contained in their LNM volumes in later publications: a brief written (or e-mail) request for formal permission is sufficient.

Addresses:

Professor J.-M. Morel, CMLA,
École Normale Supérieure de Cachan,
61 Avenue du Président Wilson,
94235 Cachan Cedex, France
E-mail: Jean-Michel.Morel@cmla.ens-cachan.fr

Professor F. Takens, Mathematisch Instituut,
Rijksuniversiteit Groningen, Postbus 800,
9700 AV Groningen, The Netherlands
E-mail: F.Takens@rug.nl

Professor B. Teissier,
Institut Mathématique de Jussieu,
UMR 7586 du CNRS,
Équipe "Géométrie et Dynamique",
175 rue du Chevaleret,
75013 Paris, France
E-mail: teissier@math.jussieu.fr

For the "Mathematical Biosciences Subseries" of LNM:

Professor P.K. Maini, Center for Mathematical Biology,
Mathematical Institute, 24-29 St Giles,
Oxford OX1 3LP, UK
E-mail: maini@maths.ox.ac.uk

Springer, Mathematics Editorial I, Tiergartenstr. 17,
69121 Heidelberg, Germany,
Tel.: +49 (6221) 487-8259
Fax: +49 (6221) 4876-8259
E-mail: lnm@springer.com